

A comparative study of nitrogen uptake and nitrification rates in sub-tropical, polar and upwelling waters

Marie Catherine Raïssa Philibert

A thesis presented for the degree of Doctor of Philosophy
in the Department of Oceanography,
Faculty of Science,
University of Cape Town,
South Africa.

Supervisors: Dr H. Waldron and Dr D. Clark

April 2015

The copyright of this thesis vests in the author. No quotation from it or information derived from it is to be published without full acknowledgement of the source. The thesis is to be used for private study or non-commercial research purposes only.

Published by the University of Cape Town (UCT) in terms of the non-exclusive license granted to UCT by the author.

Plagiarism Declaration

I know the meaning of plagiarism and declare that all of the work in this dissertation, save for that which is properly acknowledged, is my own.

The following publication is based partly on Chapter 3:

Philibert, R., Waldron, H., and Clark, D.: A geographical and seasonal comparison of nitrogen uptake by phytoplankton in the Southern Ocean, *Ocean Sci.*, 11, 251-267, doi:10.5194/os-11-251-2015, 2015.

Signed:_____

Date: __/__/2015

Abstract

Nitrification is the oxidation of ammonium to nitrate through a two step biological process. Nitrification in the euphotic zone has, in the past, been considered negligible even though quantifying this process correctly is important when linking carbon export to nitrate uptake by phytoplankton. However, studies of both nitrogen uptake and nitrification rates in surface waters are rare.

This thesis presents such data for the Southern Ocean and St-Helena Bay, located in the Southern Benguela upwelling system. Using ^{15}N tracers, Nitrogen uptake and regeneration rates were measured in the Southern Ocean (during a winter cruise in July 2012 and a summer cruise in February-March 2013) and St-Helena Bay (during three studies in November 2011, March 2012 and March 2013).

In St-Helena Bay, the upwelling (bloom) cycle was one of the main drivers of the nitrogen cycle. As the bloom cycle started, nitrate uptake rates ($5.47 - 670.48 \text{ nmol} \cdot \text{L}^{-1} \cdot \text{h}^{-1}$) and nitrite regeneration ($4.36 \pm 1.28 - 22.83 \pm 1.63 \text{ nmol} \cdot \text{L}^{-1} \cdot \text{h}^{-1}$) were high but the contribution of nitrification to the nitrate demand was low. Nitrite regeneration at this time could have been driven by phytoplankton excretion. In contrast, at the end of the bloom cycle, nitrate uptake rates were low and was exceeded by nitrate regeneration rates ($25.34 \pm 6.16 - 82.74 \pm 34.41 \text{ nmol} \cdot \text{L}^{-1} \cdot \text{h}^{-1}$). Nitrite regeneration decreased and was most likely due to ammonium oxidation at this stage of the upwelling cycle.

Nitrification in the Southern Ocean was more variable than in St-Helena Bay. It was only detected at five stations out of fifteen and the accuracy of the high nitrite oxidation rates ($37.21 \pm 9.13 - 217 \pm 88 \text{ nmol} \cdot \text{L}^{-1} \cdot \text{h}^{-1}$) observed can only be assessed with repeat measurements. Nitrate uptake rates ranged from 0.07 to $57.00 \text{ nmol} \cdot \text{L}^{-1} \cdot \text{h}^{-1}$ while ammonium uptake rates ranged from 0.81 - $160.94 \text{ nmol} \cdot \text{L}^{-1} \cdot \text{h}^{-1}$. The nitrogen uptake rates were similar for both seasons. Using multivariate statistical approach, it was found that during winter, in the Southern Ocean, light and ammonium availability were the most important factors regulating nitrogen uptake while in the late summer, changes in the mixed layer depth had a larger effect.

This study provides new observational data for two undersampled regions and contributes to further the mechanistic understanding of the factors regulating nitrogen uptake and nitrification in the Southern Ocean and St-Helena Bay.

Acknowledgements

I would like to thank my supervisors, Dr Howard Waldron and Dr Darren Clark, for their guidance, support and advice.

I would like to acknowledge various funders. This PhD has been in large part funded by the EU FP7 Greenseas project. I am grateful to the University of Cape Town for the yearly international students' scholarship as well as the grant which has allowed me to travel to Plymouth for laboratory analyses. The funding which I received from NRF-SANAP under the SAMMOC programme for two years is greatly appreciated. I am very grateful for the Departmental bursary which I received for this last year of my PhD.

A special thank-you to the numerous people who have helped me with field work in St-Helena Bay; I am very grateful to Pieter Truter for driving the boat and helping to set up experiments in St-Helena Bay and to Raymond Roman who drove all the way to Cape Town from Port Owen to fetch chemicals I needed. I have really appreciated the help of Ffion Atkins, Luke Gregor and the students from the Taught Masters course in 2012 and 2013. I am also grateful to Richard Bellerby for providing me with the data about the phytoplankton community structure.

I would like to acknowledge the officers and crews of the RV SA Agulhas II (for a great winter cruise in the Southern Ocean) and of RV SA Agulhas (for the summer cruise). Big, big thanks to MJ Gibberd for conducting the experiments and sample collection during the summer cruise. I would also like to extend my gratitude to Dr Sandy Thomalla for helping with the summer cruise and providing me with sorted cruise data.

I am also grateful for the friendly working environment in the Department of Oceanography; for the tea-time discussions; to Claire Khai and Emlyn Balarin for doing such a great job and making my life easier. Thanks to the cool office, Room 118: Ceini, Sarah and Brett (who have all left us!), Thulwane, Luke and Izzy (and Wizard). A massive thanks to Luke and Izzy for shipping the samples I forgot in Cape Town when I went to Plymouth for lab work!

Thanks to the Plymouth Marine Laboratory for giving access to their facilities. I am very grateful to the PML staff and students who have been very helpful and made me feel so welcome in Plymouth. I am also very thankful to my family and friends (old and new) in the UK for making my stays in the UK so much better!

Finally, I am very thankful to my friends and family for their support and encouragement. Thanks to my mum and my aunt Vé who have been so good about keeping in touch with me. A special thought (and dedication) to my dad, who has always believed that I could do whatever I wanted and was so proud of me. Last but not least, I am extremely grateful to Timothy Povall for making me breakfast every day and encouraging me in moments of self-doubt.

Contents

Abstract	i
Acknowledgements	ii
List of Figures	viii
List of Tables	xi
List of Abbreviations	xiv
1 Introduction and literature review	1
1.1 Introduction	1
1.2 The nitrogen cycle	2
1.2.1 Major reactions of the nitrogen cycle	2
1.3 Export production and the f-ratio	5
1.4 Nitrification	6
1.4.1 Impact of nitrification on the nitrogen cycle	7
1.4.2 Nitrification rates	8
1.5 Factors regulating nitrification	10
1.5.1 Nitrifiers	10
1.5.2 Light	10
1.5.3 Substrate availability	12
1.5.4 Oxygen	13
1.5.5 Temperature	13
1.6 Summary and research questions	14
1.6.1 Thesis structure	15

2	General methods	17
2.1	Introduction	17
2.2	Nutrients, dissolved oxygen and chlorophyll concentrations	17
2.2.1	Ambient concentrations of nitrate and nitrite	17
2.2.2	Ambient concentrations of ammonium	19
2.2.3	Chlorophyll concentrations	19
2.2.4	Dissolved oxygen concentrations	20
2.3	Nitrogen cycling methods	20
2.3.1	Method overview	20
2.3.2	Incubations	20
2.3.3	Uptake experiments	21
2.3.4	Determination of ammonium and nitrite oxidation rates	22
2.3.5	Dye purification and quantification	26
2.3.6	Calculation of nitrification rates	28
3	A seasonal and geographical comparison of nitrogen uptake by phytoplankton in the Southern Ocean	31
3.1	Introduction: The biological pump in the Southern Ocean	31
3.2	Methods	32
3.2.1	Sampling and analytical methods	32
3.2.2	Statistical analysis	36
3.3	Results	37
3.3.1	Hydrographic data and nutrients	37
3.3.2	Nitrogen and Carbon uptake rates	48
3.3.3	Biogeochemical controls on primary productivity	54
3.4	Discussion	57
3.4.1	Comparison of nitrogen uptake rates with previous studies	57
3.4.2	Carbon export	58
3.4.3	Biogeochemical controls on primary productivity	61
3.5	Conclusion	65
4	Nitrification in the Southern Ocean	67
4.1	Introduction	67
4.2	Methods	68
4.2.1	Sampling	68
4.2.2	Addition of ^{15}N tracers and incubations	68

4.2.3	Determination of isotopic ratios and nitrification rates	69
4.2.4	Differences between the methods used in the winter and summer cruises	71
4.2.5	Data analysis	72
4.2.6	Nitrogen fluxes in summer: a box model	74
4.3	Results	75
4.3.1	Did significant nitrification occur?	75
4.3.2	Nitrogen fluxes in the summer: a box model	79
4.3.3	Nitrite profiles	84
4.4	Discussion	85
4.4.1	Are uncertainties in the measurements obscuring nitrification?	85
4.4.2	Comparison against previously reported rates	90
4.4.3	Decoupling of ammonium and nitrite oxidation	91
4.4.4	Seasonal differences in nitrification rates	92
4.4.5	Factors affecting nitrification	93
4.5	Comparison with models	96
4.6	Conclusion	97
5	The importance of nitrification for the nitrogen cycle in the Southern Benguela upwelling system	99
5.1	Introduction	99
5.2	Methods	100
5.2.1	Sampling	100
5.2.2	Incubations	100
5.2.3	Nitrogen uptake and regeneration rates	102
5.3	Results	102
5.3.1	Environmental conditions - Timing within the upwelling cycle	102
5.3.2	Nitrogen uptake rates	105
5.3.3	Nitrification rates	108
5.4	Discussion	110
5.4.1	Comparison of Nitrogen uptake rates with previous estimates	110
5.4.2	Nitrification rates	112
5.4.3	Changes in the nitrogen cycle within upwelling cycles	113
5.4.4	Implications of high nitrification rates for carbon export in the Benguela upwelling system	119
5.5	Conclusion	120

6	Synthesis and conclusions	121
6.1	Thesis aims	121
6.2	What are the nitrification rates in the Southern Ocean and in the Southern Benguela upwelling system?	121
6.3	What is the contribution of nitrification to nitrate demand in these two regions?	122
6.4	Seasonal differences in the nitrogen cycling	123
6.5	Outlook	125
	Bibliography	125
A	CTD stations for the winter cruise	145
B	Nitrate and nitrite profiles for the Southern Ocean stations	147

List of Figures

1.1	The major reactions of the nitrogen cycle reproduced from Gruber (2008)	3
1.2	Simplified view of the biological pump	6
1.3	Specific nitrification with depth	12
2.1	Schematic of the method for the measurement of nitrification rates	21
2.2	Breakthrough curve of Sudan-1 injected on two types of SPE cartridges	25
2.3	Concentration of NO_2^- or NO_3^- recovered from the biotage and sigma cartridges for 7 different samples	27
3.1	Cruise track for the two cruises	34
3.2	POC vs PON concentrations for the winter and summer cruises	36
3.3	Temperature and salinity sections for leg 1 of the winter cruise	38
3.4	Chlorophyll and dissolved oxygen concentrations for leg 1 of the winter cruise	39
3.5	Temperature and Salinity data for leg 2 of the winter cruise	40
3.6	Chlorophyll and dissolved oxygen concentrations for leg 2 of the winter cruise	41
3.7	Surface concentrations of NO_3^- and Si(OH)_4 for leg 1 of the winter cruise.	42
3.8	Temperature and salinity data for Process Station A during the summer cruise.	43
3.9	Chlorophyll and dissolved oxygen concentrations for Process Station A during the summer cruise.	44
3.10	Temperature and salinity data for Process Station B during the summer cruise.	45
3.11	Chlorophyll and dissolved oxygen concentrations for Process Station B during the summer cruise.	46
3.12	Silicate and nitrate profiles for the summer cruise	47
3.13	Nitrogen uptake rates corrected according to Eppley et al. (1977)	49
3.14	Ammonium uptake rates corrected according to Kanda et al. (1987)	49
3.15	Total primary productivity from ^{13}C uptake vs Total primary productivity estimated from ^{15}N uptake	51
3.16	Nitrate and ammonium uptake rates profiles for the summer cruise	53
3.17	Cluster analysis for all the stations including underway stations	55

3.18	RDA triplot showing the effect of environmental parameters on the nitrogen uptake regime	56
3.19	Comparison of nitrate and ammonium uptake rates with previous studies	60
4.1	Comparison of nitrate and nitrite concentrations measured from the GC-MS and concentrations measured by FIA on board	70
4.2	Effect of increasing sample size on GC-MS response	71
4.3	Winter cruise: Sample size (MSD response) for all stations.	72
4.4	Summer cruise: Sample size (MSD response) for all stations	73
4.5	Box plots showing the $^{15}\text{N}/^{14}\text{N}$ ratio comparing the "pre" sample of station 15N-5	74
4.6	Box model for fluxes of ammonium, nitrate and nitrite	75
4.7	Comparison of the "pre" and "post" $^{15}\text{N}/^{14}\text{N}$ ratios for winter ammonium oxidation (NO_2^- production) samples	77
4.8	Comparison of the "pre" and "post" $^{15}\text{N}/^{14}\text{N}$ ratio for winter nitrite oxidation samples	78
4.9	Results of the box model for fluxes of ammonium, nitrate and nitrite	79
4.10	Ammonium concentrations before and after incubation for selected stations during the summer cruise	83
4.11	A typical nitrite profile and the processes which could contribute to such a profile.	84
4.12	Nitrite concentration profiles for the winter cruise for stations	86
4.13	Concentration of ^{14}N and ^{15}N before and after incubation at CTD 4 for the enrichment experiment	88
4.14	Comparisons of the "pre" enrichment ratio for the enrichment and dilution experiments during the summer cruise.	89
4.15	Comparisons of the "pre" and "post" $^{15}\text{N}/^{14}\text{N}$ ratio for the dilution experiment at CTD 1 of the summer cruise	90
4.16	N^* for stations located in the Polar Frontal Zone for both the summer and winter cruises.	94
5.1	Location of St Helena Bay station	101
5.2	Sea-Surface temperature obtained from MODIS satellites for 28 November 2011 to 01 December 2011.	103
5.3	Temperature and salinity profiles for March 2012 and March 2013.	104
5.4	Evolution of chemical and biological variables during the three field surveys	106
5.5	Nitrate and ammonium uptake	107
5.6	Dominant phytoplankton groups for stations Mar2013-1A (Tuesday), Mar2013-2A (Wednesday) and Mar2013-3A (Thursday)	116
5.7	Pathways for the production (sources) and consumption (sinks) of nitrite, adapted from Lipschultz (2008)	117
5.8	Nitrification and nitrate uptake rates at selected stations.	118
6.1	Summary of nitrogen cycling rates in the Southern Ocean and St Helena Bay (Benguela upwelling system)	124

A.1	CTD positions for the winter cruise	145
B.1	Nitrate and nitrite profiles to maximum depth for the summer cruise	147
B.2	Nitrate and nitrite profiles to maximum depth for the summer cruise (cont.)	148
B.3	Nitrate and nitrite profiles to 200 m for the summer cruise	149
B.4	Nitrate and nitrite profiles to 200 m for the summer cruise (cont.)	150

List of Tables

1.1	Summary of reported ammonium oxidation and nitrite oxidation rates	11
2.1	Samples used for the comparison of biotage and sigma cartridges	26
2.2	Changes in the composition of the mobile phase during the purification step by HPLC	26
3.1	Primary productivity station details for the SOSCEX summer cruise in February-March 2013	33
3.2	Winter depth integrated nitrogen uptake rates	50
3.3	Winter primary production estimates from ^{13}C measurements at 8 CTD stations	51
3.4	Summer depth-integrated nitrogen uptake rates	52
3.5	Spearman correlation matrix of uptake rates and environmental variables for the summer cruise with the associated p-values.	56
3.6	Overview and comparison of integrated nitrogen uptake rates ($\text{mmol}\cdot\text{N}\cdot^{-2}\text{m}\cdot^{-1}\text{d}$).	59
4.1	Southern Ocean nitrification stations	68
4.2	Results of the Mann-Whitney test for the winter cruise.	76
4.3	Results of the Mann-Whitney test for the summer cruise	77
4.4	Ammonium and nitrite oxidation in the Southern Ocean	78
4.5	Results of the box-model for nitrate concentrations	80
5.1	Nitrogen uptake and nitrification rates in St-Helena Bay during surveys in November 2011, March 2012 and March 2013	109
5.2	Phytoplankton community structure from Tuesday (Mar2013-1A) to Thursday (Mar2013-3A).	115

Chapter 1

Introduction and literature review

1.1 Introduction

In terms of matter, the Earth is a closed system (Schlesinger and Bernhardt, 2013). Most matter that is found on Earth was present at its formation and has been recycled ever since by biological, chemical and geological processes as extraterrestrial inputs since then have been minimal (Schlesinger and Bernhardt, 2013). The latter are essential for life as they make the necessary elements available and contribute to the regulation of climate. In order to gain a better understanding of these processes, they have been represented by biogeochemical cycles. The concept of biogeochemical cycles is considered to stem directly from work by Sergei Winogradsky (Dworkin, 2012; Gorham, 1991). He was amongst the first to realise that the conversions between oxidised and reduced species of sulfur and nitrogen were part of the "cycles of life" (Dworkin, 2012). Biogeochemical cycles are characterised by the places where the elements are stored (the reservoirs or the exchange pools), the size of the various reservoirs, the amount of time for which they are stored (the residence time) and the rate at which they are exchanged between reservoirs (the exchange flux rate). Such cycles can be created for each element even though a key aspect in the study of biogeochemical systems is the interdependence of the major cycles. For instance, the carbon and nitrogen cycles are connected by processes such as photosynthesis, respiration, deposition and decomposition of organic matter in the ocean.

The marine carbon cycle is particularly important as the ocean is the largest reservoir of carbon on Earth (Emerson and Hedge, 2008). It stores about 38 000 Pg (10^{15} g) while the atmospheric and terrestrial reservoirs contain about 600 and 2000 Pg respectively (Emerson and Hedge, 2008). The sequestration of carbon in the ocean occurs through two pathways known as the biological and the solubility pumps (Volk and Hoffert, 1985). The solubility pumps depends on the difference in the solubility of carbon dioxide, CO_2 , in warm surface and cold deep waters (Volk and Hoffert, 1985). This is tied to thermohaline circulation but cannot by itself account for all of the carbon sequestered by the ocean.

The biological pump is a result of the processes through which particulate organic matter and calcium carbonate are created biologically before being removed from the euphotic zone (Volk and Hoffert, 1985). Primary production by phytoplankton is the dominant process of the biological pump. Through photosynthesis and nutrient uptake, phytoplankton generate particulate organic matter. Eventually, most of the particulate organic matter is remineralised while the rest sinks exporting and sequestering carbon in the deep ocean. This has been described by Volk and Hoffert (1985) as the soft-tissue pump and plays an important role in linking the carbon cycle to other biogeochemical cycles such as the nitrogen and phosphorus cycle. In this model, the efficiency of the soft-tissue pump was based on the availability of nitrate, NO_3^- , and phosphate, PO_4^- (Volk and Hoffert, 1985). This relationship leads to a biological pump, which is not geographically uniform and is more active in high nutrient regions such as upwelling systems and areas experiencing strong vertical

mixing (Yool, 2011). In addition, climate change due to anthropogenic CO₂ emissions is expected to affect primary production by phytoplankton and the biological pump (Raven and Falkowski, 2002; Wanninkhof, 2013; Riebesell et al., 2007). Increased sea-surface temperature is expected to result in increased stratification. At low latitudes, this leads to a decrease in nutrient influx from depth and consequently, to a decrease in phytoplankton primary productivity (Bopp et al., 2001; Boyce et al., 2010). In contrast, at high latitudes, increased stratification can alleviate the light limitation faced by phytoplankton and stimulate growth (Boyd et al., 2010; Bopp et al., 2001). Increased CO₂ concentrations can also have more direct effects on phytoplankton. Despite the fact that inorganic carbon is not limiting for marine phytoplankton (Raven and Falkowski, 2002), phytoplankton have been shown to increase their consumption of carbon under high CO₂ conditions (Riebesell et al., 2007).

While anthropogenic pressures to the carbon cycle attract most of the attention, the nitrogen cycle is also experiencing changes. Through nitrogen fertilisers, humans are fixing an increasing amount of nitrogen and thus accelerating natural processes of the nitrogen cycle leading to changes in terrestrial, freshwater and coastal ecosystems (Canfield et al., 2010; Gruber, 2008). This has serious implications for the marine nitrogen cycle, which is very dynamic and therefore likely to exhibit substantial changes. In addition, new scientific developments are showing that processes like marine nitrogen fixation and nitrification are more important than previously thought. These processes affect the carbon cycle and the amount of carbon exported from the surface ocean (Gruber, 2008). Furthermore, changes in the availability of nitrogen can have major impacts on phytoplankton and consequently future climate. For this reason, it is important to understand the nitrogen cycle in order to better constrain carbon export. For instance, increased stratification is expected as sea-surface temperature rises. This would decrease the influx of nutrients from the deep ocean.

This literature review details the links between the marine carbon and nitrogen cycles, with a particular attention to nitrification, the biologically mediated conversion of ammonium to nitrate. First, it gives a short overview of the nitrogen cycle and its major reactions. A description of export production and the f-ratio, a proxy used to estimate carbon export, is given. The limitations of the f-ratio are also briefly discussed. Then, the nitrification process and its impact on the nitrogen cycle are detailed. This is followed by a summary of nitrification rates reported in the literature. The factors regulating the process are then considered. Finally, the aims of this thesis and the thesis structure are detailed.

1.2 The nitrogen cycle

Gruber (2008) provides an excellent overview of the nitrogen cycle which he described as the “most complex and fascinating biogeochemical cycle”. In the marine environment, nitrogen exists in a large number of chemical species and in oxidation states ranging from +5 to -3 (see figure 1.1) (Gruber, 2008; Ward, 2011b; Chapman, 1986). The only other element to exhibit such chemical diversity is carbon. This diversity, which stems from the element’s electronic configuration, allows nitrogen to play multiple roles in biologically mediated reactions: it can act as both an electron donor and acceptor (Ward, 2011b). As such, it can undergo a wide range of reactions (figure 1.1). The next section gives a brief description of the major reactions in the nitrogen cycle.

1.2.1 Major reactions of the nitrogen cycle

Assimilation of nitrate and ammonium

Marine phytoplankton take up nitrate and ammonium and convert it into organic nitrogen in order to synthesise their organic matter. This conversion of inorganic nutrients to organic matter is often seen as the base of

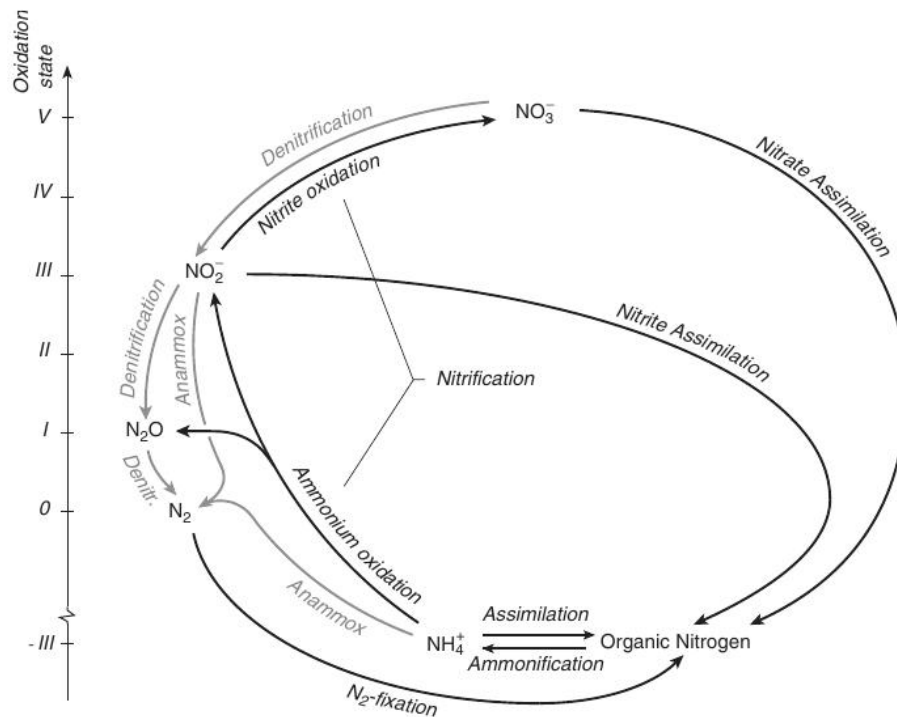


Figure 1.1: The major reactions of the nitrogen cycle reproduced from Gruber (2008)

the food web since this organic matter supports organisms at higher trophic levels (Falkowski, 2012). This reaction is quantitatively the most important reaction of the marine nitrogen cycle. Phytoplankton generally prefer ammonium as it is already in a reduced form (oxidation state -3) and therefore requires less energy for assimilation (Zehr and Ward, 2002). The assimilation of nitrate (NO_3^-) which is more energetically demanding, requires the nitrate reductase enzyme. The latter is crucially present in most phytoplankton since nitrate (NO_3^-) is more abundant than ammonium (Gruber, 2008).

Nitrogen has been identified as the proximate limiting element for biological productivity in the ocean and strongly affects other biogeochemical cycles, particularly the carbon cycle (Tyrrell, 1999; Yool, 2011; Moore et al., 2013). The proximate limiting nutrient influences primary productivity in the short term and addition of this nutrient stimulates phytoplankton growth (Tyrrell, 1999). As they assimilate nitrogen, phytoplankton also take up carbon and phosphate to build their organic matter. Given the cellular demands (Hedges et al., 2002), the elements are generally assimilated in a fixed ratio, which was first observed by Redfield (1934). This ratio has been used to link the various biogeochemical cycles and will be discussed in more details in section 1.3.

Remineralisation and denitrification

Remineralisation is the conversion of organic nitrogen back to the inorganic nitrate. This takes place through ammonification and nitrification. Ammonification is performed by heterotrophic bacteria for which the oxidation of organic carbon to CO_2 is a source of energy. The organic nitrogen is released as ammonium because the heterotrophic bacteria are unable to oxidise it further (Gruber, 2008). Ammonium (as well as urea) is also regenerated through excretion by zooplankton (Fernández and Farías, 2012).

Nitrification is a two-step process. First, ammonium is oxidised to nitrite (NO_2^-) and the latter oxidised to nitrate (NO_3^-). For a long time, this process was thought to be performed only by chemotrophic bacteria but in the last ten years, the role of archaea has also been identified (Wuchter et al., 2006). Archaea are chemotrophic unicellular organisms which are part of a different biological domain to bacteria due to differences in their

biochemical and genetic makeup and form the third domain of life after Eukaryotes and Bacteria (Wuchter et al., 2006).

Remineralisation generally needs oxygen but the organisms responsible for these processes are often chemically flexible and can use other electron acceptors. For instance, nitrate is often used as an electron acceptor in denitrification, which leads to the production of nitrogen gas (N_2) and the loss of fixed nitrogen. Denitrification generally occurs in oxygen minimum zones, such as the Black sea, the Peruvian and Northern Benguela upwelling ecosystems, where the oxygen concentrations are below $5 \mu\text{mol} \cdot \text{L}^{-1}$ (Tyrrell and Lucas, 2002; Devol, 2008). In these regions, denitrification accounts for 20 – 40% of total global nitrogen losses from the ocean (Kuypers et al., 2005; Lam et al., 2009). Denitrification is a step-wise process and is only considered complete when N_2 is actually lost from the system. NH_4^+ and NO_2^- are both formed as intermediaries in this process. However, when examining the stoichiometry of denitrification and the resulting nitrogen budget, it was found that the concentrations of NH_4^+ was lower than expected. This led to a hypothesised pathway for the loss of ammonium. This pathway, anammox, the anaerobic oxidation of ammonium by nitrite, was then confirmed by a number of studies as well as the identification of bacteria capable of carrying out this process (Devol 2008 and references therein).

During nitrification and denitrification, small amounts of nitrous oxide (N_2O) are found. N_2O production associated with nitrification generally occurs in low oxygen areas. Since N_2O is a greenhouse gas, variations in its concentrations can lead to climate change. This is the most direct link between the ocean nitrogen cycle and the Earth's climate.

Nitrogen fixation

As mentioned above, denitrification results in loss of fixed nitrogen from the ocean. For a steady state to prevail, denitrification needs to be balanced by processes such as nitrogen fixation - the conversion of N_2 into nitrogen species which can be used by phytoplankton. Globally, benthic denitrification accounts for a loss of $95 \pm 20 \text{TgN} \cdot \text{y}^{-1}$ and water column denitrification for $80 \pm 20 \text{TgN} \cdot \text{y}^{-1}$ (Gruber and Sarmiento, 1997). Global marine nitrogen fixation is approximately $110 - 140 \text{TgN} \cdot \text{y}^{-1}$ (Codispoti et al., 2001; Gruber and Sarmiento, 1997; Deutsch, Curtis et al., 2007; Aumont et al., 2015). This amounts to a nitrogen deficit of about $60 \text{TgN} \cdot \text{y}^{-1}$ and result in net nitrogen loss from the ocean. However, there are still a number of questions about whether this deficit is real or results from underestimates of nitrogen fixation. Such underestimates have been attributed to methodological aspects (Mohr et al., 2010; Großkopf et al., 2012). This is also reflected in a new biogeochemical model by Aumont et al. (2015) who estimate that the sources of nitrogen (nitrogen fixation) slightly exceed the sinks (denitrification). Estimating nitrogen fixation correctly can also have an impact on carbon export estimates. In most studies, nitrogen fixation is viewed as negligible and consequently, primary production fuelled by this fixed nitrogen is not considered as "new" production. As mentioned earlier, this can result in a 7% underestimate of the f-ratio and carbon export (Henson et al., 2011).

Given its importance in the global nitrogen and carbon budgets and the questions surrounding the process, gaining an understanding of its distribution and driving factors is necessary. Nitrogen fixation rates are affected by the distribution of photoautotrophic nitrogen-fixing organisms; while *Trischodesmium* is the most studied, other organisms such as unicellular bacteria and cyanobacteria have also been shown to contribute to this process (Großkopf et al., 2012). These organisms have high-iron requirements and for this reason, nitrogen fixation is positively correlated with high iron concentrations (Berman-Frank et al., 2001). Nutrient distribution also impacts the process. Nitrogen fixation is usually stimulated in environments where other sources fixed nitrogen have been exhausted but where phosphorus is still available in excess (Deutsch, Curtis et al., 2007). Climate change is likely to also have an effect on nitrogen fixation. Temperature rise, changes in nutrient distributions as well as increases in dust (and therefore, iron) inputs are likely to contribute to an increase in nitrogen fixation.

1.3 Export production and the f-ratio

Primary production is the base of the food chain. It supports all metabolism in the ocean both through grazing and sinking material (Ward, 2011a; Falkowski, 2012). Photosynthesis is the main input of organic carbon into the surface ocean (Gruber, 2008; Ward, 2011b; Doney, 2010; Herr, 2009). Other nutrients such as phosphates and silicates (which is, of course, only required by silicious algae) are also taken up at the same time as carbon and nitrogen. In 1934, Alfred Redfield established that the average plankton had a molar ratio of carbon, nitrogen and phosphorus (Yool, 2011). This ratio is now known as the classic Redfield ratio, 106 C: 16 N: 1 P (Redfield, 1958). It has been used as a tenet of marine biogeochemistry and has been particularly useful in modelling nutrient cycles and the links between them. Deviations from the Redfield ratio have also been used to identify distribution of processes such as uptake, nitrification and denitrification (Deutsch and Weber, 2012; Yool, 2011). These processes contribute to the biological pump, or as (Gruber, 2008) puts it, the “biological loop”. Part of the organic matter, which results from uptake of nutrients, is remineralised to ammonium and other regenerated nutrients (e.g urea) within the euphotic zone while part of it (about 20% Laws et al. (2000)) sinks and is sequestered below the permanent thermocline (maximum mixing depth) (Falkowski et al., 2003). The regenerated ammonium provides the substrate for regenerated production by phytoplankton as well as for ammonium oxidation. The sinking organic matter is also remineralised to ammonium and subsequently to nitrate within the oceans interior. Eventually (over long time scales) the inorganic forms are transported back to the euphotic zone through physical processes. The cyclical nature of this process is the basis for the use nitrate uptake as a proxy for carbon export (figure 1.3a).

Export production is the fraction of particulate organic matter which sinks to the deep ocean and results in the sequestration of carbon (Falkowski, 2012; Eppley and Peterson, 1979; Buesseler, 1998). It is therefore a factor regulating the concentration of CO₂ in the atmosphere. If the biological pump ceased, atmospheric CO₂ would increase by more than 200 ppm (Gruber, 2008). On the other hand, if it was 100% efficient, [CO₂] would decrease by more than 100 ppm. Quantifying export production is important as it gives insight into the vertical structure of the water column (for example, where ammonium and nitrite maxima might be found) and how it might change in the future (Gruber, 2008). Export production can be measured directly using sediments traps, which collect particulate matter as it sinks (Henson et al., 2011). However, this system can prove to be impractical (Falkowski et al., 2003). For this reason, proxies are often used despite their limitations.

The f-ratio (

$$f = \frac{\rho_{\text{NO}_3}}{\rho_{\text{NO}_3} + \rho_{\text{NH}_4} + \rho_{\text{urea}}} \quad (1.1)$$

, where ρ_{NO_3} , ρ_{NH_4} and ρ_{urea} are the uptake rates for nitrate, ammonium and urea respectively) is a common proxy used to estimate the strength of the biological pump (Eppley and Peterson, 1979). Primary production fuelled by nutrients such as ammonium and urea is referred to as regenerated production (Dugdale and Goering, 1967). This is based on the assumption that the sources of the nutrients are distinct. Ammonium and urea are formed through the remineralisation of particulate organic matter in the euphotic zone. By contrast, nitrate, which drives “new” production, is produced by remineralisation of particulate organic matter in the deep ocean and brought to the surface through upwelling and vertical mixing (Dugdale and Goering, 1967). In fact, “New” production is driven by any nutrient that is not regenerated within the euphotic zone. For instance, nitrogen fixation might be an important source of new nutrients, especially in subtropical gyres (Falkowski et al., 2003).

For the fraction of new production (from nitrate) over total production to be used as a proxy for export, the rate of organic nitrogen export and the rate at which new nitrogen becomes available needs to be in balance for the phytoplankton to maintain itself (the steady-state assumption). Other assumptions on which the f-ratio relies include adherence to the Redfield ratio and the absence of nitrification and nitrogen fixation within the

euphotic zone (Dugdale and Goering, 1967; Joubert et al., 2011). In most studies, nitrogen fixation is not included as a source of "new" nutrients. Approximately $140 \text{ Tg} \cdot \text{N} \cdot \text{y}^{-1}$ It is estimated that excluding nitrogen fixation result in a 7% underestimate in carbon export (Henson et al., 2011).

It was thought that nitrification was completely inhibited by light. This implied that no nitrate is formed in euphotic zone and the calculation of the f-ratio as shown in equation 1.1 rests on this assumption. However, there is significant evidence that nitrification does occur in the euphotic zone of various environments (Bianchi et al., 1997, 1999; Clark et al., 2006; Dore and Karl, 1996; Feliatra and Bianchi, 1993; Fernández et al., 2009; Yool et al., 2007) and that accounting for the regeneration of nitrate changed the f-ratio significantly (figure 1.3b). For instance, in the model presented by Yool et al. (2007), the simulated global average of the f-ratio between 1995-2004 was found to be 0.577 if regenerated nitrate is not taken into account, but when this factor is included in the model, the f-ratio decreased to 0.260. It is therefore important to consider the nitrification process when estimating new production from nitrate production over appropriate time-scales. For instance, investigating the seasonal variations in nitrification with the euphotic zone (or above the permanent thermocline) will provide insight into its potential contribution to nitrate demand by phytoplankton. Observational data will also allow for better constraints for models which incorporate nitrification.

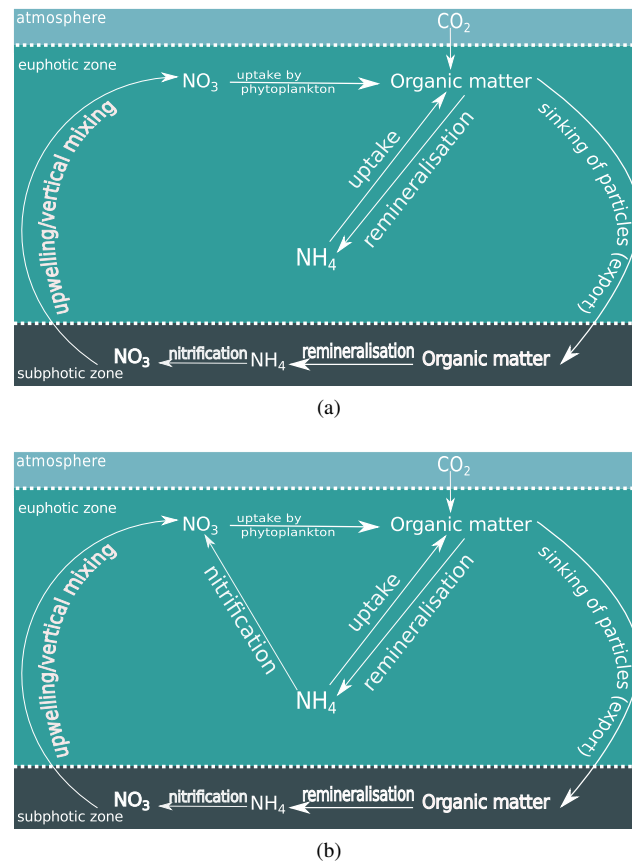
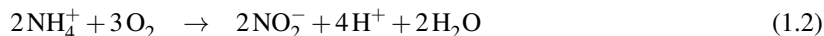


Figure 1.2: Simplified view of the biological pump

1.4 Nitrification

Nitrification, an aerobic process, is the biologically mediated oxidation of ammonium to nitrate. The process was first discovered in soils where nitrification remediates the loss of nitrate through denitrification (Dworkin, 2012). Nitrification occurs in two separate steps. The ammonium is first oxidised to nitrite (Eq. 1.2), which is then converted to nitrate (Eq. 1.3). The two reactions are thermodynamically favourable. They can occur

through biological processes as first suggested by Louis Pasteur (Dworkin, 2012). Nitrification can also be the result of photochemical processes but, in the ocean the contribution of photochemical nitrification is probably minor (Ward, 2008).



Most of the nitrification in the ocean is performed by nitrifying microorganisms (Ward, 2008). Nitrifiers are classified under three categories: Ammonium oxidising bacteria (AOB), ammonium oxidising archaea (AOA) and nitrite oxidising bacteria (NOB) (Ward, 2008). AOB and NOB were first isolated from soils by Sergei Winogradsky. His work on nitrification has led to the idea of biogeochemical cycles as well as to the discovery of chemolithotrophy (the ability of microorganisms to derive energy by oxidising inorganic nutrients) (Dworkin, 2012). Since then, nitrifiers have been discovered in a wide range of environments including the urban heating system of Moscow (Daims et al., 2011) and the human skin (Whitlock and Feelisch, 2009).

While no organism is known to perform both reactions, AOB and NOB both descend from a common photosynthetic ancestor. The biochemistry and physiology of AOB and NOB (with an emphasis on AOB) have been studied through cultures and field studies (Norton, 2011; Daims et al., 2011). The genera *Nitrosococcus*, *Nitrosomonas* and *Nitrospira* all include AOB. There are four confirmed genera of NOB: *Nitrobacter*, *Nitrococcus*, *Nitrospina*, and *Nitrospira* and a candidate genus "Nitrotoga". *Nitrococcus* and *Nitrospina* are strictly marine genera and NOBs from these genera have not been identified or isolated from any other environments (Daims et al., 2011).

The potential for archaeal ammonium oxidation was first recognised by (Venter et al., 2004) who identified the ammonia-monooxygenase enzyme in *Crenarchaeota*. The ubiquitousness of AOA and their role in the nitrification process was established shortly afterwards (Wuchter et al., 2006). AOA also show great diversity as different communities dominate in different habitats such as sediments or water columns. Important variations have also been observed in between sites (Francis et al., 2007). AOA are more abundant in the marine environment than AOB (Ward, 2011b; Francis et al., 2005) and whether this results in a higher contribution to ammonium oxidation is debatable (Hatzenpichler, 2012). This is being addressed through the increasing number of studies examining the physiology of AOA and comparing its contribution to ammonia oxidation with that of AOB (Martens-Habben et al., 2009). Due to their different physiologies, AOA and AOB are able to occupy separate niches (Fernández and Farías, 2012; Santoro et al., 2013; Beman et al., 2012). These differences include their affinities for ammonium and resistance to light - AOA have a higher affinity for ammonium (Martens-Habben et al., 2009) and are more sensitive to light than AOB (Merbt et al., 2012).

1.4.1 Impact of nitrification on the nitrogen cycle

Nitrification is a particularly interesting process as it creates a link between the most oxidised (oxidation state +5) and the most reduced (oxidation state -3) nitrogen species in the marine environment (Ward, 2011b). It also links other critical processes of the marine nitrogen cycling such as remineralisation and nitrogen assimilation (Carini et al., 2010; Ward, 2011b).

While nitrification does not influence the net nitrogen inventory of the ocean directly (unlike denitrification which leads to the loss of nitrogen from the ocean), it determines the distribution of nitrogen amongst important pools (Carini et al., 2010; Ward, 2011b). In oxygenated oceans, the abundance of ammonium is influenced by the rates of ammonium oxidation by AOB and AOA and of ammonium uptake by other microorganisms

and phytoplankton. Furthermore, the nitrification-denitrification balance plays an important role in regulating the nitrogen inventory both in the natural environment (marine and terrestrial) and managed systems, such as waste water treatment plants (Ward, 2011b). In the coastal oceans, coupled nitrification-denitrification removes a large proportion of nitrogen pollution originating from terrestrial inputs before it can reach the open ocean. As such, it partially separates the open ocean from anthropogenic changes in the terrestrial nitrogen cycle (Francis et al., 2005)

Nitrification also impacts the vertical distribution of nitrogen species. Nitrite (NO_2^-) and ammonium often have maximum concentrations between 50 and 80 m depth. The concentrations then decrease with depth indicating their roles as intermediates in the nitrogen cycle. They accumulate where production is greater than consumption (Gruber, 2008). In the deeper parts of the euphotic zone, where NH_4^+ uptake is limited by light, NH_4^+ consumption is likely to occur through nitrification (Gruber, 2008; Ward and Zafriou, 1988; Ward and O'Mullan, 2005). The primary nitrite maximum (PNM) on the other hand is enigmatic (Lomas and Lipschultz, 2006). It has been suggested that the PNM is a result of the decoupling of the two nitrification steps while others suggest that reduction of nitrate by phytoplankton has a larger role to play. There has been a number of studies attempting to resolve this question but it appears that the mechanisms leading to the formation of the PNM vary regionally and seasonally (Olson, 1981b; Santoro et al., 2013; Beman et al., 2013). While the earlier studies (e.g Lomas and Lipschultz (2006)) focused on differentiating nitrite production by phytoplankton and AOB, more recent studies have shown that differences in activities and distribution of AOA and AOB could also have an impact on the PNM (Martens-Habbena et al., 2009; Merbt et al., 2012). AOA and AOB also have different photoinhibition and affinities for ammonium. AOA are known to be more sensitive to light than AOB (Merbt et al., 2012) but given their very high affinities for ammonium (Martens-Habbena et al., 2009), they might fare better when in competition with phytoplankton.

Finally, as previously mentioned, nitrification within the euphotic zone breaks down the "new" and "regenerated" production paradigm. If nitrate is formed in areas where nitrate uptake is possible, part of the nitrate pool has to be reclassified as a regenerated nutrient. In this case, the question is "what are the rates of nitrification in the euphotic zone?."

1.4.2 Nitrification rates

Techniques for the measurement of nitrification have improved and are now much more sensitive (Ward, 2011b; Yool et al., 2007; Ward, 2011a). (Ward, 2008) compiled euphotic nitrification rates in a variety of environments (coastal upwelling systems, oligotrophic mid oceanic gyres) with a range of nutrient concentrations and depths. Table 1.1 reproduces some of the euphotic zone nitrification rates presented by Ward (2008) and includes rates reported in more recent studies. It is to be noted that many of these studies report only NH_4^+ oxidation (for example Sutka et al. (2004); Grundle et al. (2013)) and not nitrite oxidation. Others have measured "net nitrification" as the oxidation of NH_4^+ to NO_3^- using $^{15}\text{NH}_4^+$ tracers (Fernández et al., 2009). This method is referred to as R_{NO_3} from $^{15}\text{NH}_4$ in table 1.1. Others measure a combined rate of NH_4 and NO_2 oxidation using isotopic dilution techniques (Cavagna et al., 2014; Souza et al., 2014; Bronk et al., 2014; Santoro et al., 2013; Carini et al., 2010) (referred to as NO_x isotopic dilution). Both methods assume a coupling between the two steps of nitrification even though this is not always the case (Bronk et al., 2014).

Euphotic zone nitrification breaks the connection between the supply of nitrate from depth and export production. It is difficult to evaluate this quantitatively over the whole ocean and a full annual cycle (Yool et al., 2007). For this reason, good models with the right parameters are needed. This can only happen with increased in-situ data, such as the results presented in this thesis. As mentioned in section 1.4.1, nitrification contributes to the turnover of ammonium, nitrite and nitrate. In this section, the importance of nitrification in these two roles will be considered- the regeneration of nitrate (per se), which can support primary production by phytoplankton, and a driver of dissolved inorganic nitrogen (ammonium, nitrate and nitrite) turnover.

Clark et al. (2008) provided nitrogen uptake and regeneration rates for various regions of the Atlantic Ocean including the North and South Atlantic gyres and the Northwest African upwelling region. Their data showed that nitrification (ammonium oxidation and nitrite oxidation) can contribute to very rapid turnover of the nitrite and nitrate in all of the sampled regions. Given that ammonium regeneration was much faster than ammonium oxidation, the latter accounted for $< 10\% - 50\%$ of the ammonium pool turnover whereas most of the nitrite turnover was attributed to nitrite regeneration. The nitrate pool could also be completely replaced by nitrite oxidised within the euphotic layer. In the complementary papers by Bianchi et al. (1999) and Bianchi and Feliatra (1999), it was found that 30-100% of nitrite at the PNM of NW Mediterranean basin was produced through ammonium oxidation and 7-20% of the nitrate concentration was produced through nitrite oxidation. Beman et al. (2013) estimated that the PNM could be formed within 2 - 4 days. In one case, the PNM could have potentially been formed within less than a day. Under non-upwelling conditions, ammonium oxidation was the most important pathway for the consumption of ammonium in the surface layers at a station off the coast of Chile (Molina et al., 2012). These studies highlight the role of nitrification in the turnover of nitrogen species. They also show that there is a large variation within and between regions.

Nitrite oxidation is the process which brings the classification of nitrate as a strictly new nutrient into question. While the rates of nitrite oxidation are usually low, they can be of the same order of magnitude as the rates of nitrate uptake by phytoplankton (Ward et al., 1989; Dore and Karl, 1996; Clark et al., 2008; Fernández and Raimbault, 2007). For instance, in Monterey Bay, 15 - 27 % of nitrate assimilation is supported by nitrification while 21 - 33% of the ammonium pool was used up by nitrifiers (Wankel et al., 2007). This has been shown in different regions including the Mediterranean sea (Bianchi et al., 1999; Bianchi and Feliatra, 1999; Diaz and Raimbault, 2000), the North East Atlantic (Fernández and Raimbault, 2007; Fernández et al., 2005), the Peruvian upwelling (Fernández et al., 2009), the Californian upwelling (Beman et al., 2013), the Iberian upwelling (Clark et al., 2011) and the Northern Benguela upwelling (Benavides et al., 2014). Ward et al. (1989) measured nitrification and nitrate uptake simultaneously in the Southern California Bight, however, they used to different models to calculate the uptake and nitrification rates. As a result, the contribution of nitrification to nitrate demand at the surface was not clear, averaging 0.37% for one model and 15.4% for the other.

In several studies which directly compared coastal and open ocean (Bianchi et al., 1999; Grundle et al., 2013; Raimbault et al., 1999; Bronk et al., 2014) higher contributions of nitrification to nitrate demand in the coastal ocean was the consistent finding. In the open ocean, nitrification rates can be of the order of $1 - 100 \text{ nmol} \cdot \text{L} \cdot \text{d}^{-1}$ (Ward, 2011a; Yool et al., 2007) and has been detected to depths up 3000m. Dore and Karl (1996) measured nitrification and N_2O production at the ALOHA station, which is expected to be representative of the subtropical mid-ocean gyres. Ammonium oxidation rates in their study ranged between $1 - 137 \text{ nmol} \cdot \text{L} \cdot \text{d}^{-1}$ whereas nitrite oxidation ranged from undetectable to $137 \text{ nmol} \cdot \text{L} \cdot \text{d}^{-1}$. Dore and Karl (1996) did not measure near-surface nitrification but concluded that the process might have been significant based on the N_2O as well as the net nitrogen uptake. On one cruise, they also found that nitrification in the euphotic zone represented between 47 - 142% of nitrate uptake rates.

Only 7 of the studies cited here (Grundle et al., 2013; Clark et al., 2011, 2014; Benavides et al., 2014; Bronk et al., 2014; Cavagna et al., 2014; Fernández et al., 2009; Fernández and Farías, 2012; Ward et al., 1989) measured rates of nitrification and nitrate uptake simultaneously. Nitrate regeneration can lead to the isotopic dilution of $^{15}\text{NO}_3^-$ tracers and result in underestimate of uptake. The extent to which such isotopic dilution affects the rate measurements changes as both nitrification and nitrate uptake rates can be highly variable. Furthermore, many assume coupling between ammonium and nitrite oxidation and that the nitrite is only formed through ammonium oxidation. However, this is not always true (Clark et al., 2011; Füssel et al., 2012; Fernandes et al., 2014) and there are other possible sources of nitrite (Lipschultz, 2008). These alternate sources of nitrite have the potential to stimulate nitrite oxidation and it is therefore important to measure the two processes independently. Furthermore, nitrite and ammonium oxidation are often spatially

separated, leading to the formation of the PNM. It is only by separating the two processes that the balance between the processes producing and consuming nitrite can be investigated.

1.5 Factors regulating nitrification

For a better modelling of nitrification, especially given its relationship to carbon export, it is important to understand the factors which can affect the process location and rates. Both field observations and laboratory cultures can be used to this effect. Laboratory cultures have often been used and can provide a testable, repeatable environment where conditions can be varied. However, often the relationships observed in laboratory cultures are not repeated in natural assemblages (Ward, 2008; Bianchi et al., 1997; Olson, 1981a). This is because organisms not present in cultures might contribute to the process in the natural environment. Furthermore, competition with other organisms - for example competition for ammonium between phytoplankton and ammonium oxidisers - are not reproduced in pure cultures. For this reason, field observations can help in understanding the environmental factors which affect nitrification. While the influence of light has been known and studied for a long time, other factors are gaining increasing relevance. For instance, understanding the effect of pH on nitrification is becoming increasingly important to predict how the ecosystem will respond to ocean acidification (Fulweiler et al., 2011; Beman et al., 2010; Clark et al., 2014). The distribution of nitrifying organisms, specifically AOA, has also come into focus since their discovery. This section summarises the influence of light, oxygen, microbial community and substrate availability on nitrification.

1.5.1 Nitrifiers

Most nitrification in the marine environment is biologically mediated and therefore, it cannot happen without the organisms able to perform this reaction. These organisms occupy a unique niche as they have inflexible nutritional requirements. Thus, environmental variables which affect the distribution of these organisms will also regulate the distribution of nitrification rates. Autotrophic nitrifiers use ammonium or nitrite as their only source of energy whereas heterotrophic nitrifiers, which are rare in the marine environment (Alonso-Sáez et al., 2012; Ward, 2008), can use either ammonium or organic substrates. Autotrophic nitrifiers are more likely to be found in the surface layers and down to 1000 m but the effects of substrate availability on nitrification rates are not fully understood. The abundance of nitrifier genes and nitrification rates are generally well correlated (Santoro et al., 2010, 2013; Beman et al., 2013). It is to be noted, however, that the presence of certain genes does not in itself imply high activity and that studies estimating both activity and abundance of these organisms are required (Merbt et al., 2012).

1.5.2 Light

Light is one of the most important factors affecting nitrification. Nitrification has been shown to be very strongly inhibited by UV (Guerrero and Jones, 1996a,b) and for this reason, it was assumed that it did not occur or was negligible within the euphotic zone. Several studies have shown nitrification rates increasing with depth (and hence, reduced light availability) (Ward and O'Mullan, 2005; Bianchi et al., 1997). For instance, Grundle et al. (2013) observed maximum ammonium oxidation rates at the lowest light intensity for all stations. However, as described in section 1.4, nitrifiers and nitrifying activities are detected even in surface sea-water showing that the relationship between nitrification rates and depths is not always clear-cut. For instance, dark periods, which are long enough, allow nitrifiers to recuperate/repair their cells after exposure to UV (Horrigan et al., 1981) and could explain the prevalence of these organisms in surface waters and the sun-lit water column. Nitrifiers' physiological sensitivity to light as well as the reduced competition

Reference	Publication year)	Region	Season	Depth (m)	Ammonium oxidation ($\text{nmol} \cdot \text{L}^{-1} \cdot \text{h}^{-1}$)	Nitrite oxidation ($\text{nmol} \cdot \text{L}^{-1} \cdot \text{h}^{-1}$)	Method
Miyazaki et al. (1973)	1973	Sagami Bay, Japan	Summer	Photic zone	2100	-	15 N tracers
Miyazaki et al. (1973)	1973	Sagami Bay, Japan	Autumn	Photic zone	1600	-	15 N tracers
Olson (1981a)	1981	Southern California Bight	All seasons	0	0-0.03	-	15 N tracers
Olson (1981a)	1981	Central North Pacific	Summer	109-150	0.09-0.030	-	15 N tracers
Olson (1981a)	1981	Ross Sea (Southern Ocean)	Summer	0-30	0.37	-	15 N tracers
Olson (1981a)	1981	Scotia Sea (Southern Ocean)	Spring	0-90	0-0.54	-	15 N tracers
Bianchi et al. (1997)	1997	Southern Ocean	Spring	60	0.8-1.4	0.2-0.8	Inhibitors
Bianchi and Feliatra (1999)	1999	Mediterranean sea	Spring	-	-	3-21	Inhibitors
Raimbault et al. (1999)	1999	Equatorial Pacific ocean	Spring (Austral)	0-140	-	< 0.2-1.7	R_{NO_3} from $^{15}\text{NH}_4$
Diaz and Raimbault (2000)	2000	Mediterranean sea	Spring	5-60	-	0.4-1.3	R_{NO_3} from $^{15}\text{NH}_4$
Ward (2005)	2005	Monterey Bay	All seasons	0-80	< 0.8-3.3	-	15 N tracers
Fernández and Raimbault (2007)	2007	NE Atlantic	Spring and winter	0-30	-	0-0.83	R_{NO_3} from $^{15}\text{NH}_4$
Clark et al. (2008)	2008	Oligotrophic and equatorial Atlantic	Autumn	euphotic zone	0-0.41	0.017-1.2	^{15}N isotopic dilution
Clark et al. (2008)	2008	Northwest African upwelling	Autumn	euphotic zone	0.05-0.23	0-0.35	^{15}N isotopic dilution
Fernández et al. (2009)	2009	Peruvian upwelling	Spring/summer	surface	-	0.13-0.25	R_{NO_3} from $^{15}\text{NH}_4$
Carini et al. (2010)	2010	Gulf of Mexico	Summer	3-16	0.08-8.8	up to 150	NO_x isotopic dilution
Santoro et al. (2010)	2010	California current	Summer	25-500	7.2-130	-	Inhibitors
Painter (2011)	2011	Iceland basin	Summer	0-125	0.03-3.7	0.03-24.8	^{15}N tracers
Newell et al. (2011)	2011	Arabian Sea	Autumn	50-200	0.03-3.7	0-8.3	$^{15}\text{NH}_4$ tracer + inhibitors
Clark et al. (2011)	2011	Iberian upwelling	Summer	0-80	0.03-3.7	0.58-16	$^{15}\text{NO}_2$ tracer
Fernández and Farias (2012)	2012	Coastal waters off Chile	All seasons	80-120	0-15	below dl - 34 ± 12	$^{15}\text{NH}_4$ tracer
Füssel et al. (2012)	2012	Northern Benguela upwelling	Autumn/Winter	0-200	below dl - 23 ± 15	below dl - 8 ± 5	$^{15}\text{NH}_4$ tracer
Beman et al. (2012)	2012	California current	Summer	0-55	0.03 ± 0.03 - 9 ± 22	below dl - 8 ± 5	Inhibitors
Santoro et al. (2013)	2013	California current -Inshore	Autumn	0-55	below dl to 4.0	below dl - 8.9	$^{15}\text{NO}_2$ tracer
Santoro et al. (2013)	2013	California current -Offshore	Autumn	0-75	below dl to 4.0	30-150	NO_x isotopic dilution
Grundle et al. (2013)	2013	Subarctic North Pacific	All seasons	0-75	below dl to 4.0	2.5-9.1	NO_x isotopic dilution
Beman et al. (2013)	2013	California current	Summer	0-50	0.20-1.9	0.05-29	^{15}N isotopic dilution
Souza et al. (2014)	2014	Northern Chukchi Sea	Summer	0-50	0.20-1.9	below dl - 125	NO_x isotopic dilution
Bronk et al. (2014)	2014	West Florida Shelf	Autumn	0-140	0.20-1.9	below dl - 125	NO_x isotopic dilution
Clark et al. (2014)	2014	Subarctic	Summer	0-140	0.20-1.9	below dl - 125	NO_x isotopic dilution
Cavagna et al. (2014)	2014	Southern Ocean	Spring	0-140	0.20-1.9	below dl - 125	NO_x isotopic dilution

Table 1.1: Summary of reported ammonium oxidation and nitrite oxidation rates. The methods used for the measurement of nitrification rates summarised here include inhibitors, ^{15}N tracers and isotopic dilution (separating ammonium and nitrite oxidation), "net nitrification" (the oxidation of NH_4^+ to NO_3^- using $^{15}\text{NH}_4^+$ tracers referred to as R_{NO_3} from $^{15}\text{NH}_4^+$) and combined rate measurements of NH_4^+ and NO_2^- oxidation using isotopic dilution techniques (referred to as NO_x isotopic dilution).

with phytoplankton would suggest that nitrification rates should increase linearly with depth and be at a maximum below the euphotic zone, but this does not happen. Nitrification rates have been found to peak at the base of the euphotic zone due to the substrate availability (Beman et al., 2012; Olson, 1981b; Ward, 2005; Bianchi et al., 1997; Olson, 1981b). In addition, in the datasets collated by Yool et al. (2007), there was no correlation between depth and specific ammonium oxidation rates (where ammonium oxidation was divided by ammonium concentrations) as seen in figure 1.3.

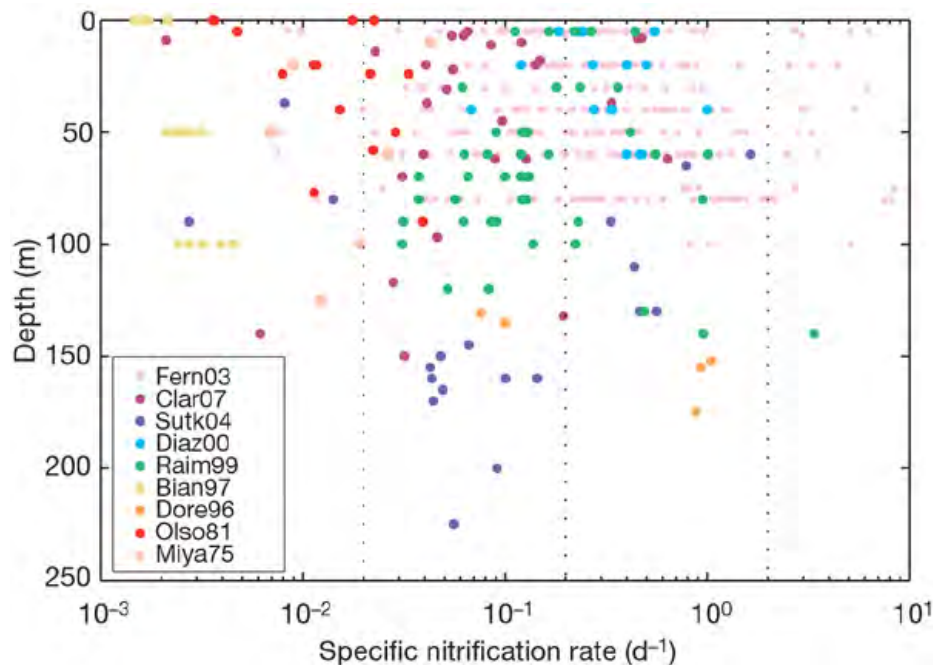


Figure 1.3: Specific nitrification with depth, reproduced from Yool et al. (2007). The datasets shown in this plot are originally from the following studies: Fern03 (Fernández, 2003), Clar07 (Clark et al., 2007), Sutk04 (Sutka et al., 2004), Diaz00 (Diaz and Raimbault, 2000), Raim99 (Raimbault et al., 1999), Bian97 (Bianchi et al., 1997), Dore96 (Dore and Karl, 1996), Olso81 (Olson, 1981a) and Miya75 (Miyazaki et al., 1975)

1.5.3 Substrate availability

Changes in substrate availability are expected to be a controlling variable in determining the AOA, AOB and NOB community composition but there are contradictory findings relating to their effects. For instance, in culture experiments, it has been shown that increased ammonium concentration lead to increased ammonium oxidation rates (e.g Martens-Habbenha et al. (2009)), however this has not been reproduced in natural assemblages and consequently to increased nitrification (Ward, 2008; Bianchi et al., 1997; Olson, 1981a). While there are sensible explanations (mentioned above) for the differences between culture and field observations, such differences support the idea that the combination of factors controlling nitrification are not linear.

Nevertheless, nitrification is linked to the supply of ammonium and the vertical flux of organic matter (Ward, 2011b). Given that organic matter is the substrate for ammonium regeneration, as the latter decreases with depth, so does the supply of ammonium and ammonium oxidation rates. When nitrite and ammonium oxidation are coupled, nitrite oxidation also peaks at the same depth. Nitrite oxidation might also increase if there is a different source of nitrite such as the release of nitrite by phytoplankton. The links between nitrification and particulate organic matter can also be seen when comparing nitrification rates and nitrifier abundances under upwelling and non-upwelling conditions. At a station off the coast of Chile, nitrification was found to increase under upwelling conditions (Fernández and Farías, 2012; Levipan et al., 2014; Farías et al., 2009). Under such conditions, phytoplankton growth was found to be enhanced and ammonium (originating from

remineralised particulate matter) increased. Higher ammonium oxidation rates with higher ammonium concentration was also observed by (Grundle et al., 2013), however, the response to substrate availability was different in winter and spring/summer.

Increasing the nutrient loads in natural waters may lead to a change in the natural assemblages (Ward, 2011b). For example, Bianchi and Feliatra (1999) observed very high nitrification rates in a region which was influenced by a plume from the Rhône river. It is to be noted that the supply rate of ammonium (through ammonium regeneration) or nitrite (through either ammonium oxidation or excretion by phytoplankton) might have a greater influence than the absolute concentration of nitrate and nitrite (Ward and O'Mullan, 2005). There is contradictory evidence about which one of the two factors (concentration or supply rate) is more important. Beman et al. (2013) found no correlation between nitrite oxidation and ammonium oxidation but found a significant correlation between nitrite oxidation and nitrite concentration. This corresponded to results reported by (Olson, 1981a) who showed a strong relationship between nitrite oxidation and nitrite concentration. In contrast, Bianchi et al. (1997) did not find a significant correlation between substrate availability and ammonium/nitrite oxidation rate but observed a significant correlation between ammonium oxidation and nitrite oxidation. In this case, there was a strong coupling between ammonium and nitrite oxidation. This led them to conclude that ammonium oxidation (rather than other potential sources of nitrite such as excretion by phytoplankton) was providing the substrate for nitrite oxidation. It is also possible that factors enhancing ammonium oxidation, for example temperature or oxygen, were also enhancing nitrite oxidation in Bianchi et al.'s study.

1.5.4 Oxygen

Given that nitrification is an oxidative process, the presence of oxygen is an obvious requirement for the process (Ward, 2011a). However, both nitrite and ammonium oxidisers have been shown to survive in low oxygen environments (Ward, 2011b) and nitrification has been observed in various oxygen-minimum zones (Füßel et al., 2012; Lam et al., 2009; Zehr, 2009). Nitrification is expected to increase with oxygen concentrations. This is mainly observed in low oxygen environments, e.g the Northern Benguela upwelling system (Füßel et al., 2012). In other regions, the oxygen concentrations are above saturation for nitrification and therefore, nitrifiers are less affected by changes in the concentrations of this gas. Moreover, the relationship between ammonium oxidation and oxygen concentrations has been shown to be different in the photic and non-photoc zones. For the same oxygen concentration, lower nitrification rates were observed in the photic zone than in the non-photoc zone (Ward and Zafiriou, 1988) highlighting the interactions between the different factors influencing nitrification rates.

1.5.5 Temperature

Bacterial activity is generally expected to increase with increasing temperatures (Delille, 2004) and the rates are expected to double with every 10°C rise in temperature. Increased rates of nitrification have been observed with temperature. Ijichi and Hamasaki (2011) suggested that the distribution of different AOA species can be affected by temperature. In this study, they sampled at two different depths and incubated the samples at various temperatures. These temperature variations resulted in changes in the AOA community structure and to increases in the rates of ammonium consumption and nitrate production. Nitrate concentrations increased to a higher level at higher temperatures. The final nitrate concentrations were 60 at 4°C, 90 $\mu\text{mol} \cdot \text{L}^{-1}$ at 10°C and 150 $\mu\text{mol} \cdot \text{L}^{-1}$ at 20°C. (Berounsky and Nixon, 1990) observed higher nitrification rates in summer than in winter as well as with increased temperature in laboratory experiments. Similarly, in the Southern Ocean, Bianchi et al. (1997) found a significant positive correlation between nitrite oxidation and temperature and calculated a Q₁₀ value of 1.73 for ammonium oxidation. However, this in contrast with the results from

more recent studies (Sanders et al., 2007; Grundle et al., 2013; Smart, 2014; DiFiore et al., 2009; Grzyski et al., 2012) which found that nitrification was more important under the colder winter conditions than under the warmer summer ones. Using a mass-balance approach, Sanders et al. (2007) suggested an increased importance of nitrification in winter in the Southern Ocean. This was corroborated by (DiFiore et al., 2009) and Smart (2014) who examined the $\delta^{15}\text{N}$ of the nitrate pool in the Southern Ocean. Finally, Grzyski et al. (2012) reported a higher bacterial diversity in winter than in summer in the coastal Antarctic peninsula. The relative abundance of chemolithoautotrophs (organisms which derive energy from the oxidation of inorganic compounds) was higher in winter (18-37%) than in summer (1%). More specifically, they observed the presence of the ammonia oxidiser *Ca.N. maritimus* in winter but not in summer. Such findings are in line with the comment by Ward (2008) who suggests that in marine ecosystems, temperature is not a major factor affecting nitrification rates as nitrifiers are usually adapted to the environment in which they are found. This is an absolute necessity as nitrifiers have been found in a variety of environments such as temperatures ranging from 0.2 to 97 °C (Erguder et al., 2009).

1.6 Summary and research questions

The ocean plays an important role in the global carbon cycle as it stores about 38 000 Pg (10^{15} g) of carbon. Carbon is taken up into the ocean through the biological and solubility pumps. The solubility pump is based on physical processes which takes carbon dioxide rich surface waters to depth whereas the biological pump is driven by phytoplankton. The latter produce organic matter, which eventually sinks. This effectively removes carbon from the surface layers and this carbon can be sequestered at depths for a long period. Given its importance for the removal of carbon from the upper ocean and lower atmosphere, phytoplankton primary productivity contributes to the regulation of climate. However, it is likely to be affected by anthropogenic carbon emissions as the latter impacts the water column stratification and hence, nutrient and light availability. In order to quantify how much carbon is taken up and sequestered by the ocean, proxies based on the links between the carbon and nitrogen cycles are often used. To produce their organic matter, phytoplankton require elements other than carbon. These include nitrogen and phosphorus. On average, phytoplankton take up the different elements in a fixed ratio, which was first described by Alfred Redfield. Therefore, by knowing how much nitrogen phytoplankton are using, one can estimate how much carbon is taken up. However, phytoplankton are able to use different type of nitrogen-containing compounds (nitrogen species) and the source of these nitrogen species can be separated. Nitrate was considered to be a "new" nutrient which is only formed outside of the euphotic zone and brought to the surface through physical processes. Ammonium and urea were considered to be "regenerated" nutrients formed only within the euphotic zone. Nitrate being used by phytoplankton has to be in balance with the rate of organic nitrogen export for the phytoplankton to maintain itself. Therefore, the fraction of primary production fuelled by nitrate over total primary production would correspond to the amount of exported organic matter. This rests on the assumption that nitrification, the oxidation of ammonium to nitrate, is completely inhibited by light and does not occur within the euphotic zone. This is, however, a false assumption as nitrification as well as nitrifying organisms have been observed in the euphotic zone in various regions.

Nitrification is a two step process. First ammonium is oxidised to nitrite and the latter converted to nitrate. Ammonium oxidation is performed by AOB and AOA while nitrite oxidation is performed by NOB. Being a biological process, the factors affecting nitrification are directly linked to their impact on the physiology of nitrifying organisms. For instance, nitrifiers are potentially sensitive to light explaining why nitrification increases with depth. However, AOA, AOB and NOB have differential light sensitivities as well as different potential for recovery after having been exposed to light. These organisms are extremely important for the nitrogen cycle as they affect the distribution of nitrogen amongst important pools as well as the vertical profiles of these nitrogen species. Nitrification can provide more than 100% of the nitrate demand and contribute to

the rapid turnover of ammonium, nitrite and nitrate. The "variations in degrees of separation between nitrate assimilation and regeneration seasonally and geographically" is one of the major unknowns in nitrification research (Ward, 2011b). This separation is affected both by the factors controlling nitrogen uptake as well as those controlling nitrification.

This thesis aims to address this gap and provide observational data for two undersampled regions, the Benguela Upwelling system and the Southern Ocean. By comparing different environmental conditions and seasons, this study aims to provide a better understanding of factors controlling nitrification and nitrogen uptake. The regulating factors are often complex and non-linear and vary across time and spatial scales (Murawski et al., 2010; Salihoglu et al., 2013), but by comparing across ecosystems and through time, the intention is to answer a broader set of questions as well as test the generality of assumptions made. Such findings can contribute to the refining of carbon export estimates and climate models and to provide better predictions of both local and global changes.

With the overarching objective of investigating the significance of nitrification in the Benguela upwelling and Southern Ocean, the specific research questions addressed in this thesis are as follows:

- What are the nitrification rates in the Southern Ocean and in the Southern Benguela upwelling system?
- What is the contribution of nitrification to nitrate demand in these two regions?
- What are the seasonal or event-driven differences in nitrogen cycling for these two regions?

1.6.1 Thesis structure

The present chapter, chapter 1, is a literature review highlighting the links between the carbon and nitrogen cycle. It provides an introduction to important aspects of the nitrogen cycle and discusses the role of nitrification in the linkages between the carbon and nitrogen cycle.

Chapter 2 describes the general methods applied in this study. These methods were applied during field work and following laboratory work for both regions. Each subsequent chapter also highlights deviations from the general methods where relevant.

The importance of nitrification is often seen relative to its contribution to nitrate uptake. Quantifying nitrate uptake and demand therefore contributes to answering the second research question. Chapter 3 discusses nitrogen uptake rates in the Southern Ocean. It also examines the biogeochemical controls of the nitrogen uptake regime in this region using multivariate statistical analyses. Chapter 4 reports the rates of nitrification in the Southern Ocean, directly answering the first research question. These nitrification rates were measured simultaneously to the nitrate uptake rates reported in chapter 3. Both chapters offer a comparison of nitrogen cycling processes during a summer and a winter cruise. As such, they address the third question and examine the seasonal differences in the nitrogen cycle of the Southern Ocean.

Chapter 5 examines nitrification and nitrogen uptake rates in the Southern Benguela upwelling system during three field surveys. Differences in nitrogen cycling under different upwelling conditions are discussed. Nitrification rates and nitrogen uptake rates are compared. The timing within an upwelling cycle influences the different nitrogen cycling processes. The impact of this effect on the nitrogen cycle and in particular nitrification is considered.

Chapter 6 provides a synthesis of the previous three chapters effectively comparing the importance of nitrification in the two regions. It summarises the thesis and the rates measured before discussing potential future work.

Chapter 2

General methods

2.1 Introduction

The aim of this chapter is to describe in detail the procedures followed for the measurement of nitrification and nitrogen uptake. Field work was conducted in St-Helena Bay (Benguela upwelling system) on three separate occasions (November 2011, March 2012 and March 2013) for a week at a time. In the Southern Ocean, a winter cruise was conducted in July 2012 and a summer cruise in February 2013. Experimental details such as sampling locations and any deviations from the general method, are given in the relevant chapters. This also applies to statistical analyses used in each chapter.

Contextual information such as nutrient, dissolved oxygen and chlorophyll-a concentrations are required for a better understanding of the conditions under which nitrification occurs. The nutrient concentrations are also required for the calculation of nitrogen uptake rates. The first part of this chapter describes how nutrient, dissolved oxygen and chlorophyll concentrations were measured. The second part of the chapter is a description of the method for the measurement of nitrification rates which has been adapted from Clark et al. (2007). All chemicals were supplied by Sigma-Aldrich Co. unless stated otherwise.

2.2 Nutrients, dissolved oxygen and chlorophyll concentrations

2.2.1 Ambient concentrations of nitrate and nitrite

Ambient concentrations of nitrite were measured manually according to methods by described Grasshoff et al. (1983). Nitrate (as part of nitrate + nitrite, NO_x) concentration was either measured manually according to the same manual or using a Lachat Flow Injection autoanalyser (FIA). When using the FIA, the QuikChem® Method 31-107-04-1-C (Egan, 2008) was followed. If there are no systematic sampling errors, the precision of the $\text{NO}_3^- + \text{NO}_2^-$ is $\pm 0.04 \mu\text{mol} \cdot \text{l}^{-1}$ (Grasshoff et al., 1983).

To measure the nitrate and nitrite concentrations manually, an azo-dye was developed in 5 mL of the samples and standards by adding sulfanilimide solution (0.1 mL), followed by N-(1-naphthyl)-ethylenediamine dihydrochloride solution (NEDI, 0.1 mL). The sulfanilimide solution was made by dissolving sulfanilimide (1 g) in a solution of 37% Hydrochloric acid, HCl (10 mL) and deionised water (60 mL) in a 100 mL volumetric flask. This solution was then made up to 100 mL with deionised water. The NEDI solution consisted of NEDI (0.1 g) dissolved in deionised water (100 mL). The absorbances were read using a Spectronic™ Helios™ Epsilon™ spectrophotometer set at a wavelength of 540 nm.

As nitrate concentrations cannot be measured directly, the nitrate in the samples and standards was reduced to nitrite (see below) before the development of azo-dye. The concentration of nitrite (from unreduced samples) was subtracted from this value to obtain the nitrate concentrations.

Preparation of standards

Separate nitrate and nitrite standards were prepared. Anhydrous analytical grade sodium nitrite was dried at 110°C for an hour before dissolving 0.345 g in 1000 mL deionised water. This solution, which had a nitrite concentration of $5\text{ mmol}\cdot\text{L}^{-1}$, was preserved with chloroform (1 mL) in a dark bottle. A $10\text{ }\mu\text{mol}\cdot\text{L}^{-1}$ nitrite solution, to be used as a working standard, was prepared by diluting 0.2 mL of the concentrated stock solution to 100 mL with deionised water. A range of nitrite standards (0, 2.5, 5, 7.5 and $10\text{ }\mu\text{mol}\cdot\text{L}^{-1}$) was prepared by adding the $10\text{ }\mu\text{mol}\cdot\text{L}^{-1}$ nitrite standard (0, 1.25, 2.50, 3.75 and 5 mL) to deionised water (5, 3.75, 2.50, 1.25 and 0 mL) in 5 test-tubes.

A $5\text{ mmol}\cdot\text{L}^{-1}$ nitrate standard was made from anhydrous sodium nitrate, NaNO_3 , (0.425 g) in the same way as the $5\text{ mmol}\cdot\text{L}^{-1}$ nitrite solution. Nitrate standards in the same range were made by diluting the $5\text{ mmol}\cdot\text{L}^{-1}$ nitrate standard (0.05, 0.1, 0.15 and 0.2 mL respectively) in deionised water (100 mL).

Reduction of nitrate to nitrite

Nitrate needs to be reduced to nitrite quantitatively before synthesising azo-dyes to determine the nitrate concentrations (section 2.2.1) and isotopic ratios (section 2.3.4). This was done using a copperised cadmium column as described by Grasshoff et al. (1983). The column was prepared by first washing a sufficient amount of cadmium with acetone, followed by deionised water. The granules were then rinsed with dilute HCl (1:5 37% HCl:water ratio) and deionised water before being treated with copper sulphate (12.8 g copper sulphate in 1 L deionised water). A glass tube was connected to the peristaltic tubing and filled with dilute ammonium chloride. It was packed with the copperised cadmium, which was stored in this medium when not in use. The column was activated by passing a sufficient volume of the “nitrate bomb” (cadmium column activator) through. To prepare the “nitrate bomb”, Potassium nitrate, KNO_3 (0.5055 g) was dissolved in deionised water (500 mL) to make a $10\text{ mmol}\cdot\text{L}^{-1}$ solution. 1 mL of this solution was made up to 100 mL with deionised water to give a $100\text{ }\mu\text{mol}\cdot\text{L}^{-1}$ solution.

The pH of each nitrate standard and sample was to a pH of 8.5 (using a solution of either Tris or buffered ammonium chloride, NH_4Cl , buffered to a pH of 8.5) before being passed through the copperised cadmium column to be reduced. A sufficient amount of sample or standard was passed through the column to clear it of any previous sample. Then, 5 mL of the sample or standard was collected in a test-tube and the same procedure as the one for nitrite determination was followed.

Efficiency of cadmium column

For a quantitative reduction, an efficient cadmium column is needed. A nitrate-nitrite standard, consisting of $5\text{ mmol}\cdot\text{L}^{-1}\text{NO}_2^-$ (0.5 mL) and $5\text{ mmol}\cdot\text{L}^{-1}\text{NO}_3^-$ (0.5 mL) in 500 mL deionised water, was used to test the efficiency of the column. This was done regularly by reducing the nitrite- nitrate standard through the column and collecting 5 mL of the resulting product. 5 mL of the unreduced sample was also collected in a test-tube. The azo-dye was synthesised in both test-tubes by adding sulfanilimide followed by NEDI as described above.

If the column is 100% efficient, the reduced sample should have an absorbance that is twice that of the non-reduced one. Efficiency was calculated as shown below:

$$\text{Efficiency} = 100 \times \left(\frac{\text{Absorbance reduced sample} - \text{Absorbance non-reduced sample}}{\text{Absorbance non-reduced sample}} \right). \quad (2.1)$$

2.2.2 Ambient concentrations of ammonium

For determination of ammonium concentrations, the method developed by Holmes et al. (1999) was used in conjunction with the improvements made by Taylor et al. (2007). Using this method, the precision of the ammonium concentration is expected to be $\pm 0.06 \mu\text{mol} \cdot \text{L}^{-1}$ (Holmes et al., 1999) if there are no systematic errors. The latter improved on the equation and method to measure and correct for background fluorescence as detailed below.

NH_4Cl (2.674g) was dissolved in deionised water (1L) to prepare a $50 \mu\text{mol} \cdot \text{L}^{-1} \text{NH}_4$ stock solution, which was in turn diluted to generate standards for the calibration curve. A working reagent, containing orthophthaldialdehyde (OPA, $2 \text{g} \cdot \text{L}^{-1}$), Sodium tetraborate ($40 \text{g} \cdot \text{L}^{-1}$), Sodium sulfite ($40 \text{mg} \cdot \text{L}^{-1}$) and ethanol ($50 \text{mL} \cdot \text{L}^{-1}$), was reacted with each sample and standard to measure the ambient concentrations of ammonium. This working reagent, which is stable for at least three months, was stored in an opaque container and allowed to stand for a day before use.

A Turner Designs 1-AU field fluorometer with a UV-module (optical kit n^o 10-303) was used to measure fluorescence for the determination of ambient ammonium concentrations.

Each sample (10 mL) was placed in a 60mL sample bottle. OPA (5mL) was added to each sample and standard before mixing. The samples and standards were then allowed to react in the dark for a minimum 2.5 hours and a maximum of 3.5 hours. After the reaction has gone to completion, the raw (uncorrected) fluorescence, $F_{\text{sampleobs}}$, was read using the UV module of the Turner Trilogy fluorometer.

Background fluorescence was measured for both deionised water and the sample as follows. Deionised water (10 mL) and the sample (10 mL) were placed in separate reagent bottles. OPA (5 mL) was added to each and the fluorescence was noted immediately (Taylor et al., 2007). This was recorded as t_0 fluorescence. Sample t_0 fluorescence ($F_{\text{sample}t_0}$) from the samples' fluorescence (F_{sampleNH_4}) while deionised water t_0 fluorescence is subtracted from the raw fluorescence of the standards as shown:

$$F_{\text{sampleNH}_4} = F_{\text{sampleobs}} - F_{\text{sample}t_0}. \quad (2.2)$$

The ammonium concentrations were not corrected for the matrix effect (Holmes et al., 1999; Taylor et al., 2007). The matrix effect was found to be quite variable even for samples coming from the same body of water. As it was difficult to assess whether the variability was due to differences in the samples themselves or due to errors, the matrix effect was not accounted for in this study. Furthermore, the matrix effect is likely to be smaller with smaller volumes of sample (Holmes et al., 1999).

2.2.3 Chlorophyll concentrations

Chlorophyll concentrations were either measured in-situ by calibrated Wetlab sensors attached to a rosette or manually. Wetlab sensors were cross-calibrated against manually measured chlorophyll-a concentrations from bottle samples. To determine chlorophyll concentrations manually, the seawater samples (250 mL) were filtered and the volume filtered noted. The filter paper was placed in 90% acetone (9 mL) and allowed to stand for 24 hours in the freezer. The fluorescence was then read on the Turner design trilogy fluorometer using the Chl-a N/A module. The Chl-a N/A module was calibrated using a range of chlorophyll standards.

2.2.4 Dissolved oxygen concentrations

Dissolved oxygen concentrations were also determined either in-situ by calibrated Wetlab sensor attached to a rosette or manually using the Winkler method as described by Grasshoff et al. (1983). When Wetlab oxygen sensors were used, they were cross-calibrated with manual bottle measurements.

2.3 Nitrogen cycling methods

2.3.1 Method overview

In this study, uptake rates were measured for nitrate and ammonium, and regeneration rates for nitrate and nitrite. Nitrate and ammonium uptake rates were determined through the enrichment of ^{15}N in the particulate matter according to methods by Collos (1987) while nitrate and nitrite regeneration were measured through the isotopic dilution of the ^{15}N tracer as per methods described by Clark et al. (2007). Ammonium regeneration was not measured for logistical reasons. Figure 2.1 represent a schematic of the method used for the measurement of nitrification rates which will be described in more details in following sections.

2.3.2 Incubations

Bulk samples were amended with $\text{Na}^{15}\text{NO}_3$, and $\text{Na}^{15}\text{NH}_4$ in order to measure nitrate and ammonium uptake. The sample used for measuring nitrate uptake was also used to measure nitrate regeneration (nitrite oxidation). A third sample was amended with $\text{Na}^{15}\text{NO}_2$ to measure the nitrite regeneration. Nitrite uptake was not measured as it is considered negligible in the study regions Olson (1981a). A 10% enrichment was considered optimal and the amount of tracer to be added was based on historical data. The concentrations of tracer in each experiment will be given in the relevant chapters. The tracer was allowed to mix for about 10 minutes after which the bulk samples were split into two.

The first subsample was filtered immediately and the filtrate collected for further processing. The second part of the bulk samples were placed in clear, Nalgene bottles. The samples were incubated either in-situ or on deck under simulated in-situ conditions. Incubation times ranged from 6 - 24 hours. Following the incubation, the samples were filtered. The filters were used for the determination of nitrogen uptake rates and the filtrates for the determination of nitrification rates. The samples which were not incubated are referred to as the “pre” sample (or time zero, T_0). This sample was used as the baseline from which any change was measured after incubation. The incubated samples are referred to as “post” samples (or time final, T_f).

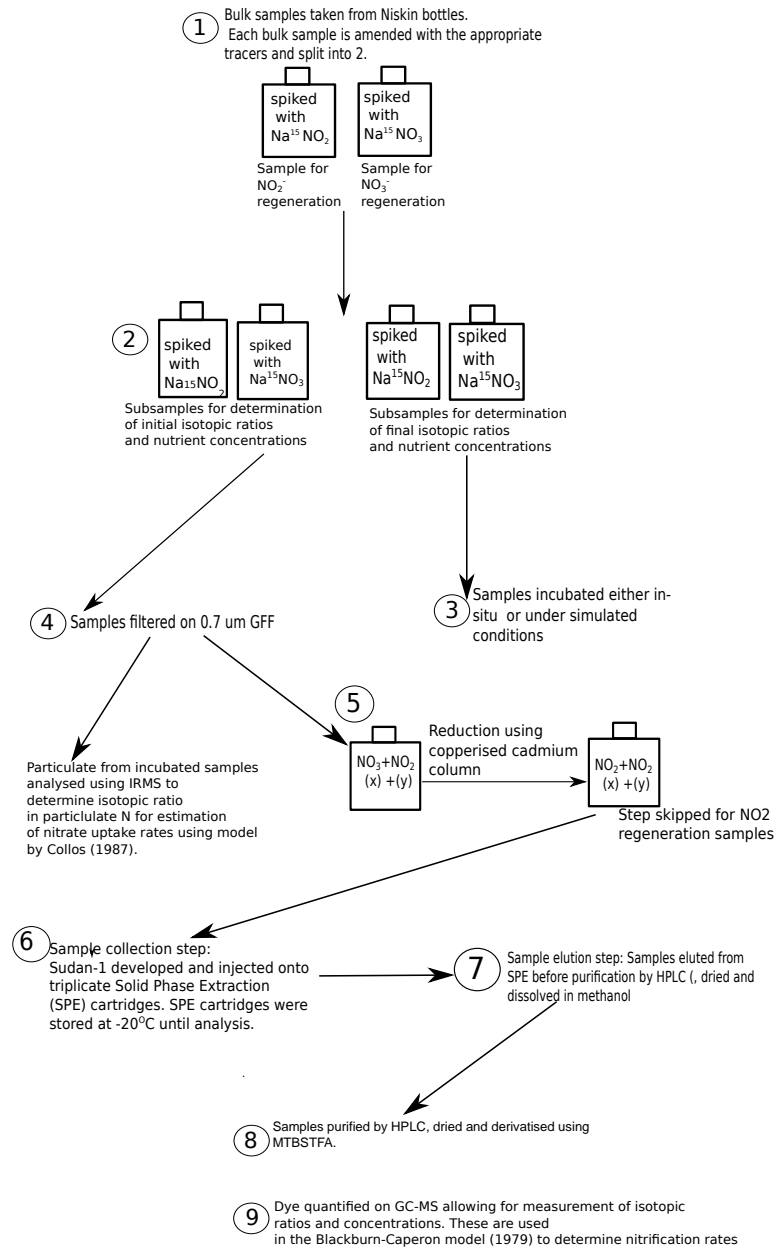


Figure 2.1: Schematic of the method used for the measuring nitrite and nitrate regeneration rates (adapted from Clark et al. (2007)) as well as nitrate uptake rates. An internal standard was used for the quantification of the dye. During earlier phases of the study, the internal standard was added during the sample elution step but during later phases of the study, it was added during the sample collection step as discussed in section 2.3.4.

2.3.3 Uptake experiments

The isotopic ratios were determined at the Archeometry facility at the University of Cape Town. The filters were dried in an oven at about 60°C for 24 hours. The dried filters were enclosed into tin capsules. The samples were then combusted in an elemental analyser and the gases transferred to an Isotope ratio mass spectrometer (IRMS) using a gas control unit. In-house standards, which had been calibrated against the International Atomic Energy Agency (IAEA) standards, were used to verify that there was no instrument drift. The results from this analysis provides the isotopic ratios as well as the amount of particulate carbon and nitrogen on the filters.

Specific uptake rates for NO_3^- and NH_4^+ were calculated as described by Collos (1987):

$$v = \frac{a_p - a_{nat}}{t \times (a_{enr} - a_{nat})}$$

where a_p is the final atom enrichment percent (AE%) in the particulate matter, a_{nat} is the natural abundance of ^{15}N and a_{enr} is the AE% of the water sample (initially labelled fraction) and t is the incubation time. Absolute uptake rates were obtained by multiplying the specific uptake rate by the concentration of nitrogen in the particulate matter. The a_{nat} is the natural abundance of ^{15}N was taken from machine standards. The carbon and nitrogen content of each sample was determined using a standard (Valine) of known carbon and nitrogen content by weight. Cross-laboratory comparisons have shown the accuracy of this measurement to be within 1% of the true value. The standard deviation of the atom enrichment percent on standards with natural concentrations of ^{15}N was 0.39%. This precision is expected to be lower for enriched samples but a good estimate is not available as enriched standards were not used. The lack of an exact estimate on this precision precludes from estimating the error on the uptakes rates through error propagation. However, it is expected that the relative standard deviation for these measurements would be $\pm 10\%$ as calculated by (Cavagna et al., 2011) given the similarities in the methods. The equation by Collos (1987) is used here because they account for the uptake of multiple sources of nitrogen (discussed in chapter 3).

At selected stations during the winter cruise in the Southern Ocean, a dual-spiking approach was used to measure carbon and nitrogen uptake at the same time (Slawyk et al., 1977). At these stations, the water samples were amended with $100\text{nmol} \cdot \text{L}^{-1}$ $^{13}\text{CO}_3$ (in the form the bicarbonate salt) in addition to the ^{15}N tracer. A recorded volume of seawater was filtered on a $0.7\mu\text{m}$ GFF to determine particulate organic carbon (POC) and particulate organic nitrogen (PON) concentrations. The GFF was exposed to fuming HCl to remove all inorganic carbon. The POC and PON content were determined using the elemental analyser coupled with IRMS. Dissolved inorganic carbon (DIC) was measured according to methods described in Dickson et al. (2007). For stations where DIC measurement was not available, an average DIC value of $2100\text{nmol} \cdot \text{L}^{-1}$, based on measured values during the winter cruise, was assumed. The carbon uptake rates were calculated in a similar manner to nitrogen uptake using the AE% of ^{13}C instead of ^{15}N . The specific ^{13}C uptake was multiplied by the POC concentration to determine the absolute uptake rate. The use of POC values from samples which have not been incubated is expected to introduce some biases in the estimates of carbon export (Legendre and Gosselin, 1997). However, given that the changes in POC are expected to be small over 24 hours in the Southern Ocean due to slow growth, this is expected to be minimal. At each station, the value reported is the average of carbon uptake rate from the bottle spiked with $^{15}\text{NH}_4$ and that spiked with $^{15}\text{NO}_3$.

2.3.4 Determination of ammonium and nitrite oxidation rates

Generation of Sudan-1

Synthesis of Sudan-1, an azo-dye, from the nitrite and nitrate (first reduced to nitrite) in sea-water samples allows for the determination of enrichment ratios and ambient concentrations. Sudan-1 was synthesised by adding the following reagents to the seawater samples. Concentrated (37%) HCl was diluted to make 3M HCl. Aniline sulphate (0.2 g) was dissolved in the latter solution (200mL). This reagent will henceforth be referred to as reagent 1. Reagent 2 was prepared by dissolving sodium hydroxide (NaOH, 24 g) and 2-naphtol (0.416 g) in deionised water (200mL). These two reagents, which are added to the sea-water to develop Sudan-1, were kept for only 24 hours. The Sudan-1 was acidified using 1 M Citric acid, made up from monohydrate citric acid (21.014 g) dissolved in deionised water (100mL).

Generation of Sudan-1 for Nitrite regeneration (ammonium oxidation)

To determine the isotopic ratio and concentrations of nitrite in the nitrite-spiked filtrates from the incubations (section 2.3.2), Sudan-1 was developed in the samples using a method adapted from Clark et al. (2007). Reagent 1 was added to each subsample. Small increments of reagent 2 were added to the mixture until its pH increased to about 8. The incubated sample was also filtered and the same procedure was followed. During the first part of the project (November 2011, March 2012 surveys in St Helena Bay as well as the winter cruise in the Southern Ocean), the dye was allowed to develop for 12 hours. The dye development time was changed to half an hour for later field work (March 2013 in St-Helena Bay and summer cruise to the sub-antarctic region) as this has been shown to provide a better dye recovery (Clark et al., 2014).

Generation of Sudan-1 for Nitrate regeneration (Nitrite oxidation)

The nitrate-spiked filtrates from the incubations were passed through a cadmium column containing copper-impregnated cadmium in order to reduce all the nitrate to nitrite. The column was cleared of any previous sample and a sufficient amount of "pre" and "post" samples for the generation of Sudan-1 was reduced. Sudan-1 was synthesised as above.

The samples for both nitrite and nitrate regeneration were acidified by adding a sufficient amount of 1 M citric acid to change the pH to about 5-6 before being extracted under vacuum on pre-conditioned solid phase extraction (SPE) cartridges

Solid phase extraction

SPE cartridges were used to extract Sudan-1 which had been developed in sea-water. The sea-water was passed through conditioned cartridges, which selectively retained the desired analytes. Before quantification, the latter were eluted from the cartridge by using an appropriate solvent.

SPE cartridges were conditioned by drawing methanol (5 mL) through until the level of solvent was just above the C18 phase. The methanol was then diluted with deionised water by successive 5 mL additions until it could be assumed that only deionised water was present. Finally, 1% NaCl solution (2×5 mL) was injected onto the column, which was not allowed to run dry once the conditioning process had started. The samples were then acidified to pH 5.0-6.0 using 1 M citric acid.

The dye was collected on triplicate SPE cartridges. The volume injected depended on ambient concentrations measured. In the Benguela upwelling system, volumes were kept at 5 – 10 mL for NO_2^- samples and 2.5 mL for NO_3^- samples. In the earlier experiments, the internal standard was added to samples after elution from the SPE cartridges (Section 2.3.5). However, at a later stage, the deuterated Sudan-1 standard was injected onto the SPE cartridges with the sample rather than after elution.

The SPE cartridges were stored frozen before the extraction, purification by HPLC and analysis by GC-MS as described in section 2.3.5.

During a pilot study in False Bay, the recovery of Sudan-1 from Empore C18 (Sigma catalogue n^o 66873-U) cartridges was very low. This indicated that a more appropriate SPE cartridge had to be selected. Furthermore, nominally similar cartridges sometimes yield different dye recovery. Any loss in recovery results in underestimates of nitrogen regeneration rates. It is therefore required to optimise the extraction of the analytes to ensure quantitative retention of the analytes.

The first optimisation step was the selection of the type and amount of sorbent. This was based to the properties of the analyte, the nature of the sample matrix and the analytical methods to be used (Colin F.,

2003; Hennion, 1999; Poole et al., 2000; Ferreira et al., 2004; Bielicka-Daszkiewicz and Voelkel, 2009). It is well established that for Sudan-1 in sea-water, a reversed-phase sorbent is the most appropriate (Clark et al., 2007; Preston et al., 1998).

The breakthrough volume, V_b , is the largest volume which can be injected onto the cartridge without any loss in recovery. It is an important factor when determining the suitability of a SPE cartridge (Colin F., 2003; Hennion, 1999; Poole et al., 2000; Ferreira et al., 2004; Bielicka-Daszkiewicz and Voelkel, 2009).

Measurement of breakthrough volume

SupelcleanTM LC-18 SPE Tube (57054, Sigma) and ENV+ spe columns (200MG/10ML, Biotage- IS915-0020-H) cartridges were compared using sea-water collected in False Bay. SupelcleanTM LC-18 SPE Tube will be referred to as Sigma SPE cartridge and the ENV+ spe columns (200MG/10ML, Biotage- IS915-0020-H) as the biotage (ENV+) cartridge.

The concentration of nitrite in a sea-water sample was measured as in section 2.2.1. Sudan-1 was developed in sea-water amended with $30 \mu\text{mol} \cdot \text{L}^{-1} \text{NO}_2^-$. This concentration was used as such NO_3^- concentrations are typical of Southern Ocean waters as well as recently upwelled waters in the Benguela upwelling system. The pH of the sample was adjusted to pH 5-6 using citric acid. Various volumes (1.5, 2.0, 2.5, 3, 5 mL) of the Sudan-1 solution were injected onto conditioned SPE cartridges. The resulting eluent was spotted onto thin layer chromatography (TLC) plates next to pure Sudan-1 and to a portion of the sea water which had not been passed through SPE. The TLC was developed in a 50:50 water-methanol mix. The cartridges were then rinsed with 5 mL of deionised water.

No breakthrough of Sudan-1 was detected by TLC and the “breakthrough” curves were not conclusive. The recovery of Sudan-1 by sigma cartridges was lower than by biotage cartridges. However, in terms of identifying the breakthrough volume itself, the curve shown in figure 2.2 is inconclusive. First, its shape does not correspond to a typical breakthrough curve. On a typical breakthrough curve, the amount recovered increases to a maximum before flattening out. In this case, a peak in the amount of Sudan-1 was present at 2.5 mL for both brands of cartridges. However, the amount recovered when a 5 mL sample was injected increased for the sigma cartridge but decreased for the Biotage cartridge. Unfortunately these samples were not replicated as they were part of a trial during the method development phase. Due to the lack of replication, it is not possible to identify the correct pattern and outliers. This trial provided, however, a strong basis for injecting internal standards with the seawater samples rather than adding at elution time. In doing so, the internal standard and sample would be retained in similar proportions and losses of Sudan-1 from the SPE cartridge. This is specially the case if other organics are interfering with the SPE extraction. In this case, the potential presence of other organic compounds, which would be retained preferentially, could explain the shape of the breakthrough curve. At lower volumes the SPE cartridges are able to retain both the unknown compounds and Sudan-1 quantitatively. At higher volumes the unknown compounds might be retained preferentially and Sudan-1 would no longer be retained quantitatively. This would result in decreasing amounts of Sudan-1 being recovered at higher volumes.

Another issue relating to these breakthrough experiments is the fact that the concentration of NO_2^- measured by GC-MS follows the same pattern as the mass recovered. In an ideal situation, the concentration of NO_2^- would stay constant until the column is saturated and the dye is no longer retained quantitatively. This could be tested more rigorously by comparing recoveries from standards made in deionised water and samples in sea-water.

To summarise, the breakthrough curves seen here do not correspond to the expected shape (linear until saturation). However, more rigorous measurements of the breakthrough volumes are required. Nevertheless, this provided with justification to inject the internal standard onto the SPE cartridge at the same time as the

seawater sample. This was done for the summer cruise in the Southern Ocean in February 2013 and the field campaign in St-Helena Bay in March 2013 but not for earlier field work.

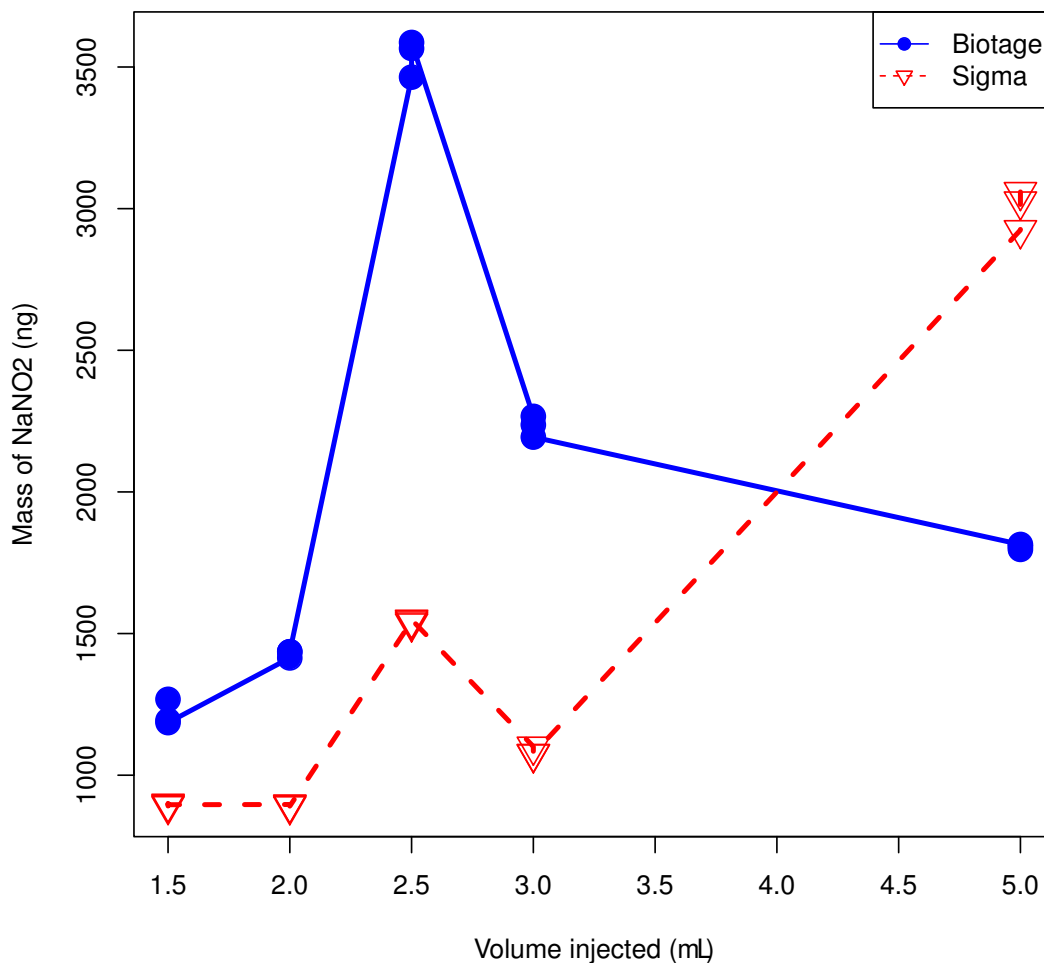


Figure 2.2: Breakthrough curve of Sudan-1 injected onto Sigma and Biotage SPE cartridges. This breakthrough curve shows variable recoveries of Sudan-1 and supported a change in the method. In the earlier part of the study, the internal standard was injected at the time of elution from the SPE whereas in the latter parts, it was injected onto the SPE with the sample to account for any losses during this step.

Field Recovery measurement

In order to identify appropriate SPE cartridges, the recovery of the dye is measured. The recovery efficiency from standards made in deionised water might be misleading as the numerous organic compounds present in seawater are absent from standards made in 1% sodium chloride (NaCl). In order to compare different types of cartridges more effectively, samples were injected onto different types of cartridges during field work in St-Helena Bay. 7 different samples which include samples for the measurement of ammonium oxidation, nitrite oxidation as well as efficiency standards were used (table 2.1). During field work in St-Helena Bay in November 2011, samples were injected onto the sigma cartridges and the biotage ENV+ cartridges (samples 1 - 5 on figure 2.3) while in March 2012, samples were injected onto the sigma and ISOLUTE® C18 (500MG/6ML, Biotage 220-0050-C) (samples 6 - 7 on figure 2.3). No major differences were observed in the recovery of Sudan-1 was observed (figure 2.3). The sigma cartridge was used for the first two field campaigns in St Helena Bay (November 2012 and March 2012). The ISOLUTE® C18 (500MG/6ML, Biotage 220-0050-C) was used on all subsequent fieldwork to be more consistent with the methods by Clark et al. (2007, 2014). It is to be noted that during these experiments, the recovery of the

analyte was low - between 7.5 and 29% for the Biotage cartridges and between 7 and 55% for the Sigma cartridges. Such low recoveries are troublesome as they can lead to an underestimate of the nitrification rates. However, as discussed in section earlier, the recovery of the analyte was improved at later stages of the study by adding the internal standard during the sample collection step rather than during the sample elution one.

Sample number	Sample type	Analyte	Concentration (nmol · L ⁻¹)
1	Sea water	NO ₂ ⁻	293
2	Sea water	NO ₃ ⁻	23900
3	Sea water	NO ₃ ⁻	10500
4	Sea water	NO ₃ ⁻	13500
5	Standard in 1% NaCl solution	NO ₃ ⁻	18300
6	Sea water	NO ₂ ⁻	725
7	Sea water	NO ₃ ⁻	19300

Table 2.1: Samples used for the comparison of biotage and sigma cartridges. The sample type indicates whether a sea-water sample or a standard was used. The analyte indicates whether the concentration of NO₂⁻ or NO₃⁻ was used. Finally, the concentration reported in the table are concentrations measured manually.

2.3.5 Dye purification and quantification

Ethyl acetate (2mL) was added to each of the SPE cartridges and drawn through under vacuum to elute samples. The latter were collected into test-tubes into which a deuterated Sudan-1 internal standard (Clark et al., 2007) had been added. The eluted sample was transferred to another test-tube before evaporating the ethyl acetate using a Zymark Turbo-vap (high capacity evaporating unit using oxygen-free nitrogen). The remaining solid was dissolved in methanol (0.2mL) and placed in 0.5 – mL Eppendorf Safe-Lock Micro-centrifuge Tube and centrifuged for five minutes. This separated some white particulate material and a clear solution, which was transferred to GC vials.

A 1100 series preparative HPLC system (Agilent Technologies), comprising of a C18 column (Gemini-NX 5u C18 110A, 250 x 4.6 mm), Security Guard Cartridges (Gemini-NX C18 4 x3.0 mm), two preparative pumps (G1361A), an autosampler (G1313A), a diode array detector (DAD, G1315B) and an automated fraction collector (G1364A), was used to purify samples extracted from the SPE cartridges.

The samples (150µL) were injected onto the HPLC column. The various components of the sample were separated using gradient elution. This means that the composition of the carrier was altered at different time steps as shown in table 2.2.

Only the fraction containing mostly Sudan-1 was collected. The collection window was identified by separating a series of the deuterated standard dissolved in methanol. During the separation, the DAD monitored

Time	Methanol (%)	Deionised water (%)	Flow rate (mL/min)
0	50	50	1
10	50	50	1
38	75	25	1
40	100	0	1
46	100	0	1
50	50	50	1
55	50	50	1

Table 2.2: Changes in composition of the mobile phase with time during the separation of Sudan-1 from interferences by HPLC. Table replicated from Clark et al. (2007)

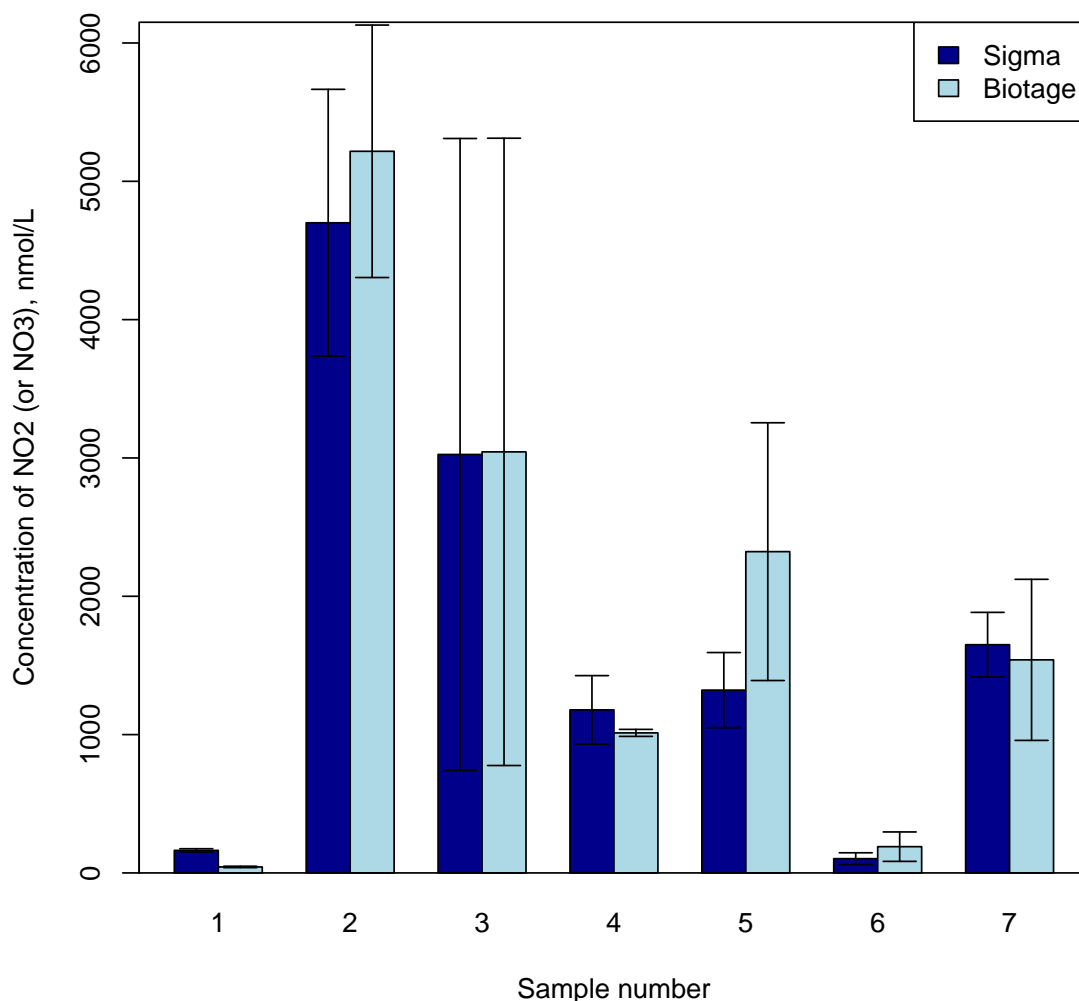


Figure 2.3: Concentration of NO_2^- or NO_3^- recovered from the biotage and sigma cartridges for 7 different samples described in table 2.1. These samples include samples which were taken for the measurement of ammonium oxidation, nitrite oxidation as well as efficiency standards.

the absorption of the 330 nm and 480 nm wavelengths as large absorptions at those wavelengths indicated the presence of Sudan-1 (Clark et al., 2007). The sample fractions eluted during this time were transferred to test-tubes. These fractions comprising of Sudan-1, which was dissolved in a methanol-water mix, were evaporated using the Turbo-vap. The residue was dissolved in methanol (100 μL), transferred to GC vials and blown to dryness and stored over silica for 24 hours. The samples were then ready for derivitisation.

The silylating reagent, a 10% of N- methyl-N-tert-butyldimethylsilyltrifluoroacetamide (MTBSTFA, Sigma-Aldrich, UK) solution (50 μL) was added to the residues in the GC-vials. The MTBSTFA was purchased in 1 mL ampoules. The vials were capped and placed in the oven at 50°C for 2 hours.

The GC-MS system consisted of a Hewlett-Packard 5890 series II GC coupled to an HP5972 MSD. An HP7973 injection controller was used to inject samples in splitless mode onto the column, which was an HP-5ms column (30 m \times 0.25 mm internal diameter).

The injection port and transfer line were kept at 300°C. Optimal separation was achieved by using temperature programming (Clark et al., 2007). The initial temperature of the GC-oven was 80°C. After 1.75 min, it was

increased to 210 °C at 35 °C/min, following which it was ramped to 310 °C at 20 °C/min. This temperature was held for 3 min. Molecular ions with m/z 305.2 and 306.2, 311.2 and 312.2 were used for selected ion monitoring (SIM). Molecular ions with m/z 305.2 and 306.2 represent the fraction of ^{14}N and ^{15}N in the sample while m/z 311.2 and 312.2 represent the same fractions in the deuterated internal standard. The sample Sudan-1 and the deuterated internal standard co-eluted at about 10 min. A peak is observed for each of the molecular ions and the peak areas were integrated for quantitative and isotopic analysis. Each sample was analysed three times.

2.3.6 Calculation of nitrification rates

The integrated peak areas represent the mass of Sudan-1 recovered. This is then used to calculate concentrations of $^{14}\text{NO}_2$ and $^{15}\text{NO}_2$ from the samples using

$$C_{\text{sample}} = \frac{A_{\text{peak}}}{A_{s_1}} \times m_{s_1} \times \left(\frac{N : S_1}{14.01 \times V_s} \right). \quad (2.3)$$

where using C_{sample} is the concentration of NaNO_2 in the sample, A_{peak} and A_{s_1} are the peak areas for the sample at m/z 305.2 and the internal standard at m/z 311.2 respectively, m_{s_1} is the mass of Sudan-1 deuterated standard added to the sample. $N : S_1$ ($14.01/248.48 = 0.0564$) is the mass ratio of the sample nitrogen to Sudan-1 in one mole of the compound in the deuterated standard, V_s the volume of seawater initially injected onto the SPE and 14.01 the atomic mass of nitrogen.

The $^{15}\text{N}/^{14}\text{N}$ ratios were equivalent to the ratio of the areas of the peaks at m/z 305.2 and 306.2 respectively. Before proceeding to further analyses, outliers were removed by determining whether they were significantly different from the other replicates for the sample.

A, the atom enrichment percent (AE%) is calculated from R, $^{15}\text{N}/^{14}\text{N}$ of the sample, and Rnat, the background $^{15}\text{N}/^{14}\text{N}$ ratio according to the equation by Preston et al. (1998):

$$A = 100 \times \frac{(R - R_{\text{nat}})}{1 + (R - R_{\text{nat}})} \quad (2.4)$$

The calculation of nitrification rates were based on the Blackburn-Caperon model as described by Clark et al. (2007). The model used for ammonium oxidation, Ox_a is shown in equation 2.5.

$$Ox_a = \frac{\ln(A_{t_a}/A_{o_a})}{\ln(S_{t_a}/S_{o_a})} \times \frac{S_{o_a} - S_{t_a}}{t_a} \quad (2.5)$$

A_{o_a} and S_{o_a} are, respectively the atom enrichment percent (AE%) and the concentration of NO_2^- in $\text{nmol} \cdot \text{L}^{-1} \cdot \text{h}^{-1}$ for the "pre" sample (section 2.3.2). A_{t_a} and S_{t_a} are the corresponding "post" values and t_a is the incubation period.

A similar equation using the relevant values for nitrate only was used for nitrite oxidation. The concentrations of nitrate only before and after incubation are used. The corresponding AE% were calculated using Ro_n and Rt_n , the pre and post incubation $^{15}\text{N}/^{14}\text{N}$ ratio for nitrate only. However, given that Sudan-1 was synthesised in the presence of ambient nitrite, the combined concentrations and enrichment ratios of $\text{NO}_2^- + \text{NO}_3^-$ were measured. These values were corrected using the equations from Sweeney et al. (1978) as cited by Clark et al. (2007) to obtain Ro_n , the enrichment related to nitrate only:

$$Ro_n = \frac{(\alpha \cdot R_a) - Ro_{an}}{(\alpha - 1)} \quad (2.6)$$

,

where R_a is the natural abundance ratio of $^{15}\text{N}/^{14}\text{N}$ for NO_2^- , Ro_{an} is the pre-incubation $^{15}\text{N}/^{14}\text{N}$ for $\text{NO}_2^- + \text{NO}_3^-$ concentration and α is the ratio of NO_2^- concentration (Sa) to $\text{NO}_2^- + \text{NO}_3^-$ concentration (So_{an}):

$$\alpha = \frac{Sa}{So_{an}}. \quad (2.7)$$

Rt_n was calculated in the same manner but Ro_{an} was replaced with Rt_{an} and So_{an} with St_{an} . As Sa was not measured in the post-incubation samples, it is assumed to be constant.

Each sample was injected onto three SPE cartridges and each SPE was analysed three times. The error in the nitrification rates was obtained by propagating the standard deviation in the results ($\text{NO}_2^-/\text{NO}_3^-$ concentrations and $^{15}\text{N}/^{14}\text{N}$) obtained from each analysis.

Chapter 3

A seasonal and geographical comparison of nitrogen uptake by phytoplankton in the Southern Ocean

3.1 Introduction: The biological pump in the Southern Ocean

In the Southern Ocean, low temperature, low light, strong vertical mixing and iron limitation restrict the uptake of nitrogen and ultimately phytoplankton growth. The concentrations of iron in the Southern Ocean are low due to the lack of terrestrial inputs. The role of these low iron concentrations in limiting phytoplankton growth and nitrate uptake is well-established (De Baar et al., 1990; Martin et al., 1990; Moore et al., 2007; Falkowski et al., 1998; Cochlan, 2008; Boyd et al., 2010; Boyd, 2002). Furthermore, phytoplankton in a strongly mixed environment, such as the Southern Ocean, are not exposed to light sufficiently long for efficient nutrient uptake and growth (Mitchell et al., 1991; Venables and Moore, 2010). This is compounded by the low incident light. The combination of these “bottom-up” controls and “top-down” controls such as grazing (Behrenfeld, 2010) results in the High Nutrients Low chlorophyll (HNLC) conditions for which the Southern Ocean is well-known. Despite this, the Southern Ocean plays an important role in the global marine carbon cycle. Carbon fluxes in this region accounts for about 4 % of global carbon fluxes (Takahashi et al., 2009). This is achieved through a combination of the solubility pump and the biological pump. The solubility pump encompasses the physical processes, such as mixing of surface water masses to the deeper layer, which remove carbon dioxide from the surface. The biological pump is driven by the sinking and subsequent sequestration of organic matter produced by phytoplankton through photosynthesis.

The Southern Ocean is subdivided by distinct frontal features which have been observed in the Antarctic Circumpolar current (ACC) (Orsi et al., 1995). These frontal features (from North to South, the Subtropical, the Subantarctic and the Polar Fronts) separate three surface water regimes and affect the distribution of phytoplankton as well as other “biogeographical” patterns (Pollard et al., 2002; Sambrotto and Mace, 2000). In addition, the deep water masses formed in the Southern Ocean play an important role in supplying nutrients to the low-latitudes (Sarmiento et al., 2004). This nutrient supply to the sub-tropics and tropics is effectively controlled by nutrient uptake in the Polar Frontal Zone (south of the Polar front) and Subantarctic Zone (north of the Polar front) where the Antarctic Intermediate Water and Subantarctic Mode water are formed. The efficiency of the biological pump for carbon export and nutrient transfer to thermocline waters is still debated. In order to resolve this debate, an understanding of seasonal variations on biogeochemical features and phytoplankton productivity is needed (Boyd, 2002; Sambrotto and Mace, 2000). Given the zonation resulting from

the frontal features of the ACC, the Southern Ocean is a complex region with diverse ecological provinces and the effects of seasonality vary from region to region (Le Moigne et al., 2013; Thomalla et al., 2011a). For this, numerous studies compare nitrogen uptake based on their location with respect to the fronts (Sambrotto and Mace, 2000; Thomalla et al., 2011b; Joubert et al., 2011; Westwood et al., 2011; Cavagna et al., 2011).

There is, however, a paucity of observational data in the Southern Ocean, especially for the winter season as most cruises in the Southern Ocean have been confined to spring and summer. As a result, the influences of seasonality on phytoplankton dynamics, nitrogen uptake and consequently the efficiency of the biological pump in the Southern Ocean are still not completely resolved over an annual cycle. Researchers are turning to remote sensing and modelling in order to overcome the logistical constraints of ship-based measurements (e.g. poor spatial and temporal resolution) (Henson et al., 2011; Vichi et al., 2007) but these two approaches have their limitations. Remote sensing data needs to be calibrated against observational data and in the Southern Ocean, satellite observations for the winter season can be limited by the sun angle as well as cloud cover (Vernet et al., 2012). There is little data to initialise and validate biogeochemical models which derive primary production from environmental and physical conditions such as light availability and nutrient concentrations (Vichi et al., 2007; Bissett et al., 1999).

In this chapter, primary production rates, which were estimated using ^{15}N and ^{13}C tracers, are presented. Nitrate (NO_3^-) and ammonium (NH_4^+) uptake rates were measured in the Southern Ocean during the austral winter of 2012 and in the late summer of 2013 using ^{15}N tracers. Carbon uptake was estimated using ^{13}C tracers for selected stations during the winter cruise. While summer (or early autumn) rates are common, this dataset is a rare instance of primary production rates for winter (Cota et al., 1992). Consequently estimates of new production and carbon export are presented with the aim of investigating seasonal patterns as well as the significance of primary production in winter. The nitrogen uptake rates from this study are compared to rates measured in winter and other seasons to highlight the fact that nitrogen uptake in winter, while low, is still significant.

Finally, the biogeochemical factors controlling nutrient uptake by phytoplankton are explored. Given that phytoplankton respond to the biogeochemical setting and that the latter is controlled by the frontal positions, the fronts should play a role in controlling nitrogen uptake by phytoplankton. In this study, the extent to which the nitrogen uptake regime is bounded by the fronts of the ACC is examined. Using multivariate analyses, the potential factors for the variability in nitrogen uptake rates are explored to determine which ones (nutrients, light, temperature, mixed layer depth) play a more important role in regulating primary productivity. The factors controlling nitrogen uptake during the summer and winter seasons are discussed. This provides for a better mechanistic understanding of factors controlling nitrogen uptake by phytoplankton and can contribute to the development of biogeochemical models.

3.2 Methods

3.2.1 Sampling and analytical methods

The present study consists of two cruises which are part of the Southern Ocean Seasonal Cycle Experiment (SOSCEX). The first cruise, referred to as the winter cruise, was undertaken aboard the RV SA Agulhas II from the 10 to 29 July 2012 and consisted of two legs. Leg 1 extended from Cape Town to the ice margin along the GoodHope Line. The Goodhope line is a monitoring line between South Africa and Antarctica, which was established in 2004 (Ansorge et al., 2005). Leg 2 stretched from the ice margin to Marion Island (Fig. 3.1). The summer cruise was conducted on board the RV SA Agulhas from the 15 February 2013 to 11 March 2013. Nitrogen and carbon uptake rates were estimated at 2 stations along the Goodhope line and 2 process stations (A and B) within the Subantarctic Zone. The sampling locations for the summer cruise are shown in black on

Fig. 3.1. The aim of the process stations was to sample the same parcel of water repeatedly and observe the effects of short-term changes. As such, each process station consisted of several Conductivity, Temperature, Depth (CTD) stations where nitrate uptake was measured. Process Station A was initialised by deploying a float on 25 February 2013 at 42°39' S 8°41' E. However, the float was deployed incorrectly and a new float had to be deployed two days later when this station was next occupied. This Lagrangian float measured conductivity, temperature, pressure and photosynthetically available radiation using built-in sensors. Process Station B did not have a float but was sampled continuously by a glider. The latter measured the same variables as the float as well fluorescence and two wavelengths ($\lambda=470$ and 700) of optical backscattering. Each dive cycle took approximately 5 hours to complete and covered an average horizontal distance of 2.8 km, rendering a temporal resolution of 2.5 hours and spatial resolution of 1.4 km between profiles. Table 3.1 shows the summer stations where nitrogen and carbon uptake rates were measured.

Temperature and salinity were measured by a rosette-mounted Sea-Bird Conductivity Temperature Depth (CTD) sensor. Chlorophyll *a* and oxygen measurements were obtained from calibrated Wetlab sensors attached to the same rosette. During the first leg of the winter cruise, the CTD was cast three times a day (06:00, 12:00 and 21:00 LT) along the GoodHope Line whereas on the track between the ice-shelf and Marion Island, it was cast at pre-determined locations. Temperature profiles were also obtained from Expendable Bathythermographs and Underway CTD deployments at 2 h intervals. Figure 3.1 only shows the stations where nitrogen uptake was measured whereas figure A.1 in appendix A shows all of the CTD stations in the winter cruise.

The study region was divided into 4 zones based on the temperature criteria of Orsi et al. (1995): the Subtropical (defined as the region north of the Subtropical Front), the Subantarctic (defined as north of the Subantarctic Front), the Polar Frontal (defined as north of Polar Front) and the Antarctic zones (defined as south of the Polar Front). The Subantarctic Zone was the target of the summer cruise while most of the winter stations were found in the Polar Frontal and the Antarctic zones. However, for the second leg, only CTDs were taken and the spatial resolution was not fine enough to establish the position of the fronts. The positions of the fronts are shown on the western side of the study area (figure 3.1).

Date	Station number	Process Station	Latitude (°S)	Longitude (°E)
23/2/2013	CTD 1		49.266	2.056
24/02/2013	CTD 2		46.965	4.506
25/02/2013	CTD 4	A	42.645	8.687
28/02/2013	CTD 7	B	43.506	7.186
01/03/2013	CTD 8	A	42.741	8.811
02/03/2013	CTD 9	B	43.423	7.178
03/03/2013	CTD 11	A	42.676	9.189
04/03/2013	CTD 13	B	43.518	7.131
05/03/2013	CTD 14	A	42.644	9.431
07/03/2013	CTD 15	A	42.615	9.597

Table 3.1: Primary productivity station details for the SOSCEX summer cruise in February-March 2013. Samples were taken at two process stations where the aim was to follow a single parcel of water over several days and at two stations outside of the Subantarctic Zone

Nutrient concentrations were determined on board: NO_3^- and $\text{Si}(\text{OH})_4$ using a Lachat Quick-Chem Flow injection autoanalyser; NO_2^- and PO_4^{3-} manually according to methods described by Grasshoff et al. (1983) and NH_4^+ using the fluorometric method described by Holmes et al. (1999) with improvements by Taylor et al. (2007). For the summer cruise, samples for NH_4^+ concentrations were frozen and analysed at a later stage. If there are no systematic sampling errors, the precision of the $\text{NO}_3^- + \text{NO}_2^-$ concentration is $\pm 0.04 \mu\text{mol} \cdot \text{L}^{-1}$ (Grasshoff et al., 1983) and the ammonium concentration $0.06 \mu\text{mol} \cdot \text{L}^{-1}$ (Holmes et al., 1999).

Water samples for the measurement of NO_3^- and NH_4^+ uptake rates were obtained at the early morning CTD stations. During the winter cruise, samples at the CTD stations were taken at the depth of the fluorescence

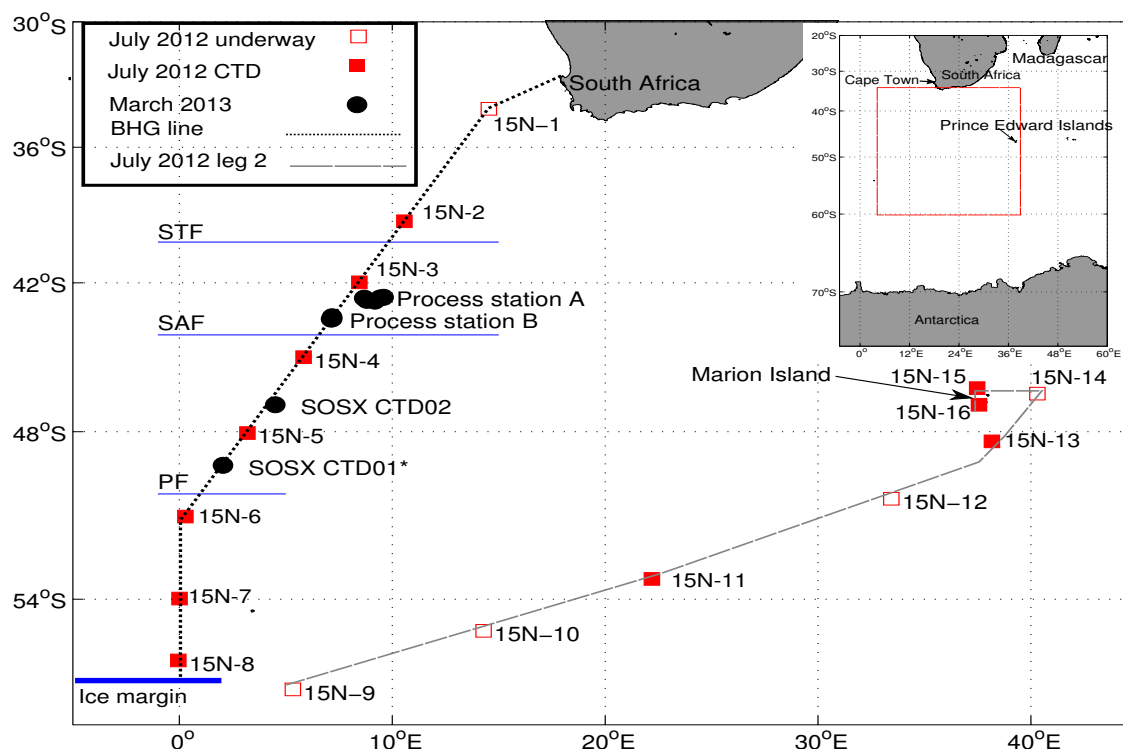


Figure 3.1: Cruise track for the two cruises. Leg 1 of winter cruise extended from Cape Town to the ice margin 58° S and Leg 2 from the ice margin to Marion Island. The winter frontal and ice margin positions are indicated by the blue lines. STF represents the Subtropical Front, SAF the Subantarctic Front and PF the Polar Front. The frontal positions were determined according to the criteria by Orsi et al. (1995) (see section The black dotted line (BHG line) shows the Bonus GoodHope line while the grey dashed line shows the cruise track on leg 2 of the winter cruise.

maximum and at the 1 % light depth. Alternatively, on days where the ship did not stop for an early morning CTD cast due to bad weather or sampling plans, samples were taken from the underway water system. Underway samples were collected from 5 m using a mono-pump. This type of pump is recommended for supplying major research vessels with uncontaminated seawater supply as it minimises the damage to phytoplankton cells. For the summer cruise, samples were collected from 4 depths representing 55, 30, 10 and 3 % of surface irradiance. Those light depths were determined during a cast on the afternoon prior to sample collection.

2 L water samples from each depth were amended with $\text{Na}^{15}\text{NO}_3$ ($1 \mu\text{mol} \cdot \text{L}^{-1}$) and $^{15}\text{NH}_4\text{Cl}$ ($0.1 \mu\text{mol} \cdot \text{L}^{-1}$ in winter and $0.05 \mu\text{mol} \cdot \text{L}^{-1}$). These values were based on expected ambient nutrient concentrations and kept constant throughout the cruise. The resulting enrichments were between 5 and 160 % for NH_4^+ and 3 and 52 % for NO_3^- . On the winter cruise, the samples were incubated for 24 h on deck under simulated in situ light depths of 1 % and 55 % sPAR. For underway stations, samples were only incubated at the 55 % light depth. On the summer cruise, the samples were incubated for 12 h under simulated in situ light depths corresponding to the sampling depth (55, 30, 10 and 3 % sPAR). During both cruises, the temperature was kept at sea-surface temperature by using a continuous flow of sea-water. The incubations were terminated by filtering onto $0.7 \mu\text{m}$ GF/F Whatmann filters (GFF). The particulate on the filter was analysed for nitrogen content and isotopic enrichment using an elemental analyser coupled to an isotope ratio mass spectrometer (IRMS). The carbon and nitrogen content of each sample was determined using a standard of a known carbon and nitrogen content by weight (Valine). Cross-laboratory comparisons have shown the accuracy of this measurement to be within 1% of the true value. The relative standard deviation of the atom enrichment percent on standards with natural concentrations of 15N was 0.39% This precision is expected to be lower for enriched samples

but a good estimate is not available as enriched standards were not used. The lack of an exact estimate on this precision precludes from estimating the error on the uptakes rates through error propagation. However, it is expected that the relative standard deviation for these measurements would be $\pm 10\%$ as calculated by (Cavagna et al., 2011) given the similarities in the methods.

Specific uptake rates for NO_3^- and NH_4^+ were calculated as described by equation (4') from Collos (1987):

$$v = \frac{a_p - a_{nat}}{t \times (a_{enr} - a_{nat})}$$

, where a_p is the final atom enrichment percent (AE%) in the particulate matter, a_{nat} is the natural abundance of ^{15}N (AE% in the particulate at the start of incubation) and a_{enr} is the calculated AE% of the water sample (initially labelled fraction) and t is the incubation time. Absolute uptake rates were obtained by multiplying the specific uptake rate by the concentration of nitrogen in the particulate matter. In addition, a recorded volume of sea water (obtained from the same CTD cast) was filtered on a $0.7 \mu\text{m}$ GFF to determine particulate organic carbon (POC) and particulate organic nitrogen (PON). The GFF was exposed to fuming HCl to remove all inorganic carbon. The POC and PON content were determined using the elemental analyser coupled with IRMS.

For each of the winter CTD stations, the daily ammonium and nitrate uptake rates were integrated over the mixed layer depth according to equation 3.2.1:

$$\frac{\rho_{N55} + \rho_{N1}}{2} \times \text{MLD}$$

where ρ_{N55} and ρ_{N1} are the nitrogen uptake rates at the 55% and 1% light depth only. The mixed layer depth (MLD) was identified from the temperature profiles as the first depth where the temperature differs from the 25 m temperature by more than 0.2°C (de Boyer Montégut et al., 2004). The 25 m depth was used as it is the shallowest depth common to all CTD casts. It is to be noted that this estimate of integrated uptake rates might contain a large error as nitrogen uptake were only measured for two light levels.

For the summer, the average nitrogen (ammonium and nitrate) uptake rates between consecutive light depths was calculated and multiplied by the difference in depth between the two light depths. For example, the depth integrated nitrogen uptake rate between the 55 and 30% light depth was calculated as follows

$$\rho_{N55-30} = \frac{\rho_{N-55} + \rho_{N-30}}{2} \times D_{30} - D_{55}$$

, where ρ_{N-55} and ρ_{N-30} are the nitrogen uptake rates at the 55% and 30% light depth while D_{55} and D_{30} are the corresponding depths for the 55% and 30% light depth. This was repeated with the other light depths measured during this cruise (10 and 3%). The sum of the integrated uptake rates for each depth section was converted to a daily rate to obtain the integrated nitrogen uptake rate over the euphotic zone.

The hourly nitrate uptake rates were multiplied by the light period at the sampling location whereas the ammonium uptake rate was multiplied by the light period plus half of the dark period to account for dark uptake (Cavagna et al. (2011) and references therein). The average light period during the summer cruise was 14 hours. The integrated nitrogen uptake ($\int \rho_N$ in $\text{mmol} \cdot \text{N} \cdot \text{m}^{-2} \cdot \text{d}^{-1}$) was converted to carbon units according to equation 3.1 below:

$$\text{PP} = \int \rho_N \times (\text{POC}/\text{PON}) \times 12. \quad (3.1)$$

where PP primary productivity in $\text{mg} \cdot \text{C} \cdot \text{m}^{-2} \cdot \text{d}^{-1}$, POC/PON is the C:N molar ratio in the particulate organic matter and 12 the molar mass of carbon. POC was determined by filtering a fixed volume of sample onto a GFF. The DIC collected onto the GFF was fumed off with HCl. The POC content were determined using an isotope ratio mass spectrometer (IRMS). Linear regressions of the measured POC and PON concentrations were done for each cruise (figure 3.2). The regression coefficient was used as an average POC/PON ratio. For the winter cruise, this value was found to be 6.7 (based on 143 measurements) and for the summer cruise 7.0 (based on 131 measurements). Total primary productivity was obtained by adding PP resulting from ammonium and nitrate uptake.

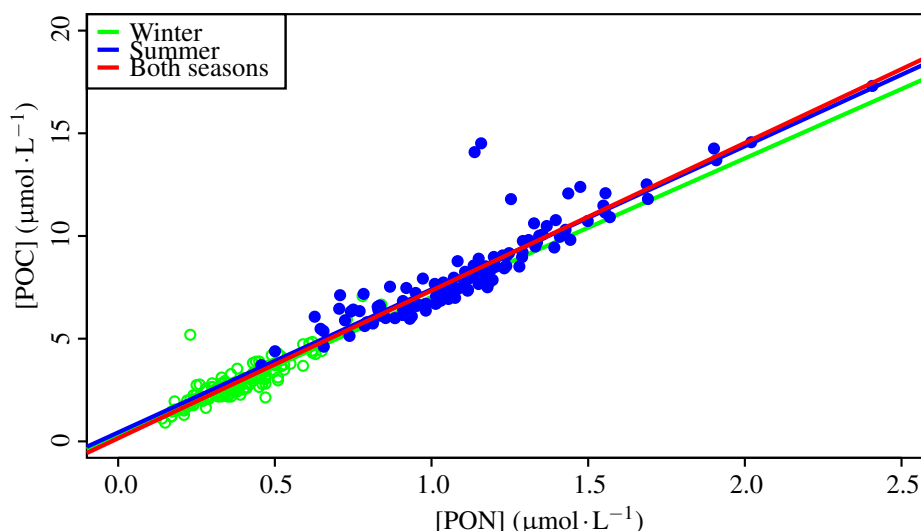


Figure 3.2: POC vs PON concentrations for the winter and summer cruises. The green open circles represent the winter data and the blue closed circles the summer data. The green line represents the linear fit of the winter POC vs PON (gradient = 6.7, $r^2 = 0.77$) and the blue line is for the linear fit of the summer POC vs PON (gradient = 7.0, $r^2 = 0.81$). The red line is for a linear fit using the data from both seasons (gradient = 7.2, $r^2 = 0.94$).

For 8 CTD and 4 underway stations during the winter cruise, a dual-spiking approach was used to measure carbon and nitrogen uptake at the same time. At these stations, the water samples were amended with $100 \text{ nmol} \cdot \text{L}^{-1}$ $^{13}\text{CO}_3$ (in the form the bicarbonate salt) in addition to the ^{15}N tracer. Dissolved inorganic carbon (DIC) was measured according to methods described in Dickson et al. (2007). For stations where DIC measurement was not available (stations 15N-4, 15N-7, 15N-8 and 15N-14), an average DIC value of $2100 \text{ nmol} \cdot \text{L}^{-1}$, based on measured values during the winter cruise, was assumed. The carbon uptake rates were calculated in a similar manner to nitrogen uptake using the AE% of ^{13}C and the POC concentration instead of AE% of ^{15}N and the PON concentration. At each station, the value reported is the average of carbon uptake rate from the bottle spiked with $^{15}\text{NH}_4^+$ and that spiked with $^{15}\text{NO}_3^-$.

3.2.2 Statistical analysis

A multivariate statistics approach was employed on this dataset in order to investigate the biogeochemical controls over nitrogen uptake and test the hypothesis that the nitrogen uptake regime was controlled by the fronts in Southern Ocean.

The statistical approach and the interpretation of the results are based largely on material from Borcard et al. (2011). The analysis was done in R using the vegan package. The hypothesis tested here was whether clusters

which were derived from the nitrogen uptake rates would be separated by the Subtropical (STF), Subantarctic (SAF) and Polar (PF) fronts. First, a cluster analysis was performed using the physical and biogeochemical variables for each station (temperature, chlorophyll, nutrients) to confirm whether these variables were constrained by the fronts. This cluster analysis was compared with a cluster analysis of the nitrogen uptake rates (response variables). Finally, a redundancy analysis (RDA) was performed. A RDA combines a principal components analysis, which identifies the major sources of variations in a dataset, to multiple regressions. The RDA was done twice for the winter dataset: the first using the CTD stations only and the second using all the stations. Using the CTD stations, where nitrogen uptake was estimated at 2 light depths and for which the mixed layer depths were known, allows for a quantification of the role of the MLD in regulating nitrogen uptake. When including the underway stations, only the 55% light depth was used and the MLD was not included as a parameter as it was not available for these stations. For the summer cruise, an RDA on the two process stations was not possible due to the limited number of complete observations. Instead, the correlations between the uptake rates and environmental variables were investigated. These results were also limited by the number of observations and are presented here as a qualitative investigation into the factors controlling nitrogen uptake rates.

3.3 Results

3.3.1 Hydrographic data and nutrients

Winter cruise

The first leg of the winter cruise followed the GoodHope line and crossed the Subtropical Front, Subantarctic Front and Polar front. While the temperatures and salinity decreased with latitude, the transitions at the fronts were not sharp. Mixed layer depths (white dashed line on figures 3.3 and 3.4) ranged between 43m (CTD 22, latitude -57.7643) and 255m (CTD 6, latitude -43.0938). Chlorophyll concentrations generally decreased southwards with a maximum chlorophyll in the Subtropical Zone ($0.33 \mu\text{g} \cdot \text{L}^{-1}$ at 20m). However, in the Polar Frontal Zone, this trend was not observed. The maximum chlorophyll ($0.27 \mu\text{g} \cdot \text{L}^{-1}$ at 30m) for this region was measured at CTD 9 (latitude -46.1082 °N). The dissolved oxygen concentration increased southwards (from $5.16 \text{mL} \cdot \text{L}^{-1}$ at CTD 1 in the Subtropical Zone to $7.83 \text{mL} \cdot \text{L}^{-1}$ at CTD 22 in the Antarctic Zone) while temperature and chlorophyll decreased.

During leg 2, sampling was carried out from the ice edge to Marion Island in a straight line and then around the island in an anti-clockwise direction. Figure 3.5 shows the temperature and salinity profiles and figure 3.6 the chlorophyll and dissolved oxygen profiles for leg 2. The profiles are shown by station number rather than by latitude there are overlaps in the latitudes due to the circular nature of this leg. There is a sharp temperature transition between CTD stations 25 and 26 showing the shift between the Antarctic Zone and Polar Frontal Zone. This sharp transition, however, was not observed in the other parameters. The shallower stations close to the island (CTDs 30 and 31) had warmer waters than the deeper, further stations (CTDs 32 and 29) while the salinity was more or less uniform (figure 3.5). The maximum chlorophyll ($0.25 \mu\text{g} \cdot \text{L}^{-1}$) was observed at CTD 30, which was the closest to Marion Island. This also corresponded to a decrease in dissolved oxygen (figure 3.6).

On leg 1, the concentration of nitrate, $[\text{NO}_3^-]$, and phosphate, $[\text{PO}_4^{3-}]$ in the mixed layer increased southwards despite some slight deviations from this trend (CTD 11 and 12 on figure 3.7). The concentration of silicic acid, $[\text{Si}(\text{OH})_4]$ remained constantly low until the Polar front (figure 3.7). After this point, $[\text{Si}(\text{OH})_4]$ increased rapidly towards the ice-edge. The nutrients patterns were similar on leg 2 with low $[\text{Si}(\text{OH})_4]$ throughout the Polar Frontal Zone and higher $[\text{NO}_3^-]$ at the stations further south (data not shown). As

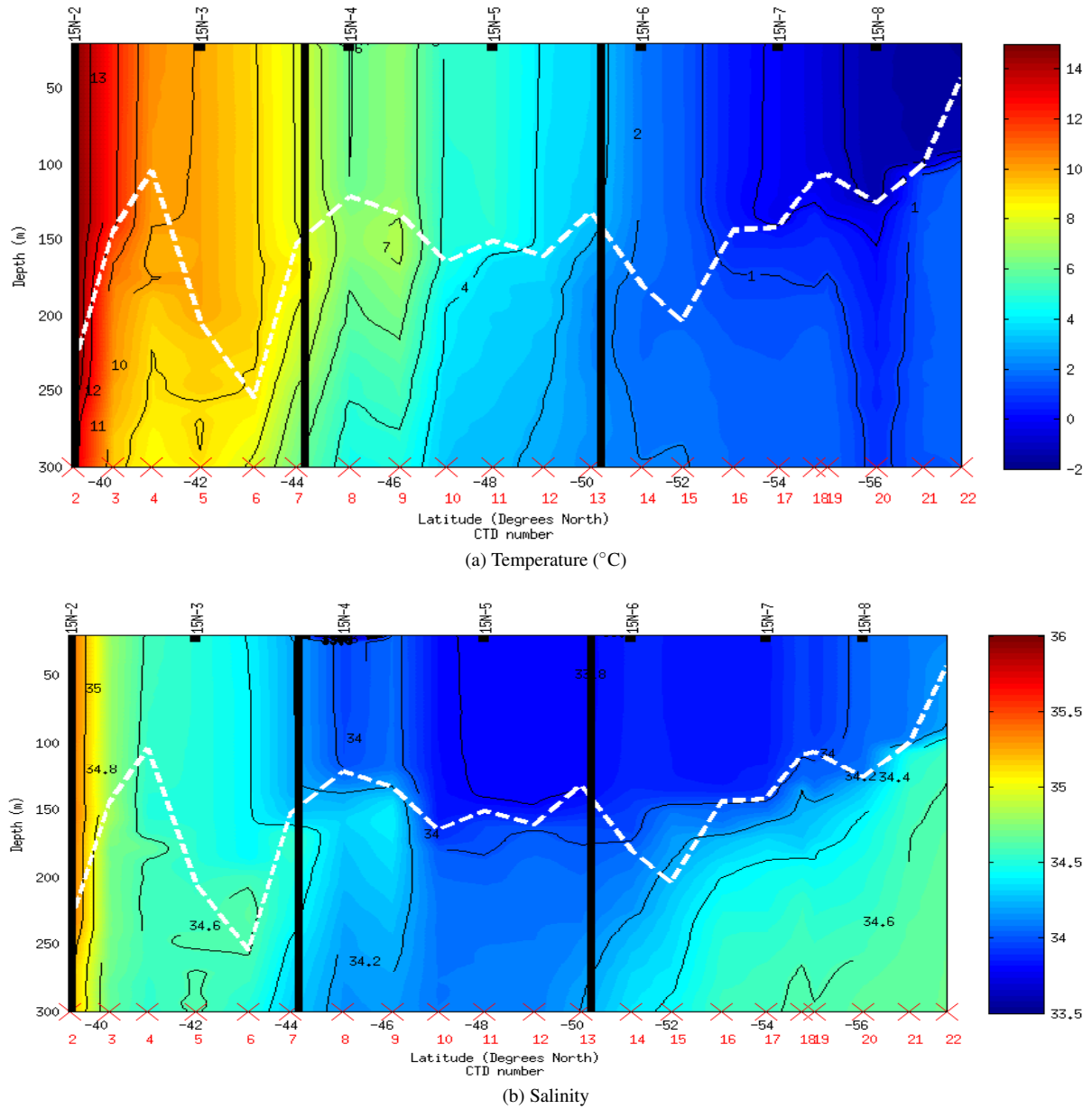


Figure 3.3: (a) Temperature ($^{\circ}\text{C}$) and (b) Salinity (psu) sections for leg 1 of the winter cruise: (a) Temperature ($^{\circ}\text{C}$) (b) (c) Chlorophyll ($\mu\text{g} \cdot \text{L}^{-1}$) (d) Oxygen ($\text{mL} \cdot \text{L}^{-1}$). The red crosses and numbers represent all the CTD stations during this leg. The stations where nitrogen uptake was measured are indicated by the black rectangles and "15N-" number at the top of each plot. The solid black lines from left to right show the positions of STF, SAF and the PF and the white dashed line shows the mixed layer depths.

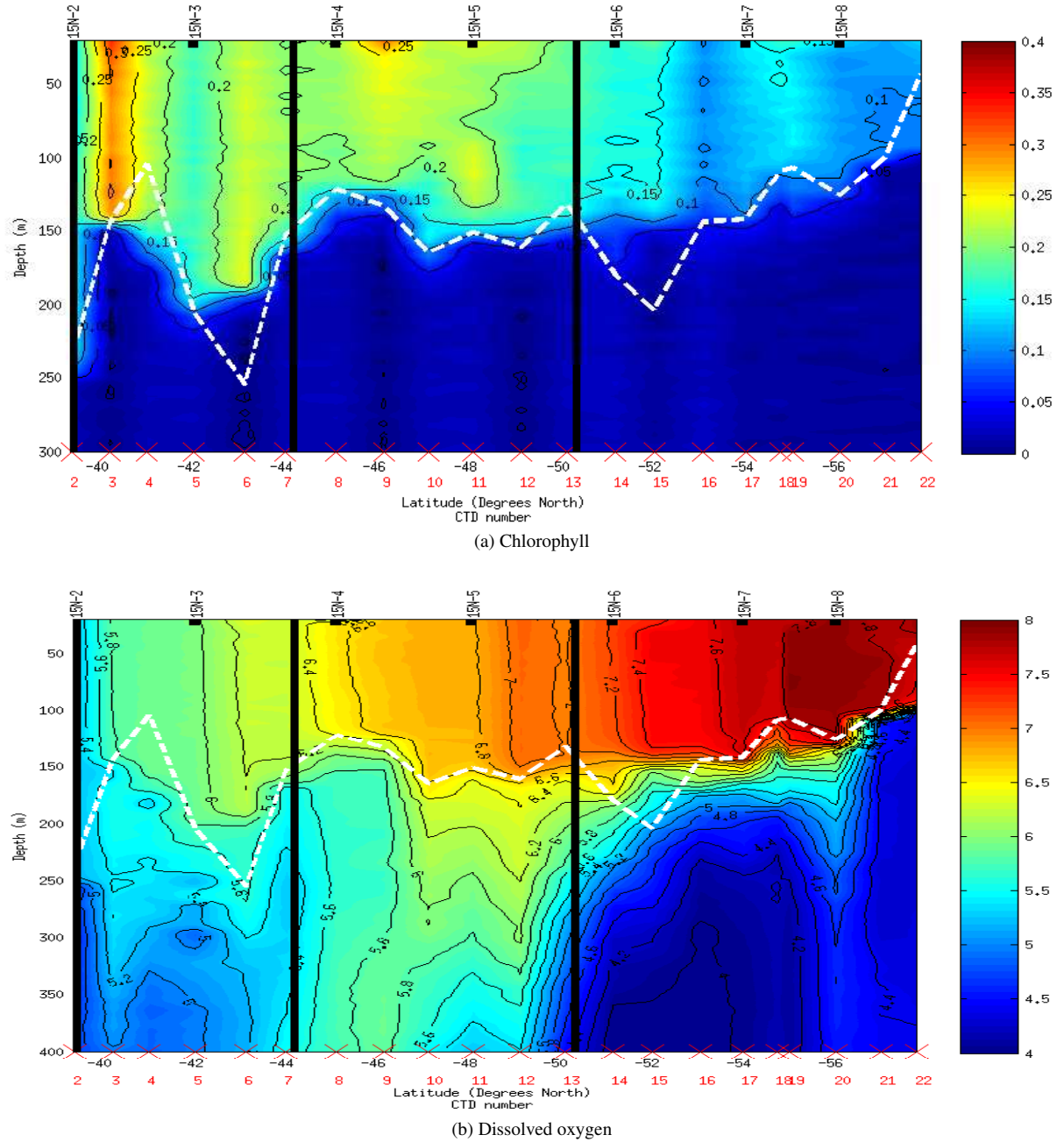


Figure 3.4: (a) Chlorophyll ($\mu\text{g} \cdot \text{L}^{-1}$) and (b) dissolved Oxygen ($\text{mL} \cdot \text{L}^{-1}$) concentrations for leg 1 of the winter cruise. The red crosses and numbers represent all the CTD stations during this leg. The stations where nitrogen uptake was measured are indicated by the black rectangles and "15N-" number at the top of each plot. The solid black lines from left to right show the positions of STF, SAF and the PF and the white dashed line shows the mixed layer depths.

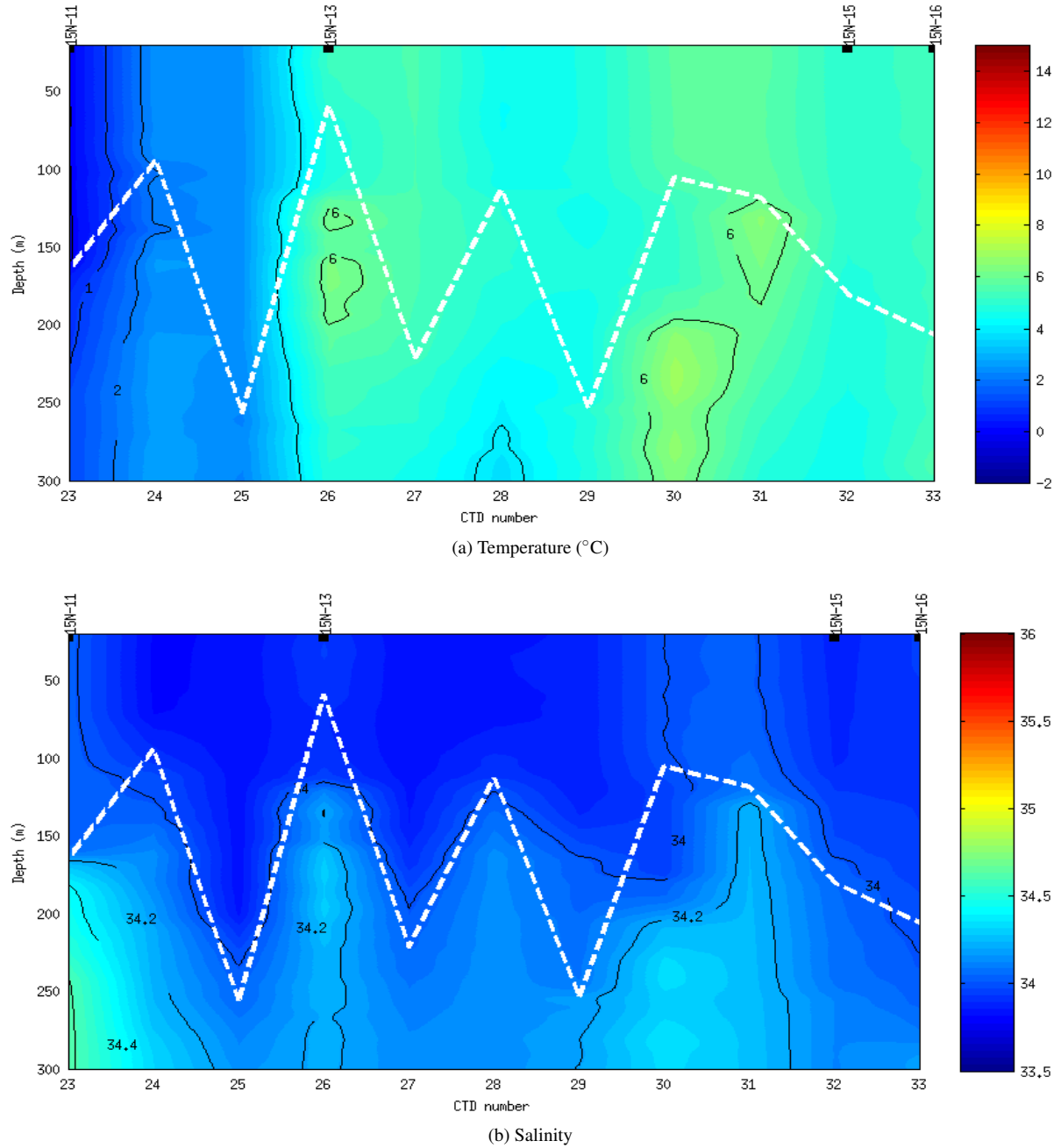


Figure 3.5: (a) Temperature (°C) and (b) Salinity (psu) data for leg 2 of the winter cruise: The profiles are shown by station number rather than by latitude there are overlaps in the latitudes due to the circular nature of this leg. The distance between the stations is not shown at scale. The white dashed line represents the mixed layer depths. The stations where nitrogen uptake was measured are indicated by the black lines and "15N-" number at the top of each plot.

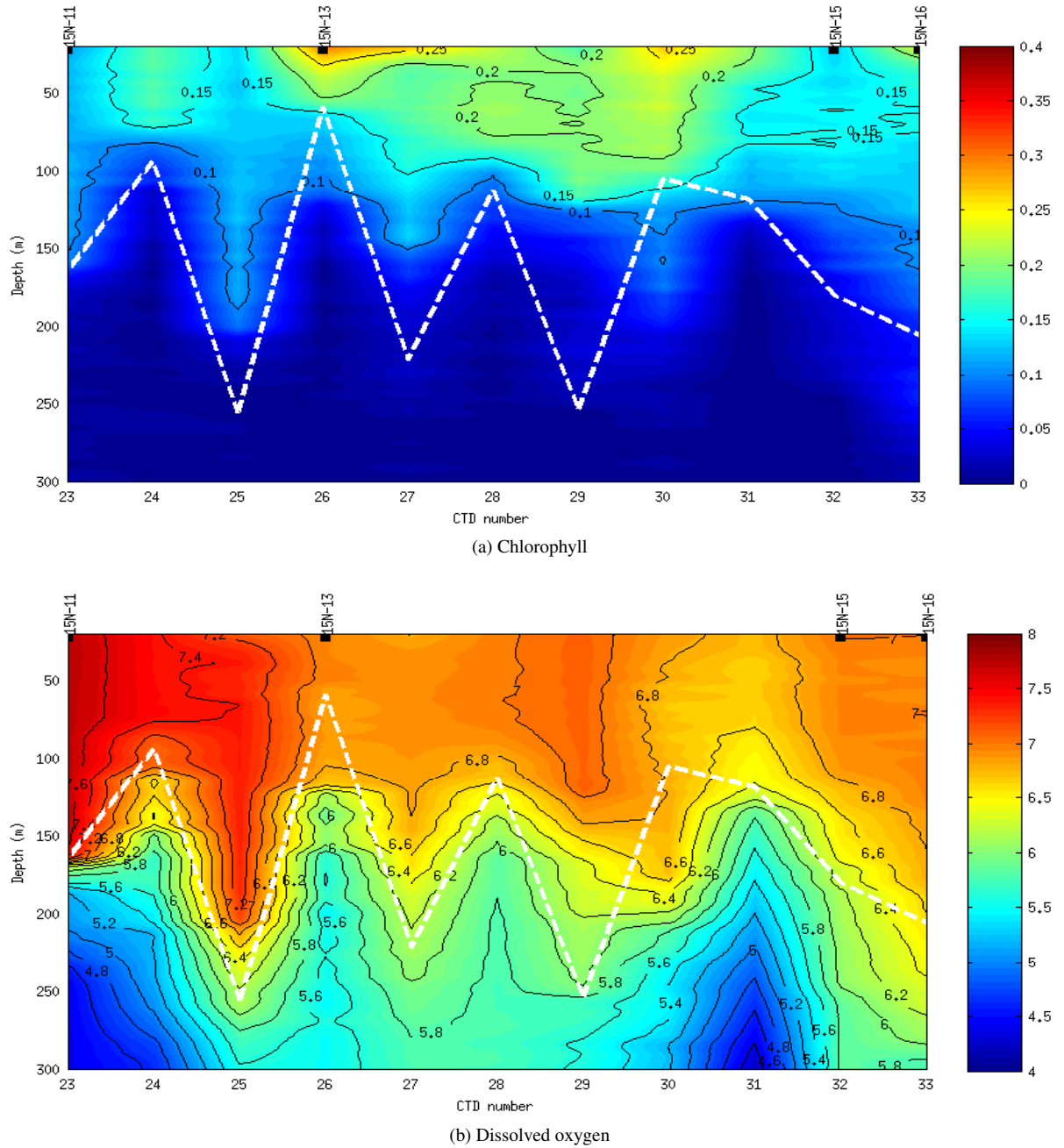


Figure 3.6: (a) Chlorophyll ($\mu\text{g} \cdot \text{L}^{-1}$) and (b) dissolved Oxygen ($\text{mL} \cdot \text{L}^{-1}$). concentrations for leg 2 of the winter cruise. The profiles are shown by station number rather than by latitude there are overlaps in the latitudes due to the circular nature of this leg. The distance between the stations is not shown on scale. The white dashed line represents the mixed layer depths. The stations where nitrogen uptake was measured are indicated by the black lines and "15N-" number at the top of each plot.

chlorophyll increased closer to Marion Island (CTD 30,31), $[\text{NO}_3^-]$ within the mixed layer was lower than at stations further away (CTD 32 and 33).

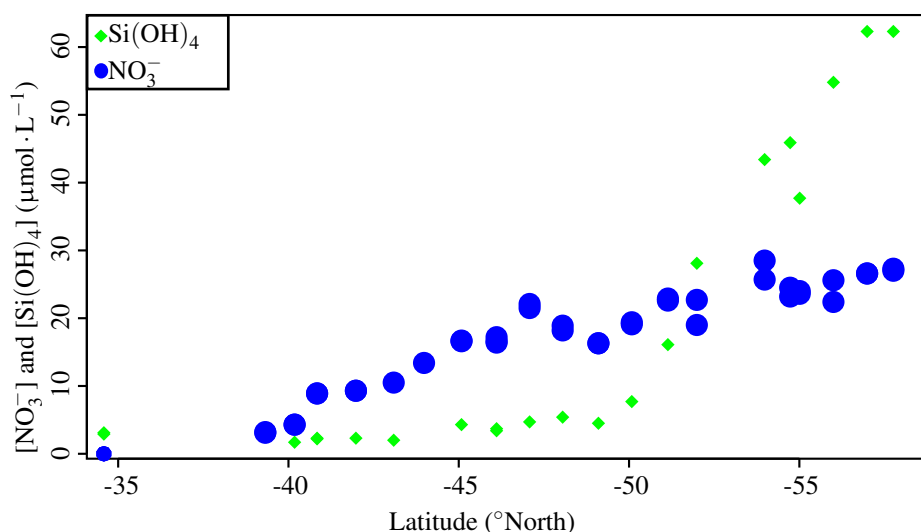


Figure 3.7: Surface $[\text{NO}_3^-]$ and $[\text{Si}(\text{OH})_4]$ for leg 1 of the winter cruise. Surface is defined as depths less than 40 m in this case.

Summer cruise

For the summer cruise, samples were taken at two process stations within the Subantarctic Zone as well as two stations within the Polar Frontal Zone. Temperature, salinity, chlorophyll and oxygen profiles were plotted for each of the process stations and show the evolution of the hydrographic variables throughout the process study. Temperatures through the euphotic zone at Process Station A (figures 3.8 and 3.9) were between 10 and 12°C. A mixing event occurred between the 3 March and 7 March. The mixed layer depth increased from its shallowest at 37 m to a maximum of 76 m. This brought colder, deeper water to the surface and reduced the average temperature. This was accompanied by a decrease in salinity. A decrease in chlorophyll was observed. Process Station B (figures 3.10 and 3.11) showed cooler temperatures (between 9 and 10°C) than station A. The mixed layer depths were deeper than at Process Station A ranging from 65 to 85 m. The mixed layer deepened between the 28th February and 4 March. Though this did not result in large differences in temperature, salinity and oxygen, there was a clear decrease in chlorophyll concentration between these two sampling dates. Nutrient profiles are shown in figure 3.12.

Within the Subantarctic Zone, the temperature differences between the summer and winter cruise within the mixed layer were minimal. However, as expected, the water column was more stratified in summer as expected given the weather conditions and shallower mixed layers. The difference in stratification was also seen from the salinity profiles. In summer, the water below the mixed layer was more saline than in winter. Summer chlorophyll concentrations were about twice their winter values while differences in oxygen concentrations were small. In winter, the depth of the euphotic zone was always shallower than that of the mixed layer. For this reason, the biomass was seen only within the mixed layer. This contrasts with the summer cruise where chlorophyll was occasionally observed below the mixed layer depth indicating that the euphotic depth was deeper than the mixed layer.

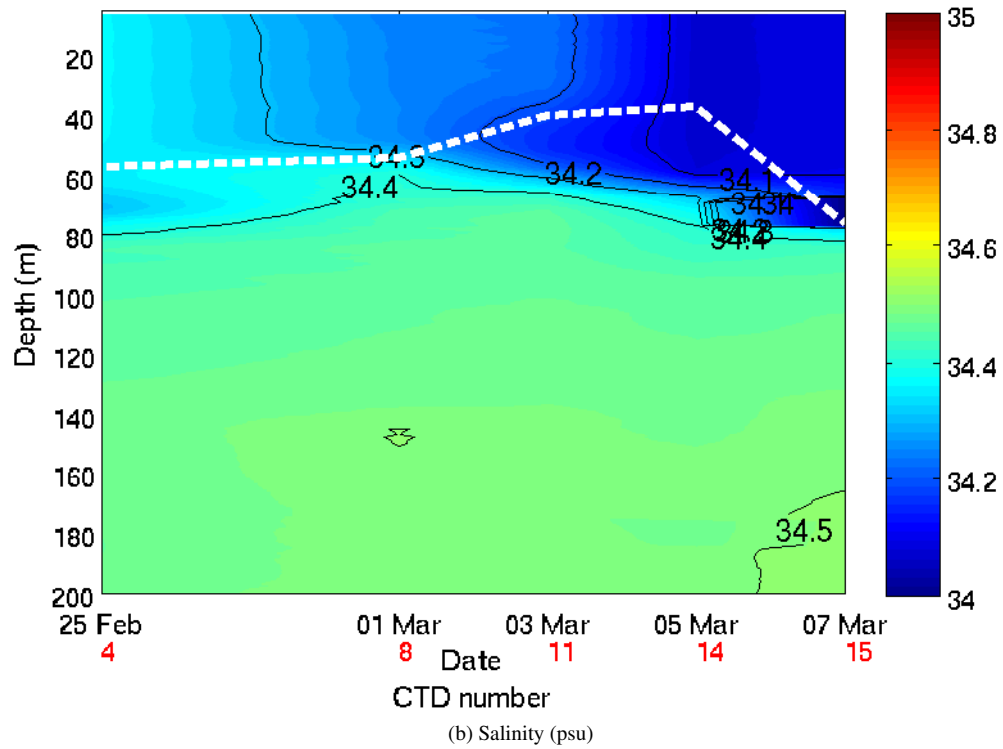
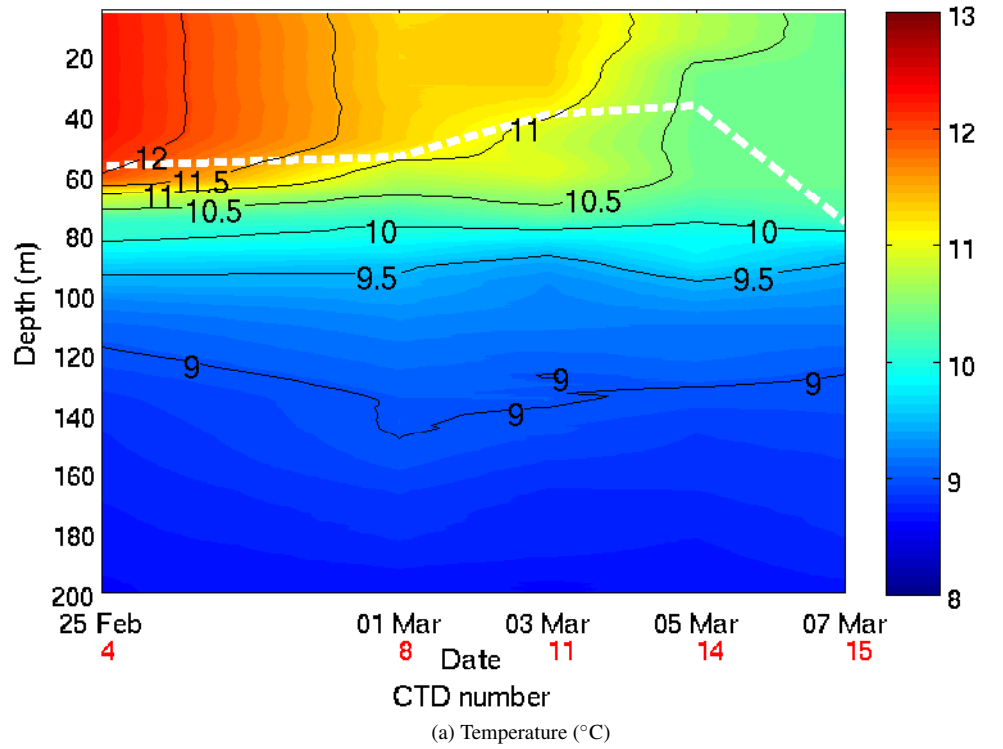


Figure 3.8: (a) Temperature (°C) and Salinity (psu) sections for Process Station A during the summer cruise. The MLD, which was identified from the temperature profiles as the first depth where the temperature differs from the 25 m temperature by more than 0.2°C (de Boyer Montégut et al., 2004)

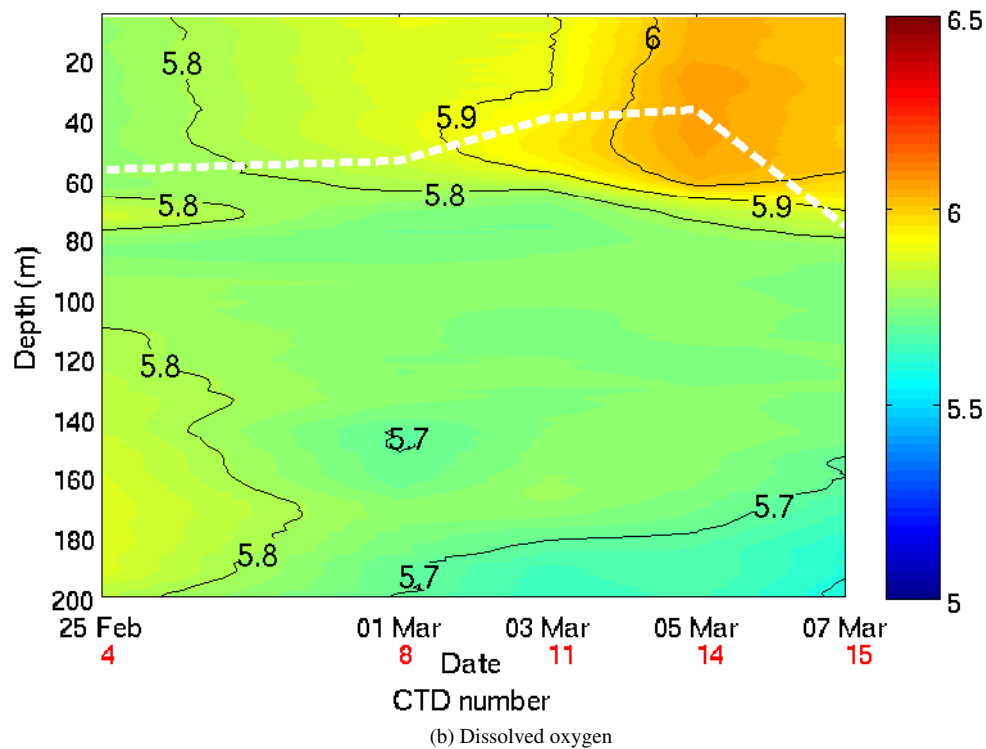
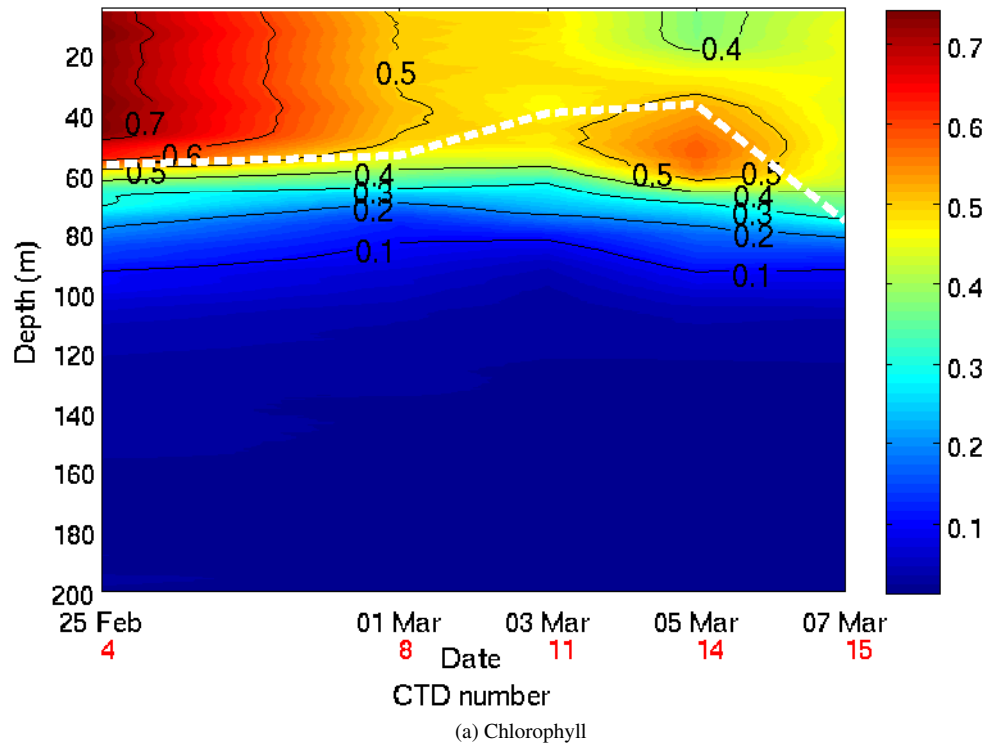


Figure 3.9: (a) Chlorophyll ($\mu\text{g}\cdot\text{L}^{-1}$) and (b) dissolved Oxygen ($\text{mL}\cdot\text{L}^{-1}$) for Process Station A during the summer cruise. The CTD number is shown in red for each date. The white dashed lines represent the MLD, which was identified from the temperature profiles as the first depth where the temperature differs from the 25 m temperature by more than 0.2°C (de Boyer Montégut et al., 2004)

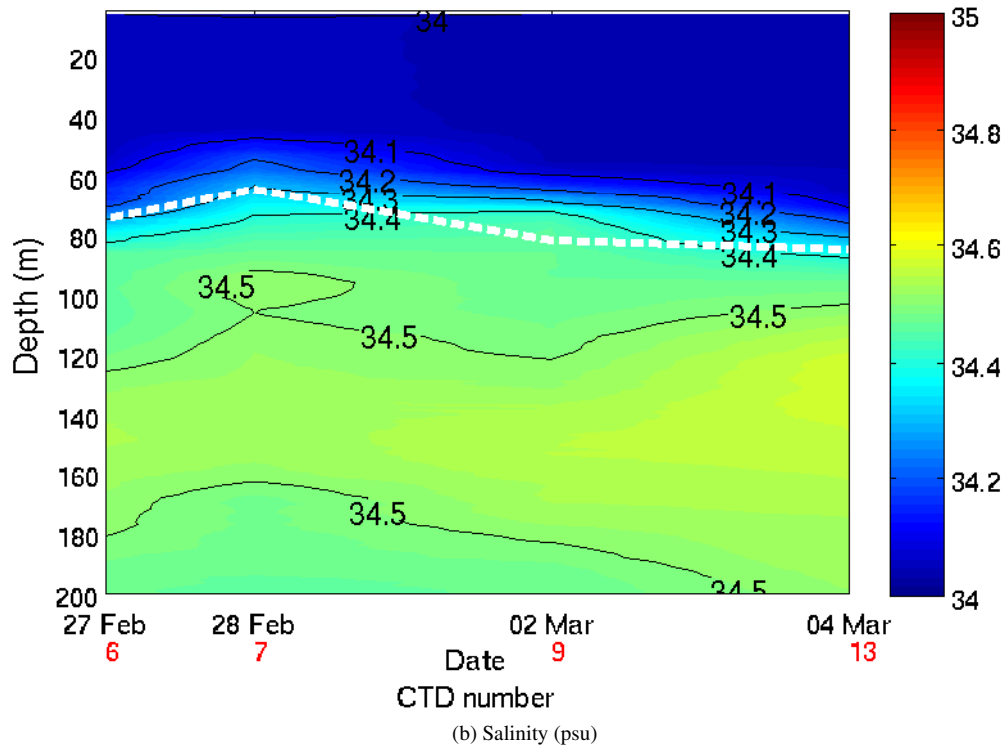
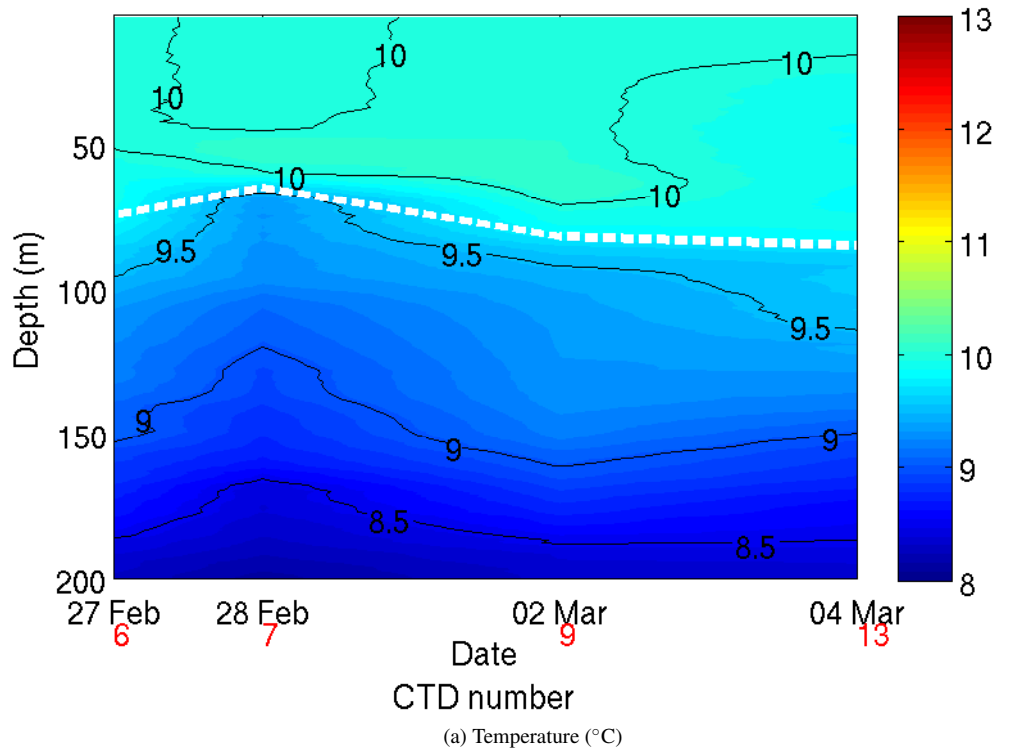


Figure 3.10: (a) Temperature (°C) and Salinity (psu) sections for Process Station B during the summer cruise. The MLD, which was identified from the temperature profiles as the first depth where the temperature differs from the 25 m temperature by more than 0.2 °C (de Boyer Montégut et al., 2004)

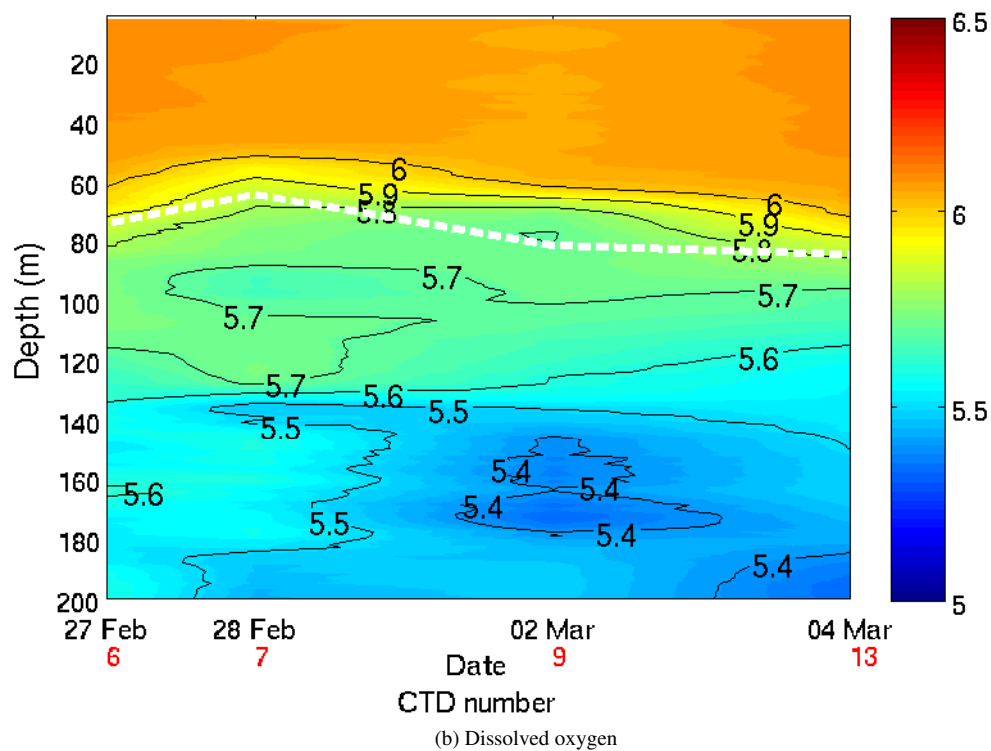
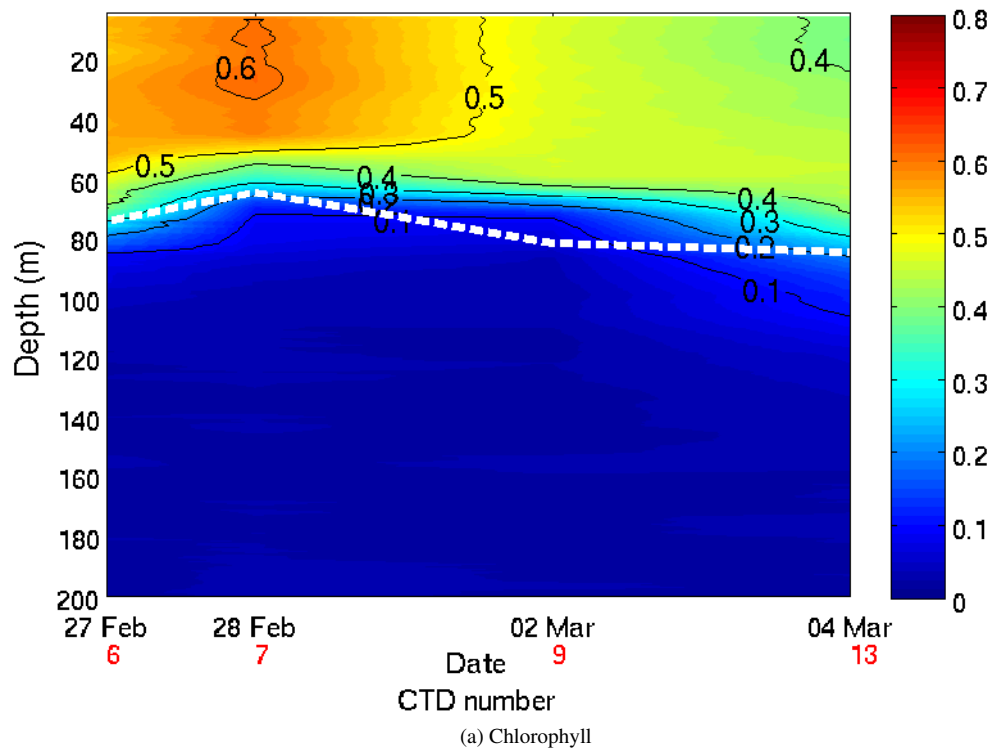


Figure 3.11: (a) Chlorophyll ($\mu\text{g} \cdot \text{L}^{-1}$) and (b) dissolved Oxygen ($\text{mL} \cdot \text{L}^{-1}$) for Process Station B during the summer cruise. The CTD number is shown in red for each date. The white dashed lines represent the MLD, which was identified from the temperature profiles as the first depth where the temperature differs from the 25 m temperature by more than 0.2°C (de Boyer Montégut et al., 2004)

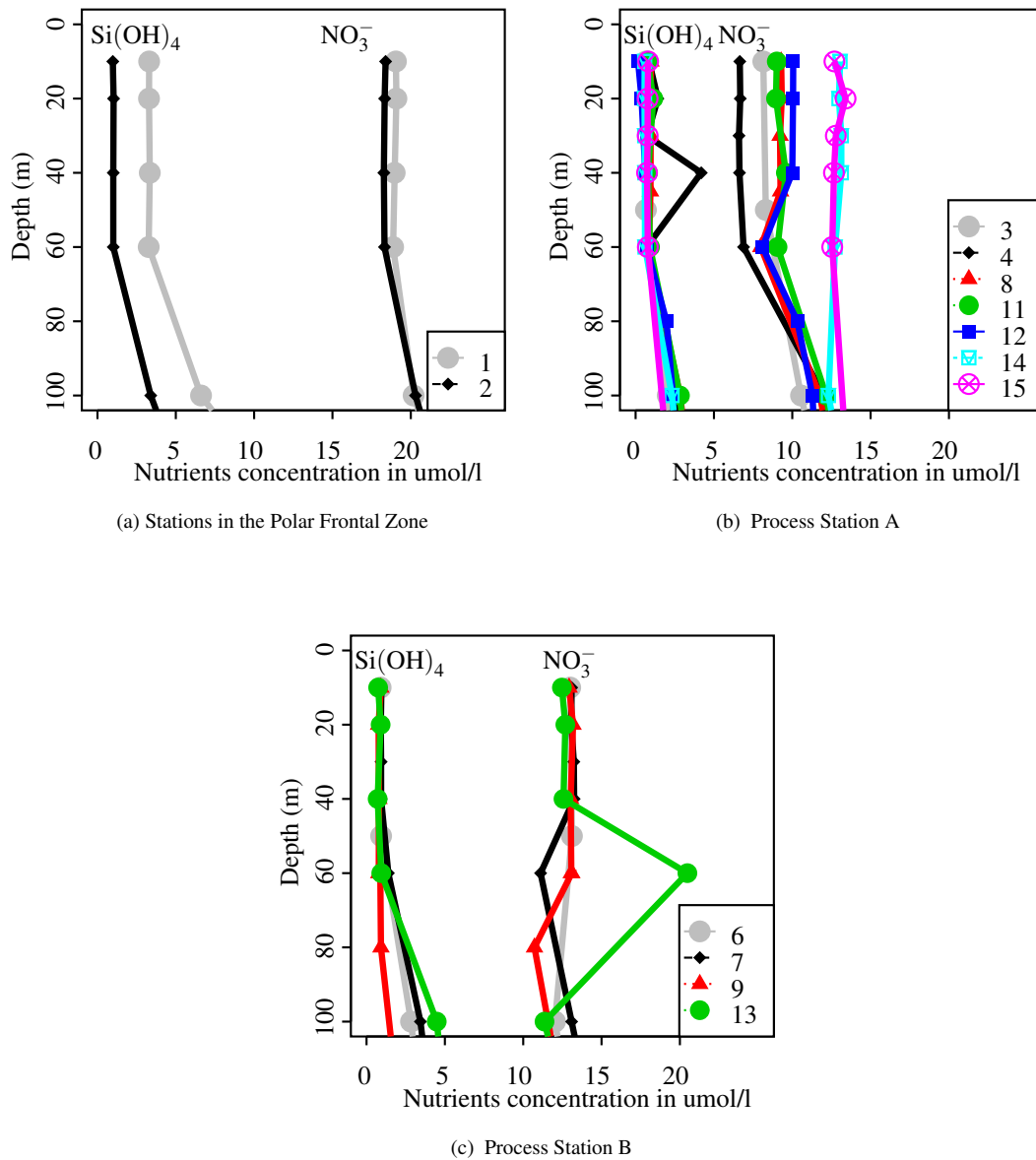


Figure 3.12: Silicate and nitrate profiles (a) for the stations in the Polar Frontal Zone (b) Process Station A (c) Process Station B during the summer cruise. The profiles shown here on from each of the casts at the two process stations and at the two stations outside the Polar Frontal Zone (CTD 1 and 2). The numbers in the legends represent the CTD numbers. The silicate concentrations were consistently low throughout the cruise while nitrate concentrations showed more variation. This is seen mostly at process station A where nitrate concentrations increased for CTD 14 and 15.

3.3.2 Nitrogen and Carbon uptake rates

This section provides a short description of the nitrogen uptake rates for the two seasons. Specific, absolute and depth-integrated rates are presented here. Specific nitrogen uptake rates (v) allow for comparison of uptake and growth rates independent of biomass whereas the absolute uptake rates represent the uptake in relation to the particulate nitrogen. The depth integrated rates allow for estimates of nutrient uptake throughout the water column.

It is to be noted that isotopic dilution arising from NH_4^+ regeneration has not been accounted for as samples for the regeneration of NH_4^+ were lost. Due to environmental constraints, urea concentrations and uptake rates were not measured despite being a potentially important fraction of regenerated production (Joubert et al., 2011). Other potential sources of regenerated production such as dissolved organic nitrogen (e.g amino acids) and nitrate regenerated by nitrification were also not accounted for. These omissions in the regenerated production estimates do not affect the new production estimates but they highlight the limitations of the f -ratio as an indicator of carbon export as they lead to underestimates in regenerated production. Nitrification can also lead to the isotopic dilution of the nitrate pool and a resulting underestimate of nitrate uptake. Such underestimates would also affect the f -ratio. Nitrification has been observed during summer in the Southern Ocean (Bianchi et al., 1997) and DiFiore et al. (2009) have estimated that this process could represent up to 6 % of NO_3^- uptake during this season. The role of nitrification in replenishing nutrients over the winter season has been hypothesised previously (Sanders et al., 2007) and has been confirmed by a recent study on the natural abundances of $\delta^{15}\text{N}$ and $\delta^{18}\text{O}$ (Smart et al., 2015). In this thesis, nitrification rates were measured simultaneously to nitrate uptake rates (chapter 4). However, nitrification was only measured at one light depth (55%) and was only detected at five stations out of fifteen. The nitrate uptake rates were not corrected for nitrification due to the large uncertainties in the measured nitrification rates (chapter 4).

Equating nitrate uptake to new production also rests on the assumption that nitrogen fixation is negligible. While the contribution of nitrogen fixation was expected to be low in the Southern Ocean (Berman-Frank et al., 2001), this nevertheless brings the use of the f -ratio as a proxy for carbon export into question.

In addition, in this study, the equation by Collos (1987) was used instead of the one by Dugdale and Goering (1967). The latter, which subtracts the AE% in the particulate matter at the end of the incubation from the AE% of the initially labelled pool, does not account for the use of multiple sources of nitrogen. When the phytoplankton uses an unlabelled source of nitrogen at the same time as a labelled one, the resulting enrichment in the particulate matter is underestimated. Collos (1987) have shown that the equation used here accounts this bias.

However, there are other sources of errors which are not corrected for. Part of the DIN taken up by phytoplankton is sometimes released as DON instead of being assimilated into the cells. When this is not accounted for, nitrogen uptake rates might be underestimated as this nitrogen is lost from the particulate pool (Bronk et al., 1994; Glibert et al., 1985; Laws, 1984). The high tracer additions can result in stimulation of the phytoplankton growth and artificially high uptake rates. Rates corrected for high tracer additions were obtained from the model by (Eppley et al., 1977) and compared with the rates presented here. There were so significant differences between the two datasets (figure 3.13). As mentioned above, the isotopic dilution of the tracer for both ammonium (Glibert et al., 1982a) and nitrate (Ward et al., 1989; Clark et al., 2007) might lead to underestimates of the uptake rates. Furthermore, if regeneration rates are high, it might also lead to a situation where isotopic equilibrium is reached i.e equal isotopic enrichment in the particulate matter (phytoplankton cells) and in the aqueous pool (Glibert et al., 1985). The effect of isotopic dilution can be estimated using the model by Kanda et al. (1987) (figure 3.14). The ratio of regeneration to true uptake rates, a , is used as a correction factor. The plot shows the corrected ammonium uptake for values of $a = 0.5$ and $a = 2$ as these represent the range of ' a ' expected in the open ocean. This again did not show significant differences (figure 3.14).

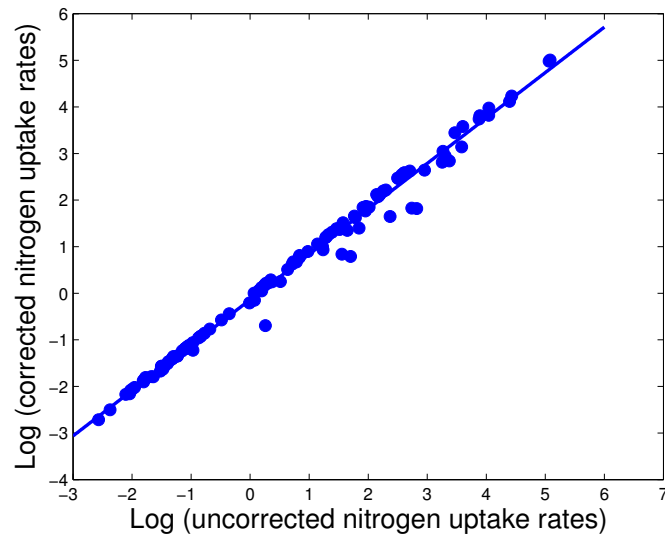


Figure 3.13: Comparison of uncorrected nitrogen uptake rates and those corrected for large enrichments according to the equation by Eppley et al. (1977). With few exceptions, no significant differences were seen

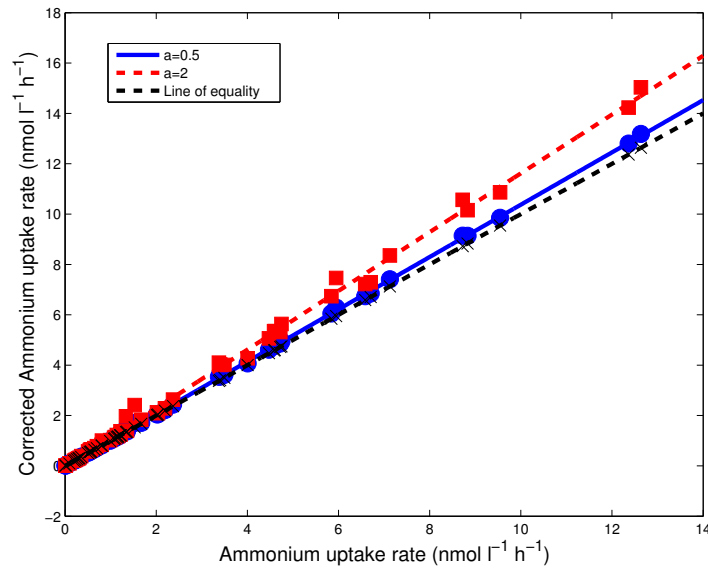


Figure 3.14: Comparison of uncorrected ammonium uptake rates and those corrected for isotopic dilution to the equation by Kanda et al. (1987). The ratio of regeneration to true uptake rates, a , is used as a correction factor. The plot shows the corrected ammonium uptake for values of $a = 0.5$ and $a = 2$ as these represent the range of ' a ' expected in the open ocean.

Uptake rates for the winter cruise

For the winter cruise, the specific nitrate uptake rates, v_{NO_3} , ranged between 0.002 and 0.107 (mean = $0.017 \pm 0.026 \text{ d}^{-1}$) at the 55 % light depth. At the 1 % light depth, the specific nitrate uptake ranged between 0.003 and 0.034 (mean = $0.009 \pm 0.009 \text{ d}^{-1}$). However, when excluding station 15N-1, located in the Subtropical Zone, the mean was $0.007 \pm 0.004 \text{ d}^{-1}$. Specific ammonium uptake rates, v_{NH_4} , averaged 0.073 ± 0.094 ($0.006 - -0.376$) d^{-1} for the 55 % light depth and 0.085 ± 0.116 ($0.0004 - 0.416$) d^{-1} for the 1 % light depth.

The absolute nitrate uptake rates, ρ_{NO_3} averaged 8.89 ± 14.38 ($1.28 - -57.00$) $\text{nmol} \cdot \text{L}^{-1} \cdot \text{d}^{-1}$ and absolute ammonium uptake rates, ρ_{NH_4} , 31.91 ± 40.91 ($2.31 - -158.05$) $\text{nmol} \cdot \text{L}^{-1} \cdot \text{d}^{-1}$ at 55 % sPAR. At the 1 % light depth, the average ρ_{NO_3} was 5.98 ± 9.71 ($1.07 - -35.98$) $\text{nmol} \cdot \text{L}^{-1} \cdot \text{d}^{-1}$. When excluding station 15N-1, the average ρ_{NO_3} was 3.25 ± 2.36 ($1.07 - -8.95$) $\text{nmol} \cdot \text{L}^{-1} \cdot \text{d}^{-1}$. The average ρ_{NH_4} at the 1 % light depth was 35.44 ± 40.06 ($0.17 - -160.94$) $\text{nmol} \cdot \text{L}^{-1} \cdot \text{d}^{-1}$.

The specific ^{13}C uptake, $v_{^{13}\text{C}}$ at the 55% light depth ranged from 0.01 – 0.067 d^{-1} with an average of 0.06 d^{-1} . The absolute ^{13}C uptake, $\rho_{^{13}\text{C}}$, had a mean of 232.86 ($34.82 - 779.01$) $\text{nmol} \cdot \text{C} \cdot \text{L}^{-1} \cdot \text{d}^{-1}$. At the 1% light depth, the minimum $v_{^{13}\text{C}}$ was 0.01 and the maximum 0.11 d^{-1} . The average $\rho_{^{13}\text{C}}$ was 173.39 $\text{nmol} \cdot \text{C} \cdot \text{L}^{-1} \cdot \text{d}^{-1}$ while the lower and upper estimates were 19.78 and 410.09 $\text{nmol} \cdot \text{C} \cdot \text{L}^{-1} \cdot \text{d}^{-1}$. In this data set, the 55 % light depth nitrate uptake rate at station 15N-6 was much higher than other nitrate uptake rates in the Antarctic zone. It was also much higher than the corresponding nitrate uptake rate at the 1 % light depth. It is considered as an outlier for further statistical analyses as it exceeds the mean by more than 2 standard deviations. On the other hand, the ammonium uptake rates for station 15N-1 were not excluded as they might have been much higher than the average ammonium uptake rate in the data set due the geographical position of this station as well as the higher ammonium concentrations observed at this station.

Table 3.2 shows the integrated nitrate uptake rates for the CTD stations from the winter cruise. Integrated ρ_{NO_3} ranged from 0.17 to 5.19 (mean = 1.14 ± 1.50) $\text{mmol} \cdot \text{m}^{-2} \cdot \text{d}^{-1}$ and integrated ammonium uptake from 0.60 to 32.8 (mean = 6.72 ± 9.54) $\text{mmol} \cdot \text{m}^{-2} \cdot \text{d}^{-1}$.

Total production estimated from the nitrogen uptake was compared to the total production estimated from the ^{13}C uptake. Figure 3.15 shows a plot of total production estimated from ^{13}C uptake against total primary production estimated from ^{15}N uptake. The plot also includes a line of equality (an $x=y$ line). Points lying on this line represent samples where the two estimates were equivalent. Points below the line represent those where the nitrogen gives an overestimate of carbon uptake and vice-versa for points above the line. A t-test showed that there were no differences between the log transformed ^{13}C and ^{15}N estimates of primary production (p value = 0.4434). The data was log transformed so that it fitted with the normality assumption.

Station number	Latitude	Longitude	Zone	SST	MLD	[NH ₄ ⁺]	[NO ₃ ⁻]	Depth integrated		
								Chlorophyll-a	ρ_{NH_4}	ρ_{NO_3}
	°N	°E		°C	m	$\mu\text{mol} \cdot \text{L}^{-1}$	$\mu\text{mol} \cdot \text{L}^{-1}$	$\text{mg} \cdot \text{m}^{-2}$	$\text{mmol} \cdot \text{N} \cdot \text{m}^{-2} \cdot \text{d}^{-1}$	$\text{mmol} \cdot \text{N} \cdot \text{m}^{-2} \cdot \text{d}^{-1}$
15N-2	-39.34	10.57	STZ	15	236	0.25	3.15	33.22	13.12	1.02
15N-3	-41.98	8.46	SAZ	10	206	1.7	9.30	33.09	32.86	0.34
15N-4	-45.08	5.84	PFZ	6.9	200	0.06	16.57	22.30	1.70	1.31
15N-5	-48.05	3.2	PFZ	5.4	151	0.35	18.18	30.78	8.32	0.61
15N-6	-51.14	0.28	AZ	2	178	0.19	22.90	22.73	0.60	5.20
15N-7	-53.98	0.01	AZ	0.9	142	0.1	28.46	17.40	1.70	0.22
15N-8	-56	-0.04	AZ	-1	126	0.46	25.57	13.22	2.13	0.45
15N-11	-53.31	22.19	AZ	0.4	165	1.8	20.00	18.57	8.03	0.21
15N-13	-48.37	38.17	PFZ	5.4	59	0.07	16.44	12.95	0.81	0.17
15N-15	-46.31	37.48	PFZ	5	180	below dl	16.06	19.91	2.00	0.57
15N-16	-46.96	37.56	PFZ	5.4	206	below dl	16.66	24.79	2.73	2.46

Table 3.2: Winter depth integrated Chlorophyll-a, ρ_{NO_3} and ρ_{NH_4} from ^{15}N estimates with the associated $[\text{NO}_3^-]$ and $[\text{NH}_4^+]$ at the 55% light depth only. The depth integrated nitrogen uptake rates were calculated from the nitrogen uptake rates at the 55% and 1% light depth.. The station positions are indicated in figure 3.1 and the corresponding hydrographic data is shown in figures 3.3, 3.4, 3.5 and 3.6.

Station number	Zone	Depth integrated	
		New PP ($\text{mg} \cdot \text{C} \cdot \text{m}^{-2} \cdot \text{d}^{-1}$)	Total PP ($\text{mg} \cdot \text{C} \cdot \text{m}^{-2} \cdot \text{d}^{-1}$)
15N-2	STZ	61.9	860
15N-4	PFZ	503	1150
15N-7	AZ	24.2	208
15N-8	AZ	16.7	95.7
15N-11	AZ	8.00	313
15N-13	PFZ	18.0	106
15N-15	PFZ	124	559

Table 3.3: Winter primary production estimates from ^{13}C measurements at 8 CTD stations. "New" production was calculated by multiplying total production measuring using the ^{13}C tracers by the f-ratio calculated from the ^{15}N measurements of nitrogen uptake. These rates represent the average of duplicate measurements for each station. The station positions are indicated in figure 3.1 and the corresponding hydrographic data is shown in figures 3.3, 3.4, 3.5 and 3.6. The rates are shown to three significant figures

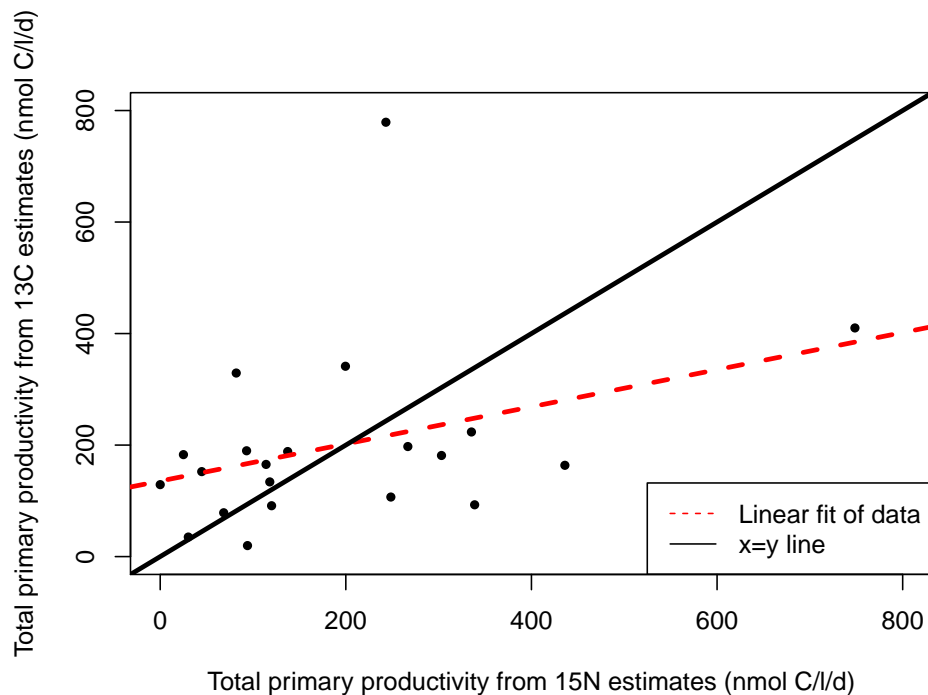


Figure 3.15: Total primary productivity from ^{13}C uptake vs Total primary productivity estimated from ^{15}N uptake. The black straight line is an $x=y$ line while the red dashed line represents a linear fit of the data shown ($r^2 = 0.127$). The values shown here included both the 55% and 1% light depth.

Uptake rates for the summer cruise

For the summer cruise, more detailed depth profiles were available (figure 3.16). CTDs 1 and 2 were the two stations outside the Subantarctic Zone and process study. They showed similar nitrate uptake profiles (figure 3.16a). The glider station however has lower subsurface nitrate uptake rates than the Polar Frontal Zone station. At Process Station A (figure 3.16c), nitrate uptake increased between the CTD stations conducted on 25 February 2013 (CTD 4) and 5 March 2013 (CTD 14). Between CTD 14 and 15, there was a change in nitrate uptake pattern. CTD 4, 8, 14 all showed a subsurface maximum in terms of nitrate uptake. This maximum value was found at the 10% light depth for CTD 4 and 14 but was shallower at CTD 8. For CTD 15, the nitrate uptake rate at 20 m (30% light depth) represented a minimum rate. This rate then surprisingly increased with depth to the 1% light level. It is possible that nitrate uptake rate through the water column did not differ much and that the differences seen are due to standard errors in the measurements.

At Process Station B (figure 3.16e), two of the stations CTD 7 and 9 showed nitrate uptake rates which decreased with depth. Differences between CTD 7 and 9 were minimal. At the 55% light depth, nitrate uptake for CTD 13 was very similar to the two other stations. However, nitrate uptake rates at this station were much larger subsurface, with a maximum at 20 m.

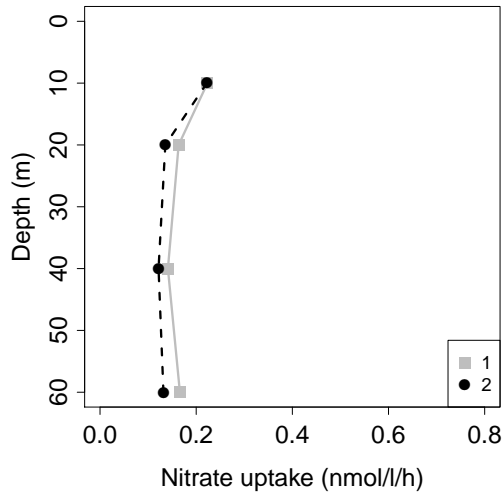
As mentioned before, ammonium regeneration rates were not measured during this study. This is likely to result in an underestimate of ammonium uptake rates. Potential ammonium regeneration rates for the summer cruise were estimated using a box-model and can reach up to $37.13 \text{ nmol} \cdot \text{L}^{-1} \cdot \text{h}^{-1}$ (section 4.3.2). Therefore it is important to consider the ammonium uptake rates presented here as conservative estimates.

At Process Station A, three ammonium uptake profiles were available (figure 3.16d). For CTD 4 and 14, ammonium uptake decreased with depth. At CTD 15, however, ammonium uptake increased with depth. Those patterns were opposite to the nitrate uptake pattern. At Process Station B, ammonium uptake rates were only available for a few points (3.16f). CTD 7 showed a greater ammonium uptake rate than CTD 9 and 13 at the 60 m depth (0.3% light depth). For CTD 13, like the nitrate uptake, ammonium uptake was maximum at 20 m. As expected, the subsurface maximum in chlorophyll at CTD 14 coincided with the maximum uptake rate. At CTD 4 and 8, the subsurface minimum of chlorophyll was at the subsurface maximum of nitrate uptake.

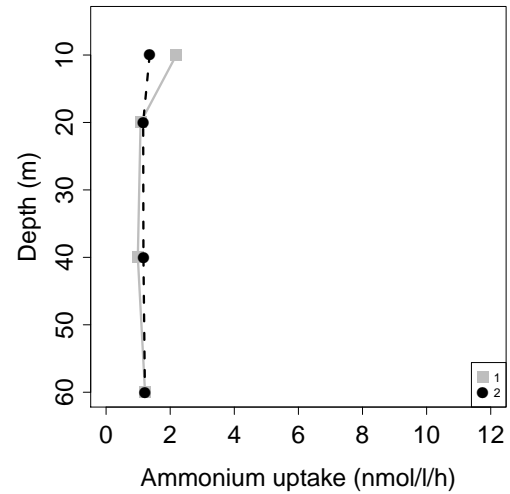
The integrated summer uptake rates are shown in Table 3.4. During the summer cruise, the mean integrated nitrate uptake rate was $0.20 \pm 0.09 \text{ mmol} \cdot \text{N} \cdot \text{m}^{-2} \cdot \text{d}^{-1}$ with a range between $0.10\text{--}0.38 \text{ mmol} \cdot \text{N} \cdot \text{m}^{-2} \cdot \text{d}^{-1}$. The integrated ammonium uptake rate averaged $4.39 \pm 3.21 \text{ mmol} \cdot \text{N} \cdot \text{m}^{-2} \cdot \text{d}^{-1}$ and ranged from $1.12\text{--}9.05 \text{ mmol} \cdot \text{N} \cdot \text{m}^{-2} \cdot \text{d}^{-1}$.

Process Station	Date	Lat °N	Long °E	SST °C	MLD m	[NH ₄] μmol · L ⁻¹	[NO ₃] μmol · L ⁻¹	Depth integrated		
								Chlorophyll-a mg · m ⁻²	ρ_{NH_4} mmol · N · m ⁻² · d ⁻¹	ρ_{NO_3} mmol · N · m ⁻² · d ⁻¹
A	26 Feb 2013	-42.645	8.6867	12.19	57	0.05	6.65	40.07	2.86	0.13
A	1 Mar 2013	-42.7412	8.8111	11.27	54		9.29	25.95		
A	3 Mar 2013	-42.7758	9.1892	11.23	37	0.31	9.01	16.77		0.17
A	5 Mar 2013	-42.6436	9.4306	10.72	69	0.93	13.05	31.69	9.05	0.32
A	7 Mar 2013	-42.6153	9.5967	10.28	76	0.34	12.69	32.29	6.57	0.23
B	28 Feb 2013	-43.5064	7.1858	9.96	65	0.30	13.09	34.69		0.20
B	2 Mar 2013	-43.4233	7.1785	10.02	82		12.93	31.35		0.21
B	4 Mar 2013	-43.5178	7.1315	10.03	85	0.41	12.47	33.49	5.60	0.38

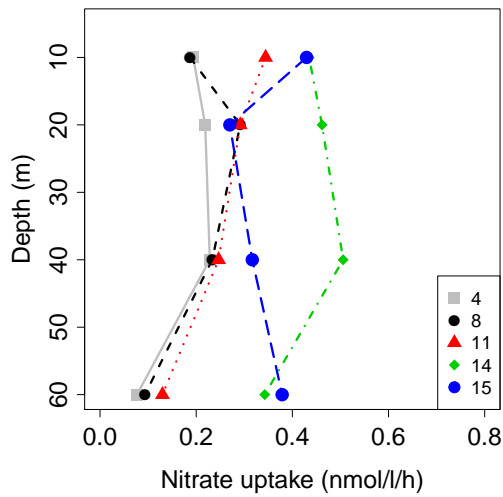
Table 3.4: Summer depth-integrated ρ_{NH_4} , ρ_{NO_3} and Chlorophyll-a concentrations and associated SST, MLD (mixed layer depth), [NH₄] and [NO₃]. [NO₃] and [NH₄] are given for the 55 % light depth only. The corresponding station details are shown in table 3.1 and the hydrographic data is shown in figures 3.8,3.9, 3.10 and 3.11



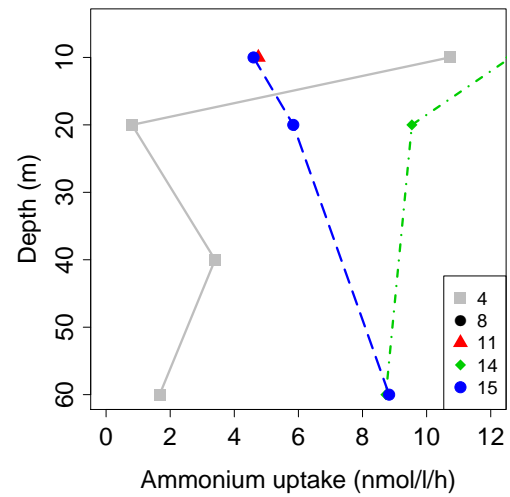
(a) Nitrate uptake in the Polar Frontal Zone



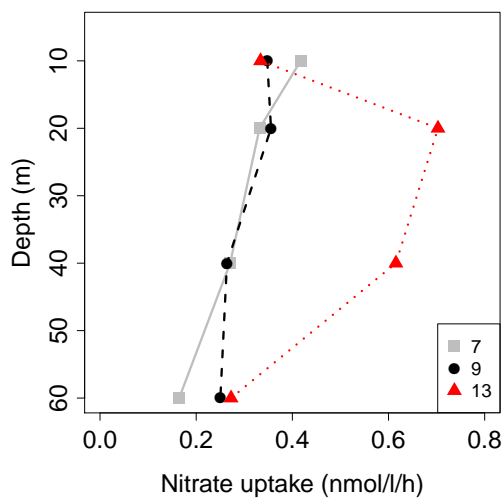
(b) Ammonium uptake in the Polar Frontal Zone



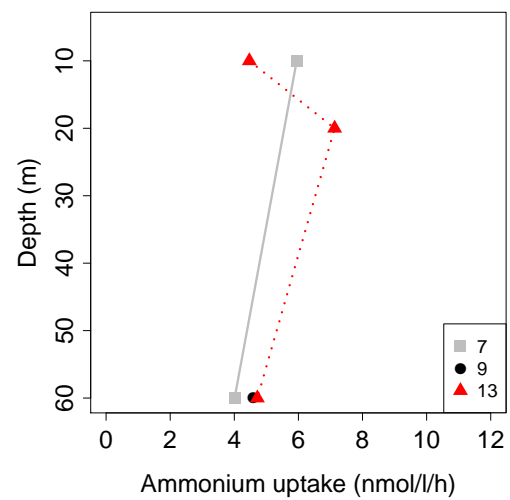
(c) Nitrate uptake at Process Station A



(d) Ammonium uptake at Process Station A



(e) Nitrate uptake at Process Station B



(f) Ammonium uptake at Process Station B

Figure 3.16: Nitrate and ammonium uptake rates profiles for the summer cruise. In the left-hand column, nitrate uptake profiles are shown for the Polar Frontal Zone stations (3.16a), process station A (3.16c) and process station B (3.16e). In the right-hand column, the ammonium uptake profiles are shown for the Polar Frontal Zone stations (3.16b), Process station A (3.16d) and Process station B (3.16f). The uptake rates presented here were not corrected for isotopic dilution and are likely to be underestimates. The effects of isotopic dilution will be discussed further in chapter 4.

3.3.3 Biogeochemical controls on primary productivity

Winter cruise

A multivariate statistical analysis was performed to determine which one of the environmental variables had the most influence on nitrate and ammonium uptake by phytoplankton. The normality of all the variables was examined using a Shapiro-Wilk test as this is a requirement for the multivariate analysis. Nitrate concentrations were found to be normal while the uptake rates, ammonium and silicic acid concentrations were normalised through a log transformation.

The first step of the analysis was a cluster analysis. The hypothesis tested here was whether clusters, based the response variables, would be separated by the fronts (Subtropical, Subantarctic and Polar fronts). Two cluster analyses were undertaken one based on the environmental variables at the 50% and 1% light depths and the other on the uptake rates. The environmental clustering showed clusters which were separated by the fronts (figure 3.17a). This was an expected as the location of the fronts and the delineation of the different regions (Subtropical, Subantarctic, Polar frontal and Antarctic zones) is based on environmental parameters. In the cluster analysis based on the uptake rates, stations did not follow such clear cut separation across the fronts (figure 3.17b). Stations, situated far from each other geographically, had similar responses. For e.g stations 15N-3 and 15N-11 were placed in the same cluster. When using only the CTD stations for the cluster analysis, 15N-2, however, was identified as a Subantarctic Zone station rather than a Subtropical Zone station where it is actually located. This could be due to its proximity to the Subtropical front. While surface parameters at this station were typical of the Subtropical front, the transition was not so clear in deeper waters. For the rest of the analysis, 15N-2 will be considered as a subantarctic station rather than a subtropical one.

A RDA was then performed. The RDA combines a principal component analysis and multiple regressions. The process identifies sets of axes along which most of the variation can be explained. As stated previously, in this analysis, station 15N-6 was considered as an outlier and not used because it had a very high nitrate uptake rate. On the plot, the angle between the blue lines represent the strength of the correlation between the environmental parameters. Acute angles represent positive correlations whereas obtuse angles represent negative correlations. Stronger positive correlations are shown by smaller angles while a 180° angle represents a correlation of -1. A 90° angle indicates no correlation. The length of the arrows shows the significance of the regressions between a particular variable and the response variables. The angle between the blue arrows and red lines shows the correlation between the environmental parameter and each response variable.

The controlling factors included in the analysis were the day length and MLD as measures of light limitation, SST and nutrient concentrations ($[\text{NO}_3^-]$, $[\text{NH}_4^+]$, $[\text{NO}_2^-]$). The $\text{Si}(\text{OH})_4$ and PO_4^{3-} were not included in the analysis as they are strongly colinear with the NO_3^- concentrations. Such strong colinearity results in additional variation which is insignificant. While SST and day length were also strongly correlated, they were included in the analysis in order to determine which of the two factors has a larger influence on the uptake rates.

The RDA plot is shown in figure 3.18. The angle between the arrow representing day length and nitrate uptake was smaller than between SST and nitrate uptake. This implies that day length had a more important role in the regulation of nitrate uptake than SST. Ammonium concentration was positively correlated to ammonium uptake and negatively correlated to nitrate uptake. Though the MLD was negatively correlated to nitrate uptake, the length of its representative arrow indicates that it did not contribute significantly to the variation in the uptake rates. Similar results were obtained with an RDA which included all the underway stations and the specific uptake rates and excluded the MLD.

The unadjusted and adjusted R^2 values for the RDA were 0.74 and 0.36 respectively. This gives an indication of the proportion of variance that can be explained through this analysis. A permutation test confirmed (p

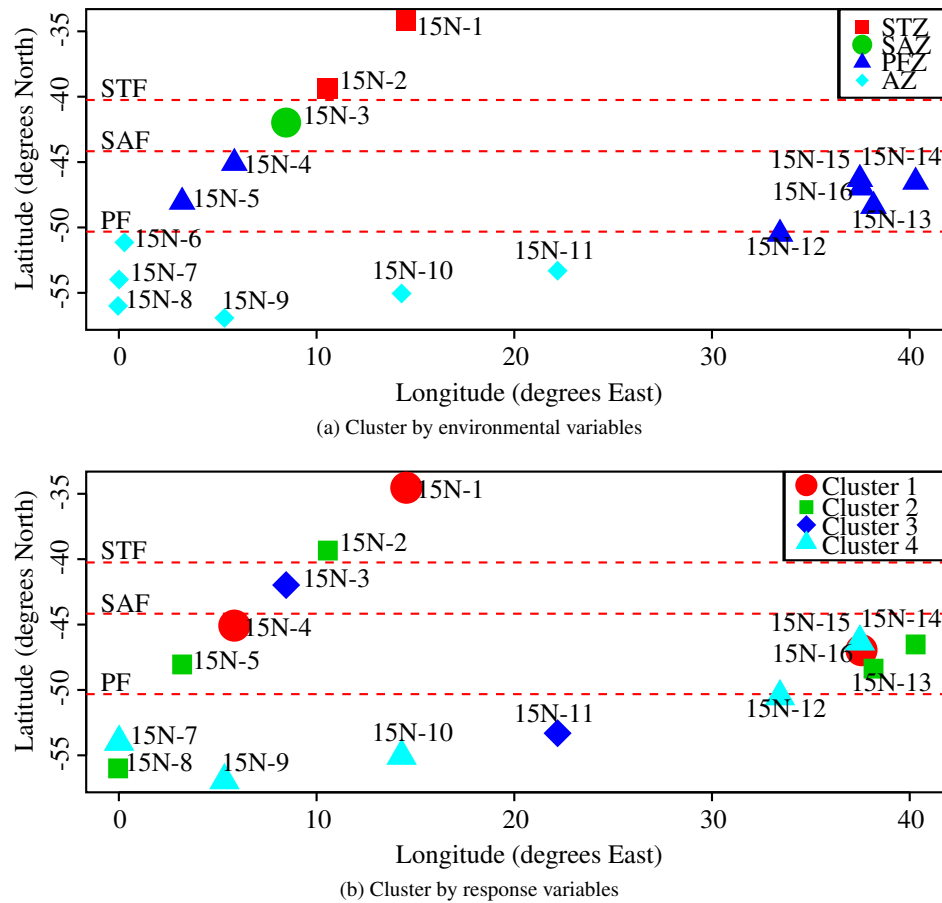


Figure 3.17: Cluster analysis for all the stations including underway stations. The cluster analysis groups the stations based on their similarities. The clusters are arbitrarily numbered and each cluster is shown by a different symbol. Figure 3.17a shows the clusters based on environmental parameters in terms of temperature, chlorophyll and nutrients concentration. In this case, the clusters are separated by the fronts. Figure 3.17b shows the clusters based on the uptake rates. These clusters were not confined by the fronts i.e stations in the same clusters are not always found in the same region

value 0.0967) that the RDA was significant and that the relationship between the environmental parameters and uptake rates was not random. Given this information, it was possible to perform a “forward selection” of parameters (Borcard et al., 2011). This process identified day length and ammonium concentration as the two parameters which influenced the variation in uptake rates the most. The controlling factors in this RDA explain 36% (adjusted R^2) of the variation in the uptake rates. This value has to be adjusted as the RDA employs multiple regressions. Each regression is a hypothesis test. At each iteration, the probability of making a type I error (where a relationship that is not significant is seen as significant) increases and this needs to be accounted for. The algorithm used here has been shown to be conservative (Borcard et al., 2011). This would mean that the parameters used here explain more than 36% of the variation in nitrogen uptake.

Relationship between uptake rates and hydrographic parameters during the summer cruise

A correlation matrix was done for the summer cruise (table 3.5). As the mixed layer depth increased, SST decreased as shown by the strong negative correlation between the two parameters. This also corresponded to an increase in the concentration of nitrate, nitrite, ammonium and phosphate concentrations. Silicate concentration was the only nutrient concentration to decrease with deeper vertical mixing. Both ammonium and nitrate uptake increased when the mixed layers were deeper even though the chlorophyll concentrations decreased.

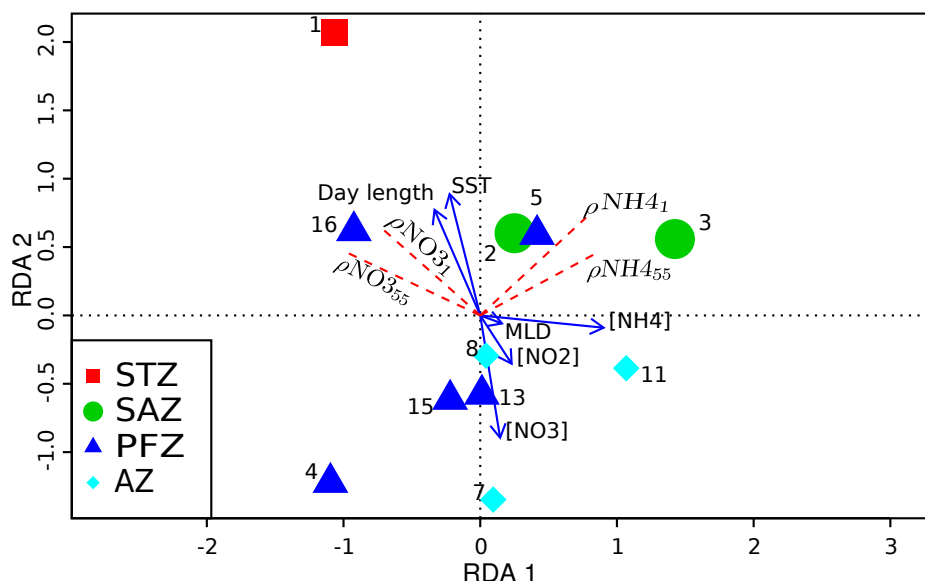


Figure 3.18: RDA triplot. The stations are labelled based on the zone in which they are located. The numbers in the legend represent the CTD stations. The red line are the response variables: ρNO_3 , and ρNO_3 represent ρNO_3 at the 1 % and 55 % light depths respectively and ρNH_4 and ρNH_4 the ρNH_4 at the same light depths. The uptake rates were log-transformed. The blue arrows represent the environmental parameters: SST is the sea-surface temperature, $[\text{NO}_2]$, $[\text{NO}_3]$ and $[\text{NH}_4]$ the concentrations of nitrite, nitrate and ammonium. The numbers for each station are the 15-N station numbers. The angle between the blue lines represent the strength of the correlation between the environmental parameters while the angle between the blue arrows and red lines shows the correlation between the environmental parameter and each response variable. Acute angles represent positive correlations whereas obtuse angles represent negative correlations. Stronger positive correlations are shown by smaller angles while a 180 °angle represents a correlation of -1. A 90 °angle indicates no correlation. The length of the arrows shows the significance of the regressions between a particular variable and the response variables.

	v_{NH_4}	p value	ρ_{NH_4}	p value	v_{NO_3}	p value	ρ_{NO_3}	p value
SST	-0.23	0.43	-0.13	0.67	-0.66	0.01	-0.47	0.09
$[\text{NH}_4^+]$	0.66	0.01	0.54	0.05	0.62	0.02	0.5	0.07
$[\text{NO}_3^-]$	0.32	0.27	0.42	0.13	0.56	0.04	0.57	0.03
$[\text{NO}_2^-]$	0.37	0.19	0.35	0.22	0.56	0.04	0.29	0.32
$[\text{Si}(\text{OH})_4]$	-0.4	0.15	-0.46	0.09	-0.31	0.28	-0.27	0.36
$[\text{PO}_4^{3-}]$	0.25	0.38	0.23	0.44	0.46	0.1	0.41	0.15
[Chl]	0.16	0.59	0.33	0.25	-0.19	0.52	-0.05	0.86
MLD	0.36	0.21	0.29	0.31	0.73	0	0.62	0.02

Table 3.5: Spearman correlation matrix of uptake rates and environmental variables for the summer cruise with the associated p-values. v_{NH_4} and v_{NO_3} are the specific ammonium and nitrate uptake rates while ρ_{NH_4} and ρ_{NO_3} are the absolute uptake rates. SST is the sea-surface temperature and MLD the mixed layer depth. $[\text{NH}_4^+]$, $[\text{NO}_3^-]$, $[\text{NO}_2^-]$, $[\text{Si}(\text{OH})_4]$, $[\text{PO}_4^{3-}]$ and [Chl] are the concentrations of ammonium, nitrate, nitrite, silicic acid, phosphate and chlorophyll.

3.4 Discussion

3.4.1 Comparison of nitrogen uptake rates with previous studies

Shipboard observations allow for a snapshot view of nitrogen uptake and primary productivity. In order to obtain a more complete image of the seasonal and interannual variability, a comparison with historical data is useful. Figures 3.19a and 3.19b compares the absolute nitrate and ammonium uptake rates for the two cruises with historical data. The historical data includes data along the GoodHope Line (Joubert et al., 2011), the Indian sector (Thomalla et al., 2011b) and data collected during three South African National Antarctic Expedition (SANAE) cruises. SANAE cruises are yearly cruises which take place between December and February in the Atlantic sector of the Southern Ocean. The data and cruise reports for the SANAE cruises are available from the Greenseas database (www.greenport.nersc.no). These data were either results from 24-hours ^{15}N incubations or presented as daily rates. The hourly summer uptake rates have therefore been converted to a daily rate to allow for comparison. As described in section 3.2.1, the hourly nitrate uptake rate was multiplied by the light period and the hourly ammonium uptake by the light period plus half of the dark period. The light period was taken as 14 hours.

The nitrogen uptake rates shown in figures 3.19a and 3.19b span several orders of magnitudes and show large variability even within single studies. It is to be noted that the geographical ranges of these studies was very wide. In terms of longitudes, the stations ranged from -36.41 to 44.27°E . Given the large spatial differences, the phytoplankton community structure as well as the biogeochemical settings vary significantly and result in large differences in nitrogen uptake rates (Boyd et al., 2010).

Winter uptake rates from previous winter and autumn studies (Cota et al., 1992; Smith and Nelson, 1990) are comparable with the current dataset. As expected, ρ_{NO_3} , v_{NO_3} and therefore $\int \rho_{\text{NO}_3}$ were lower in winter than in summer and spring. The extent of the seasonal difference varied from region to region. In the Subtropical Zone, nitrogen uptake rates were of similar order of magnitude for both seasons (Thomalla et al., 2011b). Further south, the differences between summer and winter rates increased; winter ρ_{NO_3} along the GoodHope line were between 2 - 80 times smaller than summer rates measured by Joubert et al. (2011) for similar latitudes and light depths.

The summer nitrate uptake rates presented here were lower than summer rates from most past studies (table 3.6). The nitrate uptake rates from the summer cruise were, indeed, very similar to the winter uptake rates (table 3.6 and figure 3.19a). Most of the summer studies were conducted between December and February. For instance, integrated nitrate uptake in the Subantarctic Zone from Savoye et al. (2004) were greater than our estimates. While this could be due to longitudinal variations, it is to be noted that the sampling by Savoye et al. (2004) was done in October and December. At that point, it is likely that the phytoplankton were not yet affected by nutrient limitations. While Joubert et al. (2011) sampled at a similar time of the year, their high nitrate uptake rates for Subantarctic Zone stations were due to an anti-cyclonic eddy in this region at the time of sampling. For Gandhi et al. (2012), sampling extended from December to April and the nitrate concentrations and uptake rates were comparable to the summer uptake in this dataset.

In contrast, ammonium uptake rates did not vary much seasonally or geographically (figure 3.19b). The ammonium uptake for the winter cruise was very weakly correlated to latitude. Rates from the winter and summer cruises were similar to previous studies. A preference for ammonium was observed during the two cruises. Both v_{NH_4} and ρ_{NH_4} were higher than v_{NO_3} and ρ_{NO_3} respectively. Such a preference has been observed in winter (Cota et al., 1992), summer (Semeneh et al., 1998b) and autumn (Thomalla et al., 2011b). There are instances, however, where nitrate uptake is favoured. Gandhi et al. (2012) measured higher nitrate uptake than ammonium and urea uptakes during the summer on transects in the Indian Sector of the Southern Ocean. Sambrotto and Mace (2000) observed a shift in preference from nitrate to ammonium

between December and February in the Pacific sector of Southern Ocean. Smith and Nelson (1990) also observed a preference for nitrate. However, in Smith and Nelson (1990)'s study, as the season progressed from spring into autumn, there was no shift in preferential uptake but a decrease in both uptake rates. Unavailability of nitrate or silicic acid as well as changes within the phytoplankton community structure (e.g a decrease in average cell size or shift in the dominant species) can lead to a preference for regenerated nutrients (Probyn, 1985, 1992). The smaller (seasonal and geographical) variation in NH_4^+ uptake are due to the lower energy requirements of NH_4^+ uptake compared to NO_3^- uptake as the latter needs to be reduced to NH_4^+ before it can be used by the phytoplankton (Thompson et al., 1989). The phytoplankton are able to use NH_4^+ even under severe limitations such as low light in winter and decreased nitrate, silicic acid and micronutrients such as iron in summer.

This can also be seen from the differences in chlorophyll concentrations. In the Subantarctic Zone, chlorophyll concentrations were slightly higher during the summer cruise than during the winter cruise and corresponded to the seasonal averages from satellite observations (Moore and Abbott, 2000). This was true even after mixing events which occurred during the summer cruise. Those mixing events decreased the temperature and chlorophyll concentrations within the mixed layer and increased the nutrient supply. The depth integrated chlorophyll, however, was very similar for the two seasons due to the deeper mixed layer in winter. Behrenfeld (2010) proposes that as the mixed layer gets shallower in spring and summer, the likelihood of the phytoplankton to be grazed increases. For the phytoplankton stocks to remain at the same levels, it means that phytoplankton growth had to increase in order to counteract the effects of a shallowing mixed layer and increased grazing pressure. This would imply that uptake rates had been higher than winter rates throughout the spring and summer, even though the summer primary production rates in this study were similar to winter rates. Furthermore, chlorophyll concentrations at the first CTD casts within the process study were high. The maximum at Process Station A was about $0.7 \mu\text{g} \cdot \text{L}^{-1}$ and at Process Station B, the maximum was about $0.5 \mu\text{g} \cdot \text{L}^{-1}$. The chlorophyll concentrations here were higher than those from Gandhi et al. (2012) - maximum approximately $0.5 \mu\text{g} \cdot \text{L}^{-1}$ - and Joubert et al. (2011) - $0.3 - 0.4 \text{ mg m}^{-3}$. The low chlorophyll in those previous studies highlights that the biomass was still in a positive net growth phase and was likely not to have been limited by nutrients yet explaining the variations in nitrate uptake rates - Gandhi et al. (2012) and Joubert et al. (2011) reported nitrate uptake rates which were higher than our estimates. This also applies when comparing with the rates from Savoye et al. (2004). The former study showed lower integrated chlorophyll (about 6 mg m^{-2} as opposed to $30.8 \pm 6.4 \text{ mg} \cdot \text{m}^{-2}$ in the current dataset) and higher nitrate uptake rates. These measurements were also taken during spring at a time when bloom initiation is expected (Thomalla et al., 2011a). Finally, the study reported by Thomalla et al. (2011b) presented comparable nitrogen uptake rates and integrated chlorophyll concentrations (mean = $30.6 \pm 13.0 \text{ mg} \cdot \text{m}^{-2}$). As their study took place in April, it is likely to have experienced similar conditions to the ones occurring at the time of sampling for the summer cruise.

3.4.2 Carbon export

Nitrogen uptake rates can be equated to carbon uptake as phytoplankton use both nutrients at the same time to form organic matter. Traditionally, primary production fuelled by nitrate was defined as new production while primary production from ammonium and other regenerated nutrients was defined as regenerated production (Dugdale and Goering, 1967). New production is considered to be equivalent to carbon export when integrated over a long time period (Eppley and Peterson, 1979). Average daily primary production can be extrapolated to approximate yearly production. Such estimates are useful for the improvement of current models of the global carbon and nitrogen cycles.

The dogmatic definition of new production as NO_3^- uptake and the use of the f-ratio as a proxy for carbon export has been questioned (Yool et al., 2007) and there are some inherent flaws to this approach. It relies on

Integrated ρ_{NO_3}		Integrated ρ_{NH_4}		Season	Reference
Mean	Range	Mean	Range		
0.20	0.10 - -0.38	4.39	1.12 – 9.05	March	this study
1.14	0.17–5.20	6.73	0.60 – 32.86	July	this study
3.01	1.75 – 6.58	1.06	0.55 – 2.18	March	Smith and Nelson (1990)
3.33	0.79 – 8.63	14.58	2.65 – 39.17	April	Thomalla et al. (2011b)
1.49	0.82 – 2.48	3.68	0.35 – 10.55	February	Sambrotto and Mace (2000)
4.37	1.32 – 8.86	2.34	1.62–2.91	October	Savoie et al. (2004)
5.25	1.85 -9.26	4.63	1.51- 10.06	November	Smith and Nelson (1990)
10.43	0.90 – 34.94	12.63	2.84 – 23.19	November	Waldron et al. (1995)
6.10	1.90 – 12.58	5.65	3.03 – 8.80	December	Sambrotto and Mace (2000)
1.50	0.3 – 4.1	1.1	0.8 – 1.6	December	Gandhi et al. (2012)
4.07	3.63 – 4.55	1.37	0.98 – 1.91	December	Savoie et al. (2004)

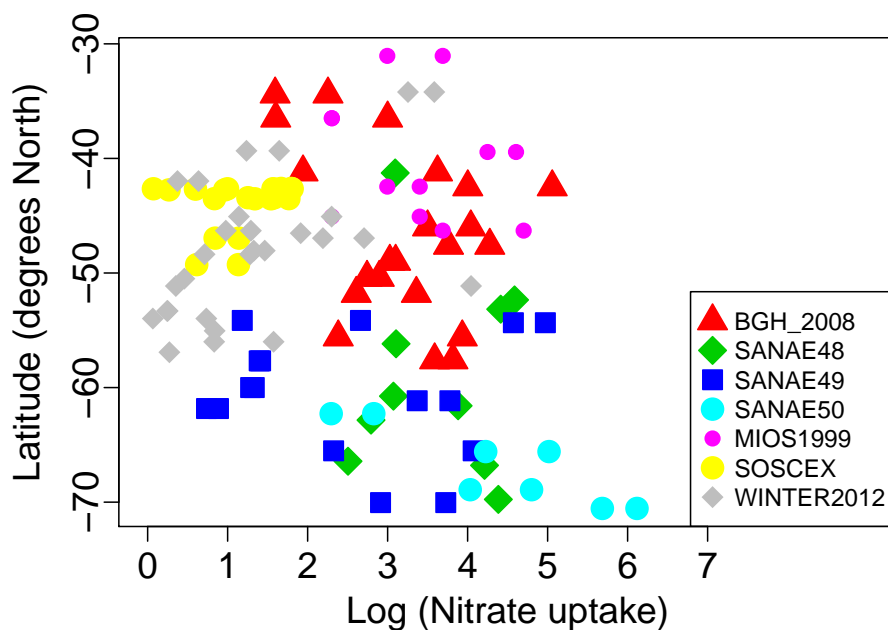
Table 3.6: Overview and comparison of integrated nitrogen uptake rates ($\text{mmol} \cdot \text{N} \cdot \text{m}^{-2} \cdot \text{d}^{-1}$) measured in the Southern Ocean. Average rates and the range are presented here.

the assumption that the phytoplankton population adheres to Redfield stoichiometry and that no nitrification occurs within the seasonal mixed layer (Yool et al., 2007; Eppley and Peterson, 1979). Nitrification has been observed during summer in the Southern Ocean (Bianchi et al., 1997) and DiFiore et al. (2009) have estimated that this process could represent up to 6% of NO_3^- uptake during this season. Furthermore, the role of nitrification in replenishing nutrients over the winter season has been hypothesised previously (Sanders et al., 2007).

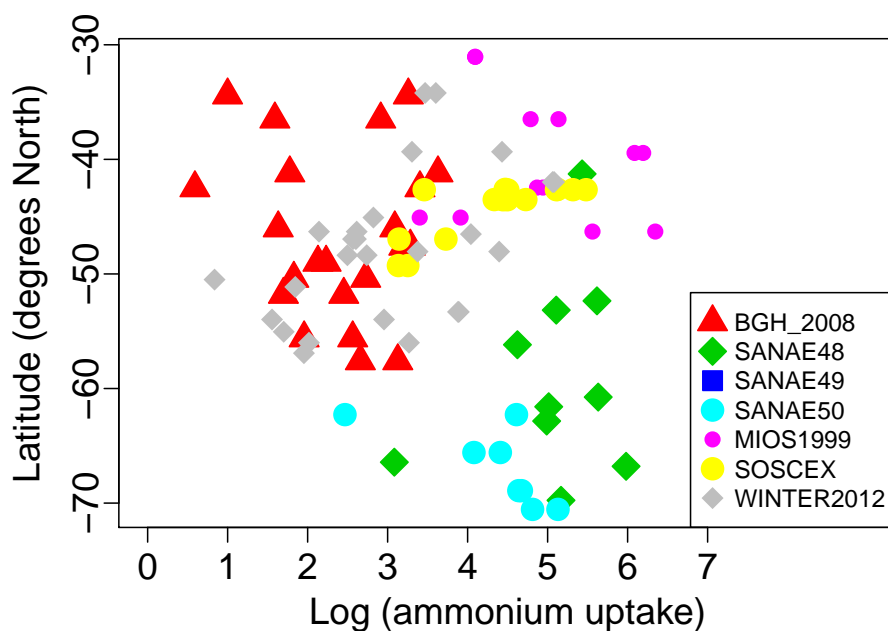
It has been shown phytoplankton in the Southern Ocean do not always exhibit Redfield behaviour (Giddy et al., 2012) and the use of the classic C:N ratio, 6.6, can therefore be problematic. However, in this study, measured C:N ratios were used, where available. This reduced the dependency on an assumed ratio. In cases where the C:N ratios had not been measured, 6.7, the gradient of the [POC] vs [PON] plot (figure 3.2), was taken as the C:N ratio. Similarly to previous observations, the deviation of the average C:N ratio from the redfield ratio was minimal (Moore et al., 2007).

Carbon uptake rates estimated using a ^{13}C tracer from the winter cruise were compared to the estimates of primary production from the ^{15}N tracers (figure 3.15). A paired t-test was applied and the differences between the two estimates were not statistically significant. However, in some cases, the ^{15}N resulted in underestimates of carbon uptake. Urea uptake was not included in the total primary production and this can lead to an underestimate of carbon uptake. Urea uptake has been shown to represent an important percentage (5.0 -74%) of total production (Gandhi et al., 2012; Savoie et al., 2004; Joubert et al., 2011; Thomalla et al., 2011a). Underestimates of carbon uptake could also arise from the fact that isotopic dilution from ammonium and nitrate regeneration was not accounted for.

Winter primary production in the Southern Ocean is generally considered as negligible. However, winter primary productivity can range between 0.08 and $0.31 \text{ g} \cdot \text{C} \cdot \text{m}^{-2} \cdot \text{d}^{-1}$ and account for 10% of annual production (Arrigo et al., 1998). These rates are lower than the estimates from the winter cruise during which primary productivity averaged $0.59 \text{ g} \cdot \text{C} \cdot \text{m}^{-2} \cdot \text{d}^{-1}$ excluding stations north of the Subtropical front are excluded. This could be due to the “snapshot” nature of shipboard in-situ observations. For stations in the Subtropical Zone, primary production peaks in autumn when the deep mixed layers allow access to the nutrient supplies (Thomalla et al., 2011a). Those stations would therefore be at their peak primary production during the winter cruise and would be contributing more to the yearly primary production at this time than in summer. Primary production rates for the Subantarctic Zone during the summer cruise were very similar to the winter rates. The peak primary production and carbon export, which coincide with the spring/summer bloom, were probably missed. The differences between this study and other summer studies in the same region highlight the intra-seasonal variations and the low seasonal reproducibility (Thomalla et al., 2011a). Integ-



(a) Comparison of nitrate uptake rates



(b) Comparison of ammonium uptake rates

Figure 3.19: Comparison of (a) nitrate uptake rates and (b) ammonium uptake rates from the summer cruise (SOSCEX) and the winter cruise (WINTER2012) and previous cruises. $\text{Log } \rho_{\text{NO}_3}$ and $\text{Log } \rho_{\text{NH}_4}$ (in $\text{nmol L}^{-1} \text{d}^{-1}$) are shown here for clarity. The data include both the 55 and 1 % light depths where available for each cruise. The summer uptake rates (SOSCEX) were converted to daily rates by multiplying the average hourly rate by the light period + half of the dark period. The data shown here include data from Joubert et al. (2011) (BGH2008), the SANAE cruises in 2009, 2010 and 2011 (SANAE48,49,50) and Thomalla et al. (2011b) (MIOS1999). The data and cruise reports for the SANAE cruises are available from the Greenseas database (<http://greenport.nersc.no>).

rated new production was higher in the Polar Frontal Zone ($56.8 \text{ mg} \cdot \text{C} \cdot \text{m}^{-2} \cdot \text{d}^{-1}$) than in the Antarctic Zone ($20.0 \text{ mg} \cdot \text{C} \cdot \text{m}^{-2} \cdot \text{d}^{-1}$). This arised from differences in v_{NO_3} rather than differences in biomass. The average chlorophyll concentrations is $0.188 \pm 0.042 \mu\text{g} \cdot \text{L}^{-1}$ for the Polar Frontal Zone and $0.108 \pm 0.044 \mu\text{g} \cdot \text{L}^{-1}$ for the Antarctic Zone. The higher biomass in the Polar Frontal Zone should correspond to an increase in carbon

export. It was most likely fuelled by NO_3^- since ρ_{NH_4} is similar in both regions. This was also indicated by a higher depth integrated f-ratio in the Polar Frontal Zone (0.36) than in the Antarctic Zone (0.11).

To fully understand the implications of winter primary productivity for carbon export, it is necessary to consider these rates in a global context. Eastern Boundary currents are considered to be the most productive regions of the ocean and potential new production in the Eastern Boundary Upwelling ecosystems ranges from $351 \text{ g} \cdot \text{C} \cdot \text{m}^{-2} \cdot \text{y}^{-1}$ (California) to $566 \text{ g} \cdot \text{C} \cdot \text{m}^{-2} \cdot \text{y}^{-1}$ (Peru) (Messie et al., 2009). The Peruvian, NW African and Benguela upwelling showed very similar potential new production (Messie et al., 2009). The potential new production for the Benguela upwelling ($517 \text{ g C m}^{-2} \cdot \text{y}^{-1}$) is comparable to estimates of new production from in-situ ^{15}N measurements which lie between 39 and $70 \text{ Tg} \cdot \text{C} \cdot \text{y}^{-1}$, (Waldron et al., 2009). If daily averages of these new production estimates are considered for an area of $6.5 \times 10^{10} \text{ m}^2$ (Waldron et al., 1998), the mean winter new production estimate in this study ($100 \text{ mg C m}^{-2} \text{ d}^{-1}$) is about 5 and 13% of the new production in the Benguela. The Southern Ocean is a much larger area ($4490 \times 10^{10} \text{ m}^2$) and this highlights the importance of this region for carbon export via the biological pump even in winter. Primary production, phytoplankton stocks (chlorophyll concentrations) and carbon export peak in spring or early summer (Sambrotto and Mace, 2000; Gandhi et al., 2012). Under such conditions, potential export production (as estimated using the f-ratio) can be up to 78% of primary production (Gandhi et al., 2012). While our results do not show major differences in f-ratios between the winter and summer seasons, the importance of the Southern Ocean for carbon export during the spring or summer bloom remains uncontested.

Using an inversion model, Gruber et al. (2009) estimated that the region south of 44°S is a weak carbon sink ($300 \text{ Tg} \cdot \text{C} \cdot \text{y}^{-1}$) matching the results by Henson et al. (2011), whereby export production is between 5 and $10 \text{ g} \cdot \text{C} \cdot \text{m}^{-2} \cdot \text{y}^{-1}$ ($225 - 450 \text{ Tg} \cdot \text{C} \cdot \text{y}^{-1}$) based on ^{234}Th export and satellite data. Extrapolating the average new production estimate from this study over a year for an area of $4490 \times 10^{10} \text{ m}^2$ results in 1200 Tg C y^{-1} . This disparity is similar to the one identified by Joubert et al. (2011): carbon export estimates derived from ^{234}Th measurements were about 2-20 times smaller than those from ^{15}N uptake. This is, of course, a very crude estimate based on the assumption of a steady state. It also does not account for the various processes such as the formation of dissolved organic carbon and remineralisation that would decrease the amount of carbon exported.

3.4.3 Biogeochemical controls on primary productivity

Given the importance of primary production and nitrogen uptake for the global carbon and nitrogen cycle, it is important to understand the factors which control these processes. This section discusses various controls on primary production for the winter and summer seasons. This was investigated using multivariate statistical analyses (sections 3.2.2 and 3.3.3).

The fronts

Fronts within the Southern Ocean separate water masses. These water masses have different thermohaline properties and nutrient compositions. It is therefore likely that they have different phytoplankton communities and nitrogen uptake regimes. A cluster analysis was done on the winter data to test this hypothesis. As seen in figure 3.17, the cluster analysis for the environmental parameters corresponded to the fronts. This was to be expected as the fronts separate waters with different environmental properties. Stations with similar nitrogen uptake regimes, however, were not separated based on their positions relative to the fronts. This shows that the frontal positions cannot be used to distinguish between nitrogen uptake regimes and that the factors controlling nitrogen uptake are not a simple linear combination of the various environmental parameters.

Temperature

Temperature has the same effect on nitrogen uptake by phytoplankton as on photosynthesis. The growth rate is halved for every drop of 10 °C. (Smith Jr. and Harrison, 1991; Tilzer and Dubinsky, 1987). Positive correlations have been observed between nitrate uptake and phytoplankton growth and temperature in the Southern Ocean (Smith Jr. and Harrison, 1991; Reay et al., 2001). At temperatures above zero °C, this relationship was no different to that of temperate phytoplankton and temperature (Smith Jr. and Harrison, 1991). Polar phytoplankton do not seem to have special adaptations to the low temperatures which they encounter in their natural environment (Smith Jr. and Harrison, 1991; Reay et al., 2001; Cochlan, 2008). At low temperatures, nitrate uptake rates are potentially limited by its transport into the cell rather than assimilation rates (Reay et al., 2001; Lomas and Glibert, 1999b; Cochlan, 2008), however, the effect of temperature on polar assemblages is not completely understood as number of culture studies have been done at temperatures which are much higher than the natural ambient temperatures (Cochlan, 2008).

In agreement with previous studies, a positive correlation was shown between temperature and nitrogen uptake during the winter cruise. However, the RDA for the winter cruise showed that the general decrease in ρ_{NO_3} and v_{NO_3} with latitude, temperature and day length during the winter cruise was more strongly correlated to day length than temperature. This is in line with differences reported between summer and winter rates. When considering summer rates from previous studies, the temperature differences are not large enough to explain the variations in the uptake rates. Furthermore, within the Subantarctic Zone, temperatures were higher during the summer cruise than the winter one. Nitrogen uptake rates on the other hand were very similar. Furthermore, during the summer cruise nitrate uptake increased when temperature decreased (table 3.5). This is in agreement with the model developed by Laws et al. (2000). In nutrient limited regions, low temperatures were linked to vertical mixing, which lead to nutrient inputs and enhanced primary production. During the summer cruise, the decreases in temperature corresponded to mixing events by increases in nutrient uptake rates.

As it has been reported for previous studies (Reay et al., 2001; Laws et al., 2000), the correlation between nitrate uptake and temperature was stronger than that between ammonium uptake and temperature during both cruises. The low dependency of ammonium uptake on temperature and the contradictory responses of nitrate uptake to temperature for the summer and winter cruises show that temperature alone cannot explain variations in the nitrogen uptake regimes. Other factors might have more impact through their interactions with each other and with temperature (Tilzer and Dubinsky, 1987; Reay et al., 2001).

Irradiance

The current dataset supports the use of light availability as one of the main drivers of nitrate uptake during the winter (Boyd, 2002; Boyd et al., 2010) but not for ammonium uptake. The amount of light available to phytoplankton is controlled by the time of the year (effectively day length) and the mixed layer depth (Smith Jr. and Harrison, 1991; Cochlan, 2008). The relationship between nitrogen uptake rates and light is similar to that of nitrogen uptake rates and inorganic nitrogen concentrations. Increasing light (or nutrients) will result in increasing phytoplankton growth up to the point of process saturation. At this maximal growth rate, the system is said to be saturated (Smith Jr. and Harrison (1991); Cochlan (2008)). However, there are contradictions to this simple relationship. Maximal rates can be found at depths with 1% and even 0.1% of the surface irradiance (Cochlan, 2008). For instance, at the summer process station A, one of the nitrate uptake profiles (CTD 15, March) showed higher nitrate uptake at 60 m rather than at 20 m. Furthermore, subsurface maxima were observed in several of the nitrate uptake profiles. This could be due to photoinhibition of nitrogen uptake (Hoffmann et al., 2008). For the winter cruise, similar uptake rates were observed in samples incubated at simulated 55% and 1% light depths. The relationship between irradiance and nitrogen uptake by

phytoplankton can also be influenced by a number of other factors such as the bloom stage and phytoplankton community structure (Smith Jr. and Harrison, 1991; Cochlan, 2008).

The use of the mixed layer depth as a determining factor for phytoplankton growth (Sverdrup, 1953) has been a classic tenet of biological oceanography. It assumes that a phytoplankton bloom is not possible if the depth of vertical mixing is deeper than the critical depth. At the critical depth, losses through respiration and other processes exceed growth from photosynthesis. Moreover, with deep vertical mixing, phytoplankton are not exposed to light for long enough to allow nutrient uptake. Consequently, growth would slow down (Mitchell et al., 1991). The winter data shows a negative correlation with the nitrate uptake as expected (as MLD decreases, nitrate uptake increases) but not with ammonium uptake. However, the MLD appears to play a limited role. The length of the arrows on the RDA plot indicate the importance of a certain arrow in explaining the variability of the dataset. The MLD arrow here was very short. It is possible that changes in MLD during the days preceding sampling have a more important effect than the MLD at the time of sampling. The effect of vertical mixing is not always instantaneous. For instance, Venables et al. (2013) have shown that the depth of mixed layer during winter on the Western Antarctic Peninsula could influence phytoplankton growth during the following summer. Furthermore, they also showed that at the time of sampling, incoming irradiance - a function of day length - was a more important control than MLD. This is because the critical depth depends on incoming irradiance - the higher the incoming irradiance, the deeper the critical depth. This is also seen in the winter dataset where day length was very strongly correlated to nitrate uptake. Day length was also one of the two factors explaining most of the variation in nitrogen uptake regime during the winter cruise. This is in agreement with the model by Vernet et al. (2012) who showed a strong correlation between the seasonal cycle of day length and primary production close to the Antarctic Peninsula. Light limitation also changes the responses of phytoplankton to other factors. For example, Tilzer and Dubinsky (1987) showed that the light:dark ratio modulated the responses of phytoplankton to low temperatures. Photosynthesis (dominant in light periods) and respiration (dominant in dark periods) have differential temperature dependencies. Therefore, when temperature changes, the amount of daylight required to maintain a balance between growth from photosynthesis and losses from respiration also changes.

In addition, light limitation can lead to a decoupling of carbon and nitrogen uptake (Smith Jr. and Harrison, 1991). Under low light conditions, nitrogen uptake saturates first leading to an increased C:N ratio. Such increased C:N ratios were not observed in our winter dataset. The C:N ratio was on average 6.8 and was not significantly different from the classic Redfield C:N ratio (6.6, p value <0.001). There was also a good agreement between estimates of primary production from ^{15}N and ^{13}C tracers. This could be due to the fact that the light periods during the winter cruise, when one would expect light limitation, were still significant. The station furthest South was located at -56.92°N and had a day length of 7.6 hours. This is located far from positions where periods of total darkness are experienced much closer to the Antarctic Peninsula (Vernet et al., 2012). During the summer cruise, the day length for all stations were very similar and this was therefore not considered as a major factor affecting the variability in uptake rates. Nitrogen uptake rates increased when mixed layer depth increased in contradiction with the idea that shallow mixed layers would reduce light limitation and enhance primary production. This shows that the changes in vertical mixing impacts controls other than light availability and that depending on the season or stage of bloom, factors such as nutrient availability might become more important than light.

Nutrients

While increased vertical mixing is purported to create unfavourable light conditions for phytoplankton growth, it can promote growth by alleviating nutrient limitations. In this section, the role of iron, silicic acid and ammonium for the nitrogen uptake regime are discussed. Nitrate concentrations were not limiting throughout the two cruises. In the winter, there is a negative correlation between nitrate uptake and nitrate

concentration. The high nitrate concentrations could be due to low nitrate uptake rates and the inability of the phytoplankton to deplete this nutrient. Phytoplankton community structure is strongly influenced by the nutrient limitations (Hutchins et al., 2001; Sedwick et al., 2002; Hoffmann et al., 2008). This will not be discussed in detail here as no data on the size or species distribution were available for these two cruises.

Iron Within the Subantarctic Zone during the summer cruise, nitrate uptake, which is more dependent by iron limitation than ammonium uptake, was very low. As the vertical mixing increased, nitrate uptake increased. The deeper mixed layers resulted in enhanced nutrient availability and consequently increased nitrate uptake. As nitrate concentrations were not limiting, other macro- and micro- nutrients are responsible for this enhanced nitrate uptake rate. Iron is the most likely candidate given its well-established role in regulating primary productivity within the Southern Ocean (Van Oijen et al., 2004; Strzepek et al., 2012; Sanders et al., 2007; Moore et al., 2007; Falkowski et al., 1998; Cochlan, 2008; Boyd et al., 2010; Boyd, 2002). However, in winter, iron limitation by itself is unlikely to be a major control. The deep vertical mixing brings up water from below the ferricline and brings up a constant supply of nutrients (Boyd, 2002; Boyd et al., 2010; Thomalla et al., 2011b). Furthermore, in iron-limited systems, islands can be a source of iron which will enhance primary production and nitrate uptake (Sanders et al., 2007). The cluster analysis also allowed to test whether the stations closer to Marion island showed higher nitrogen uptake than stations further away in the Polar Frontal Zone. No such difference was observed supporting the contention that low iron supply was not limiting at this time of year. However, during this season, an iron-light colimitation, in which light might play a more important role than iron, is plausible (Moore et al., 2007; Van Oijen et al., 2004; Strzepek et al., 2012). In autumn, when mixed layers have started deepening and nutrient supply increased, Van Oijen et al. (2004) observed no changes in uptake rates after iron additions. Strzepek et al. (2012) found in laboratory experiments that the effects of iron addition on phytoplankton growth were less pronounced under light limitation. They also suggest that the relationship between iron and light utilisation by Southern Ocean phytoplankton might be different from that in temperate phytoplankton. Iron limitation affects the nitrogen uptake regime as it influences the phytoplankton community structure (Hutchins et al., 2001; Sedwick et al., 2002; Hoffmann et al., 2008). This also results in changes in the interactions with the cycling of Si.

Silicic acid During the winter cruise, Silicic acid, $\text{Si}(\text{OH})_4$, concentration was low north of the Polar front. This corresponds to observations from previous studies (Tréguer and Jacques, 1993). The minimum $\text{Si}(\text{OH})_4$ concentration was $1.7 \mu\text{mol} \cdot \text{L}^{-1}$. At this concentration, $\text{Si}(\text{OH})_4$ is not limiting if the assemblage is dominated by non-diatom phytoplankton (Sedwick et al., 2002). Notwithstanding, phytoplankton communities can be limited by low $\text{Si}(\text{OH})_4$ concentration. A number of studies have shown co-limitations of iron and silicate (Hutchins et al., 2001; Sedwick et al., 2002; Hoffmann et al., 2008). In those studies, growth rates increased to a greater extent when both Si and Fe were added together than when either nutrient was added alone. Increases in Si can also shift the community structure from dinoflagellate dominated to diatom dominated (Hutchins et al., 2001). This results in changes to the nitrogen uptake regime - the preference for ammonium and other non-nitrate nitrogen sources is reduced. During the winter cruise, however, $\text{Si}(\text{OH})_4$ and NO_3^- concentrations were positively correlated and both southwards (polewards). Nitrate uptake rates decreased with latitude indicating that $\text{Si}(\text{OH})_4$ was not a limiting nutrient. However, its influences on the community structure during this cruise is unknown. For the summer cruise, $\text{Si}(\text{OH})_4$ was the only nutrient to decrease with increased vertical mixing and to be negatively correlated to nitrogen uptake. The silicate concentration profiles show that there was an increase below 60 m following a similar pattern to nitrate. However, there is no correlation between nitrate and silicate concentration within the euphotic zone. This could indicate a decoupling between the Si and N cycles. This arises when the recycling of organic nitrogen is high as opposed to the slow recycling of biogenic silica (Tréguer and Jacques, 1993).

Ammonium The RDA plot for the winter data (figure 3.18) shows that when ammonium is present, phytoplankton exhibit a preference for ammonium. Ammonium concentration was identified as one of the factors explaining the most of the variance in the dataset (sections 3.2.2 and 3.3.3). The presence of ammonium has two reported effects on the nitrogen uptake regime: it can either inhibit nitrate uptake or increase the specific ammonium uptake rate (Goeyens et al., 1995; Whitehouse et al., 2011; Cochlan, 2008; Smith Jr. and Harrison, 1991). The question remains as to which of the two is more effective at shifting the uptake regime from one which is mainly fuelled by nitrate to one fuelled by regenerated nutrients. Inhibition of nitrate uptake by ammonium has been reported in a number of studies (Goeyens et al., 1995; Smith Jr. and Harrison, 1991; Reay et al., 2001; Semeneh et al., 1998a), but the concentration at which this inhibition effect starts is controversial. Goeyens et al. (1995) synthesised data from 9 studies and observed the changes in nitrate depletion and ammonium availability over a full seasonal cycle. Higher ammonium availability was observed when nitrate assimilation decreased. Nitrate assimilation usually decreases after a period of sustained phytoplankton growth. Following such a bloom, the particulate organic matter is remineralised to regenerate ammonium (Goeyens et al., 1995). From our winter data, there was no correlation between ammonium and chlorophyll concentrations. There might be a lag between the peak in nitrate uptake and the remineralisation of particulate organic matter. In this case, ammonium concentrations would be more likely to correlate with chlorophyll concentrations from some preceding period rather than chlorophyll concentrations at the time of sampling. In the summer dataset, a negative correlation is observed between chlorophyll and ammonium concentrations, but this cannot be attributed to an accumulation of ammonium due to remineralisation of particulate organic matter. Mixing events during the course of the study could be responsible for entraining the organic matter and bringing ammonium formed in a different location to the process station.

As discussed in section 3.3.2, the tracer additions did not affect the ammonium uptake rates. At low ambient ammonium concentrations, ammonium uptake was lower than at high ambient ammonium concentrations. It also confirms that the shift of preference to ammonium observed through the RDA is at least partly due to increased concentrations of ammonium. In contradiction to studies which have observed a fairly constant nitrate uptake in the presence of ammonium (Whitehouse et al., 2011), the winter dataset shows that nitrate uptake decreases when ammonium concentration increases. This indicates that inhibition of nitrate uptake could also be contributing to shifting the nitrogen uptake regime.

3.5 Conclusion

In this chapter, the seasonality of primary production in the Southern Ocean was investigated. Two cruises were conducted: one in winter (July-August 2012) along the Goodhope line and one in late summer within the Subantarctic Zone (February-March 2013). Nitrate uptake rates were similar for both cruises, but ammonium uptake rates were generally greater during the summer cruise. These nitrate uptake rates were, however, lower than rates measured in other cruises undertaken in spring and early summer. Even though the rates were low, they still represent a significant portion of annual carbon flux. Primary productivity was mainly driven by ammonium during both seasons. While the regions between the ACC fronts are often considered to be uniform in terms of biogeography and phytoplankton distribution, this study shows that this is not the case when considering nitrogen dynamics. Nitrogen uptake is driven by more than a simple linear combination of environmental variables. During the winter cruise, nitrogen uptake rates decreased southwards and seemed to be limited by light rather than by nutrients. During this season, the presence of ammonium was shown to shift the nitrogen uptake regime towards increased ammonium uptake. This was a result of both inhibition of nitrate uptake by ammonium as well as concentration effects increasing ammonium uptake. During the summer, on the other hand, nutrient availability seemed to be the most important control. With increased vertical mixing and increased nutrients, nitrogen uptake rates increased even though deepening mixed layers mean that the light conditions are less favourable. The presence of ammonium is an indicator of regenerative processes.

While ammonium regeneration was not measured during this study, nitrification rates were estimated at the same time as nitrogen uptake. Nitrification can produce a high proportion of the nitrate used by phytoplankton and Chapter 4 discusses the importance of nitrification during the two cruises in the Southern Ocean.

Chapter 4

Nitrification in the Southern Ocean

4.1 Introduction

As seen in chapter 3, the biological pump drives an important proportion of carbon export in the Southern Ocean. The *f*-ratio (the proportion of primary production fuelled by nitrate uptake to total primary production) is often used as a proxy for carbon export and to evaluate the efficiency of the biological pump. Using this proxy relies strongly on the assumption that the regeneration of nitrate above the permanent thermocline is negligible over the full seasonal cycle. While the importance of euphotic zone nitrification is well established, several studies using nitrate uptake and the *f*-ratio only mention the lack of nitrification as a caveat (Joubert et al., 2011; Gandhi et al., 2012). Despite the potential importance of nitrification (between 1 - 10% of nitrate uptake in surface waters), there are very few datasets that can be used to estimate the contribution of nitrification to nitrogen demand in the Southern Ocean (Cavagna et al., 2014; Preston et al., 1998).

Furthermore rate measurements are becoming more common in other regions (Beman et al., 2013; Grundle et al., 2013; Painter, 2011; Carini et al., 2010), most nitrification rates available for the Southern Ocean date back about 20 - 30 years (Bianchi et al., 1997; Olson, 1981a; Preston et al., 1998). Such rate measurements are important as they can provide more insight into the seasonal variations of the nitrification process. Several studies have proposed that the role of nitrification in the Southern Ocean could be more important in winter (Sanders et al., 2007; Smart, 2014) than in summer (DiFiore et al., 2009). However, there are no available rate measurements to support these observations. In addition, on shorter timescales, nitrification can lead to underestimates of nitrate uptake measured using ^{15}N tracers. Nitrate regeneration would dilute the ^{15}N tracer during the incubation (Dugdale and Goering, 1967).

The nitrification rates reported in this chapter were measured at the same time as the nitrogen uptake rates from chapter 3. The aim of this chapter is to evaluate how significant nitrification is in the Southern Ocean. This chapter also aims to determine whether there are differences in the occurrence and rates of nitrification between summer and winter.

In this chapter, the rates of ammonium and nitrite oxidation are reported. Ammonium oxidation is an intermediary step that is often considered rate-limiting in the oxidation of ammonium to nitrate. Based on this assumption, ammonium oxidation to nitrite has often been used to make the additional estimate of nitrite oxidation as well. However, given the possible decoupling of the two processes, it is important to determine both rates independently. During the winter cruise, the two steps of nitrification were measured using the isotopic dilution of ^{15}N tracers. During the summer cruise, an additional experiment was undertaken where a ^{15}N tracer in the ammonium pool was used to measure the rate of ammonium oxidation.

A case by case overview of the potential uncertainties in the nitrification rates is presented given that such

uncertainties might have prevented the detection of the process. A box model of the nitrate, nitrite and ammonium fluxes from the summer cruise was constructed to determine the importance of regeneration processes which were not measured as well as to provide an idea of the accuracy of those which were measured. An analysis of the nutrient profiles was also used to investigate the balance of processes contributing to the observed state and to assess whether nitrification could have been happening deeper in the water column. Furthermore, differences in these profiles were used to consider the differences between the two seasons.

4.2 Methods

4.2.1 Sampling

At selected stations, nitrification rates were measured simultaneously with nitrogen uptake rates that have been reported in Chapter 3. All the hydrographic variables such as temperature, salinity, chlorophyll and dissolved oxygen were determined as described in chapter 3. Table 4.1 shows the locations at which nitrification was measured during the two cruises. During the winter cruise, nitrogen uptake rates were estimated at CTD and underway stations along the GoodHope line and from the ice margin to Marion Island. Nitrification experiments were only conducted at the 55% light depth at the CTD stations. During the summer cruise, nitrification experiments were conducted at the 55% light depth at CTD 1 in the Polar Frontal Zone, at 3 different occupations of process station A (CTDs 4,10,15) and 2 occupations of process station B (CTD 7, 13).

Station	Latitude (°S)	Longitude (°E)	Season
15N-2	-39.34	10.57	Winter
15N-3	-41.98	8.46	Winter
15N-5	-48.05	3.20	Winter
15N-6	-51.14	0.28	Winter
15N-7	-53.98	0.01	Winter
15N-8	-56.00	-0.04	Winter
15N-11	-53.31	22.19	Winter
15N-13	-48.37	38.17	Winter
15N-15	-46.31	37.48	Winter
15N-16	-46.96	37.56	Winter
CTD 01	-49.27	2.06	Summer
CTD 04 (A)	-42.65	8.69	Summer
CTD 07 (B)	-43.51	7.19	Summer
CTD 10 (A)	-42.78	9.19	Summer
CTD 13 (B)	-43.52	7.13	Summer
CTD 15 (A)	-42.62	9.60	Summer

Table 4.1: Southern Ocean nitrification stations. Ammonium and nitrite oxidation were measured using an isotopic dilution at all winter and summer stations. At all summer stations, ammonium oxidation was also measured using an isotopic enrichment approach. The letter in brackets indicate the process station for the summer cruise.

4.2.2 Addition of ^{15}N tracers and incubations

Nitrification rates were determined based on the method of Clark et al. (2007) and described in chapter 2. The isotopic dilution of a ^{15}N tracer was estimated to obtain rates of nitrification. The concentration of the tracers were chosen according to expected ambient nutrient concentrations and kept constant throughout the cruise as described in chapter 3 because the ambient concentrations were not available in real time. While

the objective was a 10% enrichment of the sample, it should be noted that tracer concentrations greater than 10% should not affect the results as the tracer is the end product of the reactions. In other words, it should not enhance the rates of nitrification. The following subsections describe the procedure for the amendment of the samples with the ^{15}N tracer during the summer and winter cruise. All the differences in the methods between these two cruises are summarised in section 4.2.4.

Summer cruise

In the general methods chapter, the sample preparation before incubation involves the amendment of a 4-L bulk sample with either $\text{Na}^{15}\text{NO}_2$ or $\text{Na}^{15}\text{NO}_3$ depending on the step of nitrification being measured. After allowing some time for mixing, this 4-L sample is then split into two. The first half is incubated under simulated in-situ conditions while the second half is filtered immediately. The filtrate of the latter sample is called the "pre" sample and is used as a baseline from which changes in isotopic ratios of ^{14}N and ^{15}N are to be measured. The incubated sample is filtered after incubation. Its filtrate is called the "post" sample and is used to determine the isotopic ratios and concentrations after incubation.

This procedure was followed for the summer cruise where three separate 4-L samples were amended with $\text{Na}^{15}\text{NO}_3$ ($1 \mu\text{mol} \cdot \text{L}^{-1}$), $\text{Na}^{15}\text{NO}_2$ ($0.05 \mu\text{mol} \cdot \text{L}^{-1}$) and $^{15}\text{NH}_4\text{Cl}$ ($0.05 \mu\text{mol} \cdot \text{L}^{-1}$). The samples amended with $\text{Na}^{15}\text{NO}_2$ or $\text{Na}^{15}\text{NO}_3$ were used to determine rates for the two steps of nitrification (NH_4^+ to NO_2^- and NO_2^- to NO_3^- through a measure of isotopic dilution). $^{15}\text{NH}_4\text{Cl}$ ($0.05 \mu\text{mol} \cdot \text{L}^{-1}$) was added to the third sample to determine the rate of ammonium oxidation to nitrite through a measure of the isotopic enrichment. This is henceforth referred to as the enrichment experiment. Incubations during the summer cruise lasted for 12 hours during the day. The resulting enrichment were between 3.2 and 15.0% for nitrate, 15.3 and 31.3% for nitrite and 7.9 and 102% for ammonium.

Winter cruise

By using a single bulk sample to obtain the "pre" and "post" sample, one ensures that the isotopic ratios in both samples are the same and that the changes observed after incubation are real and not due to artefacts. However, a bulk sample was not used during the winter cruise but the ^{15}N tracer was added to the pre and post samples independently. In other words, for each step of nitrification, two separate samples were amended with the ^{15}N tracer of the end product ($\text{Na}^{15}\text{NO}_2$ and $\text{Na}^{15}\text{NO}_3$ for ammonium and nitrite oxidation respectively). The "pre" sample was not incubated but the "post" sample was. Given that "pre" and "post" samples did not originate from the same bulk sample for the winter cruise, it is possible that there are some inaccuracies in the differences measured. Such errors are more likely to occur if the "pre" sample and the tracer are not allowed to mix properly. To minimise these errors, the "pre" sample was filtered about 20 minutes after the tracer had been added. The 2-L water samples were separately amended with $\text{Na}^{15}\text{NO}_3$ ($1 \mu\text{mol} \cdot \text{L}^{-1}$) and $\text{Na}^{15}\text{NO}_2$ ($0.05 \mu\text{mol} \cdot \text{L}^{-1}$). The resulting enrichment was between 2 and 52% for nitrate and 16 and 33 % for nitrite.

4.2.3 Determination of isotopic ratios and nitrification rates

Use of the internal standard and concentration measurements

Sudan-1 was generated in the samples and injected on SPE cartridges (Biotage Isolute C18 - IS220-0050-C) as described in Chapter 2 (General Methods) and by Clark et al. (2007). For the winter samples, the deuterated sudan-1 internal standard was only added when the sudan-1 was eluted from the SPE. For the summer samples, about $0.2 \mu\text{L}$ of internal standard per mL of sea-water sample was added to the sample before injection onto the SPE as this has been found to improve the measurement of nitrate and nitrite concentration by

the GC-MS (Clark et al., 2014). This is also seen from the differences in the concentrations measured during the summer and winter cruise.

When the internal standard is added after elution, any amount of sample that was lost during the sample collection step (i.e when the sample was injected onto the SPE during fieldwork) or during the sample elution step (i.e the sample is removed from the SPE column) is not quantified and this might lead to a decrease in sample recovery. Figure 4.1 shows a comparison of the nutrient concentrations measured on board and the concentrations recovered by the GC-MS. There are some major differences between the recovered concentrations and the measured concentrations. This could be due to the high ambient concentrations. Despite injecting a low sample volume (5 – 10 mL) onto the SPE, it is possible that the breakthrough volume had been exceeded and the retention was no longer quantitative.

For the summer cruise, despite the addition of the internal standard during sample collection, the concentrations measured from the GC-MS and the ones measured on-board did not always agree. They were still quite reliable as seen from the regression between the two sets of concentrations (gradient = 0.76). On the other hand, for the winter cruise, the internal standard was added at the time of elution and as a result, the GC-MS concentrations were about 10 times lower than field concentrations for the winter cruise. This is seen from the gradient of the linear regression between the two sets of concentrations (0.098).

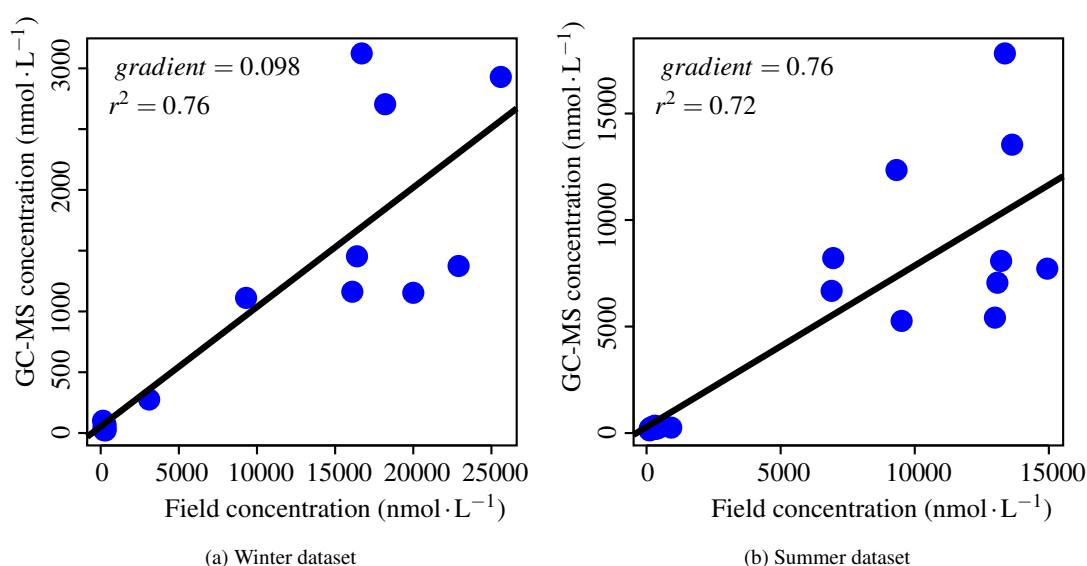


Figure 4.1: Comparison of nitrate and nitrite concentrations measured from the GC-MS (GC-MS concentration) and concentrations measured by FIA on board (field concentration) (a) winter dataset (b) summer dataset. During the winter cruise, the internal standard was added after elution of the dye from the SPE whereas in the summer cruise, the dye and internal standard were added onto the SPE at the same time. The latter method allows for a better recovery of sudan-1 and a better quantification of nitrite and nitrate concentrations.

Controlling the sample size

The amount of sample analysed by the GC-MS is a potential source of error in the $^{15}\text{N}/^{14}\text{N}$ if it results in a GC-MS response which is outside of the linear range ($< 5 \times 10^6$ AU and $> 90 \times 10^6$ AU). For samples above the upper limit, the mass spectrometry detector (MSD) shows $^{15}\text{N}/^{14}\text{N}$ ratios that are higher than the true value due to ^{14}N signal saturation. The response of the MSD does not increase at the same rate for the ^{14}N and ^{15}N mass fractions of the deuterated standards (figure 4.2). This results in different $^{15}\text{N}/^{14}\text{N}$

ratios as the amount of sample is increased (figure 4.2). Therefore, for samples which are outside the linear range, these differences will lead to uncertainties estimating the isotopic dilution. The isotopic ratio might be overestimated and consequently, the rate of isotopic dilution would also be erroneous.

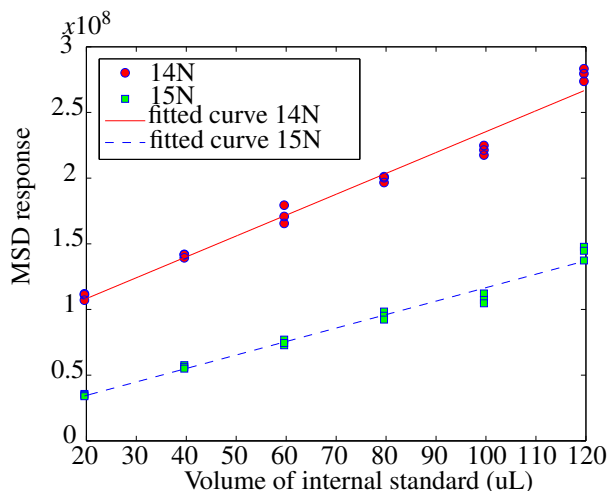


Figure 4.2: Effect of increasing sample size on GC-MS response: Responses of the 311 and 312 mass fractions of the deuterated standard representing the ^{14}N and ^{15}N mass fractions respectively

Given the high nutrient concentrations in the Southern Ocean, the sample size had to be adjusted to avoid the saturation of the mass spectrometer. The steps taken to reduce the sample size were as follows:

1. The sample volume injected onto the SPE was kept as low as possible between 5-15 ml for NO_3^- samples (NO_2^- oxidation) and about 100 ml for the NO_2^- samples (NH_4^+ oxidation). For both processes, it was ensured that the dye was visible on the SPE cartridges so that the minimum sample size would be met.
2. The samples were eluted from the SPE cartridges in ethyl acetate (2 mL). Given the large sample size for some of the samples, after elution, only 0.5 ml of the NO_3^- samples was used for HPLC. This was a first stage in sample size reduction.
3. After HPLC, all samples were dried and redissolved in methanol (200 μL) before being transferred to GC-vials. In cases of samples which showed a high response by the UV detector connected to the HPLC system (peak area higher than 200 mV), only half of the sample was transferred to GC-vials.
4. Samples which had acceptable responses on the HPLC were derivatised (made volatile) using 50 μL of derivatisation reagent while samples with high responses were derivatised in 100 μL . This would dilute the sample further and reduce the amount of material injected into the GC-MS.

Despite these adjustments to the method, it was not always possible to reduce the sample size sufficiently. Figures 4.3 and 4.4 shows the sample size for both the “pre” and “post” samples for both the NH_4^+ and NO_2^- oxidation for the winter cruise. The dotted lines show the minimum (5×10^6 AU) and maximum (90×10^6 AU) values of the linear range. For stations where the sample size was consistently too high, this may be considered as a result of the high ambient concentration preventing the detection of nitrification.

4.2.4 Differences between the methods used in the winter and summer cruises

The procedure for the sample preparation was modified between the winter and summer cruise. The differences are highlighted below:

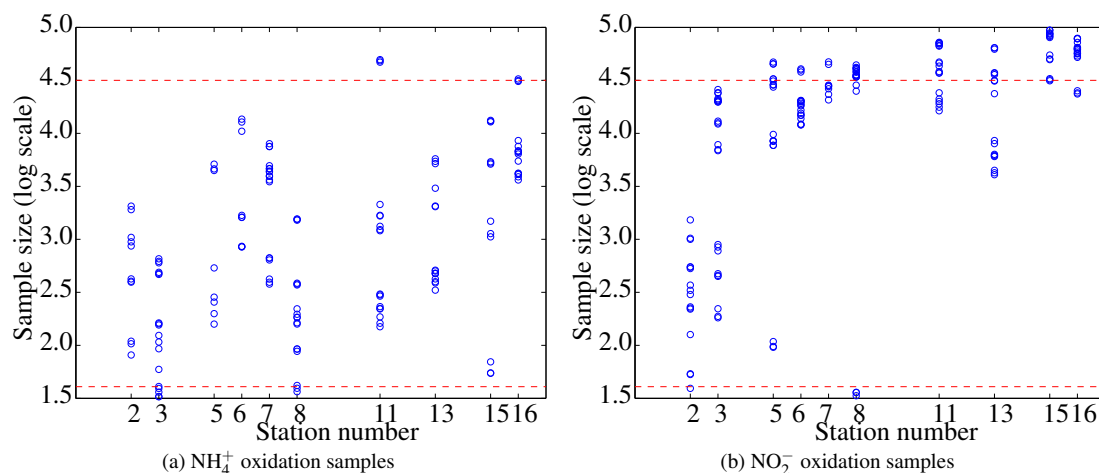


Figure 4.3: Winter cruise: The amount of sudan-1 recovered from all the SPE cartridges from the winter cruise in arbitrary units as measured by the MSD. The MSD response is shown on a natural log scale and the samples are arranged per station. The minimum and maximum values of the linear range are shown by the dotted lines. Values outside the linear range are unreliable and result in erroneous $^{15}\text{N}/^{14}\text{N}$ ratios. Figure 4.4a shows the samples used to measure ammonium oxidation through the isotopic dilution of the $^{15}\text{NO}_2$ tracer. Figure 4.4b shows the samples used to measure nitrite oxidation through the isotopic dilution of the $^{15}\text{NO}_3$

- In winter, the ^{15}N tracer was added independently to "pre" and "post" samples. "Pre" sample was allowed to stand before filtration to avoid mixing errors.
- In summer, a bulk sample was amended with the ^{15}N tracer. The bulk sample was split into two parts—one which was incubated and one which was not.
- In winter, the internal standard was added after sudan-1 was eluted from the SPE cartridges.
- In summer, the internal standard was added to the sudan-1 generated in the sample before it was injected onto the SPE.
- Samples from the summer cruise were more reliable as the MSD responses were consistently within the linear range.

4.2.5 Data analysis

For each "pre" and "post" sample, the dye was injected onto 3 SPE cartridges. Each SPE was analysed 3 times on the GC-MS. A Kruskal-wallis test was applied to each set of samples to see whether the isotopic enrichment from any of the three SPE was significantly different from the others. Box-plots showing the $^{15}\text{N}/^{14}\text{N}$ ratio (see figure 4.5 for an example), sample size and nutrient concentrations from each SPE were plotted and compared to the other two corresponding cartridges to identify outliers. Outliers were identified visually for the $^{15}\text{N}/^{14}\text{N}$ ratio and nutrient concentration:

1. If the notches of the box-plot overlapped this meant that the two samples were not different.
2. If all three samples were different from each other, none of them was considered as an outlier.
3. Similarly, if two samples were different from each other but both overlapped with the third sample, none of them was considered as an outlier.

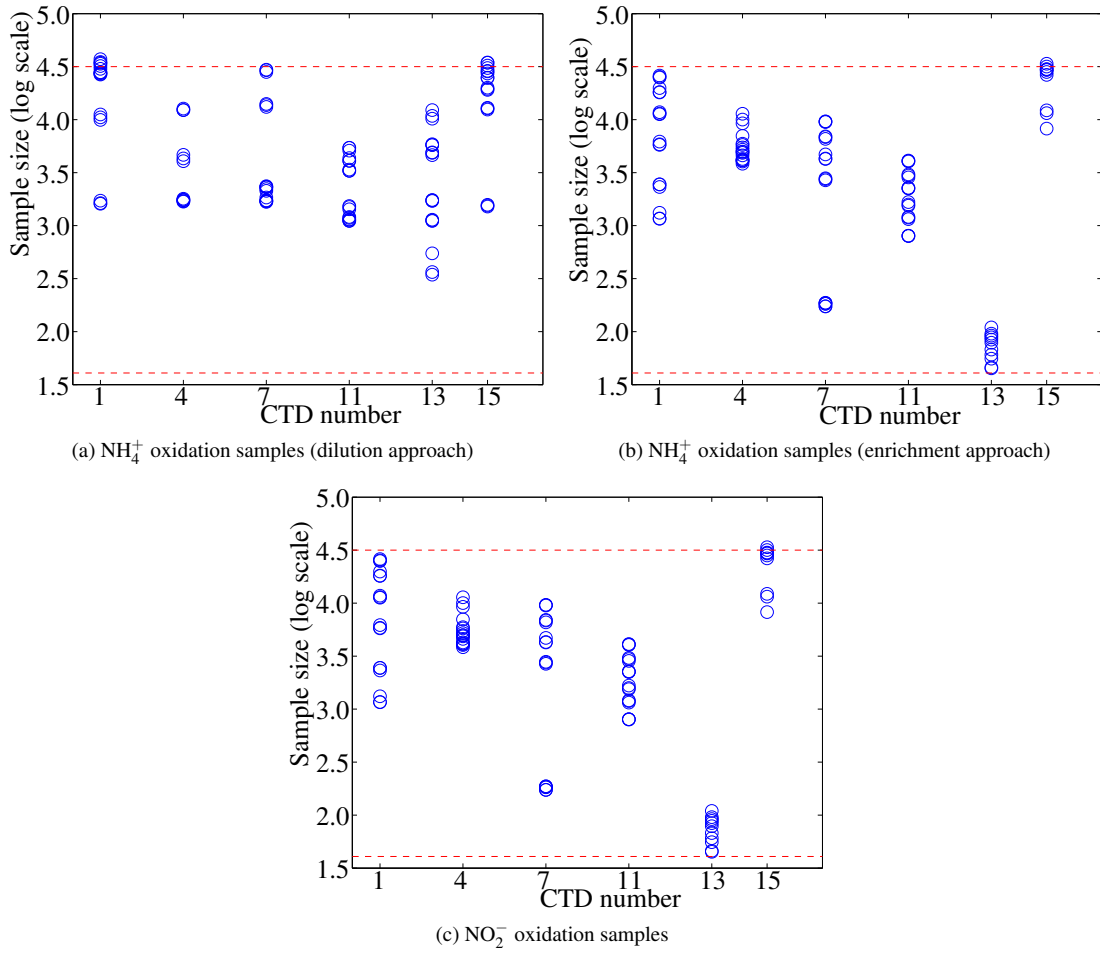


Figure 4.4: Summer cruise: The amount of sudan-1 recovered from all the SPE cartridge in arbitrary units as measured by the MSD. The MSD response is shown on a natural log scale and the samples are arranged per station. The minimum and maximum values of the linear range are shown by the dotted lines. Values outside the linear range are unreliable and result in erroneous $^{15}\text{N}/^{14}\text{N}$ ratios. Figure 4.5a shows the samples used to measure ammonium oxidation through the isotopic dilution of the $^{15}\text{NO}_2$ tracer. Figure 4.5b shows the samples used to measure ammonium oxidation by the addition of $^{15}\text{NH}_4$ tracer and subsequent enrichment of the nitrite pool. Figure 4.5c shows the samples used to measure nitrite oxidation through the isotopic dilution of the $^{15}\text{NO}_3$

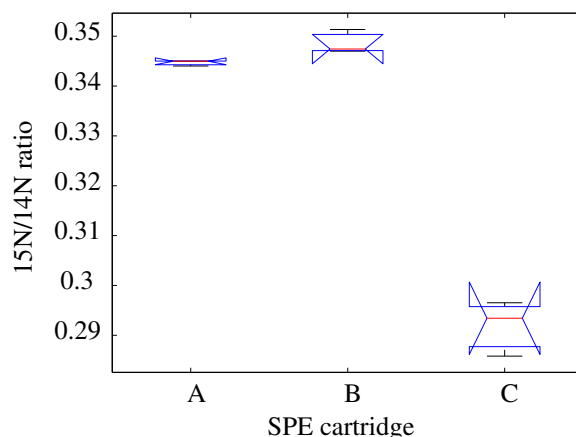


Figure 4.5: Box plots showing the $^{15}\text{N}/^{14}\text{N}$ ratio comparing the "pre" sample of station 15N-5. Each sample was injected onto triplicate SPE. Each box-plot results from triplicate measurements made from one SPE cartridge. Outliers were identified visually. In this example, SPE C was discarded.

In some cases, two different replicates were identified as outliers when using the $^{15}\text{N}/^{14}\text{N}$ ratio and nutrient concentrations. In such cases, the outlier identified from the concentrations was discarded. In total, data from 33 out of 122 SPEs were discarded.

Once the outliers had been removed, a Mann-Whitney test at a significance level of 0.05, was done comparing the median isotopic ratio ($^{15}\text{N}/^{14}\text{N}$ ratio) of the "pre" and "post" samples. This test identifies whether there is a significant difference between the two "pre" and "post" ratios. For the experiments using isotopic dilution, the "post" ratio of $^{15}\text{N}/^{14}\text{N}$ should decrease if nitrification is significant. Nitrification rates were only calculated for samples where a significant decrease in isotopic ratio was observed from the pre to post samples. For the enrichment experiment, the same test was applied to compare the pre and post samples. It differs from the dilution experiment as $^{15}\text{N}/^{14}\text{N}$ ratio should increase in the case of significant nitrification.

Nitrifications rates using the isotopic dilution method were calculated according to the equations described in chapter 2. No ammonium oxidation rates using the isotopic enrichment method as enrichment of the nitrite pool was not observed in these experiments.

4.2.6 Nitrogen fluxes in summer: a box model

For the summer cruise, nutrient data from "pre" and "post" incubation samples was used to produce a box-model. This conceptual model was based on the expected fluxes of nitrate, nitrite and ammonium. Its aim is to investigate the disparities between the measured fluxes and observed differences in concentration. As such, it contributes to the evaluation of missing components such as ammonium regeneration. It also allows for the calculation of net nitrification rates where suitable to allow for a comparison with the measured rates.

Ammonium originates from regeneration processes and is consumed through uptake by phytoplankton and oxidation by nitrifying organisms. Nitrite is produced either by phytoplankton excretion or by the oxidation of ammonium. The only nitrite sink in this model is the oxidation of nitrite. Nitrate is the end product of this reaction and is subsequently consumed through uptake by phytoplankton. In the phytoplankton cell, nitrate is first reduced to nitrite. The latter is further reduced to ammonium, which is incorporated into organic matter. If the phytoplankton is not able to reduce the nitrite further due to light, iron or other nutrient limitations, it accumulates in the cell and is released before reaching toxic levels (Malerba et al., 2012).

Figure 4.6 shows a schematic of the box model. Blue dotted arrows represent measured fluxes (nitrate and ammonium uptake as well as ammonium and nitrite oxidation). The release of nitrite by phytoplankton is

marked as a blue dotted arrow as it is indistinguishable from ammonium oxidation when using the isotopic dilution method. Nitrate uptake measured here is a measure of nitrate assimilation rather than depletion of nitrate. When nitrate uptake is measured using ^{15}N tracers, nitrate assimilation results in the isotopic enrichment of the particulate matter. Nitrate depletion, however, is a measure of how much nitrate is lost during the incubation time. This includes nitrate that is not incorporated into the particulate organic matter. It could be for example converted to nitrite or dissolved organic nitrogen (DON). Red arrows represent fluxes which were not measured (nitrite uptake and ammonium regeneration). Ammonium regeneration is shown as a red arrow directly from the phytoplankton cell even though phytoplankton do not release ammonium directly. Ammonium is usually regenerated by bacterial action (Goeyens et al., 1995; Whitehouse et al., 2011). At each station, an integration of flux rates for each nutrient over the incubation period was taken. The expected change in concentration over this time was then compared to the measured value.

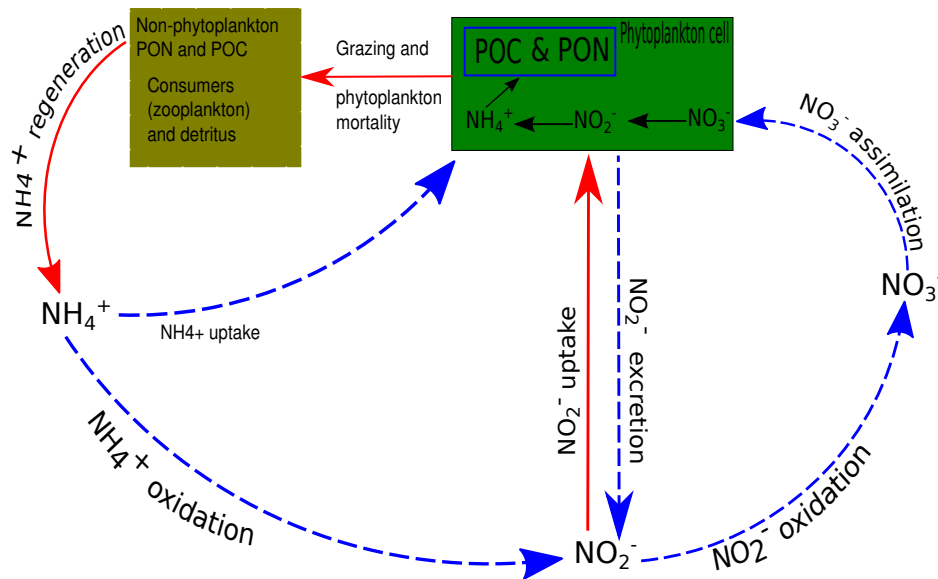


Figure 4.6: Box model for fluxes of ammonium, nitrate and nitrite. The green box represents phytoplankton cells inside which nitrate and nitrite are reduced to ammonium before assimilation. Blue dotted arrows represent measured fluxes while red arrows show those that were not measured. It is to be noted that the excretion and uptake of dissolved organic nitrogen by phytoplankton is not shown here.

4.3 Results

4.3.1 Did significant nitrification occur?

This section shows at which stations significant nitrification occurred and presents the rates for these stations. After removing outliers from the isotopic ratios measured through the GC-MS, a Mann-Whitney test was performed on the "pre" and "post" ratio to determine whether significant nitrification occurred during the incubation. The significance level was set at $\alpha = 0.05$.

For both cruises, the two steps of nitrification were measured separately. Ammonium oxidation measured through the isotopic dilution of the NO_2^- tracer will be referred to as nitrite production as this method does not discriminate between nitrite release by phytoplankton and ammonium oxidation. Table 4.2 shows the results of the Mann-Whitney tests for the winter cruise. Table 4.3 shows the results for the summer cruise. P values < 0.05 indicate that there is a significant difference between the median of the "pre" and "post" samples at the 95% level. This does not, however, indicate which one had a higher isotopic ratio and whether or not significant nitrification was observed. For stations where a significant difference was observed between

the pre and post, bar graphs comparing the isotopic ratios were plotted. Table 4.4 shows a summary of the estimated nitrification rates at the end of this section.

Station	NO_2^- production	NO_2^- oxidation
15N-2	0.258	0.002*
15N-3	0.328	0.863
15N-5	0.002*	0.004*
15N-6	0.224	-
15N-7	-	0.529
15N-8	0.002*	0.094
15N-11	0.937	0.015*
15N-13	0.0004*	0.066
15N-15	0.316	0.589
15N-16	0.689	0.272

Table 4.2: P values for the Mann-Whitney test comparing the "pre" and "post" $^{15}\text{N}/^{14}\text{N}$ ratios for each station of the winter cruise. P values below 0.05 (highlighted with asterisks) indicate a significant difference between the "pre" and "post" sample.

For the winter cruise, only stations 15N-5, 15N-8 and 15N-13 showed significant differences for the nitrite production samples with p-values of 0.002, 0.002 and 0.0004 respectively. From the bar graphs (figure 4.7), it can be seen that significant NO_2^- production occurred at station 15N-5 and station 15N-13. For station 15N-8, the "post" sample had a higher isotopic ratio than the pre sample. This could be due to a lack of mixing in the "pre" sample. Nitrite production rates were $3.21 \pm 0.21 \text{ nmol} \cdot \text{L}^{-1} \cdot \text{h}^{-1}$ and $0.824 \pm 0.298 \text{ nmol} \cdot \text{L}^{-1} \cdot \text{h}^{-1}$ for station 15N-5 and 15N-13 respectively.

With respect to nitrite oxidation, stations 15N-2, 15N-5 and 15N-11 showed differences between the "pre" and "post" samples. Station 15N-2, however, showed an enrichment (increase in $^{15}\text{N}/^{14}\text{N}$ ratio) after incubation. However, it can be stated that significant nitrification occurred at stations 15N-5 and 15N-11 as these stations showed an isotopic dilution. Nitrite oxidation rates were $123 \pm 8 \text{ nmol} \cdot \text{L}^{-1} \cdot \text{h}^{-1}$ and $37.2 \pm 9.1 \text{ nmol} \cdot \text{L}^{-1} \cdot \text{h}^{-1}$ for stations 15N-5 and 15N-11 respectively.

During the summer cruise, the rates of nitrite production were measured using an isotopic dilution approach as well as an isotopic enrichment approach (see section 4.2.2). The aim of comparing two different approaches was to differentiate between ammonium oxidation and nitrite production from other sources. In the dilution experiment (measuring NO_2^- production), only CTD 13 showed a significant isotopic dilution of the nitrite pool. There was an increase in $^{15}\text{N}/^{14}\text{N}$ at the other stations which presented a significant difference (CTDs 1,4 and 7, table 4.3). The nitrite production rate at CTD 13 was $6.10 \pm 1.06 \text{ nmol} \cdot \text{L}^{-1} \cdot \text{h}^{-1}$. In the samples which had been amended with $^{15}\text{NH}_4\text{Cl}$ (NH_4^+ oxidation enrichment experiment), a significant decrease in $^{15}\text{N}/^{14}\text{N}$ ratio of the nitrite pool was observed at CTDs 4,11 and 13 instead of the expected increase. For the nitrite oxidation samples, CTDs 1,4 and 11 showed significant differences between the "pre" and "post" $^{15}\text{N}/^{14}\text{N}$ ratio (table 4.3). However, only CTD 11 showed nitrite oxidation ($217 \pm 88 \text{ nmol} \cdot \text{L}^{-1} \cdot \text{h}^{-1}$) through a dilution of the $^{15}\text{NO}_3$ tracer.

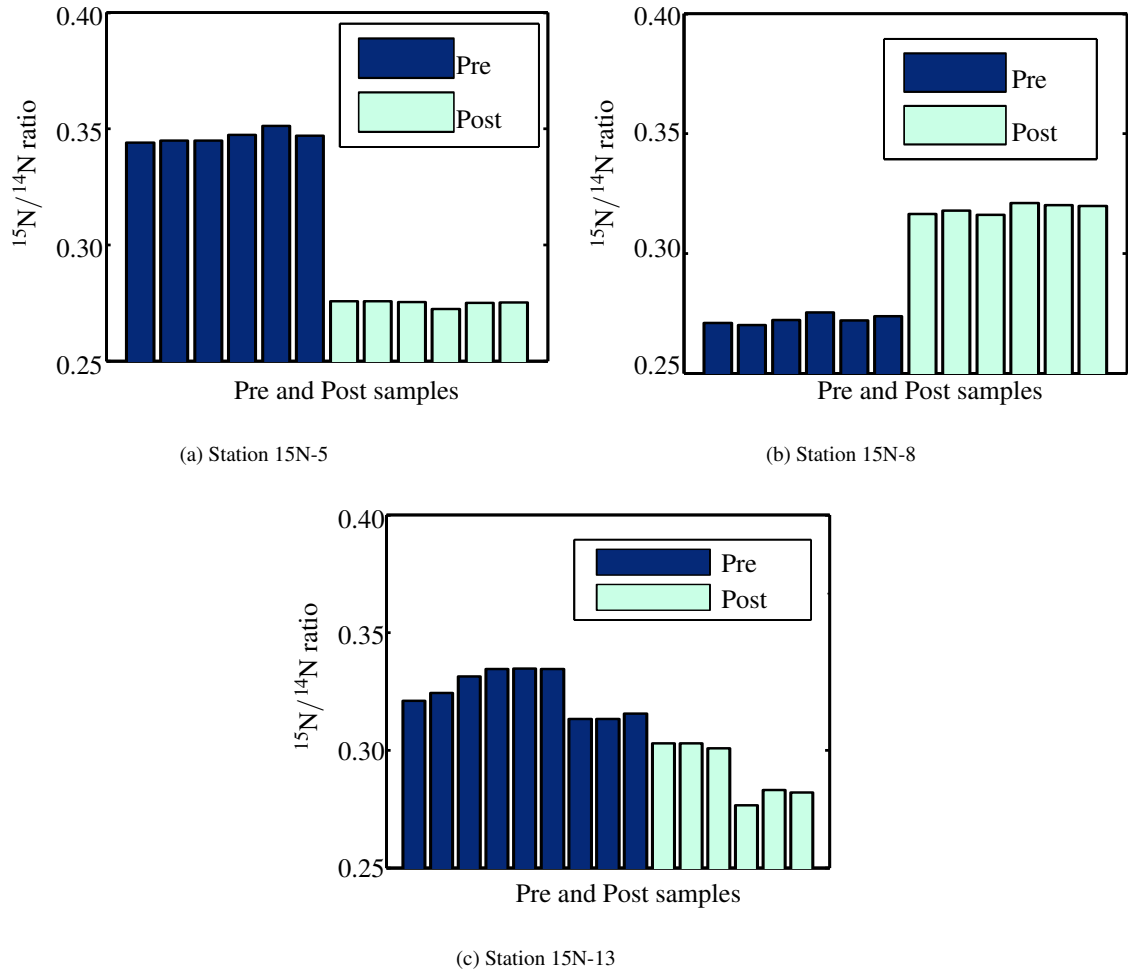


Figure 4.7: Comparison of the "pre" and "post" $^{15}\text{N}/^{14}\text{N}$ ratios for winter ammonium oxidation (NO_2^- production) samples which showed a significant difference between the "pre" and "post" samples. In these samples, the isotopic dilution of the $^{15}\text{NO}_2$ tracer was expected. Samples where an isotopic dilution was not observed imply an error (see section 4.4.1). Nitrification rates were only calculated for stations which showed an isotopic dilution. Bar plots are shown for (a) Station 15N-5, (b) Station 15N-8 and (c) Station 15N-13. The bar plot represent the repeated $^{15}\text{N}/^{14}\text{N}$. For each stations, the $^{15}\text{N}/^{14}\text{N}$ was measured 9 times (3 SPE X 3 replicate measurements for each SPE). The bar plots only show the $^{15}\text{N}/^{14}\text{N}$ after the outliers have been removed.

CTD	NO_2^- production	NH_4^+ oxidation	NO_2^- oxidation
1	0.036*	1.000	0.0004*
4	0.002*	0.000*	0.004*
7	0.002*	0.776	0.328
11	0.689	0.026*	0.0004*
13	0.002*	0.004*	0.456
15	0.087	0.065	0.388

Table 4.3: P values for the Mann-Whitney test comparing the "pre" and "post" $^{15}\text{N}/^{14}\text{N}$ ratios for each station of the summer cruise. P values below 0.05 (highlighted with asterisks) indicate a significant difference between the "pre" and "post" sample.

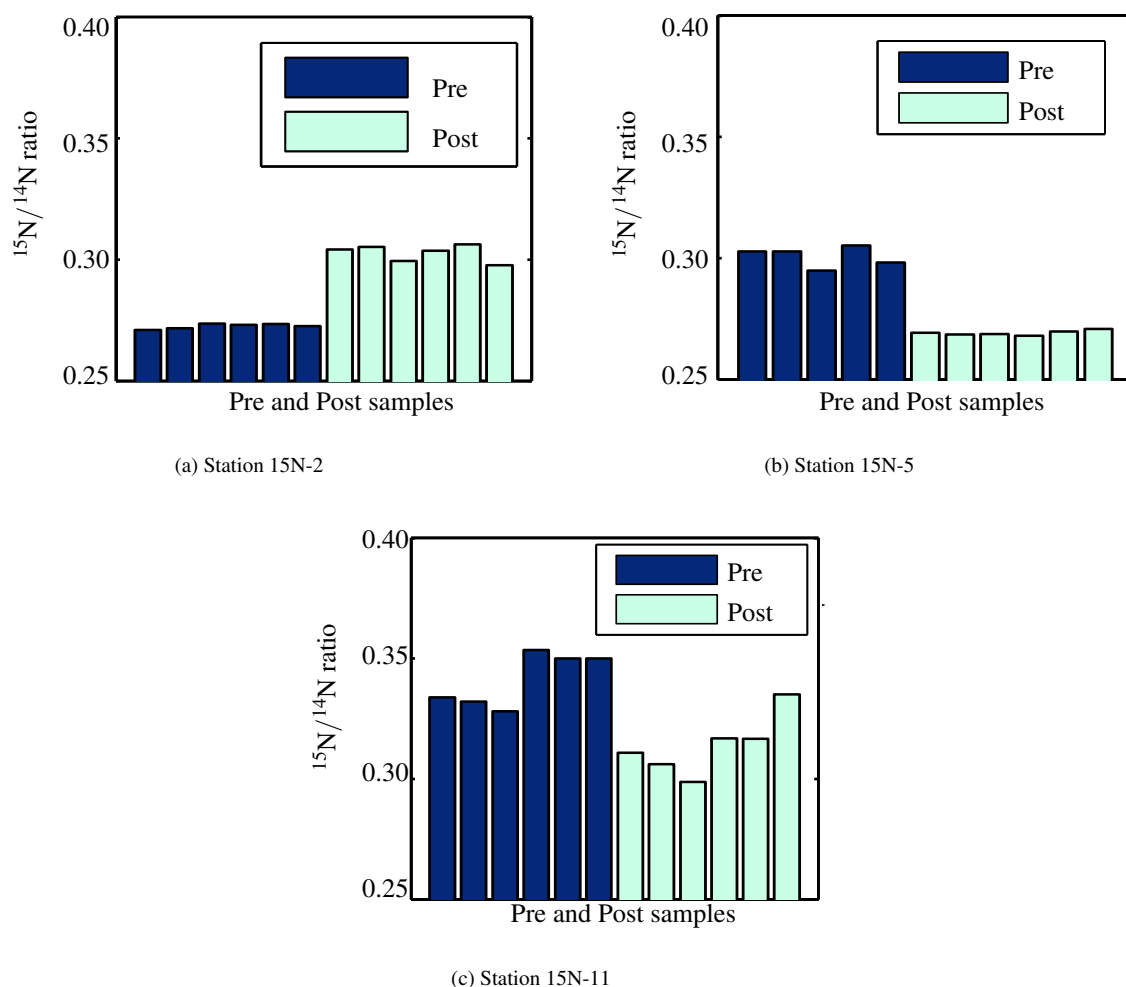


Figure 4.8: Comparison of the "pre" and "post" $^{15}\text{N}/^{14}\text{N}$ ratios for winter nitrite oxidation samples which showed a significant difference between the "pre" and "post" samples. In these samples, the isotopic dilution of the $^{15}\text{NO}_3$ tracer was expected. Samples where an isotopic dilution was not observed imply an error (see section 4.4.1). Nitrification rates were only calculated for stations which showed an isotopic dilution. The $^{15}\text{N}/^{14}\text{N}$ ratios of the nitrate pool are shown for (a) Station 15N-2, (b) Station 15N-5 (c) Station 15N-11. The bar plot represent the repeated $^{15}\text{N}/^{14}\text{N}$. For each stations, the $^{15}\text{N}/^{14}\text{N}$ was measured 9 times (3 SPE X 3 replicate measurements for each SPE). The bar plots only show the $^{15}\text{N}/^{14}\text{N}$ after the outliers have been removed.

Station	Season	NH_4^+ oxidation	$[\text{NH}_4^+]$	NO_2^- oxidation	$[\text{NO}_2^-]$
15N5	winter	3.38 ± 0.22	350	122 ± 8	310
15N11	winter	NA	1790	37.2 ± 9.1	220
15N13	winter	0.824 ± 0.298	70	NA	310
CTD 11	summer	NA	310	217 ± 88	210
CTD 13	summer	6.08 ± 1.06	1130	NA	220

Table 4.4: Ammonium and nitrite oxidation rates with the associated substrate concentrations for both cruises in the Southern Ocean. Rates are given in $\text{nmol} \cdot \text{L}^{-1} \cdot \text{h}^{-1}$ and shown to three significant figures. The concentration of $[\text{NH}_4^+]$ and $[\text{NO}_2^-]$ are $\text{nmol} \cdot \text{L}^{-1}$. NA here indicates that a significant nitrification rate could not be calculated.

4.3.2 Nitrogen fluxes in the summer: a box model

Concentrations of nitrate and nitrite measured using the GC-MS (Chapter 2) were used in this box model. Ammonium concentrations were measured as described in chapter 2. Given that “pre” and “post” values were also available from the GC-MS measurements for the winter cruise, a similar box-model could have been applied. However, the winter concentrations were less reliable given that the internal standard was only added after elution of the samples from the SPE. Furthermore, “pre” and “post” ammonium concentrations were not available for the winter cruise. Figure 4.9 shows the range of nitrogen cycling rates for each of the processes. The values in blue represent measured values while those in red are values calculated through the box model.

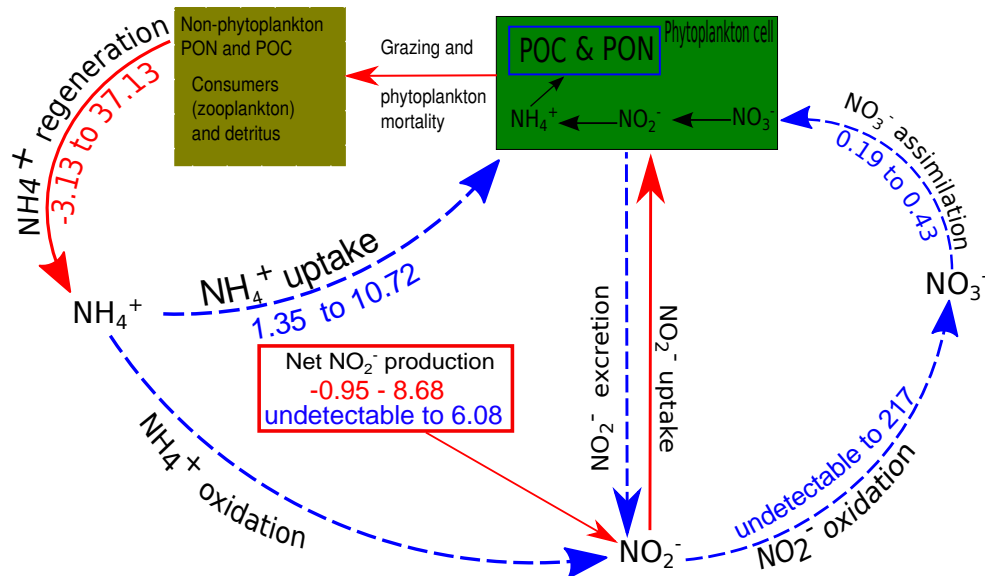


Figure 4.9: Results of the box model for fluxes of ammonium, nitrate and nitrite. Rates for each of the relevant processes are shown in $\text{nmol} \cdot \text{l}^{-1} \cdot \text{h}^{-1}$. The green box represents phytoplankton cells inside which nitrate and nitrite are reduced to ammonium before assimilation. Blue dotted arrows and values represent measured fluxes while red arrows show those that were not measured. Rates shown in red represent flux rates calculated from the box model whereas the rates shown in blue are the rates measured through isotopic dilution. The latter also include any potential release of nitrite by phytoplankton in addition to ammonium oxidation rates. Negative regeneration rates indicate that regeneration was slower than uptake and/or oxidation.

Nitrite fluxes

For nitrite concentrations, the changes from the enrichment and dilution experiments were averaged. These changes showed an accumulation of nitrite for all the stations except for CTD 15. Net nitrite production rates from the box model ranged between -0.94 and $7.58 \text{ nmol} \cdot \text{L}^{-1} \cdot \text{h}^{-1}$. The potential for ammonium oxidation is seen from elevated $^{15}\text{N}/^{14}\text{N}$ in the “pre” sample of the enrichment experiment (especially CTD 4, 11 and 13) and is confirmed by the accumulation of nitrite.

At CTD 15, the net nitrite production rate was $-0.94 \text{ nmol} \cdot \text{L}^{-1} \cdot \text{h}^{-1}$. This indicates either potential nitrite oxidation or nitrite uptake. An accumulation of nitrite was only expected at CTD 13 where measured nitrite production was $4.44 \pm 1.78 \text{ nmol} \cdot \text{L}^{-1} \cdot \text{h}^{-1}$. In this case, the observed ($91.03 \pm 120.20 \text{ nmol} \cdot \text{L}^{-1}$) and expected ($53.3 \pm 1.78 \text{ nmol} \cdot \text{L}^{-1}$) accumulation of nitrite were within a similar range.

Nitrate fluxes

Nitrate concentrations decreased over the course of most incubations indicating unequivocally that nitrite oxidation (the regeneration of nitrate) was generally slower than nitrate uptake. The observed decrease in nitrate concentration ranged from $1024 \pm 2890 \text{ nmol} \cdot \text{L}^{-1}$ at CTD 15 to $7083 \pm 798 \text{ nmol} \cdot \text{L}^{-1}$ at CTD 11. Except for CTD 1 and 13, the loss of nitrate was larger than what was expected based on the nitrate uptake rates reported in chapter 3.

A predicted “post” concentration was calculated by subtracting the losses due to nitrate uptake over the incubation from the “pre” concentration. The hourly nitrate uptake rates measured in chapter 3 were multiplied by 12 hours to estimate the nitrate drawdown by phytoplankton. The ratio of the observed “post” concentration to the predicted concentration was considered. If the observed “post” concentration is larger than the predicted value it implies that either nitrate uptake is being overestimated or that nitrification is elevating the nitrate levels. Conversely if the observed concentration is smaller than the predicted, the nitrate depletion would be higher than the nitrate uptake measured using the ^{15}N tracers. An incomplete reduction of nitrate and subsequent release of nitrite by phytoplankton or release of dissolved organic nitrogen could lead to such a situation. It could also result from an underestimation of nitrate uptake rates. The latter can also arise if the tracer is being diluted through the regeneration of nitrate (nitrite oxidation) during the course of the incubation.

For instance, at CTD 11, which showed significant isotopic dilution (table 4.3), the observed/predicted ratio was 0.427. It is highly likely that nitrate uptake was being underestimated due to this dilution of the tracer. The same would apply for CTD 7 and 15 which showed decreases in the $^{15}\text{N}/^{14}\text{N}$ ratios even though those decreases were not statistically significant. For CTD 15, this adds to the evidence that nitrite oxidation may have been occurring. Finally, CTD 1 and 13 showed increases in nitrate concentration. Nitrite oxidation rates would have to exceed nitrate uptake in those cases. Net nitrification rates can be obtained by dividing the increase in nitrate concentration by the incubation time. Net nitrification rates would hence be $583 \pm 189 \text{ nmol} \cdot \text{L}^{-1} \cdot \text{h}^{-1}$ at CTD 1 and $192 \pm 65 \text{ nmol} \cdot \text{L}^{-1} \cdot \text{h}^{-1}$ at CTD 13.

CTD	Pre $[\text{NO}_3^-]$ $\text{nmol} \cdot \text{L}^{-1}$	Post $[\text{NO}_3^-]$ $\text{nmol} \cdot \text{L}^{-1}$	ρ_{NO_3} $\text{nmol} \cdot \text{L}^{-1} \cdot \text{h}^{-1}$	Predicted post $[\text{NO}_3^-]$ $\text{nmol} \cdot \text{L}^{-1}$	Observed/Predicted
1	9080 ± 470	16100 ± 2220	0.22	9080	1.8
4	8210 ± 1850	6674 ± 556	0.19	8210	0.81
7	17800 ± 950	13538 ± 466	0.42	17800	0.76
11	12300 ± 220	5264 ± 767	0.34	12300	0.43
13	5420 ± 650	7717 ± 430	0.33	5410	1.43
15	8080 ± 235	7057 ± 1690	0.43	8080	0.87

Table 4.5: Results of the box-model for nitrate concentrations. Observed “pre” and “post” $[\text{NO}_3^-]$ compared with predicted final concentrations from the box-model. The final predicted concentrations were shown here were calculated by estimating the flux of nitrate from the nitrate uptake and nitrite oxidation rates over the incubation period (12 hours). The observed/predicted ratio gives an indication of the differences between the two concentrations.

Ammonium fluxes

Potential for ammonium oxidation and regeneration

Ammonium fluxes were considered in the same way as the nitrate fluxes - a predicted final concentration based only on ammonium uptake was compared to the observed “post” concentration. For ammonium, uptake and oxidation are two competing sinks whereas the only sink for nitrate is uptake by phytoplankton. The difference between the predicted and observed concentrations in ammonium concentrations can also give an indication of potential regeneration rates. If the predicted losses from the ammonium uptake rates are greater

than the observed losses, this indicates a potential for ammonium oxidation. For instance, at CTD 1, the observed losses of ammonium were $230 \text{ nmol} \cdot \text{L}^{-1}$ and the predicted $163 \text{ nmol} \cdot \text{L}^{-1}$. The difference in predicted and observed change corresponded to the accumulated nitrite ($70 \pm 122 \text{ nmol} \cdot \text{L}^{-1}$). The large error in the change of nitrite concentration is due to the differences in nitrite concentrations in the enrichment and dilution experiment.

There was a similar observation at CTD 11 where the observed ammonium loss was $94 \text{ nmol} \cdot \text{L}^{-1}$ but the losses due to ammonium uptake were expected to be $57 \text{ nmol} \cdot \text{L}^{-1}$. The potential for ammonium oxidation at this station is also seen from the average accumulation of nitrite ($53 \pm 60 \text{ nmol}$).

Disparities between the amount of ammonium potentially oxidised ($37 \text{ nmol} \cdot \text{L}^{-1}$) and the accumulation of nitrite ($53 \pm 60 \text{ nmol}$) are due to the fact that only net fluxes are being considered. The regeneration of ammonium can lead to an underestimate of ammonium depletion (through uptake and oxidation) as it replenishes the ammonium pool. On the other hand, nitrite production will be underestimated if it is slower than nitrite oxidation. At CTD 11, this is expected given the observed nitrite oxidation ($217 \pm 88 \text{ nmol} \cdot \text{L}^{-1} \cdot \text{h}^{-1}$). At such a rate, $2600 \pm 1050 \text{ nmol} \cdot \text{L}^{-1}$ of nitrite would be oxidised during the course of the incubation. However, the source of this nitrite is unaccounted from our observations and this box-model.

Depth profiles of ammonium fluxes

At CTD 1, 2 (where nitrification experiments were not conducted) and 13, depth profiles were available for the ammonium uptake as well as the “pre” and “post” incubation ammonium concentrations. Plotting the “pre” and “post” incubation ammonium profiles (figure 4.10) do not show consistent patterns of ammonium loss and accumulation with depth.

At CTD 1 (Polar Frontal Zone station), there is a loss of ammonium at the 55% light depth, corresponding to the maximum ammonium uptake rate (see figure 3.16). Below the surface, the accumulation of ammonium peaked at 20 m. These variations in accumulation and loss of ammonium between 20 and 60 m cannot be attributed to changes in uptake rates as the latter did not vary much vertically between these depths. The highest chlorophyll concentration ($0.631 \mu\text{g} \cdot \text{L}^{-1}$ before incubation) was found at 20 m. There are two possibilities for the peak ammonium concentration at 20 m. The first possibility is that the regeneration of ammonium could have been maximum at this depth (Whitehouse et al., 2011). The second would be that ammonium oxidation increased with depth and lead to a lower accumulation of ammonium at 40 m and 60 m. However, determining the relative importance of the two processes is not possible without ammonium oxidation and regeneration profiles.

At CTD 2 (Glider station), ammonium accumulation was observed at 10 m where uptake was maximum ($2.19 \text{ nmol} \cdot \text{L}^{-1} \cdot \text{h}^{-1}$). At 40 m, where uptake was minimum ($0.99 \text{ nmol} \cdot \text{L}^{-1} \cdot \text{h}^{-1}$), there was a loss of ammonium. Based solely on the uptake rates, this accumulation and loss pattern is counter-intuitive. The differences would therefore be due to changing patterns in ammonium regeneration and oxidation through the water column.

At 40 m, $74.0 \text{ nmol} \cdot \text{L}^{-1}$ of ammonium was used during the incubation. However, based on the ^{15}N measurements, only $11.8 \text{ nmol} \cdot \text{L}^{-1}$ can be attributed to ammonium assimilation by phytoplankton. The rest, $62.1 \text{ nmol} \cdot \text{L}^{-1}$ could have been oxidised to nitrite. This depth also corresponded to the maximum nitrite concentration within the euphotic zone ($300 \text{ nmol} \cdot \text{L}^{-1}$). It is likely that the importance of ammonium oxidation increased with depth. It is to be noted that given that changes in nitrite or nitrification rates were not measured at 40 m, it is also possible that some of the ammonium was converted to DON rather than nitrite (Slawyk and Raimbault, 1995). The absence of direct measurements of ammonium regeneration and the limitations of using net concentration changes preclude from drawing any conclusions with regards to the variability of ammonium regeneration with depth.

Finally, at CTD 13, the ammonium loss was observed at 10 and 40 m but accumulation at 20 m and 60 m. At 10 m, the net ammonium loss rate was $4.25 \text{ nmol} \cdot \text{L}^{-1} \cdot \text{h}^{-1}$. This is very close to the ammonium uptake ($4.47 \text{ nmol} \cdot \text{L}^{-1} \cdot \text{h}^{-1}$). Moreover, nitrite production was observed ($6.10 \pm 1.06 \text{ nmol} \cdot \text{L}^{-1} \cdot \text{h}^{-1}$) and nitrite concentration were the highest ($220 \text{ nmol} \cdot \text{L}^{-1}$) at this depth. Given the ammonium uptake and oxidation rates, the total ammonium loss should be equal $10.57 \text{ nmol} \cdot \text{L}^{-1} \cdot \text{h}^{-1}$ and a total of $130 \text{ nmol} \cdot \text{L}^{-1}$ over the course of the whole incubation. As the measured loss of ammonium was only $51 \text{ nmol} \cdot \text{L}^{-1}$, it would imply that the net ammonium regeneration rate would be $6.3 \text{ nmol} \cdot \text{L}^{-1} \cdot \text{h}^{-1}$.

To summarise, ammonium uptake rates ranged between 1.35 to $10.72 \text{ nmol} \cdot \text{L}^{-1} \cdot \text{h}^{-1}$ and while ammonium regeneration ranged from -3.13 to $37.13 \text{ nmol} \cdot \text{L}^{-1} \cdot \text{h}^{-1}$ (according to the box model). However, there were no consistent patterns of ammonium loss (through uptake or oxidation) and accumulation (through regeneration) with depth. Furthermore, in some cases, the disparities between the "pre" and "post" incubation ammonium concentrations indicate that ammonium oxidation might have been significant.

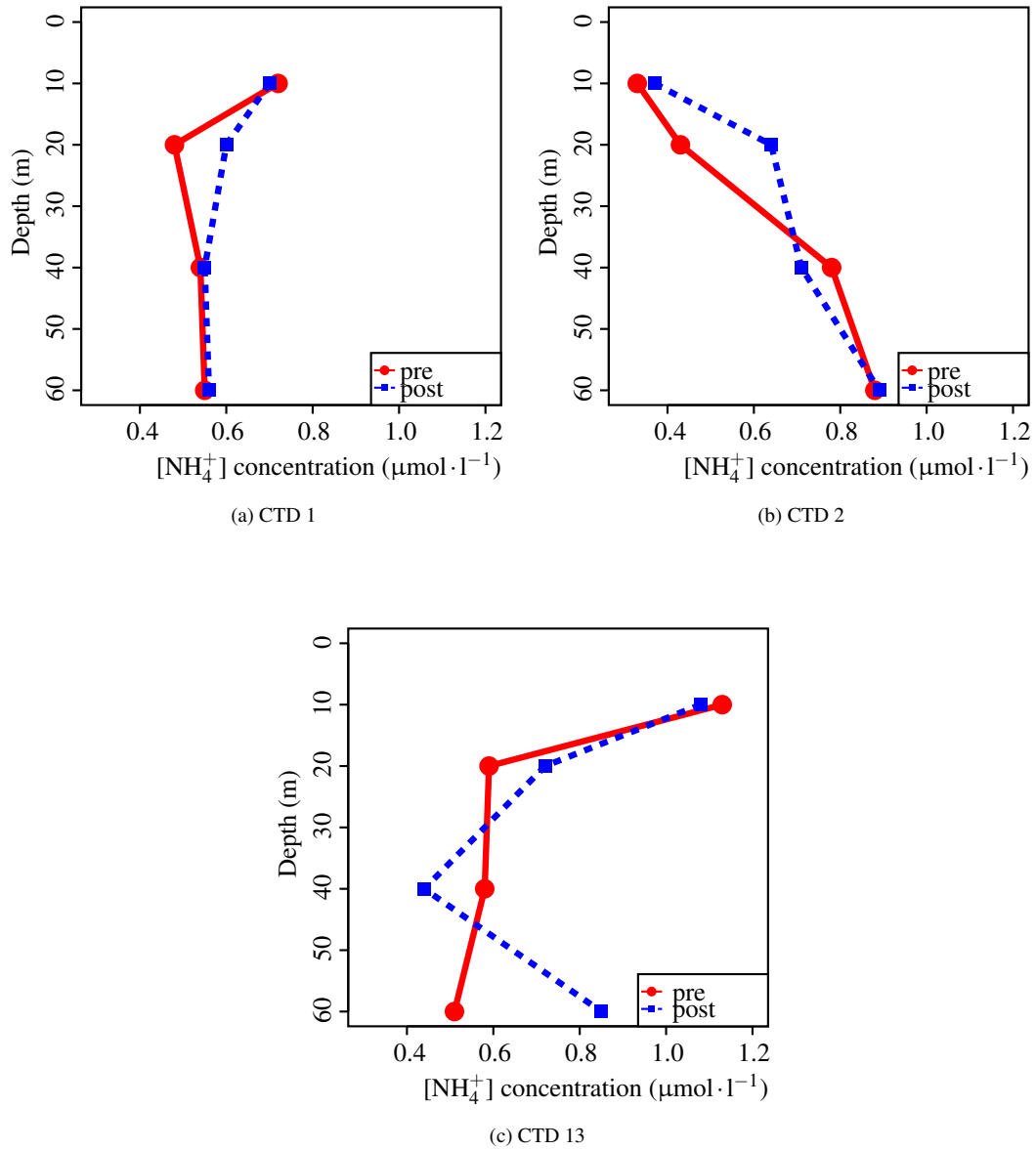


Figure 4.10: Ammonium concentrations before ("pre") and after ("post") incubation for (a)CTD 1 , (b)CTD 2 (b) and (c) CTD 13 . The red solid line represent $[\text{NH}_4^+]$ before incubation and the blue dashed line $[\text{NH}_4^+]$ after incubation

4.3.3 Nitrite profiles

This section describes nitrite profiles which provide supporting evidence for nitrification processes in the water column (Meeder et al., 2012). The nitrite profiles can also provide an overview of the distribution of processes affecting nitrite distribution. The balance between the sources (release of nitrite by phytoplankton, ammonium oxidation) and sinks (nitrite uptake by phytoplankton and nitrite oxidation) of nitrite can contribute to nitrite maxima and minima (Mackey et al., 2011; Malerba et al., 2012). Mackey et al. (2011) showed typical nitrite profile in a well stratified water column and how the importance of the various processes is expected to vary with depth (figure 4.11). The relative importance of the processes in the euphotic zone of the Southern Ocean is likely to be different from the profile presented by Mackey et al. (2011). For instance, in contrast to the processes presented in figure 4.11, the importance of nitrite assimilation in the euphotic zone of the Southern Ocean is likely to be minimal. In the presence of excess nitrate as in HNLC regions, the potential for nitrite uptake is reduced (Olson, 1981a). Mackey et al. (2011) also assume that nitrate reduction by phytoplankton is minimal within the euphotic zone because this process occurs mainly under light limited conditions. However, the phytoplankton were light-limited during the winter cruise as discussed in chapter 3. Consequently, some excretion of nitrite by phytoplankton is possible.

There are few caveats in using nutrient profiles to determine the importance of biogeochemical processes. Meeder et al. (2012) adjusted the profile depths based on density in order to extract the biogeochemical signal. This was not done here and the changes observed in nitrate and nitrite might be related to density driven changes (Omand and Mahadevan, 2013) as well as biogeochemical processes. While processes altering nutrient concentrations (e.g uptake and remineralisation) are depth dependent, the redistribution of nutrients, specially below the euphotic zone, is also affected by the positions of the isopycnals (surfaces of constant density)(Omand and Mahadevan, 2013). There is little mixing between across these surfaces which can be moved up and down by physical processes such as internal waves and eddies. As the depth of the isopycnals change, the depth profiles of the nutrients also vary. However, these changes are not due to biogeochemical processes but might appear so when density is not considered(Omand and Mahadevan, 2013; Meeder et al., 2012).

The nitrite and nitrate profiles were taken before the start of the incubation. They provide a snapshot of the nitrogen budgets. However, this does not necessarily mean that the processes, which have lead to the observed state, will continue at the same rates in a incubation bottle or even in-situ. In-situ, mixing might lead to the movement of nitrifiers, grazers and phytoplankton and affect the profiles of the different nitrogen species. Nevertheless, the nutrient profiles can provide an insight with regards to the seasonality of nitrification.

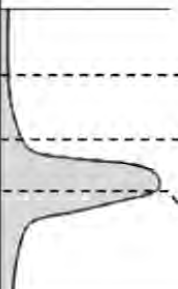
NO ₂ ⁻ inventory	Water column region	PAR (%)	NO ₂ ⁻ assimilation	NO ₂ ⁻ excretion by phytoplankton	Nitrification	
	Euphotic zone	> 1	Maximal	Minimal	Active though process is sensitive to light	
	Sub-euphotic zone	0.001- 1	Minimal	Maximal		Active though process is sensitive to light
	Upper PNM	<0.001	NA	Maximal at stratification onset, minimal activity in ongoing stratification		decoupled; NH ₄ ⁺ oxidation exceeds NO ₂ ⁻ oxidation potentially due to differential light inhibition
	Aphotic zone	<<0.001	NA	NA	NA	coupled; NO ₂ ⁻ oxidation balances NH ₄ ⁺ oxidation

Figure 4.11: A typical nitrite profile and the processes which could contribute to such a profile. This figure has been adapted from Mackey et al. (2011). At specified depths, "Maximal" or "minimal" represent the relative rates of the process within the water column and NA is shown where a process is expected to be negligible.

Figure 4.12 show nitrite profiles for the winter cruise up to the 400 m depth. Full profiles are shown in Appendix B. At station 15N-2, nitrite concentration increased from the surface to about 100 m, which is the base of the euphotic zone. It also shows a deep nitrite maximum below the MLD at about 300 m. Station 15N-3 on the other hand showed a decrease in nitrite concentration with depth and no deep nitrite maximum.

In the Polar Frontal Zone, stations 15N-13 and 15N-16 showed similar profiles (figure 4.13c). Nitrite concentrations within the mixed layer were relatively homogeneous except for a dip in nitrite concentration at the bottom of the euphotic zone at 40 – 50 m. The concentration of nitrite then decreased to zero below the mixed layer. While station 15N-15 followed a similar pattern, the nitrite minimum was shallower (about 40 m than the 1% light depth (80 m)). At station 15N-5, there were two nitrite maxima. The first nitrite maximum was present at the base of the euphotic zone. The second was found, unusually, very deep (700-1000 m) where nitrite concentrations are expected to be low (figure B.7). A nitrite minimum was present at the 55% light depth where the measured nitrite oxidation rates exceeded those of nitrite production.

Station 15N-6 in the Antarctic Zone showed a variable nitrite profile with a maximum nitrite concentration at the surface and "sudden" increases at the base of the euphotic zone and at about 300 m. A similar profile was also observed at station 15N-7. These two stations were located within the Southern branch of the PF. At station 15N-8, nitrite concentrations generally decreased with depth, the maximum nitrite concentration being at the surface. Nitrite concentration at the base of the euphotic zone were slightly elevated compared to the rest of the water column although it was still lower than the maximum nitrite at this station. Unlike the other stations in the Antarctic Zone, at station 15N-11, a minimum nitrite concentration was found at the bottom of the euphotic zone. The maximum nitrite was found at the 55% light depth. This is surprising given that measured rates of nitrification showed undetectable nitrite production but very high nitrite oxidation. As the profiles only provide a snapshot view, it is possible that the high nitrite concentration was stimulating nitrite oxidation and that a decrease in nitrite would be observed at a later stage.

During the summer cruise, the water column was expected to be more stratified. This was not always the case as some mixing events increased the mixed layer depth and increased the nutrient supply during the cruise (section 3.3.1). Nitrite maxima were observed at the bottom of the euphotic zone for CTD 1, 7 and 11 (figure 4.12). At CTD 4 and 15, nitrite concentrations within the mixed layer were variable and decreased below the euphotic zone. From CTD 4 to CTD 11 and 15, there was an increase in nitrite through the water column. The maximum nitrite concentration at CTD 13 was at the 55% light depth and decreased with depth. Within the mixed layer, a minimum nitrite concentration was observed at 40 m.

4.4 Discussion

During both cruises, the two steps of nitrification appeared to be patchy. Nitrification was not detected at all stations. Through dilution experiments, significant nitrite production was only observed at two stations out of ten during the winter cruise and at one station out of six for the summer. Nitrite oxidation was quantifiable at two winter stations and one summer station. The winter station 15N-5 was the only one where both steps of nitrification were significant. The next subsection discusses whether the lack of observable nitrification could have been due to uncertainties in the measurements.

4.4.1 Are uncertainties in the measurements obscuring nitrification?

Tables 4.2 and 4.3 show a number of samples with significant differences in isotopic ratios. However, some of these stations showed a change that was not expected i.e the "post" sample had a higher $^{15}\text{N}/^{14}\text{N}$ ratio for the dilution experiment and the reverse for the enrichment experiment. The only biological factor which

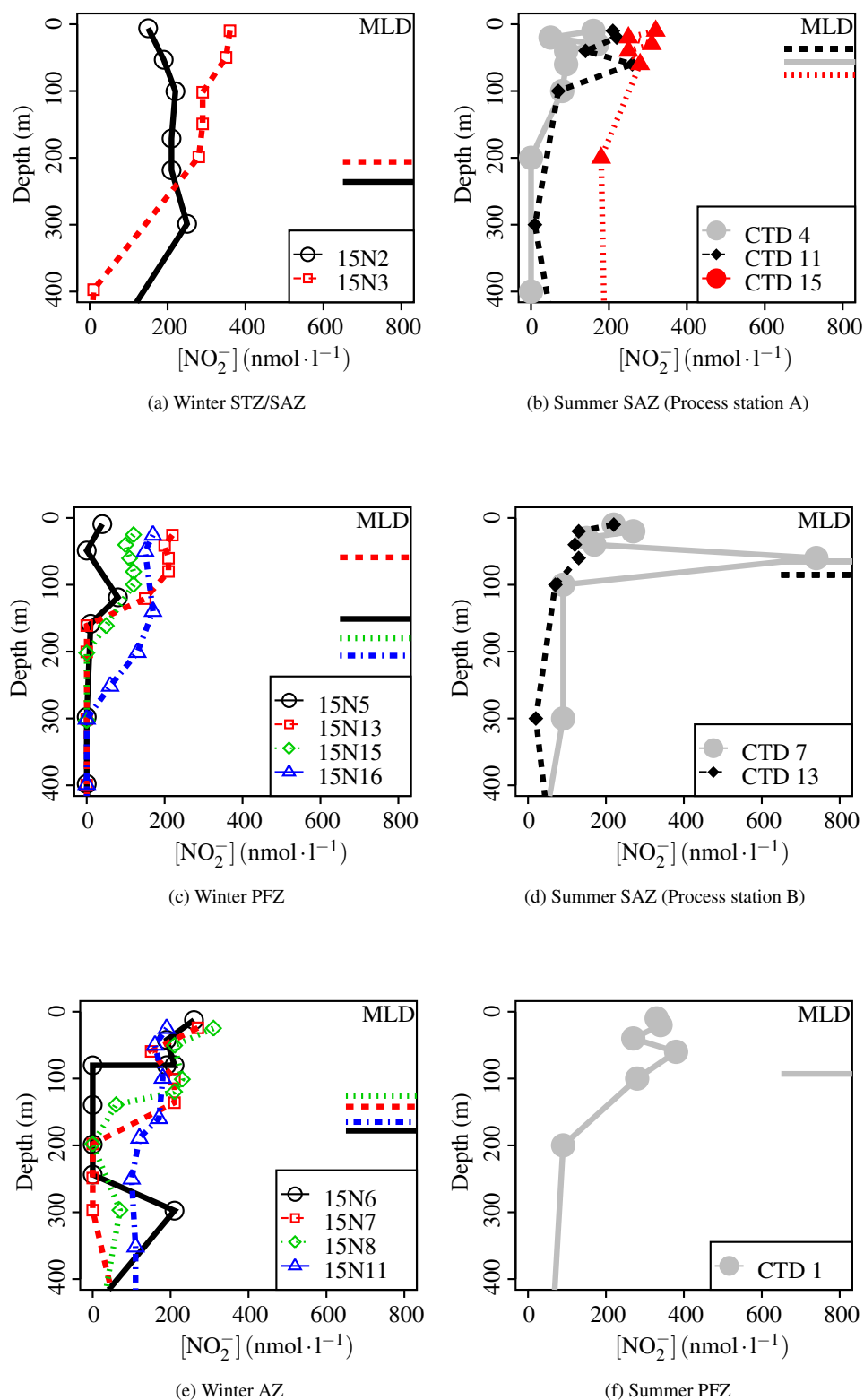


Figure 4.12: Nitrite concentration profiles for the winter cruise for stations within (a) the Subtropical/Subantarctic Zones (STZ/SAZ), (c) the Polar Frontal Zone (PFZ) (d) the Antarctic Zone (AZ) for the summer cruise and for (b) the Polar Frontal Zone station (e) Process station A (f) Process station B. The legends show the station numbers for each profile. The horizontal lines on the right of the plots represent the MLD for each station. The same line styles and colors as the nitrite profiles apply.

can affect $^{15}\text{N}/^{14}\text{N}$ is the isotope effects in biological processes as they can change the natural enrichment of the various substrate pools (Robinson, 2001). However, when adding a tracer, it is unlikely that these very small isotopic effects would be detected as the concentration of ^{15}N from the tracer (about 10% of ambient concentration of the nutrient) is much higher than the natural abundance of ^{15}N . This would therefore not be a concern in terms of the potential uncertainties in the measurements. For the winter cruise, given that the “pre” and “post” samples were not part of the same bulk sample, there is a higher risk that such errors are due to either a lack of mixing in the “pre” sample or to unequal amendments of the “pre” and “post” samples with ^{15}N . This was only observed for two NH_4^+ oxidation measurements and one nitrite oxidation measurement. However, for the summer cruise, given that the bulk sample was allowed to stand before being split into the “pre” and “post” samples, the lack of mixing and the resulting non-homogeneous bulk sample were unlikely and a more detailed analysis of the potential sources of uncertainties for each experiment was required.

Uncertainties in the summer enrichment experiment

During the summer cruise, the NO_2^- enrichment experiment was performed to determine whether nitrite was being produced primarily through ammonium oxidation or nitrate reduction. In this experiment, $^{15}\text{NH}_4\text{Cl}$ was added to the sample and the $^{15}\text{N}/^{14}\text{N}$ in the nitrite pool measured after incubation to determine the rates of ammonium oxidation. By examining $^{15}\text{N}/^{14}\text{N}$ ratio in the nitrite formed, it might be possible to identify its source. Given that the ammonium pool was enriched with ^{15}N , nitrite originating from this pool should also be enriched. On the other hand, nitrite produced by nitrate reduction would not be enriched as the nitrate pool was not labelled. In this experiment, CTDs 4, 11 and 13 showed significant decreases in isotopic ratios and increases concentrations of NO_2^- . The accumulation of nitrite indicates that nitrite production was faster than nitrite consumption. The $^{15}\text{N}/^{14}\text{N}$ ratio of this change was on average 0.249, which is the equivalent to the background $^{15}\text{N}/^{14}\text{N}$ ratio. CTD 4 can be taken as representative of the three stations. Figure 4.13 shows the change in nitrite concentration for CTD 4. The red section represents the nitrite formed during the incubation. In this case, the $^{15}\text{N}/^{14}\text{N}$ ratio of the nitrite formed during the incubation was 0.2440 implying that the source of nitrite was not enriched with ^{15}N .

If the NO_2^- formed was coming from the nitrate (unenriched source) only, the $^{15}\text{N}/^{14}\text{N}$ ratio of the nitrite pool would have been constant excluding small isotopic fractionation effects. However, a decrease in the isotopic ratio of the nitrite pool was observed. The initial enrichment of the “pre” samples (mean = 0.2837 ± 0.0134) indicates that some of the labelled ammonium was transferred to the nitrite pool. The “pre” $^{15}\text{N}/^{14}\text{N}$ ratio of the nitrite was above the background $^{15}\text{N}/^{14}\text{N}$ of an unlabelled pool. The latter is equivalent to that of the internal standard (0.2548 ± 0.0028). Given that the bulk sample was allowed to mix before being split into the pre and post sample, mixing errors are unlikely and it is possible that some of the labelled NH_4^+ was rapidly transferred into the nitrite pool. Ward et al. (1989) observed changes in isotopic ratios in an unlabelled nitrate and a labelled nitrite pool throughout time-course experiments. They observed that the nitrate pool was already labelled by their first time point after 12 minutes. After 8 hours, the isotopic ratio decreased and went back to the background value due to an isotopic dilution of the NO_2^- tracer. This resulted in a decrease in isotopic ratios from the first time point to the last. It is possible a similar pattern occurred in this study. During the 12 hour incubations, the $^{15}\text{N}/^{14}\text{N}$ in the ammonium pool could have rapidly returned to the background level in a similar way to the NO_2^- and NO_3^- tracers described by Ward et al. (1989). In studies using ammonium ^{15}N tracer to estimate uptake rates, dilution of the tracer is often cited as a cause of underestimate (Glibert et al., 1982a). Here, it would have prevented the detection of ammonium oxidation through the enrichment experiment while the ammonium uptake rates presented in chapter 3 are highly likely to be underestimates. The rates of ammonium regeneration were not measured even though they were likely to be high as seen from the box-model (section 4.3.2).

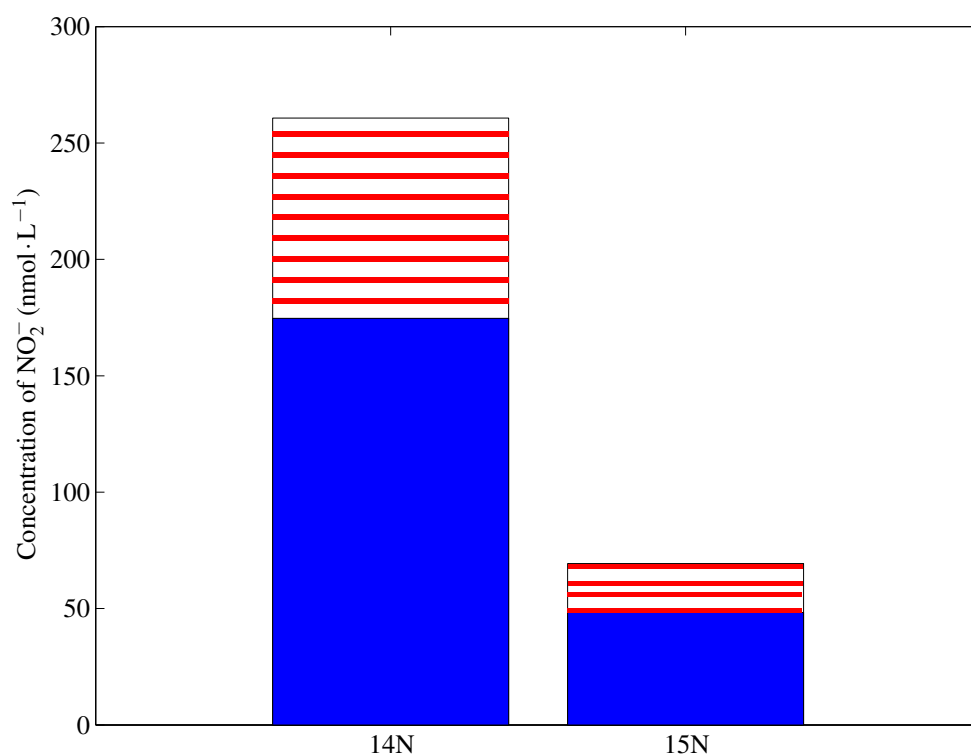


Figure 4.13: Concentration of ^{14}N and ^{15}N before (solid blue) and after (red stripes) incubation at CTD 4 for the enrichment experiment

Differences between the dilution and enrichment experiments

As mentioned earlier, the dilution and enrichment experiments were performed as an attempt to identify the source of nitrite. The two experiments also provided independent measures of nitrite concentrations before and after incubation.

To verify the samples for the dilution experiment were indeed enriched with $^{15}\text{NO}_2^-$, the enrichment ratios of the “pre” samples from the dilution experiment were compared to those from the enrichment experiment. The latter was considered to represent a baseline or ambient enrichment ratio as the nitrite pool was not labelled. Even though this pool might have already been enriched by the time the sample was filtered, this enrichment was unlikely to be as high as the enrichment of a sample to which $^{15}\text{NO}_2^-$ was added at 10% of the ambient concentration. This comparison (figure 4.14) showed that the tracer was detectable in the NO_2^- pool for the dilution experiment and that mixing should not have been an issue for most of the stations.

In the NO_2^- dilution experiments, CTD 1, 4, 7 showed significant increases in enrichment ratios. For CTD 4 and 7, it is possible that this was due to insufficient mixing. However, for CTD 4, only 2 replicates were measured and they gave very different results. Consequently, the validity of this measurement is questionable. For CTD 7, there was a very small difference between the isotopic enrichment of the “pre” sample from the dilution and enrichment experiments indicating that mixing could have been an issue. Furthermore, CTD 7 did not show a significant change in the concentrations of ^{15}N and ^{14}N . This is a contradiction to the enrichment experiment where a significant accumulation of nitrite was observed.

For CTD 1, the pre sample for the dilution experiment was highly enriched. However, the apparent increase in $^{15}\text{N}/^{14}\text{N}$ ratio after incubation could be due to the wide spread in the post sample (mean = 0.7628 ± 0.0315 , figure 4.15). Here again, there was some contradiction between the enrichment and dilution experiments. The change in nitrite concentration was not statistically significant for the enrichment experiment but was for the dilution experiments.

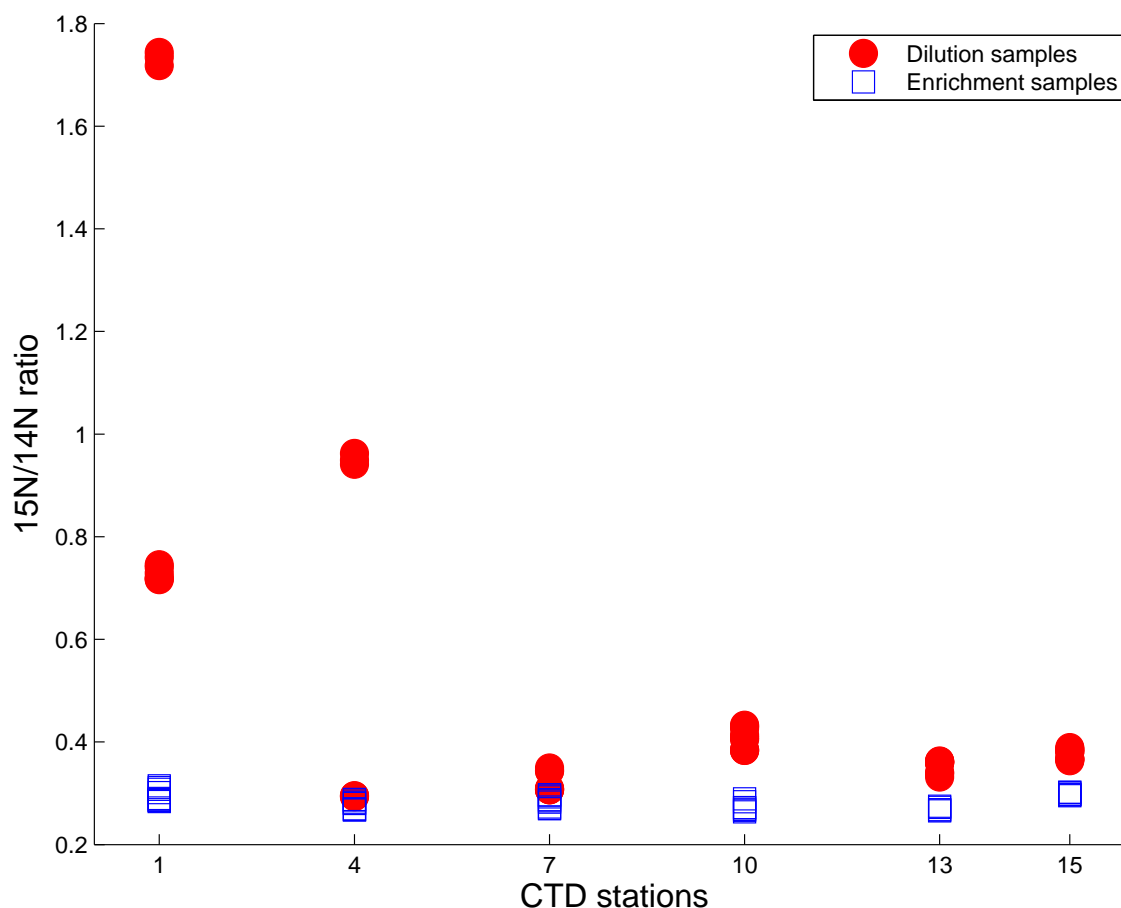


Figure 4.14: Comparisons of the "pre" enrichment ratio for the enrichment and dilution experiments during the summer cruise. This plot confirms that the nitrite pool in the dilution experiment were properly labelled with the ^{15}N tracer except at CTD 4.

In both cases (CTDs 1 and 7), the apparent significant differences in isotopic ratios could be due to the small sample size (i.e small number of observations). The efficacy of the Mann-Whitney test is reduced when there is a small number of observations. Such non-definitive results were one of the difficulties encountered when comparing the dilution and enrichment experiments for the determination of ammonium oxidation rates. This was also problematic when trying to determine the sources of uncertainties and variability.

Uncertainties in estimating NO_2^- oxidation

This section highlights the uncertainties which could have obscured nitrite oxidation during the summer cruise. In the experiments measuring the rates of NO_2^- oxidation (through isotopic dilution of a nitrate tracer), only CTD 1 and 4 showed a significant increase in isotopic ratio instead of the expected decrease.

At CTD 1, the increase in nitrate concentration was significant (p value = 0.0004). This is the first indicator of nitrate regeneration (nitrite oxidation). Such increases in concentration should be accompanied by isotopic dilutions. In this case, the source of nitrate seemed to be slightly enriched in ^{15}N (change in ^{15}N /change in ^{14}N = 0.297). While this could again be due to the mixing, it could also be due to unknowns in the isotopic mass balance i.e other nitrogen pools might have become labelled during the incubation (Slawyk and Raimbault, 1995; Ward et al., 1989). In the latter case, nitrification may have been obscured by unquantified processes.

At CTD 4, the change in ^{15}N and ^{14}N concentrations were not significant but the increase in $^{15}\text{N}/^{14}\text{N}$ ratio was. Here again, it is possible that the significant difference observed in isotopic ratio was due to the reduced

power of the Mann-Whitney test and that nitrification was not significant.

In other cases, nitrification may have been happening but the spread in the $^{15}\text{N}/^{14}\text{N}$ ratios could obscure the isotopic dilution. For instance, CTD 7,13 and 15 showed isotopic dilution, which were not statistically significant. CTD 13 also showed an increase in nitrate concentration suggesting that nitrite oxidation may have been faster than nitrate uptake.

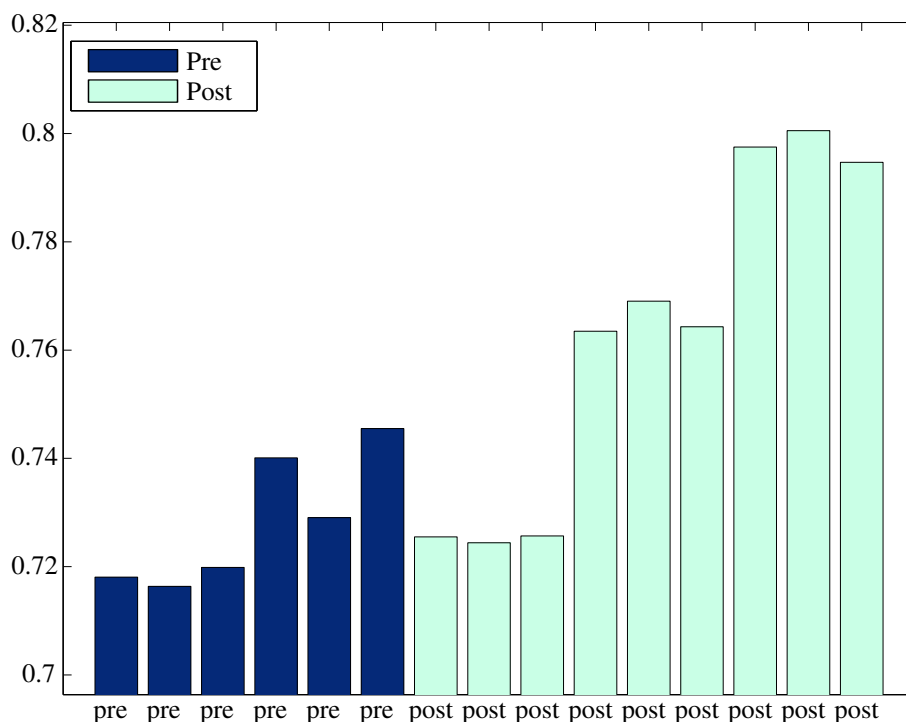


Figure 4.15: Comparisons of the "pre" and "post" $^{15}\text{N}/^{14}\text{N}$ ratio (after outliers have been removed) for the dilution experiment at CTD 1 of the summer cruise showing the wide spread of isotopic ratios

4.4.2 Comparison against previously reported rates

Ammonium oxidation/Nitrite production

The box model was used to determine net fluxes of nitrogen (NO_2^- , NO_3^- and NH_4^+) for the summer cruise. During the summer cruise, nitrite was accumulated at all the stations except CTD 15. The net nitrite production rates calculated from the box-model ranged from -0.94 to $7.58 \text{ nmol} \cdot \text{L}^{-1} \cdot \text{h}^{-1}$. At CTD 15, nitrite sinks were faster than nitrite sources. Nitrite oxidation was observed from neither the isotopic dilution nor the box model but the uptake of nitrite by phytoplankton could have been tapping into the nitrite pool (Malerba et al., 2012). At CTD 13, the potential NO_2^- production rate from the box model was very close to the measured rate. There was also a loss of ammonium confirming that ammonium oxidation was more likely than excretion of nitrite by phytoplankton. However, it could not be quantified through the enrichment experiment due to the rapid isotopic dilution of the ammonium tracer (section 4.4.1). As mentioned in section 4.4.1, the dilution of the ammonium tracer can result in underestimation of ammonium uptake or oxidation rates. Indeed, ammonium oxidation measured by isotopic dilution can be 2 - 3 times higher than when measured using tracer enrichment techniques (Carini et al., 2010).

The nitrite production rates (0.824 ± 0.298 to $6.08 \pm 1.06 \text{ nmol} \cdot \text{L}^{-1} \cdot \text{h}^{-1}$) compare well with ammonium oxidation rates presented in the literature both for the Southern Ocean and other regions. Olson (1981a) estimated ammonium oxidation rates between 0 to $0.537 \text{ nmol} \cdot \text{L}^{-1} \cdot \text{h}^{-1}$ in the Ross and Scotia sea. Bianchi

et al. (1997) measured ammonium and nitrite oxidation rates using inhibitors across a transect going from 40 °S to 54 °S for depths between 0 to 100 m. Rates of ammonium oxidation at the surface were about $1 \text{ nmol} \cdot \text{L}^{-1} \cdot \text{h}^{-1}$ for the whole transect. These rates, however, could be an underestimation. In the study by Bianchi et al. (1997), Allylthiourea (ATU) was used as an inhibitor. However, this inhibitor would not have targeted archaeal nitrifiers, which have been found to be ubiquitous in the ocean (Francis et al., 2005; Fernández and Farías, 2012). Grundle et al. (2013) reported rates between 0 and $4 \text{ nmol} \cdot \text{L}^{-1} \cdot \text{h}^{-1}$ in the subpolar North Pacific. The rates for the sub-polar North Atlantic presented by Painter (2011) were much higher (28 ± 11 to $123 \pm 11 \text{ nmol} \cdot \text{L}^{-1} \cdot \text{h}^{-1}$) and of a similar order of magnitude to the nitrite oxidation rates in this study. Painter also observed patchiness in the occurrence of nitrification as well as the influence of eddies on nitrification rates.

Nitrite oxidation

The nitrite oxidation rates measured in this study (37.2 ± 9.1 - $217 \pm 88 \text{ nmol} \cdot \text{L}^{-1} \cdot \text{h}^{-1}$) are much higher than rates presented in the literature. Maximum rates of nitrite oxidation reported range between 0.104 – $29.0 \text{ nmol} \cdot \text{L}^{-1} \cdot \text{h}^{-1}$ (Clark et al., 2014; Beman et al., 2013; Bianchi et al., 1997, 1999; Carini et al., 2010; Clark et al., 2011, 2008; Dore and Karl, 1996; Fernández et al., 2009; Fernández and Raimbault, 2007; Grundle and Juniper, 2011; Grundle et al., 2013). Bianchi and Feliatra (1999) measured maximum rates of $96 \text{ nmol} \cdot \text{L}^{-1} \cdot \text{h}^{-1}$. However, these were measured at a shallow station (about 200 m) which was influenced by a plume from the Rhône River. This resulted in enhanced nitrification rates. On the other hand, in the Southern Ocean, the euphotic nitrification rates reported by (Cavagna et al., 2014) ranged from undetectable to $125 \text{ nmol} \cdot \text{L}^{-1} \cdot \text{h}^{-1}$. While these rates are relatively close to the rates measured in the current study, they were measured through the isotopic dilution of a $^{15}\text{NO}_3^-$ tracer by both ammonium and nitrite oxidation. As such, they would represent an overestimate of nitrite oxidation unless any nitrite formed through ammonium oxidation was immediately used up by nitrite oxidation. This, however, is not always the case (see section 4.4.3).

It is possible that only the very high rates of nitrite oxidation were detectable. Nitrate concentrations during the winter cruise reached $35 \text{ } \mu\text{mol} \cdot \text{L}^{-1}$. Low nitrification rates might not produce significant decreases in the isotopic ratio when the background nitrate is so high. High rates were also derived from the box-model. The concentration of nitrate increased during the course of the incubation for CTD 1 and CTD 13. Net nitrate regeneration rates were $583 \pm 189 \text{ nmol} \cdot \text{L}^{-1} \cdot \text{h}^{-1}$ at CTD 1 and $192 \pm 65 \text{ nmol} \cdot \text{L}^{-1} \cdot \text{h}^{-1}$ at CTD 13. At neither of these stations was an isotopic dilution observed. Given observed rates in this study, the net nitrate regeneration rate from the box model for CTD 13 would be reasonable whereas the net nitrate regeneration rate at CTD 1 seems higher than expected. In order to assess the accuracy of these measurements, repeat measurements in the region are required.

4.4.3 Decoupling of ammonium and nitrite oxidation

Ammonium oxidation is often considered a rate limiting step in the conversion of ammonium to nitrite (Grundle et al., 2013; Yool et al., 2007). This is in contrast to the present study as the nitrite production rates were much smaller than the nitrite oxidation rates. Moreover, the fact that significant nitrite production and oxidation were not detected simultaneously at all stations indicates that nitrite production is not a rate limiting step. For instance, nitrite oxidation was significant at the winter station 15N-11 ($37.2 \pm 9.1 \text{ nmol} \cdot \text{L}^{-1} \cdot \text{h}^{-1}$) and at the summer station CTD 11 ($217 \pm 88 \text{ nmol} \cdot \text{L}^{-1} \cdot \text{h}^{-1}$) but nitrite production undetectable in both cases. At the winter station 15N-13 and summer CTD 13, nitrite production, at rates of 0.824 ± 0.298 and $6.10 \pm 1.06 \text{ nmol} \cdot \text{L}^{-1} \cdot \text{h}^{-1}$ respectively, were not followed by detectable nitrite oxidation. While Bianchi et al. (1997) occasionally measured nitrite oxidation rates higher than ammonium oxidation rates, they also

observed a positive correlation between the two rates. Such a coupling was not observed here. The decoupling of the two steps of nitrification is common and occur for various reasons such as differential photosensitivity of nitrite and ammonia oxidising microorganisms (Olson, 1981b; Füssel et al., 2012)

However, it is to be noted that in the present study, nitrite oxidation occurred when $[\text{NH}_4^+]$ was high. For instance, stations 15N-5 and 15N-11 were amongst those with the highest NH_4^+ concentration ($0.35 \mu\text{mol} \cdot \text{L}^{-1}$ and $1.79 \mu\text{mol} \cdot \text{L}^{-1}$ respectively at the 55% light depth (figure 3.18). Since the nitrite concentrations were correlated to ammonium concentrations, this could indicate a degree of coupling between the regeneration of ammonium, nitrite and nitrate (Souza et al., 2014). However, given the small number of observations and large variability, it is not possible to conclusively establish such a relationship.

4.4.4 Seasonal differences in nitrification rates

At first glance, it would seem that both nitrite production and oxidation rates were higher in summer than in winter. This would be in contrast with findings by Grundle et al. (2013), Smart (2014) and DiFiore et al. (2009). All three studies pointed to an increase in nitrification in winter. In the subarctic Pacific, Grundle et al. (2013) attributed this seasonal pattern to changes in the amount of incident light. However, differences between the summer and winter rates presented here might be geographical rather than seasonal. Other than CTD 1, all the summer stations were located within the Subantarctic Zone (as defined in Chapter 3). The winter station locations ranged from the Subtropical Zone to the Antarctic Zone. The seasonal patterns in those regions are not homogeneous when it comes to primary productivity and chlorophyll concentrations (Thomalla et al., 2011a). It is likely that the seasonal cycle of nitrification is not homogeneous either.

A heterogeneous pattern in nitrification would also be confirmed by the study by Smart (2014). Smart (2014) determined the profiles of $\delta^{15}\text{N}$ and $\delta^{18}\text{O}$ in the NO_3^- pool and evaluated the level of decoupling between the two in the upper water column. Deviations from 1:1 $\delta^{15}\text{N}$ - $\delta^{18}\text{O}$ relationship would be due to processes other than nitrate assimilation and the remineralisation of the resulting organic matter. Smart (2014) concluded that in winter, nitrification dominated the isotopic signature of the nitrate pool in the Antarctic Zone and that nitrification and nitrate uptake were roughly equivalent in the Polar Frontal Zone. This highlighted differential significance of nitrification across the various zones of the Southern Ocean.

It is to be noted that the study conducted by Smart (2014) was done on the same winter cruise as the present study. The $\delta^{15}\text{N}$ signature in Smart (2014) represents an integration of the processes over long timescales while instantaneous rates were measured in this study. This could explain why nitrification was not observed at every station in the study even though there is evidence pointing towards the importance of the process.

The variations between the summer nitrite profiles as well as observed nitrification rates show that differences cannot be attributed to a seasonal pattern. This is also compounded by the fact that there was only one station in the Subantarctic Zone during the winter cruise. The nitrite profiles also lacked a clear seasonal pattern. The profile at station 15N-3 in the Subantarctic Zone was similar to the profiles from CTDs 4, 13 and 15 of the summer cruise: the nitrite concentration was maximum in the surface and decreased very quickly below the mixed layer. These nitrite profiles were different from the profiles at CTDs 7 and 11. The latter showed primary nitrite maxima below the surface (figure B.1, appendix B). This indicates a high degree of intra-seasonal variability. Repeat transects with multiple stations would be required to provide more definitive conclusions.

4.4.5 Factors affecting nitrification

Role of the microbial community

In line with the studies by Grundle et al. (2013), Smart (2014) and DiFiore et al. (2009), an increased importance of nitrification in winter relative to summer can be seen from studies on the microbial ecology of the Southern Ocean. Grzymski et al. (2012) presented a metagenomic assessment of the bacterial community for the coastal Antarctic peninsula in winter and summer. In winter, they observed a higher bacterial diversity than in summer. They reported the presence of the ammonia oxidiser *Ca.N. maritimus* in winter but not in summer. Nitrite oxidisers were also detected in winter. However, they could not be identified. Furthermore, 18-37% of the winter bacterial and archaeal community showed a potential for chemolithoautotrophy (the ability of deriving energy from the oxidation of inorganic compounds). Only 1% of the summer community constituted of such organisms. Over the last decade, AOA have been shown to be ubiquitous in the world's ocean and not constrained to the deep ocean. Consequently, they could play an important role for water column nitrification in the Southern Ocean.

Depth and light availability

Nitrification is a photosensitive process and is reduced in the presence of light. Nitrification rates are therefore expected to increase with depth (Beman et al., 2012; Olson, 1981b). In this study, nitrification rates were only measured at the 55% light depth. Nitrification (both nitrite and ammonium oxidation) was not detected at all stations. Given the prevalence of nitrifiers as well as the $\delta^{15}\text{N}$ and $\delta^{18}\text{O}$ patterns, it is likely that nitrification occurred at faster, detectable rates at deeper depths which were not sampled as both processes are photosensitive. Rates of nitrification have been shown to increase with depth in the Southern Ocean (Bianchi et al., 1997; Olson, 1981b) as well as in other regions (Ward, 2005). Grundle et al. (2013) noted that the highest observed rates of ammonium oxidation were always at the lowest light depth. However, the relative light intensity is not the main controlling factor. The absolute light intensity would be more important. This is thought to explain why nitrification was still observed at the 55% light depth. Decreases in the absolute amount of incident light could have allowed the nitrifiers to recover from the photoinhibition.

The box model indicated that in some cases, nitrification could have occurred but were either undetected by the isotopic dilution or occurred at depths where it was not measured. For instance, at CTD 13 from the summer cruise, the loss of ammonium due to uptake at 40 m was about $85 \text{ nmol} \cdot \text{L}^{-1}$ but the observed ammonium loss was $133 \text{ nmol} \cdot \text{L}^{-1}$. This loss could be related to ammonium oxidation. Nitrite production was observed at the 55% light depth indicating that ammonium oxidisers were likely to be present in the water column. The same would apply for CTD 2 (Glider station) where ammonium accumulation was observed in the surface but at 40 m, an ammonium loss of $62 \text{ nmol} \cdot \text{L}^{-1}$ could not be attributed to uptake. The total ammonium loss at the latter depth was $74 \text{ nmol} \cdot \text{L}^{-1}$, but the measured uptake rates only accounted for an ammonium loss of $12 \text{ nmol} \cdot \text{L}^{-1}$. This would imply that ammonium oxidation was more increased with depth at this station.

Grzymski et al. (2012) suggested that excess N (positive N^* , $[\text{NO}_3^-] - 16[\text{PO}_4^{3-}]$) could be due to winter nitrification in the Southern Ocean. This was not consistently observed during this study. N^* was higher (more positive) at CTD 1 from the summer cruise than all of the winter Polar Frontal Zone stations (figure 4.16). This indicates, as described by Giddy et al. (2012), that the winter conditions were limiting for phytoplankton growth and corresponds to the low nitrogen uptake rates in chapter 3. At station 15N-5 where both nitrite production and oxidation was observed, N^* increased from the surface and peaked at 120 m (1% light depth). Given the strong mixing in winter, such variations in N^* are more likely to be due to regeneration processes rather than shifts in the community composition with depth (Giddy et al., 2012). This would indicate that

nitrite oxidation (nitrate regeneration) was at a maximum at the bottom of the euphotic zone as has been observed in other regions (Ward and Zafriou, 1988; Clark et al., 2008).

However, this N^* profile was very different to most of the other winter stations, both inside and outside of the Polar Frontal Zone. It is possible that the pattern in N^* observed at station 15N-5 is present because of the potential coupling between nitrite production and oxidation (section 4.4.3). Clear relationships between nitrification and N^* can only be established if reliable nitrification rates are available. At several stations in this study, the potential increase in nitrification with depth was not supported by the N^* patterns. For instance, at the winter station 15N-11, N^* at 50 m (50% light depth) was low ($-6.5 \mu\text{mol} \cdot \text{L}^{-1}$) even though nitrite oxidation was detected at this depth. The maximum N^* ($-5.23 \mu\text{mol} \cdot \text{L}^{-1}$) was found at 25 m rather than at the base of the mixed layer where nitrification is usually expected to be maximum.

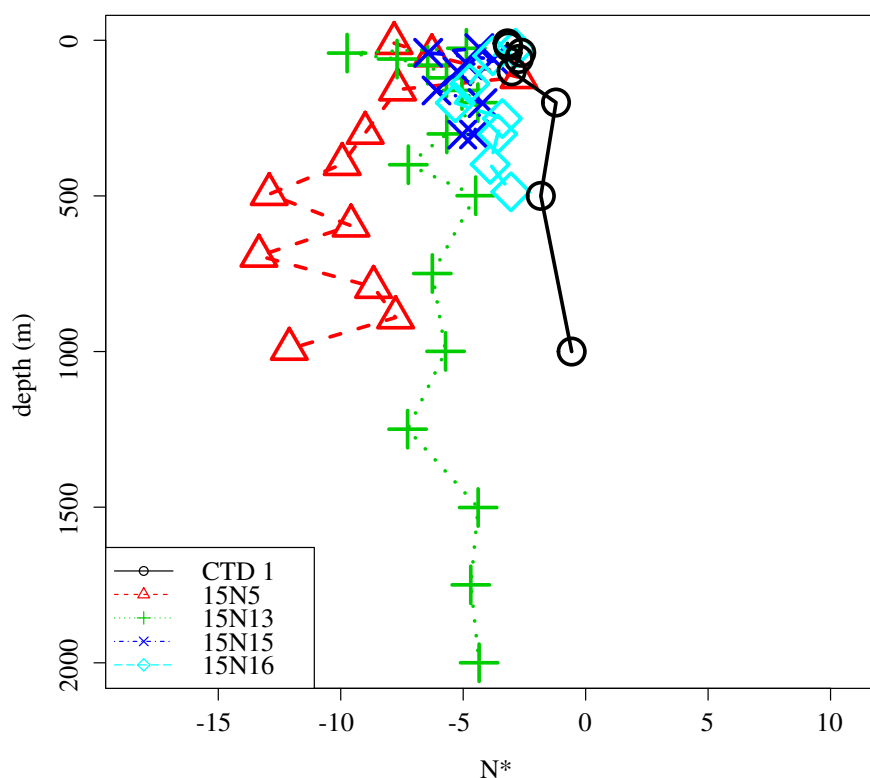


Figure 4.16: N^* for stations located in the Polar Frontal Zone for both the summer (CTD 1) and winter (15N-5, 15N-13, 15N-15, 15N-16) cruises.

The nitrite and nitrate profiles can also give an indication of nitrification processes within the water column (figure 4.12 and appendix B). For instance, the nitrite maximum at station 15N-2 was located at 300 m. The presence of this nitrite maximum indicates a potential role for nitrification at these depths. Nitrate formed below the winter mixed layer is generally considered as "new" nitrate. However, mixed layer depths in winter can reach more than 300 m (de Boyer Montégut et al., 2004). If any nitrate was being formed by nitrification at this depth and the mixed layer increased, it would have to be considered "regenerated" nitrate. This approach was taken by Yool et al. (2007) who considered any nitrate regenerated above the permanent thermocline (even if outside of the euphotic zone) as "regenerated" nitrate.

At the winter stations 15N-6 and 15N-7, the nitrite minimum coincided with nitrate maximum both within and just below the mixed layer. At both stations, nitrate peaked with concentration about $35 \mu\text{mol} \cdot \text{L}^{-1}$ just below the mixed layer. Since this peak nitrate concentration is larger than deeper nitrate concentrations where

nitrate cannot be consumed by phytoplankton, this could indicate high nitrite oxidation rates. Furthermore, these stations were located within the Antarctic zone where nitrification has a major impact on the decoupling $\delta^{15}\text{N}$ $\delta^{18}\text{O}$ in winter (Smart, 2014).

Substrate availability

15N-5 is the only Polar Frontal Zone station where nitrite oxidation was detected. Of the stations located in the Polar Frontal Zone, station 15N-5 had the lowest nitrite concentration and the highest nitrate concentration while nitrate uptake rates were similar. This is in contradiction with previous studies. Olson (1981a) and Beman et al. (2013) have shown that nitrite oxidation increases with nitrite concentration in natural assemblages.

In this study, nitrite production was higher at station 15N-5 ($3.38 \pm 0.22 \text{ nmol} \cdot \text{L}^{-1} \cdot \text{h}^{-1}$) than at station 15N-13 ($0.824 \pm 0.298 \text{ nmol} \cdot \text{L}^{-1} \cdot \text{h}^{-1}$). The main difference in biogeochemical conditions between station 15N-5 and the other Polar Frontal Zone stations was the ammonium concentrations. At stations 15N-13, 15N-15 and 15N-16, ammonium concentrations were very low (from undetectable levels to $0.07 \mu\text{mol} \cdot \text{L}^{-1}$) at both the 55% and 1% light depth. The concentrations of particulate nitrogen (PN) could be separated in two groups: 15N-5 and 15N-16 on the one hand (with PN concentrations of 6.10 and $6.38 \mu\text{g} \cdot \text{NL}^{-1}$ respectively) and 15N-13 and 15N-15 (with PN concentrations of 2.93 and $4.01 \mu\text{g} \cdot \text{NL}^{-1}$ respectively) on the other. Since nitrification was detected at one station from each of these pairs (stations 15N-5 and 15N-13) rather than only at stations in the pair with higher particulate nitrogen, the differences in particulate nitrogen do not seem to be influencing the nitrification rates as much as the presence of ammonium. This would be expected as the link between ammonium and nitrification is more direct than that between particulate nitrogen and nitrification. Particulate matter needs to be remineralised to provide the required substrate for nitrification and there are several intermediate processes which will affect the eventual availability of ammonium. Such a relationship between ammonium oxidation and the substrate concentration has only been observed in cultivated ammonium oxidizing bacteria and archaea but not in natural assemblages (Ward, 2008; Bianchi et al., 1997; Olson, 1981a).

At process station A during the summer cruise, nitrite concentration increased throughout the water column from CTD 4 to 11 and 15. This increase in nitrite throughout the water column was accompanied by an increase in nitrate. Between CTD 4 and 11, the mixed layer shoaled from 57 m to 37 m. The chlorophyll concentration between these two stations decreased from 0.7 to $0.5 \mu\text{g} \cdot \text{L}^{-1}$ (figure 3.9 in chapter 3). Ammonium concentration increased from 0 to $0.31 \mu\text{mol} \cdot \text{L}^{-1}$ between CTD 4 and 10. This could be due to grazing and release of ammonium (Whitehouse et al., 2011). Ammonium regeneration could then enhance the nitrification rates (Bianchi et al., 1997; Fernández et al., 2009). From the box model, at CTD 11, a loss of ammonium and an accumulation of nitrite was observed during the incubation. Nitrite oxidation was also observed through the isotopic dilution of the tracer at this station. Nitrification at this station could have been enhanced by the increase in availability of NH_4^+ .

The mixed layer then deepened again to 76 m at CTD 15 and chlorophyll concentrations decreased further. Nitrite and nitrate concentrations increases were detected up to 1000 m (figure B). This change is unlikely to be due to the remineralisation of sinking particles. In the deep ocean, nitrification is usually minimal as the substrate availability (NH_4^+ and organic matter) decrease with depth (Ward, 2008). While wind-induced mixing could have caused the entrainment of organic matter below the euphotic zone leading to subsurface regeneration of nutrients, it is unlikely to have caused a sudden downward flux of particles to 1000 m. Factors affecting the flux of particles downwards include the composition of the particles (community structure of the phytoplankton) and remineralisation processes degrading the particles before they reach the sequestration depth. Sinking particles would be larger particles (Lima et al., 2014) whereas nitrification is more likely to be associated with small particles (Ward, 2008).

4.5 Comparison with models

Several ecosystems model use a constant nitrification rate - e.g Serebrennikova et al. (2008) who use a constant rate of $20\text{nmol}\cdot\text{l}^{-1}\cdot\text{d}^{-1}$. This rate is much lower than the rates observed in this study. The mean ammonium oxidation rates observed here was $3.42\text{nmol}\cdot\text{l}^{-1}\cdot\text{h}^{-1}$ and the mean nitrite oxidation rates $125\text{nmol}\cdot\text{l}^{-1}\cdot\text{h}^{-1}$. Such models clearly underestimate the importance of nitrification and do not capture the variable nature of the measured rates.

An average specific nitrification rate (ammonium oxidation rate divided by ammonium concentration) of 0.21d^{-1} was obtained from the three ammonium oxidation rates measured during the two cruises in the Southern Ocean. In several models, nitrification is calculated using a constant specific rate and the ammonium concentration. While the specific rate found here is much higher than the ones used by Popova et al. (2003) - 0.03d^{-1} - and Deal et al. (2008) - 0.015d^{-1} - it is very similar to the specific rates used by Yool et al. (2007) - 0.2d^{-1} . Yool et al. (2007) used empirical evidence and datasets from various regions to estimate this parameter. As such, the specific nitrification rate is comparable to other global datasets and would support the use of this specific rate in models. However, in Yool et al's 2007 study, the substrate availability was considered the only factor affecting the absolute ammonium oxidation rates. As mentioned above, such linear relationships are not always applicable. For instance, in this study, no ammonium oxidation was observed at station 15N-11 despite the fact that this station had the highest ammonium concentration.

Other models attempt to address this by including factors such as light availability and oxygen concentrations in the defining functions (Moore et al., 2001; Grégoire and Lacroix, 2001; Martin and Pondaven, 2006; Vasechkina and Yarin, 2009; Mateus, 2012). Changes in oxygen concentrations are more likely to affect the nitrification rates under oxygen limited conditions than in regions where the oxygen concentrations are at or above saturation levels for nitrification. The oxygen concentrations measured in this study were larger than $4\text{ml}\cdot\text{l}^{-1}$ ($179\mu\text{mol}\cdot\text{l}^{-1}$) and are not expected to be limiting for this process. Some of these models restrict nitrification to darkness by only allowing it to proceed outside of the euphotic zone, below certain light levels (Stigebrandt and Wulff, 1987) or at night (Serebrennikova et al., 2008). The current study adds to the large body of evidence for nitrification within the euphotic zone. This study indeed shows that nitrification, while variable, is significant in the euphotic zone and should be constrained as such. For instance, in the model by Martin and Pondaven (2006), nitrification in the euphotic zone is allowed but depends on the fraction of surface PAR at the specified depths. The maximum nitrification rates in Martin and Pondaven's model is 0.15d^{-1} was obtained from observations in oligotrophic areas but compares well with the specific rates observed in the current study. This maximum rate, however, would be expected at the base of the euphotic zone where light availability is minimal rather at the 55% light depth where nitrification was measured in the current study. This would suggest that maximum nitrification rates in the Southern Ocean are higher than for oligotrophic regions. However, a larger dataset for the Southern Ocean is needed in order to confirm such views.

These models all represent nitrification as a single step from ammonium to nitrate. They exclude the nitrite oxidation step as nitrite concentrations are generally lower than nitrate concentrations and they assume a coupling between the two stages of nitrification. However, as discussed in section 4.4.3, this is not always the case. For instance, in this study, there is only one instance where both processes were detected (see table 4.4). The reasons for this decoupling are not always clear. They have been linked to the differential effects of light inhibition on ammonium and nitrite oxidisers (Olson, 1981a). Competition with phytoplankton can also be a factor in the decoupling between ammonium and nitrite oxidation as would the release of nitrite by phytoplankton. However, incorporating these factors and separating the two processes in models would add complexity.

While these models often assume a coupling between ammonium and nitrite oxidation, the differential effects of light inhibition on ammonium and nitrite oxidisers can often cause a decoupling between the two

processes. Competition with phytoplankton can also be a factor in such a decoupling. In this study, there is only one instance where both processes were detected at the same station. In addition, nitrite oxidation rates were found to be much higher than ammonium oxidation rates. Given this important decoupling, the single ammonium oxidation step might not be representative of nitrate regeneration on short time scales (24 hours). It is acknowledged that the addition of nitrite oxidation in the models will add to their complexity. However, a mechanistic understanding of this decoupling is required. This can be achieved through both observational and modelling studies investigating the factors controlling the nitrification rates and the differences in time-scales between the two steps.

4.6 Conclusion

In this chapter, the importance of nitrification in the Southern Ocean was considered. There is evidence from stable isotope approaches and from the microbial ecology that nitrification plays an important role in regulating the nitrate and nitrite concentrations within the mixed layer. The results from the present study show that the importance of the process at the surface (55% light depth) was very variable both in summer and winter. Using an isotopic dilution method (chapter 2), nitrite oxidation was only detected at one station out of six and nitrite production at two stations out of ten in winter. In winter, nitrite production was detected at two stations and in summer at one station. Simultaneous nitrite oxidation and production was only observed at one station in winter. In summer, an isotopic tracer approach was used to determine ammonium oxidation rate. While this approach was not successful due to the dilution of the tracer by regeneration of ammonium, the initial ("pre") sample showed an enrichment indicating that ammonium oxidation might be taking place. The rates determined here were extremely high compared to rates measured in other regions. Without repeated experiments, it is difficult to determine whether those rates are a result of methodological artefacts or an accurate representation of the importance of nitrification. For future work, nitrification rates should be measured throughout the mixed layer. From the nutrient profiles and nutrient ratios, it is likely that nitrification occurred at faster or detectable rates deeper. Time-course experiments using both isotopic dilution and tracer methods should be used to determine which proportion of nitrite is produced by ammonium oxidation and which proportion is released by phytoplankton. Furthermore, the box-model for the summer cruise in this chapter showed that the loss of nitrate expected from the observed nitrate uptake rates were much lower than the observed nitrate loss after an incubation. This could be due to a transfer of nitrate either to the nitrite pool or to unmeasured dissolved organic nitrogen pools. This should be investigated for a more accurate view of the nitrogen budgets. Finally, both from the nitrification rates and the nutrient profiles, it was not possible to establish a clear seasonal pattern in the importance of nitrification. The seasonality was also difficult to assess as the summer stations were mostly located in the Subantarctic Zone while the winter stations covered a much wider geographical range. This can only be resolved by having repeat transects during both seasons.

Chapter 5

The importance of nitrification for the nitrogen cycle in the Southern Benguela upwelling system

5.1 Introduction

Eastern Boundary Upwelling Ecosystems (EBUEs) are upwelling zones associated with eastern boundary currents (currents on the eastern margins of ocean basins) at mid and low latitudes (Quinones, 2010). In these regions, cold, nutrient-rich water from the deep ocean are brought upward due to the trade winds and the Coriolis effect (Fréon et al., 2009; Chavez and Messié, 2009; Messie et al., 2009). As this water is brought to the surface and warmed by the sun, phytoplankton are able to thrive due to the high nutrient concentrations. As a result, EBUEs are the most productive marine ecosystems and are able to support a highly productive food web. The latter accounts for 20% of the global fisheries catch highlighting the importance of EBUEs for food and livelihood strategies. This food web is reliant on the coupling between atmospheric drivers, ocean circulation and biogeochemical cycling. An understanding of these processes therefore provides societal benefits, especially in light of the anthropogenic environmental change (Fréon et al., 2009). Coastal ecosystems can be affected by changes in the local biogeochemical cycles (e.g the input of nitrogen from terrestrial sources and resulting eutrophication) as well as by global carbon emissions.

EBUEs play an important role for gas exchange and in particular carbon dioxide (CO_2) due to the high primary production in these regions. Despite covering only 1% of the ocean's surface area, they represent 11% of global new production (Messie et al., 2009). Given this disproportionate global importance, constraining the definitions of new production and carbon export models in EBUEs is necessary. For instance, new production has been defined as primary production fuelled by nitrate (Dugdale and Goering, 1967). This was based on the assumption that nitrate is not regenerated within the surface water column and that as such its use by phytoplankton can be separated from the use of "regenerated" nutrients such as ammonium and nitrate. This assumption, however, is flawed. A number of studies have shown that euphotic zone nitrification can be highly significant for the global nitrogen cycle (Yool et al., 2007; Ward, 2008). The role of nitrification in supplying "regenerated" nitrate has been shown to be important in various EBUEs (Fernández et al., 2009; Fernández and Farías, 2012; Clark et al., 2011, 2008; Beman et al., 2013; Santoro et al., 2010).

In the Benguela upwelling ecosystem, however, such studies are rare and mostly focused on the Northern Benguela (Benavides et al., 2014; Füssel et al., 2012). The Benguela upwelling system, however, is complex and comprises multiple upwelling cells (Shillington et al., 2006). Based on the different upwelling cells,

the Benguela has been divided into sub-systems representing very different ecosystem functioning. In both the Northern and Southern Benguela, the progression from a "new" to "regenerated" production regime has been well studied (Brown and Hutchings, 1987) but there is only one study discussing the changing role of nitrification within the upwelling cycle in the Northern Benguela (Benavides et al., 2014)

In this chapter, the importance of nitrification for nitrogen cycling in St-Helena Bay, located in the Southern Benguela upwelling system, is examined. Nitrogen uptake and assimilation rates were measured simultaneously as in the two previous chapters. Given that nitrification has been shown to occur in other upwelling and coastal shelf seas, it was expected that it would also occur in St-Helena Bay. The aim of this chapter was therefore to quantify the importance of nitrification under a range of environmental conditions and determine how this changes the known carbon export models for the region. In this chapter, rates of nitrification, nitrate uptake and ammonium uptake (where available) are reported. The changes in these processes depending on the timing of sampling within an upwelling cycle are examined and discussed.

5.2 Methods

5.2.1 Sampling

Nitrification rates and nitrogen uptake rates were measured simultaneously in St Helena Bay during three field campaigns in November 2011, March 2012 and March 2013 respectively. The field campaign in November 2011 represents late spring/early summer whereas the ones in March 2012 and 2013 represent the late summer/early Autumn. The three surveys followed a similar format. They started either on a Monday evening (March 2012) or on a Tuesday morning (November 2011, March 2013). From the start of each campaign to its end on the following Thursday, samples were taken from a single location either daily or twice a day. Given this format, all the data are shown according to the sampling day. While the days themselves are of no importance, they represent the evolution of the biogeochemical variables (nutrient, chlorophyll and dissolved oxygen) as well nitrogen uptake and regeneration over 3-4 days. In November 2011, sampling took place in the morning (at about 9 a.m) and the day-time nitrogen cycling rates were estimated. In March 2012, the station was sampled twice a day, once in the morning at about 9 a.m for the estimation of day-time rates and once in the evening for the estimation of night-time rates. Temperature and salinity were measured using a portable CTD. In March 2013, the rate of nitrogen uptake and nitrification were estimated for the day-time as well as for a 24 hour period. Sampling took place in the morning over three days. Table 5.1 summarises the stations in this study, indicating the incubation time and whether the rates estimated were day-time or night-time rates. The nitrogen uptake and nitrification rates are also shown in this table. Dissolved inorganic nitrogen (DIN) and dissolved oxygen concentrations were measured manually according to methods described in chapter 2.

5.2.2 Incubations

November 2011

Samples were collected from a depth of 3 m in St-Helena Bay daily from the 29th November 2011- 1 December 2011. The samples were subdivided into three 1-L subsamples which were amended with $^{15}\text{NH}_4\text{Cl}$ ($0.1 \mu\text{mol} \cdot \text{L}^{-1}$), $\text{Na}^{15}\text{NO}_2$ ($0.1 \mu\text{mol} \cdot \text{L}^{-1}$) and $\text{Na}^{15}\text{NO}_3$ ($3 \mu\text{mol} \cdot \text{L}^{-1}$) and incubated for 6 hours in day light. Another 3 subsamples from the original bulk sample were enriched with $^{15}\text{NH}_4\text{Cl}$, $\text{Na}^{15}\text{NO}_2$ and

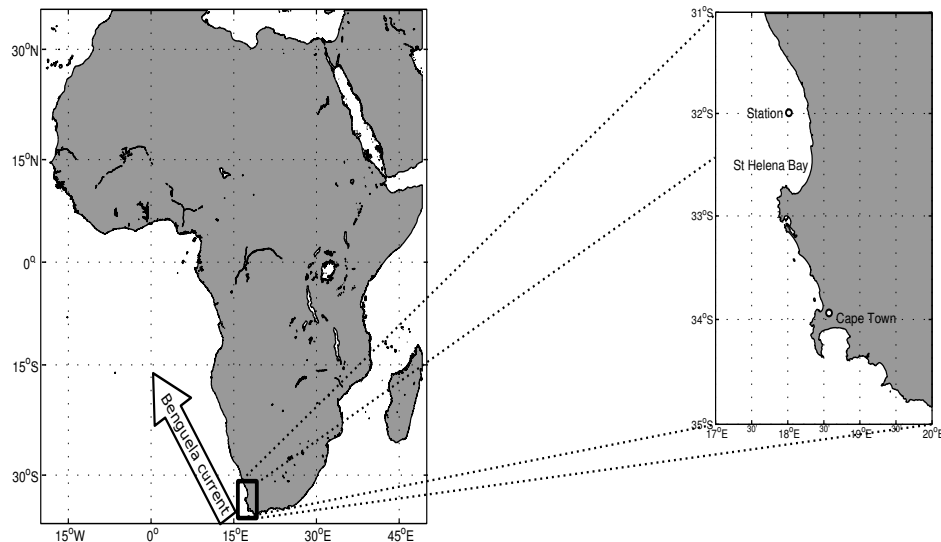


Figure 5.1: Location of St Helena Bay station

$\text{Na}^{15}\text{NO}_3$ and filtered as soon as possible. The filtrate was kept for regeneration experiments while the filters were kept for the measurements of uptake rates. The samples which had not been incubated were used to determine initial enrichment ratios and nutrient concentrations (“pre” samples). Those which had been incubated are referred to as the “post” incubation samples and were used to determine the enrichment ratios and nutrients concentrations after incubation. Both the “pre” and “post” samples were processed and prepared at the field-based laboratory before being preserved for later analysis.

March 2012

In March 2012, the samples were processed in the same way as in November 2011. However, additional night incubations were carried out. For these night incubations, water samples were collected at dusk at about 6 p.m, amended with the tracers as above and incubated overnight for 12 hours. “Pre” samples were also collected for all of these incubations. The procedure followed during these two field surveys was similar to that of the winter cruise in the Southern Ocean where the “pre” and “post” samples were amended separately. As discussed in Chapter 4, this can result in unequal amendments and increase errors in the determination of nitrification.

March 2013

In March 2013, however, this potential error was decreased by the use of a bulk sample for the “pre” and “post” samples. During this survey, each day a bulk water sample was collected from 3 m depth and the bulk sample was amended with the appropriate tracer before being split into 3 2-L subsamples. The first subsample was filtered as soon as possible (upon return at the land-based laboratory), the second was incubated for 12 hours in day light and the third for 24 hours. The sample which was not incubated served as “pre” sample for both the 12-hour and 24-hour incubations. At station Mar2013-1A, the samples were amended with the same concentrations of ^{15}N tracers as during the two previous campaigns. However, these additions were too high given that the ambient concentrations of nitrate and nitrite were much lower during this campaign. For the subsequent experiments, $0.01 \mu\text{mol} \cdot \text{L}^{-1}$ of the $^{15}\text{NO}_2^-$ and $^{15}\text{NH}_4^+$ and $0.1 \mu\text{mol} \cdot \text{L}^{-1}$ of $^{15}\text{NO}_3^-$ were added in the appropriate bottles.

5.2.3 Nitrogen uptake and regeneration rates

Nitrification rates and particulate nitrogen concentrations were determined as described in chapters 2 and 3. The nitrate uptake rate for stations Mar2013-1A and Mar2013-1B were calculated according to the equations by (Eppley et al., 1977) to account for the high tracer additions while for all the other stations, the nitrate uptake rates were corrected for isotopic dilution according to (Glibert et al., 1982b). An average AE%, R , was used instead of the calculated a_{enr} described in chapter 2. R was calculated from the AE% of the water samples before (R_0) and after (R_t) incubation as follows:

$$R = \frac{R_0}{\ln(R_0/R_t)} \times \left(1 - \frac{R_t}{R_0}\right) \quad (5.1)$$

R_0 and R_t , the "pre" and "post" enrichment ratios were obtained from same measurements as the nitrification rates (described in chapter 2). Sudan-1 was generated in the filtrates for the "pre" and "post" samples before being injected onto SPE cartridges. Again, as for the winter cruise in the Southern Ocean, in November 2011 and March 2012, the internal standard was not added onto the SPE cartridge at the same time as the sample. Rather, it was added when the dye was extracted from the SPE prior to purification by HPLC. This reduced the recovery of the sudan-1 and consequently underestimated the concentrations of nitrate and nitrite in the samples. It is therefore possible that the rates provided for these two field trips are underestimates of the real nitrification rates. In contrast, the rates estimated for the field campaign in March 2013 are more reliable as the internal standard and the samples were injected onto the SPE cartridge at the same time.

5.3 Results

5.3.1 Environmental conditions - Timing within the upwelling cycle

High nitrate concentrations ($\approx 30 \mu\text{mol} \cdot \text{L}^{-1}$), low temperatures and low particulate matter concentrations are characteristic of freshly upwelled South Atlantic Central water (SACW) (Shillington et al., 2006). When this water is exposed to the surface, its physical and biogeochemical properties change over time. This process is referred to as ageing or maturing. As the freshly upwelled water ages, the nitrate concentrations decrease while particulate matter and dissolved oxygen increase. No temperature profiles were available for the November survey. However, the sea surface temperature (about 12°C) in St-Helena Bay were characteristic of freshly upwelled waters as seen from MODIS satellite imagery (figure 5.2, data obtained from the Marine Remote Sensing Unit, <http://www.afro-sea.org.za>). The temperature and salinity profiles for Mar2012-2A to Mar2012-2D are shown in figures 5.3a and 5.3c. These profiles confirm a recent upwelling event before Mar2012-2A, when the surface water appeared to be of the High Salinity Central Water (HSCW) as defined by Shillington et al. (2006). The HSCW is expected to have a temperature of between 5 and 12°C and salinity between 34.5 and 35.5 . The differences between Mar2012-2B and Mar2012-2C, which has characteristics of the Modified Upwelled Water (Shillington et al., 2006), can be attributed to insolation. The latter is likely to have induced surface evaporation, which resulted in an increase in salinity (Brown and Hutchings, 1987). On the other hand, the changes between Mar2012-2C and D are mostly likely due to mixing. CTD profiles were not taken for Mar2012-2E and Mar2012-2F. In March 2013, the water temperature was warmer than in March 2012 and increased between Tuesday (Mar2013-1A) and Wednesday (Mar2013-2A) (figure 5.3b).

In November 2011 and March 2012, the environmental conditions were also characteristic of freshly upwelled waters. Nutrient concentrations were high and decreased as the week progressed (figure 5.4). The nitrate concentration ($30.3 \mu\text{mol} \cdot \text{L}^{-1}$) measured at Nov2011-1A, together with the low chlorophyll ($5.4 \mu\text{g} \cdot \text{L}^{-1}$) and dissolved oxygen ($4.1 \text{ mL} \cdot \text{L}^{-1}$), strongly suggests that an upwelling event had just taken place. As

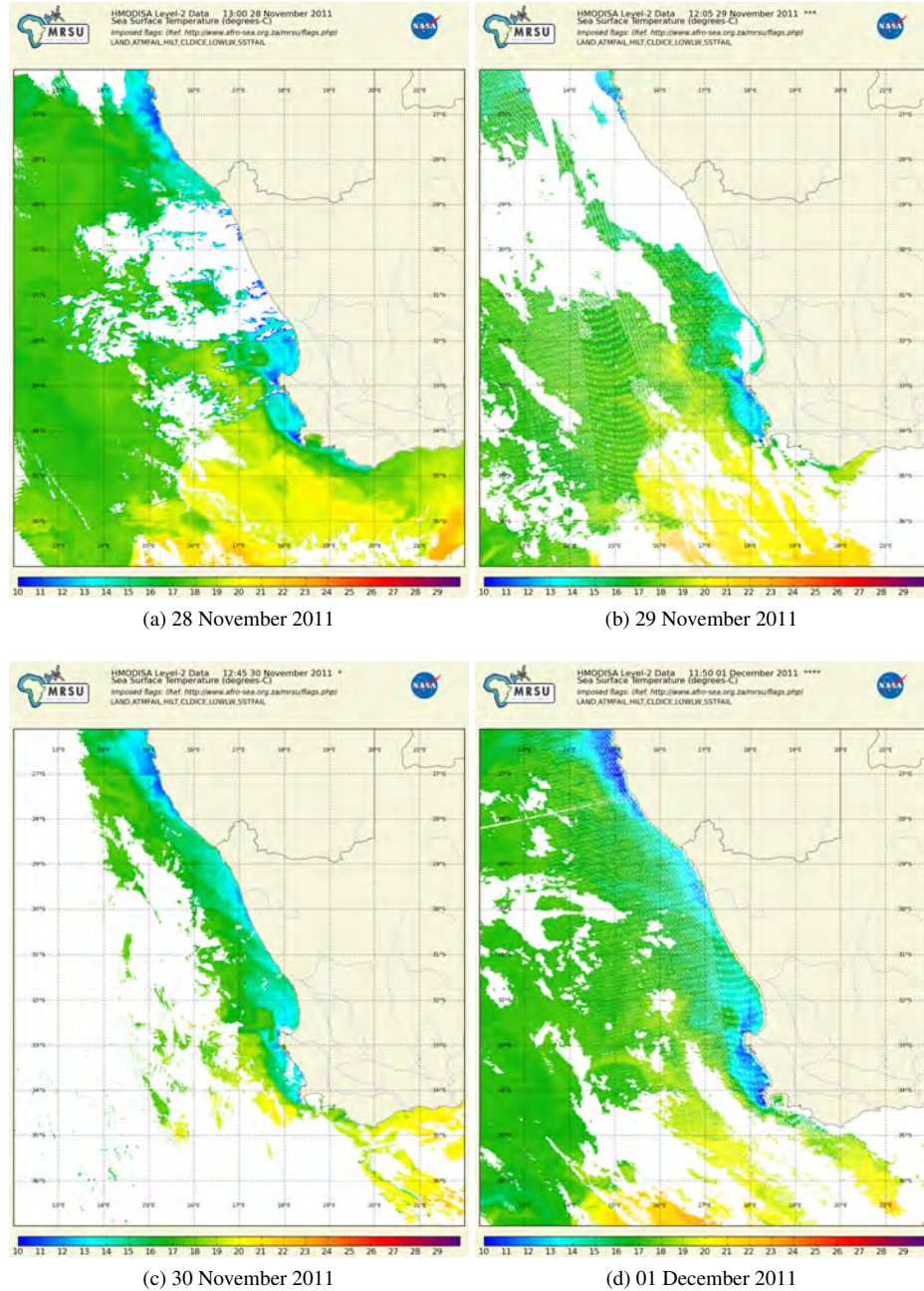


Figure 5.2: Sea-Surface temperature obtained from MODIS satellites for 28 November 2011 to 01 December 2011. These images are reproduced from <http://www.afro-sea.org.za>. During the November field survey, samples were taken on the 29 November (station Nov-1A), 30 November (Nov-1B) and 01 December (Nov-1C).. It is to be noted that the image for the 29th November 2011 does not fully cover St-Helena Bay.

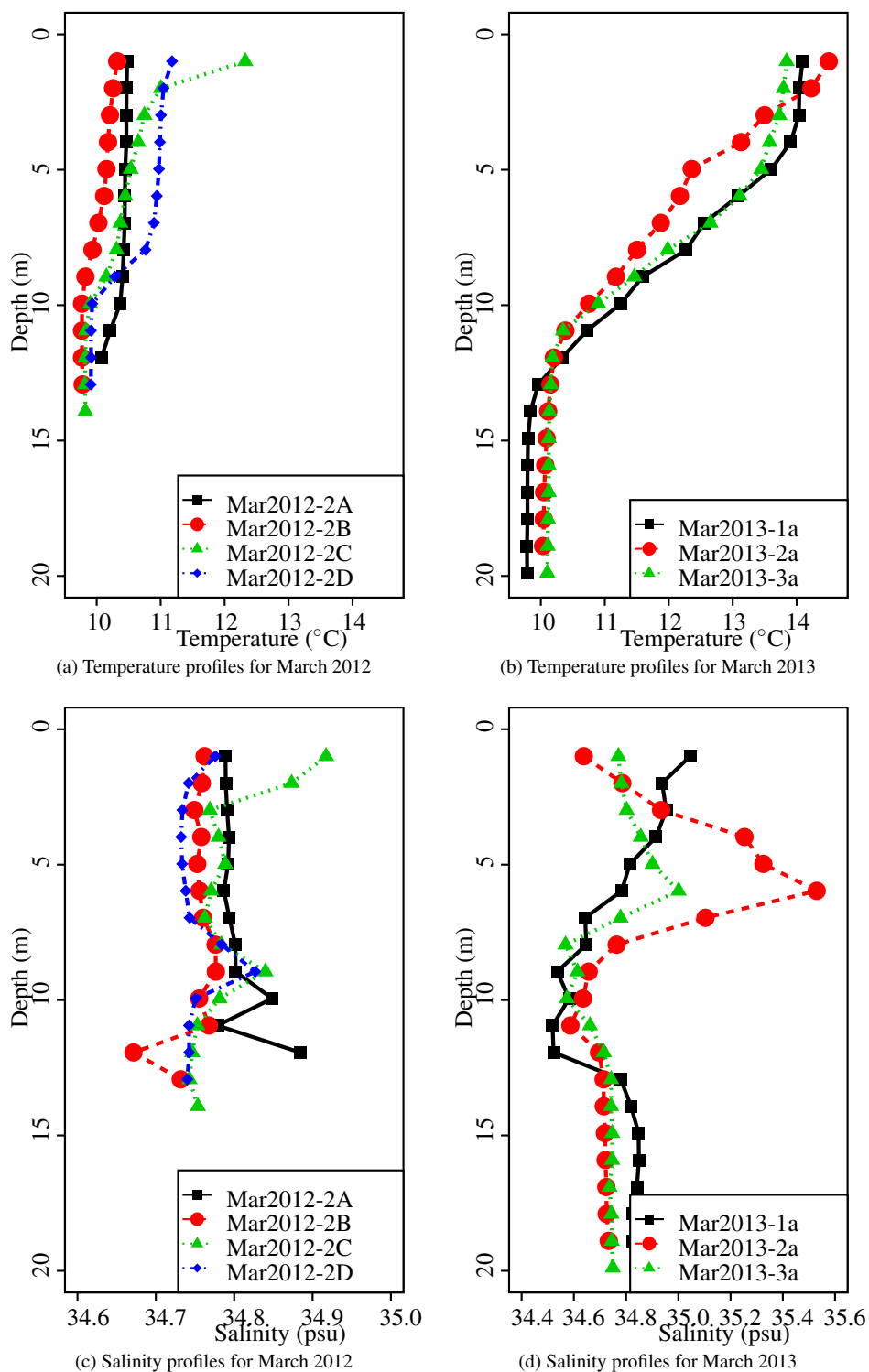


Figure 5.3: Temperature and salinity profiles for March 2012 and March 2013. Temperature and salinity measurements were done twice a day in March 2012 and in the morning in March 2013. There is no CTD data for November 2011 as the CTD was not available during this campaign.

the week progressed, the nitrate concentrations decreased while the other variables (chlorophyll and dissolved oxygen concentrations) increased implying that the water aged throughout the week (figure 5.4). The first station in March 2012, Mar2012-2A, also showed high nitrate concentrations. Again, this indicates that a fairly recent upwelling event had taken place. The nitrate concentration declined from Mar2012-2A ($32.0 \mu\text{mol} \cdot \text{L}^{-1}$) to Mar2012-2C ($16.5 \mu\text{mol} \cdot \text{L}^{-1}$). It then increased again when samples were taken at Mar2012-2D ($25.6 \mu\text{mol} \cdot \text{L}^{-1}$) before being gradually used up until Mar2012-2F ($16.1 \mu\text{mol} \cdot \text{L}^{-1}$). This indicates that either some upwelling or the advection of a different upwelling plume between stations Mar2012-2C and Mar2012-2D.

In contrast, in March 2013, the nutrient concentrations (nitrate and nitrite) remained low throughout the week (about $1 \mu\text{mol} \cdot \text{L}^{-1}$). During this field campaign, the nitrite concentrations could not be detected using the manual method. Nitrite concentrations averaging $17.2 \text{ nmol} \cdot \text{L}^{-1}$ were measured by the GC-MS (as described in chapter 2). The nitrate concentrations reported for March 2013 were also taken from the GC-MS measurements. These concentrations were reliable as the internal standard had been added onto the SPE cartridge at the same time as the sample.

The % saturation of dissolved oxygen is an indicator of biological activity as it accumulates after photosynthesis. Dissolved oxygen concentrations were higher in March 2013 ($6.8 - 9.2 \text{ mL} \cdot \text{L}^{-1}$, figure 5.4) indicating a longer period of biological activity and more mature waters. The accumulation of dissolved oxygen after photosynthesis can also be seen in March 2012 from the higher concentrations at stations sampled in the afternoon (average = $4.5 \text{ mL} \cdot \text{L}^{-1}$ at Mar2012-2C and Mar2012-2E) than at stations sampled in the morning (average = $3.1 \text{ mL} \cdot \text{L}^{-1}$ for Mar2012-2B, Mar2012-2D and Mar2012-2F). However, there was no dissolved oxygen measurement at Mar2012-2A preventing the unequivocal identification of a pattern. The difference between Mar2012-2C and Mar2012-2D was larger than the one between Mar2012-2E and Mar2012-2F (figure 5.4). This supports the idea that mixing of the water column was stronger between Mar2012-2C and Mar2012-2D than between Mar2012-2E and Mar2012-2F.

5.3.2 Nitrogen uptake rates

Nitrate uptake rates followed a similar pattern in November 2011 and March 2012. This pattern corresponds to the expected changes following an upwelling pulse and highlights that nitrogen dynamics are event-driven rather than seasonal in this region (see discussion in section 5.4.3). During these two field trips, the day-time nitrate uptake was low at the beginning of the week and increased as the week progressed (figure 5.5a). The day-time nitrate uptake rates during these two campaigns ranged from $42.84 \text{ nmol} \cdot \text{L}^{-1} \cdot \text{h}^{-1}$ to $670.48 \text{ nmol} \cdot \text{L}^{-1} \cdot \text{h}^{-1}$. Nitrate uptake rates were higher in November 2011 than in March 2012. Night-time nitrate uptake rates in March 2012 ranged from $5.47 \text{ nmol} \cdot \text{L}^{-1} \cdot \text{h}^{-1}$ to $26.71 \text{ nmol} \cdot \text{L}^{-1} \cdot \text{h}^{-1}$. Nitrate uptake rates were much lower in March 2013 when the day-time rates averaged $39.71 \text{ nmol} \cdot \text{L}^{-1} \cdot \text{h}^{-1}$. In March 2013, night time rates were included in the daily rate (measured by a 24-hour incubation), which averaged $23.77 \text{ nmol} \cdot \text{L}^{-1} \cdot \text{h}^{-1}$.

Ammonium uptake rates were only measured in November 2011 and in March 2013 (figure 5.5b). The ammonium uptake were generally greater in November 2011 (mean day-time rates = $180 \text{ nmol} \cdot \text{L}^{-1} \cdot \text{h}^{-1}$) than in March 2013 (mean day-time rates = $61.3 \text{ nmol} \cdot \text{L}^{-1} \cdot \text{h}^{-1}$). The ammonium concentrations and uptake rates measured in November 2011 were unusually high for the beginning of an upwelling cycle. The ammonium uptake rates, however, were still lower than the nitrate uptake rates as would be expected under such conditions. Station Mar2013-2A (day-time station) had a much higher ammonium uptake rate ($56.9 \text{ nmol} \cdot \text{L}^{-1} \cdot \text{h}^{-1}$) than the other stations during the March 2013 campaign. The 24-hour rates during this campaign averaged $5.17 \text{ nmol} \cdot \text{L}^{-1} \cdot \text{h}^{-1}$.

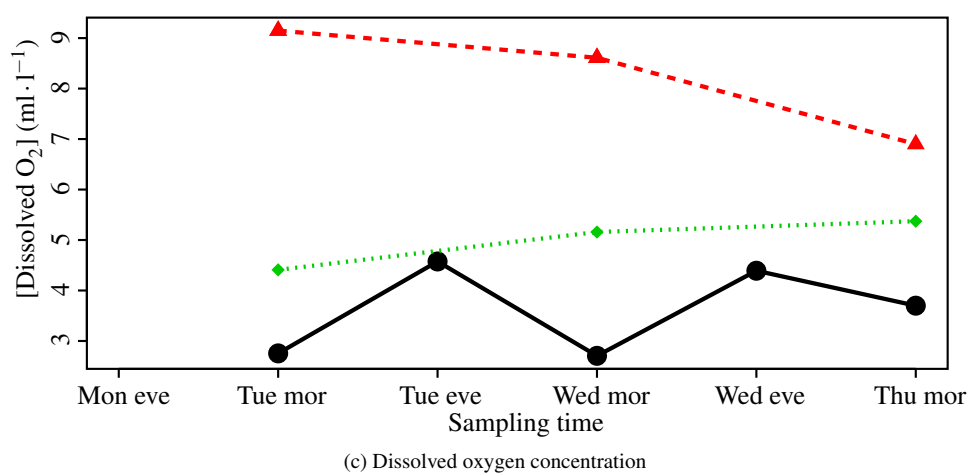
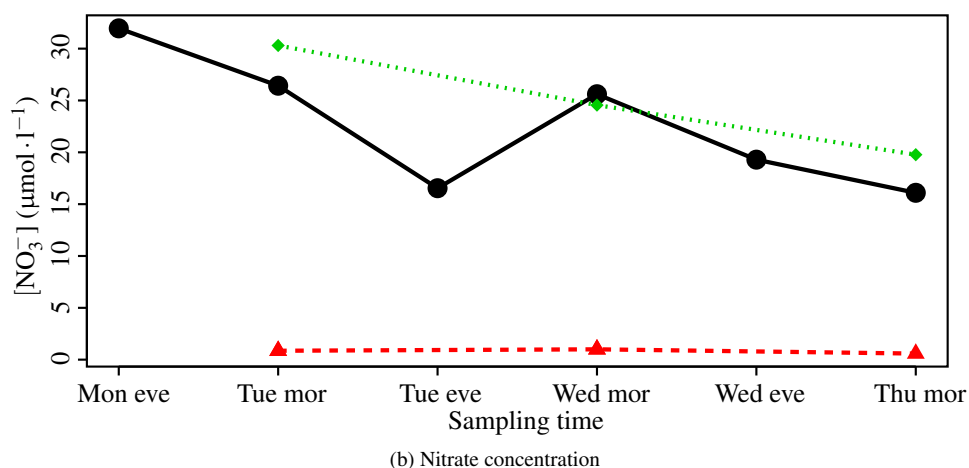
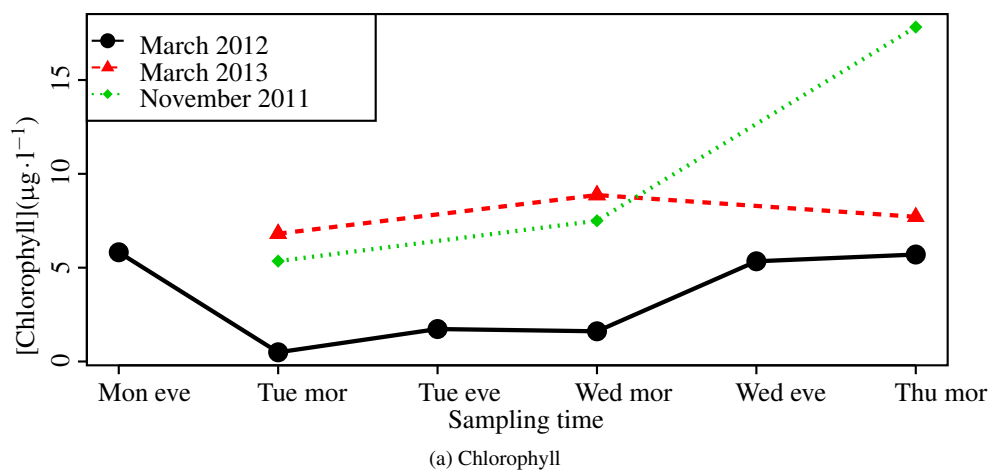
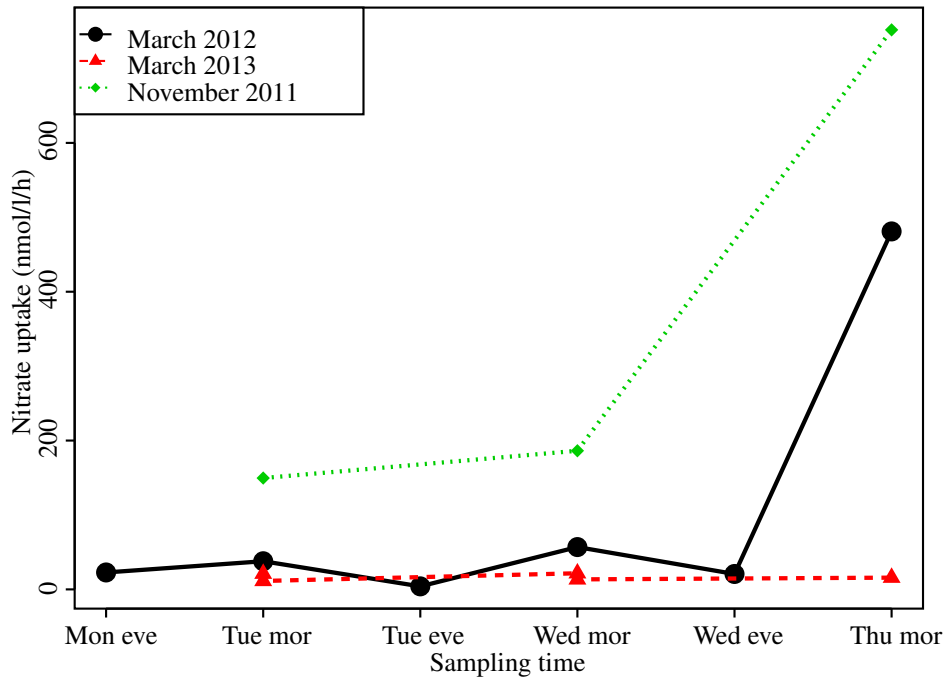
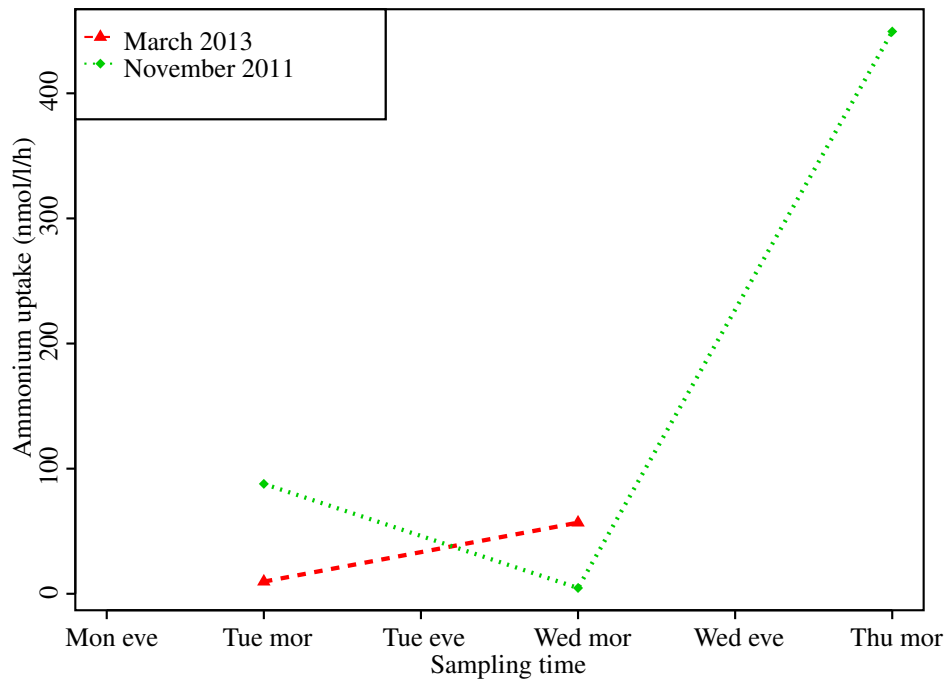


Figure 5.4: Evolution of chemical and biological variables for samples taken at a 3 m depth during the three field surveys. Nitrate, dissolved oxygen and chlorophyll concentrations are shown. The green diamonds and dotted lines represent November 2011, the black circle and solid lines March 2012 and the red triangle and dashed lines March 2013. On the sampling time labels, "mor" stands for "morning" and "eve" for "evening". Mon, Tue, Wed, Thu are for Monday, Tuesday, Wednesday and Thursday.



(a) Nitrate uptake rates



(b) Ammonium uptake rates

Figure 5.5: (a) Nitrate uptake rates (b) ammonium uptake in November 2011, March 2012 and March 2013. For March 2013, only the day-time rates are shown. On the sampling time labels, "mor" indicates that the ^{15}N incubation was started in the morning whereas "eve" indicates that the incubation was started in the evening. Mon, Tue, Wed, Thu are for Monday, Tuesday, Wednesday and Thursday.

5.3.3 Nitrification rates

Rates were estimated for the two steps of nitrification, ammonium oxidation and nitrite oxidation. As in chapter 4, after the identification of outliers, the isotopic ratio before incubation (the "pre" ratio) was compared to that after incubation (the "post" ratio) using a Mann-Whitney test. Significant differences were observed at most stations and the nitrification rates calculated as described in chapter 2 are shown in Table 5.1.

Nitrite production (Ammonium oxidation rates)

Nitrite production rates were higher in November 2011 and March 2012 than in March 2013. In November 2011, they ranged from 6.63 ± 1.7 to $20.00 \pm 10.34 \text{ nmol} \cdot \text{L}^{-1} \cdot \text{h}^{-1}$ and in March 2012, from 2.86 ± 7.54 to $22.83 \pm 1.63 \text{ nmol} \cdot \text{L}^{-1} \cdot \text{h}^{-1}$. In contrast, in March 2013, the minimum nitrite production rate at Mar2013-3A was $0.27 \pm 0.54 \text{ nmol} \cdot \text{L}^{-1} \cdot \text{h}^{-1}$ and the maximum range at station Mar2013-1A was $2.32 \pm 0.21 \text{ nmol} \cdot \text{L}^{-1} \cdot \text{h}^{-1}$. At station Mar2013-3A, the large error indicates that nitrite production was taking place but that the dilution of the tracer was not significant. This is seen from the large p-value (0.38451) for a Mann-Whitney test examining the differences between the "pre" and "post" $^{15}\text{N}/^{14}\text{N}$ ratio. Similarly, for station Mar2012-2E, the large error represents a non-significant difference between the "pre" and "post" ratio (p value = 0.73044).

No nitrite production rates are available for stations Mar2012-2B and Mar2012-2C. For these stations, the "pre" $^{15}\text{N}/^{14}\text{N}$ ratio was higher than the post ratio. The pre-incubation ratio was low (close to the background $^{15}\text{N}/^{14}\text{N}$). At these stations, the pre- and post-incubation samples were amended with the tracer separately. These two factors increase the likelihood that the difference here is due to either an unequal amendment of tracer or a lack of mixing.

Nitrite oxidation rates

Nitrite oxidation rates were much faster than nitrite production rates at all stations. They ranged from a minimum of $14.6 \pm 5.20 \text{ nmol} \cdot \text{L}^{-1} \cdot \text{h}^{-1}$ at station Mar2012-2F to a maximum of $81.7 \pm 34.4 \text{ nmol} \cdot \text{L}^{-1} \cdot \text{h}^{-1}$ at station Mar2013-2B.

Similarly to stations where nitrite production rates were not available, at stations Nov2011-1A, Mar2012-2A, Mar2012-2C and Mar2012-2D the pre-incubation $^{15}\text{N}/^{14}\text{N}$ ratio was also lower than the "post" ratio and nitrite oxidation rates could not be calculated. For stations Nov2011-1A, and Mar2012-2A, Mar2012-2C, this was likely to be due to incomplete mixing of the "pre" sample. At station Mar2012-2D, however, the "pre" $^{15}\text{N}/^{14}\text{N}$ ratio was higher than the background $^{15}\text{N}/^{14}\text{N}$ ratio, showing that the "pre" sample was enriched with ^{15}N . Mixing was therefore less likely to be the cause of the error. Moreover, the AE% obtained from the $^{15}\text{N}/^{14}\text{N}$ ratio measured by the GC-MS (11.2AE%) after the incubation was higher than the "pre" AE% calculated from the known concentrations of nitrate and ^{15}N tracer (10.6AE%). "Pre" AE% calculated in such way were used to obtain a nitrification rate for stations Mar2012-2A and Mar2012-2C. These nitrification rates were estimated to be $18.51 \pm 7.45 \text{ nmol} \cdot \text{L}^{-1} \cdot \text{h}^{-1}$ and $29.60 \pm 6.53 \text{ nmol} \cdot \text{L}^{-1} \cdot \text{h}^{-1}$. These rates are comparable to the other rates determined in this study.

Station	Date	Day	Incubation time (hours)	Day or Night	NO ₃ ⁻ ($\mu\text{mol} \cdot \text{L}^{-1}$)	NO ₂ ⁻ ($\mu\text{mol} \cdot \text{L}^{-1}$)	NH ₄ ⁺ ($\mu\text{mol} \cdot \text{L}^{-1}$)	NH ₄ ⁺ uptake ($\text{nmol} \cdot \text{L}^{-1} \cdot \text{h}^{-1}$)	NH ₄ ⁺ oxidation ($\text{nmol} \cdot \text{L}^{-1} \cdot \text{h}^{-1}$)	NO ₃ ⁻ uptake ($\text{nmol} \cdot \text{L}^{-1} \cdot \text{h}^{-1}$)	NO ₂ ⁻ oxidation ($\text{nmol} \cdot \text{L}^{-1} \cdot \text{h}^{-1}$)
Nov2011-1A	29/11/2011	Tuesday	7	Day	30.31	0.52	4.69	87.84	20.00 ± 10.34	145.15	NA
Nov2011-1B	30/11/2011	Wednesday	7	Day	24.55	0.28	0.00	4.62	17.08 ± 10.48	228.55	60.60 ± 36.00
Nov2011-1C	1/12/2012	Thursday	7	Day	19.77	0.29	9.22	449.41	6.63 ± 1.68	670.48	25.60 ± 7.70
Mar2012-2A	5/3/2012	Monday	12	Night	31.96	0.49	NA	NA	4.36 ± 1.28	23.82	NA
Mar2012-2B	6/3/2012	Tuesday	7	Day	26.42	0.28	NA	NA	NA	42.84	37.29 ± 36.71
Mar2012-2C	6/3/2012	Tuesday	12	Night	16.54	0.28	NA	NA	NA	5.47	NA
Mar2012-2D	7/3/2012	Wednesday	7	Day	25.60	0.29	NA	NA	22.83 ± 1.63	57.15	NA
Mar2012-2E	7/3/2012	Wednesday	12	Night	19.29	0.24	NA	NA	2.85 ± 7.54	26.71	15.23 ± 8.00
Mar2012-2F	8/3/2012	Thursday	7	Day	16.10	0.02	0.27	9.71	13.04 ± 2.22	531.96	14.66 ± 5.20
Mar2013-1A	12/3/2013	Tuesday	12	Day	0.86	0.02	0.27	5.49	2.32 ± 0.21	20.92	81.44 ± 20.24
Mar2013-1B	12/3/2013	Tuesday	24	24 hours	0.86	0.02	0.27	56.86	2.01 ± 0.53	8.97	25.34 ± 6.16
Mar2013-2A	13/3/2013	Wednesday	12	Day	1.00	0.01	0.82	4.87	0.78 ± 0.14	45.83	60.95 ± 14.83
Mar2013-2B	13/3/2013	Wednesday	24	24 hours	1.00	0.01	0.82	NA	0.70 ± 0.08	38.57	81.74 ± 34.41
Mar2013-3A	14/3/2013	Thursday	12	Day	0.59	0.03	NA	NA	0.27 ± 0.54	52.41	28.68 ± 1.74

Table 5.1: Nitrogen uptake and nitrification rates in St-Helena Bay during surveys in November 2011, March 2012 and March 2013. The nitrite, nitrate and ammonium concentrations are also shown. The table also indicates whether the samples were incubated during the day, night or for 24 hours as well as the length of each incubation.

5.4 Discussion

5.4.1 Comparison of Nitrogen uptake rates with previous estimates

The nitrate uptake rates (8.97 to $670.48 \text{ nmol} \cdot \text{L}^{-1} \cdot \text{h}^{-1}$) are comparable to rates previously measured in the Benguela (0 to $4000 \text{ nmol} \cdot \text{L}^{-1} \cdot \text{h}^{-1}$) (Mulholland and Lomas, 2008; Probyn et al., 1990, 1996; Rees et al., 2006; Waldron and Probyn, 1991). Rees et al. (2006) estimated nitrate uptake between reaching a maximum of $166 \text{ nmol} \cdot \text{L}^{-1} \cdot \text{h}^{-1}$ and ammonium uptake up to $42 \text{ nmol} \cdot \text{L}^{-1} \cdot \text{h}^{-1}$ in the Benguela upwelling region. Nitrate uptake rate at Nov2011-1A and Mar2012-2F were quite high compared with both historical data and the other measurements within the present dataset. Potential reasons for these high rates are discussed in section 5.4.3.

At an inshore station, Probyn (1988) observed nitrate uptake reaching a sub-surface maximum of $11.2 \text{ nmol} \cdot \text{L}^{-1} \cdot \text{h}^{-1}$ and ammonium uptake a maximum of $15.4 \text{ nmol} \cdot \text{L}^{-1} \cdot \text{h}^{-1}$. These uptake rates were associated with nitrate concentrations of about $8 \mu\text{mol} \cdot \text{L}^{-1}$ and ammonium concentrations of $0.7 \mu\text{mol} \cdot \text{L}^{-1}$. The high concentrations of nitrate ($> 16 \mu\text{mol} \cdot \text{L}^{-1}$) in November 2011 and March 2012 could explain why nitrate uptake was much higher during these two surveys than in the study by Probyn (1988). This, however, does not explain the differences between the results of Probyn (1988) and the stations in March 2013. In March 2013, higher nitrate uptake rates were observed in March 2013 than those by Probyn (1988) despite lower concentrations of nitrate. Probyn (1988) reported nitrate uptake rates between 1.32 and $29.81 \text{ nmol} \cdot \text{L}^{-1} \cdot \text{h}^{-1}$ with nitrate concentrations between 5 and $10 \mu\text{mol} \cdot \text{L}^{-1}$. In March 2013, the nitrate uptake rates ranged between 8.97 and $52.41 \text{ nmol} \cdot \text{L}^{-1} \cdot \text{h}^{-1}$ with nitrate concentrations $< 1 \mu\text{mol} \cdot \text{L}^{-1}$. On the other hand, the ammonium uptake rates in March 2013 (with the exception of station Mar2013-2A) ranged between 4.86 – $9.71 \text{ nmol} \cdot \text{L}^{-1} \cdot \text{h}^{-1}$ and were comparable to the rates presented by Probyn (1988) (3.74 to $39.46 \text{ nmol} \cdot \text{L}^{-1} \cdot \text{h}^{-1}$). Ammonium uptake rate at station Mar2013-2A ($56.8 \text{ nmol} \cdot \text{L}^{-1} \cdot \text{h}^{-1}$) was much higher than other rates measured in March 2013.

Waldron and Probyn (1991) observed nitrate uptake rates (25 – $79 \text{ nmol} \cdot \text{L}^{-1} \cdot \text{h}^{-1}$) comparable to the rates to those measured in March 2013. This was expected as the rates by Waldron and Probyn (1991) were estimated during a quiescent period with low nitrate concentrations (close to zero with the first 5 m) and high oxygen concentrations (6.98 mL at 5 m depth), similar to those encountered in March 2013. In contrast, the ammonium uptake rates presented by Waldron and Probyn (1991) were generally lower than those observed here. The ammonium uptake rates measured in November 2011 were unusually high (average day-time rates = $180 \text{ nmol} \cdot \text{L}^{-1} \cdot \text{h}^{-1}$). This is likely to be related to the high concentrations of ammonium which were observed during this survey. Such high concentrations ($< 9 \mu\text{mol} \cdot \text{L}^{-1}$) are extremely unusual (Touratier et al., 2003) and are more likely to occur later in the bloom cycle. It is therefore possible that the estimates in the current study were compromised. Only repeated measurements can help assessing how unusual such high ammonium concentrations and uptake rates are and whether these rates were realistic or not.

The preference exhibited for nitrate in the present study is in contrast to the studies by Probyn (1988) and (Waldron and Probyn, 1991). The *f*-ratio, the ratio of nitrate uptake over total N uptake, was much higher in the present study (mean= 0.69) than in Probyn (1988) (0.32). Similarly, to Rees et al. (2006), the *f*-ratio is used here as an indication of the relationship between nitrate and ammonium uptake rather than as a proxy for carbon export (Eppley and Peterson, 1979). The latter use is brought into question given the significant nitrification that has been observed in the euphotic zone in previous studies as well as this one. The usefulness of the *f*-ratio as a proxy for carbon export is discussed in section 5.4.4. An *f*-ratio higher than 0.5 represents a preference for nitrate while one lower than this value represents a preference for ammonium. It is to be noted that urea uptake was not determined for logistical reasons during the three surveys presented here. This could reduce the *f*-ratio as urea uptake can exceed both nitrate and ammonium uptake (Probyn, 1988; Probyn et al., 1990). In this study, given that similar *f*-ratios were observed at high and low nitrate concentrations, a linear relationship between the two variables (like the one presented by Rees et al. (2006)) could

not be formulated. The presence of ammonium has been shown to inhibit nitrate uptake (Semenh et al., 1998b). The concentration at which this inhibition becomes significant is controversial but has been quoted as $1 \mu\text{mol} \cdot \text{L}^{-1}$ (Semenh et al., 1998b). In March 2013, the concentration of ammonium was low (between 0.185 and $0.418 \mu\text{mol} \cdot \text{L}^{-1}$). During this survey, the inhibition of nitrate uptake was therefore unlikely. However, in November 2011, as mentioned before, the ammonium concentrations measured were very high but no inhibition of nitrate uptake was evident. This would again indicate that these ammonium measurements might not be reflecting the true concentrations and should be reconsidered.

The lack of inhibition by ammonium can also be seen in the differences between the rates presented here and those presented by (Probyn et al., 1990), who described inshore and offshore nitrogen uptake rates in aged upwelled waters. (Probyn et al., 1990) observed total ammonium uptake rates between 5.1 and $92.3 \text{ nmol} \cdot \text{L}^{-1} \cdot \text{h}^{-1}$. Although the lower end of this range is comparable to the ammonium uptake rates from March 2013, the ammonium uptake observed by (Probyn et al., 1990) was on average much faster than in the present study. In contrast, nitrate uptake in the present study was generally much higher than in (Probyn et al., 1990)'s dataset. This applied even in March 2013 when the observed environmental conditions were similar i.e samples were taken from aged upwelled waters.

It is highly likely that the ammonium presented here are underestimates. The ammonium uptake rates were corrected for the isotopic dilution of the ^{15}N tracer due to DIN regeneration. This might not cause major errors in the stations in November 2012 and day-time stations in March 2012 as the incubation period was relatively short (6-7 hours). In contrast, night-time incubations in March 2012 and those in March 2013 lasted between 12 and 24 hours. Such long incubation times result in isotopic dilutions of the ^{15}N tracer. The aim of the 24 hour incubations in March 2013 was to provide insight into the differences between day-time and night-time rates. In March 2012, samples for the day-time incubation were taken in the morning and those for the night time incubations were taken in the evening. The differences between the night and day time rates could therefore be affected by changes in the bacterial and phytoplankton community composition. The latter can arise from either vertical mixing or lateral advection. When incubating a single sample for 12 and 24 hours, only the daily changes in light availability were expected to affect the nitrogen uptake and regeneration rates. Both approaches have their merits. The shorter incubations are less likely to be affected by isotopic dilution of the tracer. However, sampling at different times might result in sampling different microbial and phytoplankton communities, specially if there is some lateral advection bringing a different parcel of water. In order to improve these experiments, the isotopic dilution of the tracer and the changes in community structure have to be accounted for. For instance, when sampling at different times, characterising the community structure would allow for a proper attribution of the differences between the day-time and night-time either as a response to light patterns or to changes in the community structure.

Diel variability in nitrogen uptake rates

In March 2012, nitrate uptake rates were determined during the day and night and were found to be markedly slower during the night. Similarly, in March 2013, the 24-hour nitrate uptake rates were lower than the nitrate uptake rate for the day-time only. Such results are expected given the decrease of nitrogen uptake at night and are also similar to the results from Probyn et al. (1996); Probyn (1988). A similar pattern was observed for ammonium uptake in March 2013. In disagreement with the results by (Probyn et al., 1990) and (Probyn et al., 1996) who observed that the ammonium uptake did not change much in the dark, the 24-hour ammonium uptake rates were lower than the day-time only rate. This would be expected given that the 24-hour incubations included a dark period. However, the 24-hour rates are also more likely to be underestimates due to the isotopic dilution of the tracers as well as potential release of DON.

5.4.2 Nitrification rates

Ammonium oxidation rates

The ammonium oxidation rates presented here ranged from 0.27 ± 0.54 at station Mar2013-3A to $22.83 \pm 1.63 \text{ nmol} \cdot \text{L}^{-1} \cdot \text{h}^{-1}$ at station Mar2012-2D. They are comparable to the only other ammonium oxidation rates available for the Southern Benguela (Rees et al., 2006). Rees et al. (2006) determined nitrification rates at the base of the euphotic zone using the nitrification inhibitor allythiourea (ATU) and applied a conversion factor of 8.3 mol NH_4^+ oxidised per mol C fixed. This conversion factor is on "the low end of published conversions factors" and could result in underestimates (Rees et al., 2006). They reported maximum rates between zero and $7.91 \text{ nmol} \cdot \text{L}^{-1} \cdot \text{h}^{-1}$. While these rates are very similar to those reported in the present study, they were estimated for samples taken from the bottom of the euphotic zone. Given the known inhibitory effect of light on ammonium oxidation (Ward, 2008), rates from the base of the euphotic zone would have been likely to be higher than the surface rates reported here. Such direct comparisons of spatially and temporally sparse datasets are a challenge as the Southern Benguela is not homogeneous (Rees et al., 2006; Brown and Hutchings, 1987); nutrient distribution and uptake rates as well as remineralisation rates differ geographically as well as seasonally (Brown and Hutchings, 1987; Gregor and Monteiro, 2013).

Ammonium oxidation rates in other upwelling systems were comparable to the rates presented here. For instance, the rates measured in March 2013 ranging from 0.27 ± 0.54 to $2.32 \pm 0.21 \text{ nmol} \cdot \text{L}^{-1} \cdot \text{h}^{-1}$ are within the same range as ammonium oxidation rates estimated by Clark et al. (2011) in the coastal waters of the Iberian peninsula ($0.06 - 3.74 \text{ nmol} \cdot \text{L}^{-1} \cdot \text{h}^{-1}$). They were also similar to the higher end of the ammonium oxidation rates observed in the Northwest African upwelling region. At 55% sPAR, the latter ranged between 0.08 and $0.22 \text{ nmol} \cdot \text{L}^{-1} \cdot \text{h}^{-1}$ (Clark et al., 2008). All of these rates were lower than those measured in the California upwelling regions (Beman et al., 2012) and in Chilean coastal waters (Fernández and Farías, 2012). Ammonium oxidation rates ranged between 0 and $14.5 \text{ nmol} \cdot \text{L}^{-1} \cdot \text{h}^{-1}$ in the California upwelling (Beman et al., 2012) while in the upwelling cell off the coast of Chile, ammonium oxidation averaged $18 \text{ nmol} \cdot \text{L}^{-1} \cdot \text{h}^{-1}$ (Fernández and Farías, 2012).

Nitrite oxidation rates

In contrast to the ammonium oxidation rates which were comparable to rates from other EBUEs, nitrite oxidation rates in this study were generally higher reaching a maximum of $81.74 \pm 34.41 \text{ nmol} \cdot \text{L}^{-1} \cdot \text{h}^{-1}$. These are the first nitrite oxidation rates presented for the euphotic zone in the Southern Benguela. In the Northern Benguela, Füssel et al. (2012) compared nitrite oxidation rates from the oxygen minimum zone (OMZ) to sources and sinks of nitrite such as the anaerobic ammonium oxidation (anammox), nitrate reduction and aerobic ammonium oxidation while nitrate regeneration in surface waters was estimated by Benavides et al. (2014). Füssel et al. (2012) estimated maximum nitrite oxidation rates of $15.5 \text{ nmol} \cdot \text{L}^{-1} \cdot \text{h}^{-1}$. In this region, nitrite oxidation was still detectable despite the low oxygen concentrations ($< 1 \mu\text{mol} \cdot \text{L}^{-1}$) and potential competition between nitrite oxidisers and anammox bacteria. These two factors could explain the higher rates observed in the present study when compared to Füssel et al. (2012). The water column in the present study was well-oxygenated and even, supersaturated in some cases. These high oxygen concentrations would therefore inhibit processes such as denitrification and anammox. The latter, which have been observed in the Benguela upwelling system (Tyrrell and Lucas, 2002; Kuypers et al., 2005; Gregor and Monteiro, 2013), are more likely to occur under oxygen minimum conditions.

The nitrite oxidation rates in the Benguela upwelling system - both from this study and Füssel et al.'s (2012) - were much higher than those measured in the Northwest African upwelling (Clark et al., 2008), off the Iberian peninsula (Clark et al., 2011) and in the California upwelling (Beman et al., 2013). In the Northwest African

upwelling, nitrite oxidation rates reached maxima of $0.17 \text{ nmol} \cdot \text{L}^{-1} \cdot \text{h}^{-1}$ and $0.34 \text{ nmol} \cdot \text{L}^{-1} \cdot \text{h}^{-1}$ at 55% and 1% sPAR respectively. Similarly, in the surface waters of the Peruvian upwelling, nitrate regeneration rates were found to be between 0.125 and $0.583 \text{ nmol} \cdot \text{L}^{-1} \cdot \text{h}^{-1}$. In the coastal waters of the Iberian peninsula, nitrite oxidation rates ranged from 0.11 to $24.76 \text{ nmol} \cdot \text{L}^{-1} \cdot \text{h}^{-1}$ (Clark et al., 2011) whereas in the California upwelling, nitrite oxidation rates up to $5.83 \text{ nmol} \cdot \text{L}^{-1} \cdot \text{h}^{-1}$ have been observed (Beman et al., 2013). While generally faster than nitrite oxidation reported previously, the nitrite oxidation rates reported in this study are realistic. The slower rates were within similar ranges to those in the other upwelling regions. For example, at station Mar2012-2F a day-time rate of $14.66 \pm 5.20 \text{ nmol} \cdot \text{L}^{-1} \cdot \text{h}^{-1}$ was observed. In addition, the faster rates are comparable to rates determined by Fernández and Farías (2012). The latter determined nitrite oxidation rates averaging $60 \text{ nmol} \cdot \text{L}^{-1} \cdot \text{h}^{-1}$ in the coastal upwelling off Chile. They were also similar to the maximum rates reported by Bianchi and Feliatra (1999), who measured maximum rates of $96 \text{ nmol} \cdot \text{L}^{-1} \cdot \text{h}^{-1}$. These were measured at a shallow station which was influenced by a plume from the Rhône River. This resulted in enhanced nitrification rates. The stations in St-Helena Bay were relatively close to the coast and could have also been influenced by riverine inputs (Monteiro and Roychoudhury, 2005).

In the study by Benavides et al. (2014), low nitrate regeneration rates were observed ($< 0.50 \text{ mmol N} \cdot \text{m}^{-2} \cdot \text{h}^{-1}$). These nitrification rates were integrated to a depth of 40 m and would therefore correspond to an average of $< 12.5 \text{ nmol} \cdot \text{L}^{-1} \cdot \text{h}^{-1}$. These nitrate regeneration rates are closer to the ammonium oxidation rates observed in the present study than the nitrite oxidation rates. While these differences could be due to riverine inputs, they can also be attributed to a decoupling between ammonium and nitrite oxidation. Benavides et al. (2014), assuming the coupling of the two nitrification steps, used a $^{15}\text{NH}_4^+$ tracer to measure the regeneration of nitrate. Ammonium oxidation is often considered a rate-limiting step in the nitrification process (Füssel et al., 2012; Grundle et al., 2013), however, the two processes are often decoupled. For instance, nitrite oxidation rates in this study were much higher than ammonium oxidation rates. This was especially true in March 2013 when ammonium oxidation and nitrite oxidation rates averaged $1.22 \text{ nmol} \cdot \text{L}^{-1} \cdot \text{h}^{-1}$ and $55.6 \text{ nmol} \cdot \text{L}^{-1} \cdot \text{h}^{-1}$ respectively. In various regions, higher rates of nitrite oxidation than ammonium oxidation have been observed (Clark et al., 2011; Beman et al., 2013, 2012; Füssel et al., 2012; Fernández and Farías, 2012). The geographical extent of this decoupling is further supported here. Under low oxygen conditions ($< 5 \mu\text{mol} \cdot \text{L}^{-1}$), the nitrite supply for nitrite oxidation can be a result of denitrification (nitrate reduction) (Füssel et al., 2012; Fernandes et al., 2014). Under the conditions observed in St-Helena Bay during this study, denitrification would have been an unlikely source of nitrite. Furthermore, the source of nitrite might change depending on the timing of sampling in an upwelling cycle as discussed in section 5.4.3.

5.4.3 Changes in the nitrogen cycle within upwelling cycles

Nitrogen uptake and phytoplankton community

The difference in conditions between the field trips in November 2011, March 2012 and March 2013 provide some insight into the changes from the beginning of an upwelling cycle to the end of an upwelling cycle. The bloom development cycle following an upwelling pulse has been well studied using various approaches (Brown and Hutchings, 1987; Pitcher et al., 1992, 1991; Waldron and Probyn, 1991). Brown and Hutchings (1987) deployed drogues in recently upwelled waters on five occasions and monitored variables such as temperature, chlorophyll and nutrients. Pitcher et al. (1991) and Waldron and Probyn (1991) studied changes at an anchor-station over 27 days. Microcosms have also been used to follow the evolution of phytoplankton biomass (Painting et al., 1989; Pitcher et al., 1992). Newly upwelled water typically has high nitrate concentrations, chlorophyll concentrations below $1 \mu\text{g} \cdot \text{L}^{-1}$ and low dissolved oxygen concentrations of about $4.0 \text{ mL} \cdot \text{L}^{-1}$. The bloom then develops over 3-4 days and nitrate uptake increases before chlorophyll concentrations reach a maximum of $10 - 20 \mu\text{g} \cdot \text{L}^{-1}$. After reaching this maximum, the bloom declines due to

nutrient limitation as well as light limitation brought about by self-shading (Lamont et al., 2014; Pitcher et al., 1992; Brown and Hutchings, 1987). The highest primary production rates are usually observed when there is a period of relaxation in the upwelling and the water column stabilises (Brown and Hutchings, 1987). St Helena Bay is influenced by a major upwelling center at Cape Columbine where the upwelling pulse and weather-influenced variability occurs over a time scale between 3 days to a week on average Waldron (1985); Touratier et al. (2003). It is therefore not surprising that the bloom development cycle follows a similar time-frame.

In accordance to previous studies, the nitrate uptake at the beginning of an upwelling cycle (in November 2011 and March 2012) were much higher than in March 2013 (representing post-bloom conditions). Furthermore, both in November 2011 and March 2012, nitrate uptake increased at the last station. This could be due to the increase in vertical stability (figure 5.3a). Both field campaigns coincidentally started at a time of active upwelling. The upwelling relaxed after a few days. In March 2012, decreased vertical mixing can be inferred from the lack of change in nutrient and chlorophyll concentrations between stations Mar2012-2E and Mar2012-2F. The increased vertical stability and the growth of biomass to a critical level could explain the sharp increase in uptake rates at the end of the week both in 2011 and 2012. Such an increase was observed despite the fact that the nitrate concentrations decreased. However, mixing of different water masses or upwelling plumes can present a challenge when attempting to establish the progression of phytoplankton biomass in upwelled waters (Brown and Hutchings, 1987). For instance, in March 2012, nitrate concentration decreased from $32.0 \mu\text{mol} \cdot \text{L}^{-1}$ to $26.4 \mu\text{mol} \cdot \text{L}^{-1}$ between stations Mar2012-2A on Monday night and Mar2012-2B on Tuesday morning. Between these two stations, the salinity decreased indicating that there had been an influx from a different water mass/ upwelling plume. Establishing a "biological progression" from the start of the field campaign (Mar2012-2A, Monday night) to its end (Mar2012-2F, Thursday) might not be entirely accurate.

The net primary production and chlorophyll concentration are not the only variables which are affected by the physical and chemical changes in the water column through an upwelling cycle. The phytoplankton community structure and nitrogen uptake regime also change (Pitcher et al., 1992). For instance, nitrate uptake is expected to dominate shortly after deep, nitrate rich waters are upwelled. Larger phytoplankton, such as diatoms, have been shown to have a preference for nitrate through size fractionated uptake experiments (Probyn et al., 1990; Probyn, 1992). They are likely to bloom at the start of an upwelling cycle when both nitrate and silicic acid are abundant (Pitcher et al., 1992; Wasmund et al., 2014). After a period of stability and quiescence, nitrate concentrations decrease and smaller phytoplankton with a preference for ammonium, such as dinoflagellates, then dominate (Pitcher et al., 1992; Probyn et al., 1990). Regenerated production (based on ammonium and urea) becomes more important in aged upwelled waters (Benavides et al., 2014). The phytoplankton community was characterised in March 2013 (data provided by R.Bellerby, Institute for Water Research, Norway). The cell volumes were calculated according to equations described in Olenina (2006) and these volumes converted to carbon content as described by Menden-Deuer and Lessard (2000). The phytoplankton cell counts were dominated by diatoms (*Bacillariophyceae* class) indicating that a bloom period had occurred (figure 5.6 and table 5.2). Similarly to results by Waldron and Probyn (1991) and Wasmund et al. (2014), the community was dominated by the *Chaetoceros spp* (68 % of total cell counts). The second most prevalent group was *Skeletonema spp*, which represented 24% of total cell count. When considering the carbon content per phytoplankton group, however, the dominance of *Chaetoceros spp* is reduced to 60% of total phytoplankton carbon content. Throughout the week, the contribution of *Chaetoceros spp* and *Bacillariophyceae* class decreased as did the total carbon (figure 5.6b). Conversely, the importance of the *Dinophyceae* class doubled from Tuesday to Thursday. Chlorophyll concentrations increased between station Mar2013-1A ($6.81 \mu\text{g} \cdot \text{L}^{-1}$) to station Mar2013-2A ($8.87 \mu\text{g} \cdot \text{L}^{-1}$) corresponding to a Carbon:Chlorophyll ratio (C:Chl) shift from 35.7 to 19.0. This community shift could be due to physical changes such as the advection of a separate water plume as it was accompanied by an increase in nitrate concentration and a change

in the temperature and salinity profile (figures 5.3b and 5.3d).

Phytoplankton group	Tuesday		Wednesday		Thursday	
	Cells L ⁻¹	Carbon content (µg·L ⁻¹)	Cells L ⁻¹	Carbon content (µg·L ⁻¹)	Cells L ⁻¹	Carbon content (µg·L ⁻¹)
<i>Dinophyceae</i>	4880	42.471	12080	54.159	11260	48.843
<i>Coccolithophyceae</i>	0	0.000	0	0.000	1200	0.022
<i>Chrysophyceae</i>	78000	1.074	11750	0.150	131600	1.805
<i>Bacillariophyceae</i>	4165 160	199.003	2669330	113.173	2028920	89.258
<i>Prasinophyceae</i>	1200	0.034	1200	0.290	0	0.000
<i>Unclassified</i>	42350	0.916	38800	0.795	42300	0.782
Total	4 291590	243.499	2733160	168.567	2215280	140.710

Table 5.2: Phytoplankton community structure from Tuesday (Mar2013-1A) to Thursday (Mar2013-3A). The cell counts (Cells L⁻¹) and carbon content per phytoplankton group for stations Mar2013-1A (Tuesday), Mar2013-2A (Wednesday) and Mar2013-3A (Thursday) are shown. The cell counts were obtained through microscopy and the carbon content calculated according to methods in Olenina (2006) and Menden-Deuer and Lessard (2000).

Differences in nitrite production

Changes in the physical and chemical settings have been shown to change to the phytoplankton community composition (Touratier et al., 2003). These changes as well as the phytoplankton community can also influence the bacterial community and consequently rates of nitrification. For instance, competition between phytoplankton and nitrifiers for ammonium could reduce either the rate of ammonium oxidation or ammonium uptake (Mulholland and Lomas, 2008). In this dataset, nitrite production rates were consistently higher in recently upwelled waters (November 2011 and March 2012) than in matured upwelled waters. This was the case even though the nitrite production and oxidation rates estimated in November 2011 and March 2012 are likely to be underestimates due to poor recoveries from the SPE cartridges. At first glance, the higher ammonium oxidation rates at the start of a bloom cycle could be attributed to lesser competition between phytoplankton and ammonium oxidisers. During this time, the demand for ammonium by phytoplankton is likely to be low as the community is dominated by large species with a preference for nitrate. At the end of a bloom cycle, species with a preference for ammonium are more abundant. This could explain why the night-time rates in March 2012 were higher than those measured in March 2013. Another possible explanation to such differences would be the increase of bacterial herbivory towards the end of an upwelling cycle (Painting et al., 1989). The impact of predators on bacterial growth and nitrification rates has been shown before (Brown et al., 1991; Lavrentyev et al., 1997; Santoro et al., 2010).

It is highly likely, however, that these two factors (competition for ammonium and predation) are not the main explanations for such differences. The day-time nitrite oxidation rates measured in November 2011 and March 2012 were much larger than the night-time rates whereas the day-time and night-time rates in March 2013 were similar. This is in contradiction the known inhibition of ammonium oxidation by light which would suggest higher nitrification rates at night. There would be two possible scenarios if competition with phytoplankton was the main driver in the differences. The first would occur if ammonium uptake was reduced at night. In this case, there would be an increase in nitrification rates due to decreased competition with phytoplankton. However, as ammonium uptake rates have been shown to be unchanged in the dark (Probyn et al., 1990), it is also possible that there would be no major changes in nitrification rates at night.

It is therefore possible that part of the nitrite pool (especially at the beginning of an upwelling) was not originating from ammonium oxidation. Unlike the nitrite production rates measured in March 2013, the rates measured in November 2011 and March 2012 were much higher than rates reported by Rees et al. (2006). The previous rates measured by Rees et al. (2006) used an inhibitor method, which involves comparing a control incubation with one where nitrifying activity is prevented by use of ATU. Rates using this method would therefore reflect only ammonium oxidation, but the rates measured by isotopic dilution could include other nitrite sources (figure 5.7) such as luxury nitrate uptake and the subsequent release of nitrite by phytoplankton

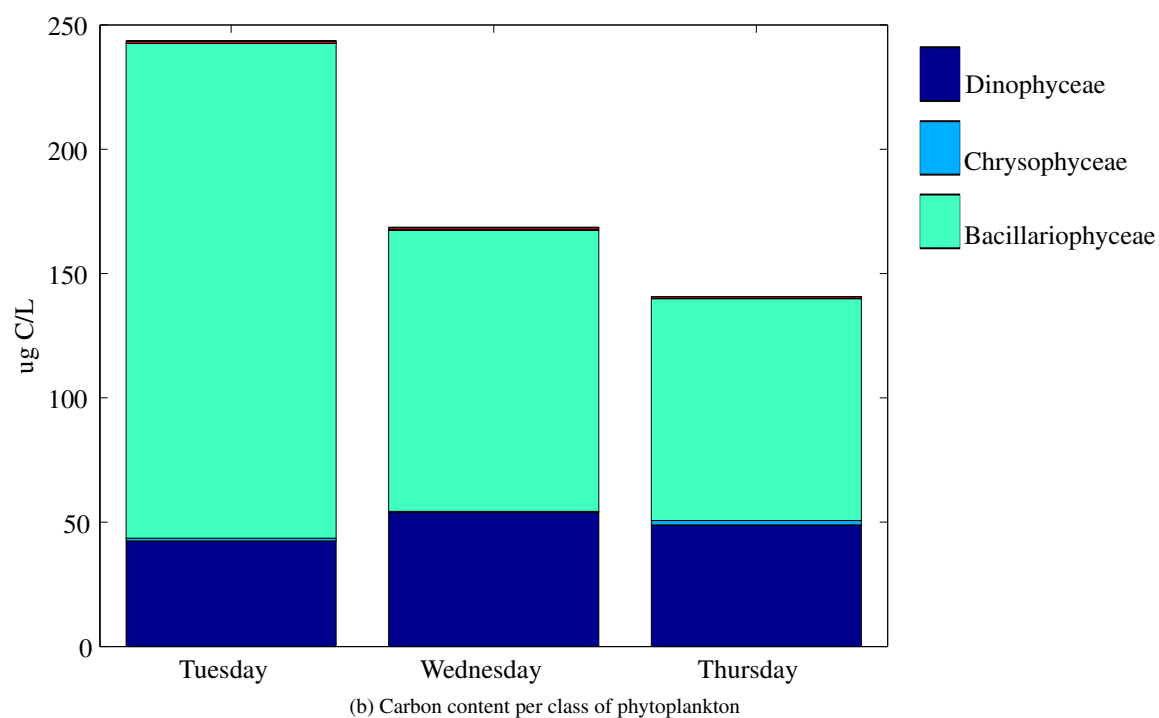
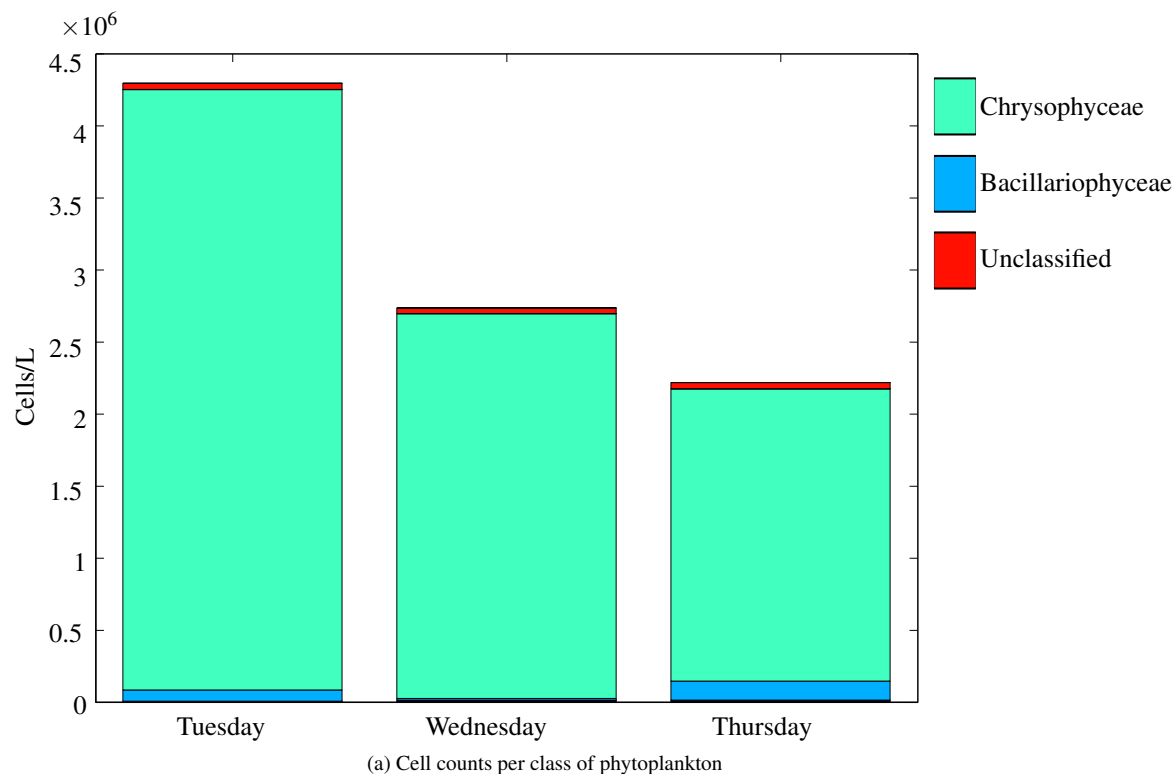


Figure 5.6: Dominant phytoplankton groups by (a) cell counts and (b) carbon content for stations Mar2013-1A (Tuesday), Mar2013-2A (Wednesday) and Mar2013-3A (Thursday). In terms of carbon content, while still minimal when compared to other groups, the importance of *Chrysophyceae* appears to increase on Thursday.

(Clark et al., 2011).

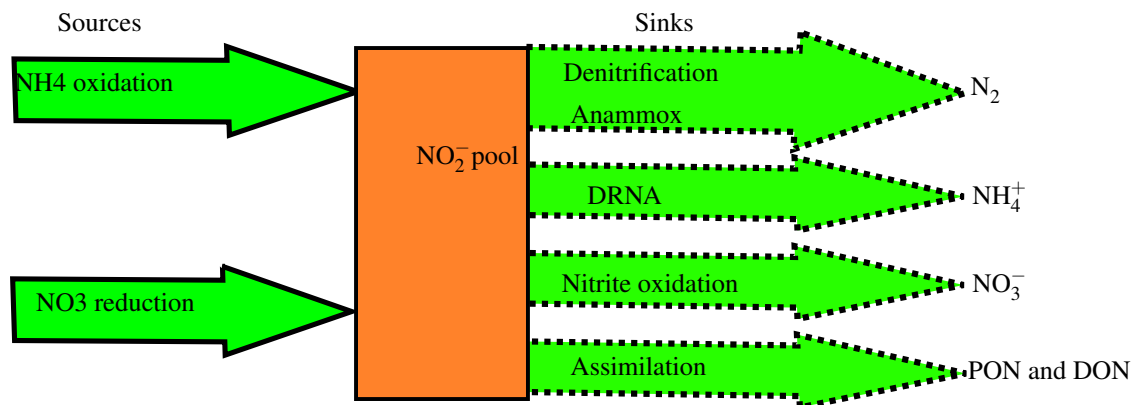


Figure 5.7: Pathways for the production (sources) and consumption (sinks) of nitrite, adapted from Lipschultz (2008)

The differences between the day-time and night-time rates at the beginning of an upwelling suggests that under these conditions, processes which are influenced by a light/dark cycle might be playing an important role in nitrite cycling. This makes the non-nutritional (luxury) uptake of nitrate more likely than denitrification. Non-nutritional nitrate uptake is a process hypothesised by Lomas and Glibert (1999a) whereby phytoplankton in a nitrate-replete environment are able to reduce more nitrate than needed for their growth. The resulting nitrite (toxic when in excess in the cells) then has to be released from the phytoplankton cells (Lomas and Glibert, 2000). Nitrite production was much lower at night when nitrate assimilation (measured as the assimilation of nitrate into the particulate matter) was also reduced. In freshly upwelled waters, the high nitrate concentrations are likely to "encourage" luxury nitrate uptake (Lomas and Lipschultz, 2006). This process is reduced when nitrate concentrations are low (e.g in March 2013). The decrease of nitrite production would then be attributed to a decrease in the release of nitrite by phytoplankton. This is further supported by the minimal differences between day and night rates in March 2013. In this case, the diel cycle of nitrite by release by phytoplankton did not affect the nitrite production rates. Tracer experiments, where a ^{15}N tracer is added to the ammonium pool and traced into the nitrite pool, were not performed but would have allowed for a more conclusive identification of the nitrite source. These differences in nitrite sources between the beginning and end of an upwelling/bloom cycle also highlight the potential decoupling between ammonium and nitrite oxidation and hence, the need to measure these rates independently.

Differences in nitrite oxidation

In contrast to nitrite production which was consistently higher at the start of an upwelling cycle than at the end, nitrite oxidation rates were similar. The one caveat in this comparison is that the nitrite oxidation rates in November 2011 and March 2012 might have been underestimated by an unquantified amount. The lack of differences between the two sets of nitrite oxidation rates could be due to this underestimate. Nevertheless, this dataset allows us to compare the contributions of nitrification to nitrate uptake (figure 5.8). At the beginning of an upwelling cycle, nitrification is expected to only contribute minimally to nitrate demand. This is seen especially at the peak of the bloom where nitrate uptake is very high (e.g stations Nov2011-1C and Mar2012-2F). In those cases, even nitrification ten times larger than those reported here would not exceed nitrate uptake. On the other hand, stations (with reliable nitrification rates) at the end of a bloom cycle showed nitrite oxidation rates consistently higher than nitrate uptake. Nitrate uptake at these stations was much lower than at that the beginning of the bloom cycle. The decrease of the nitrate uptake compounded with high nitrification rates resulted in a situation where nitrification supplied more than 100% of the nitrate demand.

Such high contributions to nitrate demand, however, are not unheard of in coastal ecosystems (Bronk et al., 2014; Clark et al., 2011) but are in stark contradiction with the results by Benavides et al. (2014). The latter estimated that nitrification supplied between 2-11% of nitrate demand. This contribution of nitrification was at its highest in matured upwelled waters with a pseudo-age between 13 and 55 days and its lowest in freshly upwelled waters with a pseudo-age of 13 days. The pseudo ages used by Benavides et al. (2014) are defined as the number of days passed between the time when the waters reached the surface at the upwelling cell and the time when they reached the oceanic stations. This definition of ageing stages is not as useful for waters closer to the coast where a bloom development cycle lasts between 6 - 7 days (Brown and Hutchings, 1987). The differences could also be due to the fact that the Northern and Southern Benguela are part of different upwelling cells (Shillington et al., 2006) and hence, have to be considered as separate systems (Hansen et al., 2014).

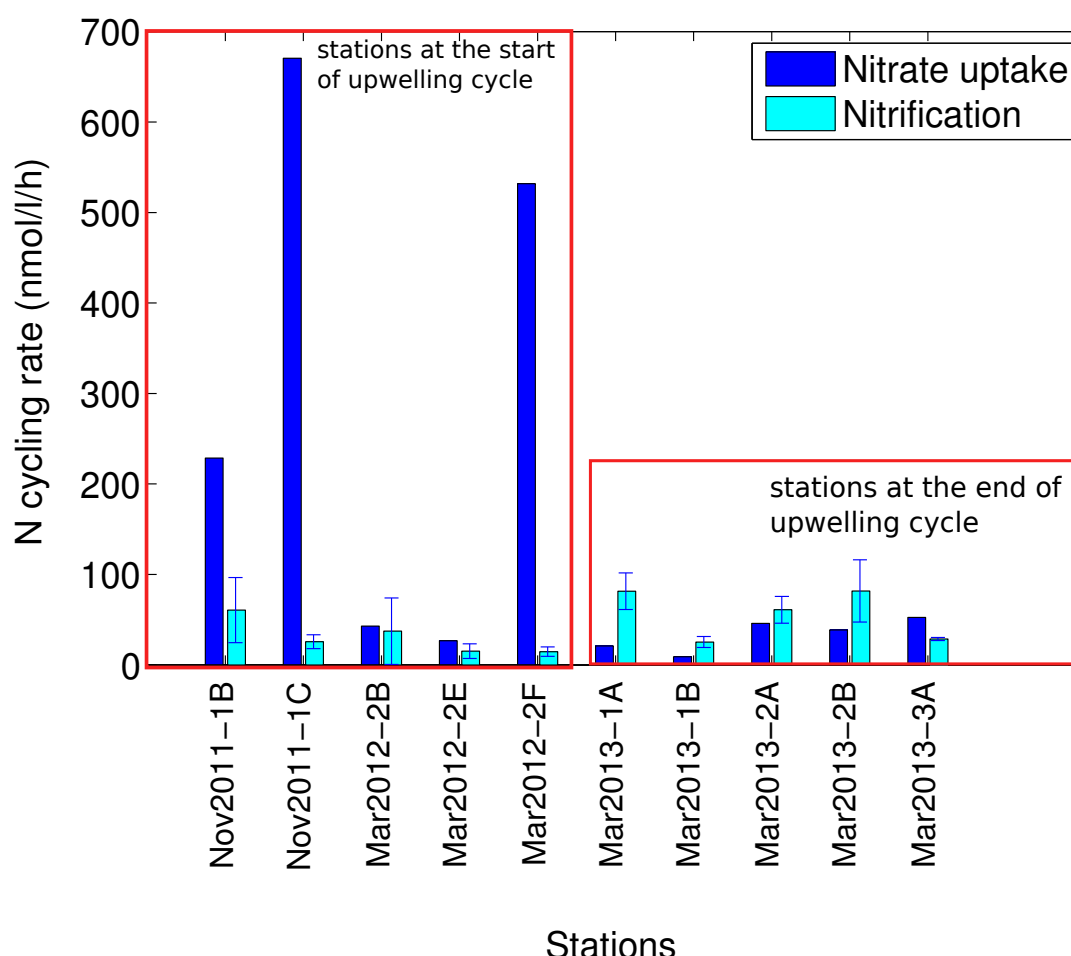


Figure 5.8: Nitrification and nitrate uptake rates at selected stations. Nitrification represented a small proportion of the nitrate demand by phytoplankton at the start of an upwelling cycle (stations in November 2011 and March 2012) whereas it consistently exceeded nitrate uptake at the end of the upwelling cycle (stations in March 2013).

The "succession" of nitrification after an upwelling event has not been investigated in other systems even though there are reports comparing nitrite oxidation under upwelling and non-upwelling conditions. Farías et al. (2009), Fernández and Farías (2012) and Levipan et al. (2014) investigated seasonal changes between the upwelling favourable summer and the non-upwelling winter off the coast of Chile. In this region, nitrification was higher during spring and summer than in fall and winter (Farías et al., 2009; Fernández and Farías, 2012) despite the fact that there was a higher diversity of nitrite oxidisers in winter (Levipan et al., 2014). These studies off the coast of Chile, however, lack the temporal resolution required to observe changes in the

short-term (3-7 days) and do not reflect the progression of nitrifying activity as upwelled waters aged.

5.4.4 Implications of high nitrification rates for carbon export in the Benguela upwelling system

The high contribution of nitrification to the nitrate pool and potentially to nitrate uptake brings into question the definitions of "new" production that have been central to many aspects marine biogeochemistry (Dugdale and Goering, 1967; Eppley and Peterson, 1979). In this study, nitrification supplied on average 35% of nitrate demand at the beginning of an upwelling cycle and consistently exceeded nitrate demand at the end of an upwelling cycle. This contribution of nitrification to nitrate demand is quite high when compared to results reported in the Central California current (25-26%, Santoro et al. 2010) and Monterey Bay (15-27%, Wankel et al., 2007). The separation of primary production between "new" and "regenerated" nitrate has been considered in the past (Waldron et al., 1992, 1998, 2009; Swart et al., 2007). In these studies, "new" nitrate was considered as the nitrate being upwelled from the SACW while "local" nitrate was the nitrate formed in the coastal shelf sediments. This separation resulted in carbon export estimates ranging from $3.9 - 7.3 \times 10^{13} \text{ g} \cdot \text{C} \cdot \text{y}^{-1}$. Based on an area of $6.5 \times 10^{10} \text{ m}^2$, these rates compared well with potential new production estimates by Messie et al. (2009) ($517 \text{ g} \cdot \text{C} \cdot \text{m}^{-2} \cdot \text{y}^{-1}$) but were likely to be overestimates of carbon export. In these studies, yearly new production was extrapolated based on estimates of upwelled nitrate in single upwelling events and the differences in upwelling intensity throughout the year were not accounted for. The potential overestimation is seen when comparing with other estimates of carbon export in the Benguela. For instance, a lower estimate of $0.72 \times 10^{13} \text{ g} \cdot \text{C} \cdot \text{y}^{-1}$ has been proposed based on modelled carbon fluxes (Waldron et al., 2009). This model used the concentrations of biogeochemical constituents at each stage of the upwelling cycle and the Ekman-driven fluxes. None of these approaches, however, considered nitrate regeneration within the water column.

Given the high proportion of regenerated nitrate, these carbon export estimates have to be revised. For instance, using dissolved inorganic carbon and total alkalinity measurements (Gregor and Monteiro, 2013) found that the Southern Benguela was only a weak sink of carbon ($-1.53 \text{ mol} \cdot \text{C} \cdot \text{m}^{-2} \cdot \text{y}^{-1}$) despite its high primary production rates. This would be the equivalent of $0.119 \times 10^{13} \text{ mol} \cdot \text{C} \cdot \text{m}^{-2} \cdot \text{y}^{-1}$. This low carbon uptake by the ocean was attributed to remineralisation processes, particularly over the shelf, and varied seasonally. This would be in agreement with the current study. Even though nitrate uptake is often high, an important proportion of the nitrate pool is regenerated and would therefore not be part of "export" production. Establishing whether the phytoplankton were using "new" nitrate originating from the SACW or nitrate formed within the water column would require a stable isotope approach (Nagel et al., 2013).

It is not possible to extrapolate the results presented here to a larger area and provide a better estimate to the overall contribution of nitrification since the rates were only measured for one depth. Integrated nitrate uptake and nitrification rates are therefore not available. In addition, the differences between shallow, near-shore ecosystems and continental shelves precludes from such extrapolations. The station in this study was located very close to the shore and the maximum depth in this study was about 20 m. This station cannot be taken as a representative of the Benguela upwelling system. For this reason, Waldron and Probyn (1992) only used data from areas deeper than 200 m to estimate carbon export from the Benguela. Gregor and Monteiro (2013) showed, in accordance with work by Chen and Borges (2009), that the near-shore was a source of CO_2 but that the continental shelf was a sink of this gas. The boundary between the areas which represented a sink of carbon and those which were a source of carbon varied seasonally and depended on the intensity and duration of upwelling as well as the extent of remineralisation processes. This would be in agreement with our results whereby remineralisation and nitrification were significant at a shallow, near-shore station. This area would therefore not be a contributor to carbon export in contrast to stations further offshore where nitrification plays a smaller role (Benavides et al., 2014).

5.5 Conclusion

In summary, nitrogen uptake and nitrification rates were measured simultaneously in St-Helena Bay, which is located within the Southern Benguela upwelling system. Three surveys were conducted and represented active upwelling and relaxation periods. Following active upwelling, temperature, salinity and dissolved oxygen were low while nitrate concentrations were high. The reverse was true in the post-bloom conditions during a relaxation period. Nitrate uptake was much higher at the start of the bloom cycle than at the end and showed an increase when the stability of the water column increased. The relative importance of nitrate uptake at the end of the upwelling cycle was greater than expected (f-ratio of 0.7). This could have been due to the fact that urea uptake was not measured. Nitrite production rates were consistently higher during the active upwelling periods. Factors which could also reduce ammonium oxidation rates include competition with ammonium due to the increased importance of small phytoplankton and predators grazing on nitrifiers. There are, however, strong doubts as to whether all of the nitrite was formed through the oxidation of ammonium. Given the differences between day-time and night-time rates at the beginning of a bloom cycle, it is possible that nitrite was released by phytoplankton following the non-nutritional uptake of nitrate. The smaller differences between day and night time rates at the end of a bloom cycle (March 2013) suggest that, during this period, ammonium oxidation was more important than nitrite release by phytoplankton. Another interesting observation in this study was the decoupling of ammonium oxidation and nitrite oxidation - the nitrite oxidation rates were much higher than the ammonium oxidation rates. The release of nitrite by phytoplankton could have been a potential source of nitrite. The nitrite oxidation rates were high compared to other upwelling regions but their contribution to nitrate uptake varied between the start and end of the bloom. While the nitrite oxidation rates measured at the beginning of an upwelling cycle in November 2011 and March 2012 could have been underestimates, they did not exceed nitrate uptake. In March 2013, reliable nitrite oxidation rates were obtained and they were consistently higher than nitrate uptake. This implies that at the end of a bloom, "new" production (i.e production fuelled by nitrate originating from outside the euphotic zone) was minimal. Given that this station was a shallow, near-shore station, this station was most likely located within an area, which is a source of CO_2 . The importance of regenerated production, whether based on "traditional" regenerated nutrients such as ammonium or urea or based on nitrate formed with the water column, is therefore expected. However, the importance of the nitrification processes potentially changes based on the timing within an upwelling cycle. However, more regular sampling is needed to confirm this pattern. One of the caveats of this study is that repeat sampling at a fixed location can be affected by the advection of different upwelling plumes. Studying the progression of nitrification and nitrogen uptake in isolated freshly upwelled water (such as a mesocosm) could prove a useful exercise to determine the changes in the contribution of nitrification to nitrogen uptake through the course of a bloom cycle. Moreover, the mechanisms behind decoupling of ammonium and nitrite oxidation as well as the source of nitrite remain an open question.

Chapter 6

Synthesis and conclusions

6.1 Thesis aims

Establishing the contribution of nitrification to the nitrogen cycle within the euphotic zone can provide insight into the fluxes between the various dissolved organic nitrogen fluxes as well as understand the vertical structure of the nutrient profiles. This thesis aimed to determine the importance of nitrification in the Southern Ocean and the Southern Benguela upwelling system by answering the following questions:

- What are the nitrification rates in the Southern Ocean and in the Southern Benguela upwelling system?
- What is the contribution of nitrification to nitrate demand in these two regions?
- What are the seasonal or event-driven differences in nitrogen cycling for these two regions?

In order to determine how important surface nitrification is in the two study regions, nitrogen uptake and nitrification rates were measured. Nitrogen uptake rates were measured using ^{15}N tracers. Nitrification rates were measured as rates of the two independent steps, ammonium oxidation and nitrite oxidation according to methods by Clark et al. (2007). These methods described in chapter 2 are based on the isotopic dilution of a ^{15}N tracer.

This chapter provides a synthesis of chapters 3 - 5 and compares nitrogen fluxes in the Southern Ocean and in St-Helena Bay (located in the Southern Benguela upwelling system). The factors controlling nitrogen uptake and nitrification in the two regions are also considered. In this chapter, the main findings are summarised in relation to the corresponding research questions.

6.2 What are the nitrification rates in the Southern Ocean and in the Southern Benguela upwelling system?

In the Southern Ocean, nitrification (at least one of the two steps) was only detected at 5 out of 15 stations using isotopic dilution approaches. The two steps of nitrification were measurable only at one station (a winter station located in the Polar frontal zone). This indicates that there is a significant decoupling between the two nitrification steps in this region. This is also seen from the fact that nitrite oxidation is much faster than ammonium oxidation. Nitrite production (ammonium oxidation) rates ranged from 0.824 ± 0.298 to $6.08 \pm 1.06 \text{ nmol} \cdot \text{l}^{-1} \cdot \text{h}^{-1}$ while nitrite oxidation ranged from 37.21 ± 9.13 to $217 \pm 88 \text{ nmol} \cdot \text{l}^{-1} \cdot \text{h}^{-1}$. While

the ammonium oxidation rates were comparable to previous studies, the nitrite oxidation rates were much higher than rates observed both in the Southern Ocean and in other regions. However, given that these nitrification rates were only detected at a minority of stations, it is possible that they are not an accurate reflection of reality. Furthermore, nitrification was only measured at 55% sPAR and could have been occurring at faster rates deeper in the mixed layer. A box-model was constructed based on nutrient concentrations before and after incubation for the summer cruise. The ammonium fluxes calculated using this box-model confirmed that ammonium oxidation was contributing to the consumption of this nutrient. In addition, the nitrite profiles as well as the N^* (the deviation of NO_3^- and PO_4^- concentrations from the Redfield ratio) also indicate the potential for deeper nitrification. This would be in agreement with results by Smart (2014) and Grzymiski et al. (2012). The former demonstrated the importance of nitrification within the winter mixed layer using a natural abundance stable isotope approach while the latter observed the presence of nitrifying organisms in the Southern Ocean during winter and summer.

In St-Helena Bay, nitrification was observed more consistently than in the Southern Ocean. Nitrite regeneration was detected at most stations. Only two stations did not show nitrite production and only 4 stations did not show nitrite oxidation. This could have been due to sampling errors. Nitrite regeneration ranged from 0.27 ± 0.54 to $22.83 \pm 1.63 \text{ nmol} \cdot \text{l}^{-1} \cdot \text{h}^{-1}$ and nitrite oxidation from 14.66 ± 5.20 to $81.74 \pm 1.74 \text{ nmol} \cdot \text{l}^{-1} \cdot \text{h}^{-1}$. In addition, nitrite oxidation rates were much higher than nitrite production indicating that the decoupling of the two nitrification steps is common globally (Clark et al., 2011; Beman et al., 2013, 2012; Füssel et al., 2012; Fernández and Farías, 2012). The nitrite production rates were comparable to those in other regions as well rates measured in the Southern Benguela using different techniques. Nitrite oxidation, while comparable to previous studies, was on the higher end of observed rates. In this study, nitrite production rates observed in the Southern Benguela and in the Southern Ocean were comparable but nitrite oxidation was generally higher in the Southern Ocean. However, as mentioned above, the occurrence of nitrification seemed to be more sporadic in the Southern Ocean and this might reduce its overall importance in this region.

6.3 What is the contribution of nitrification to nitrate demand in these two regions?

In fact, the importance of nitrification for carbon export models really lies with its contribution to nitrate demand. Figure 6.1 showed the contribution of ammonium and nitrate uptake and regeneration to the nitrogen cycle of the Southern Ocean and St Helena Bay. It also provides an indication of nitrite fluxes through nitrite production (either by ammonium oxidation or release by phytoplankton) and nitrite oxidation. Nitrate uptake rates in the Southern Ocean were much lower than in the Benguela Upwelling system. In the Southern Ocean, integrated nitrate winter uptake rates ranged from 0.17 to $5.20 \text{ mmol} \cdot \text{N} \cdot \text{m}^{-2} \cdot \text{d}^{-1}$ at 55% sPAR and summer uptake rates ranged from 0.16 to $0.65 \text{ mmol} \cdot \text{N} \cdot \text{m}^{-2} \cdot \text{d}^{-1}$. Absolute nitrate uptake rates in the Benguela were generally higher but no integrated uptake rates were available as only surface measurements were taken. The nitrification rates observed in the Southern Ocean were up to 3 orders of magnitude higher than nitrate uptake. Such a high contribution is unlikely when compared to other regions. However, it is to be noted that nitrification can be up to 6 times higher than nitrate uptake (Clark et al., 2011). In St-Helena Bay, nitrite oxidation rates represented between 3 and $> 100\%$ of nitrate uptake rates. In both regions, nitrification can be an important contributor to the regeneration of the nitrate pool and therefore not all production based on nitrate uptake can be classified as "new" production. When using the f-ratio framework and equating nitrate uptake to carbon export, the high nitrate uptake would indicate a potential for carbon export at this location. However, regions close to the coast in St-Helena Bay (where the station was located) have been identified as sources of carbon dioxide (Gregor and Monteiro, 2013). This would be supported by the high nitrogen

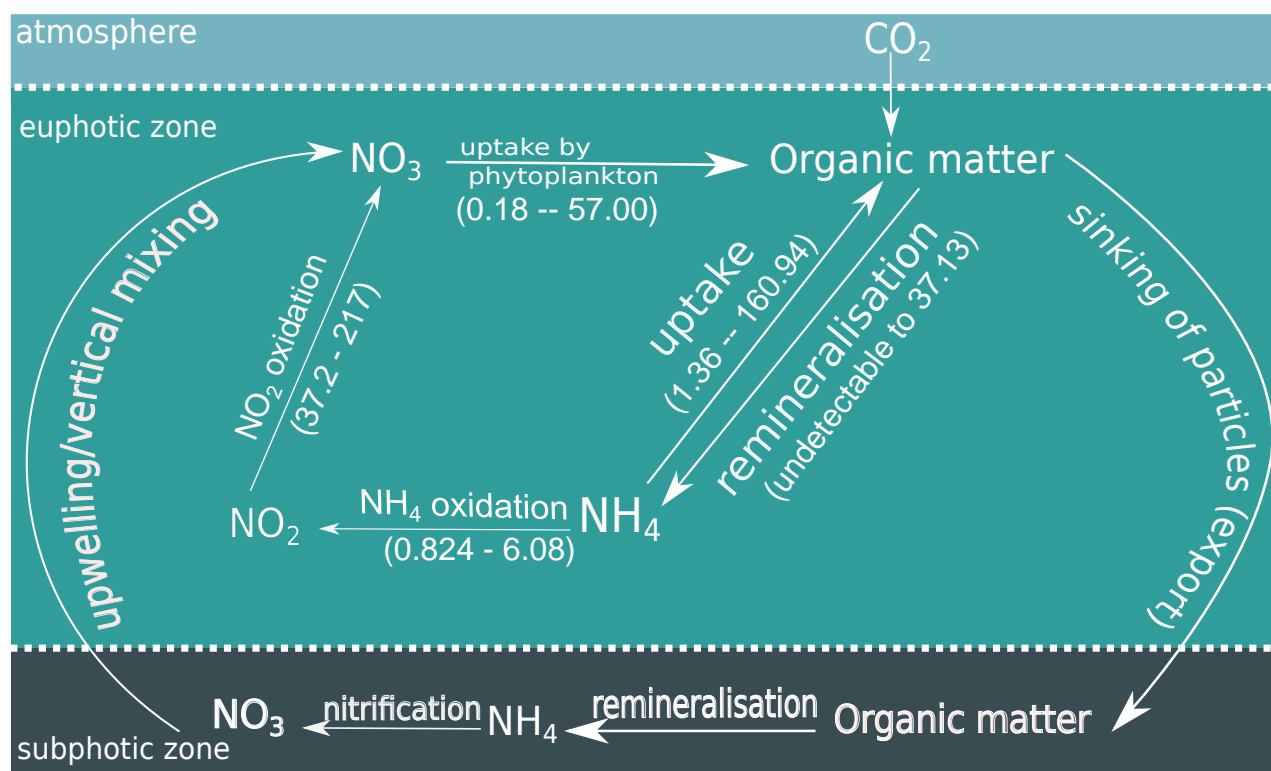
regeneration rates observed in the present study. High remineralisation rates within surface waters would indicate low export over a full upwelling cycle even if nitrate uptake is high following the influx of nutrients. This again highlights the flaws of the *f*-ratio as a proxy for carbon export.

6.4 What are the seasonal or event-driven differences in nitrogen cycling for these two regions?

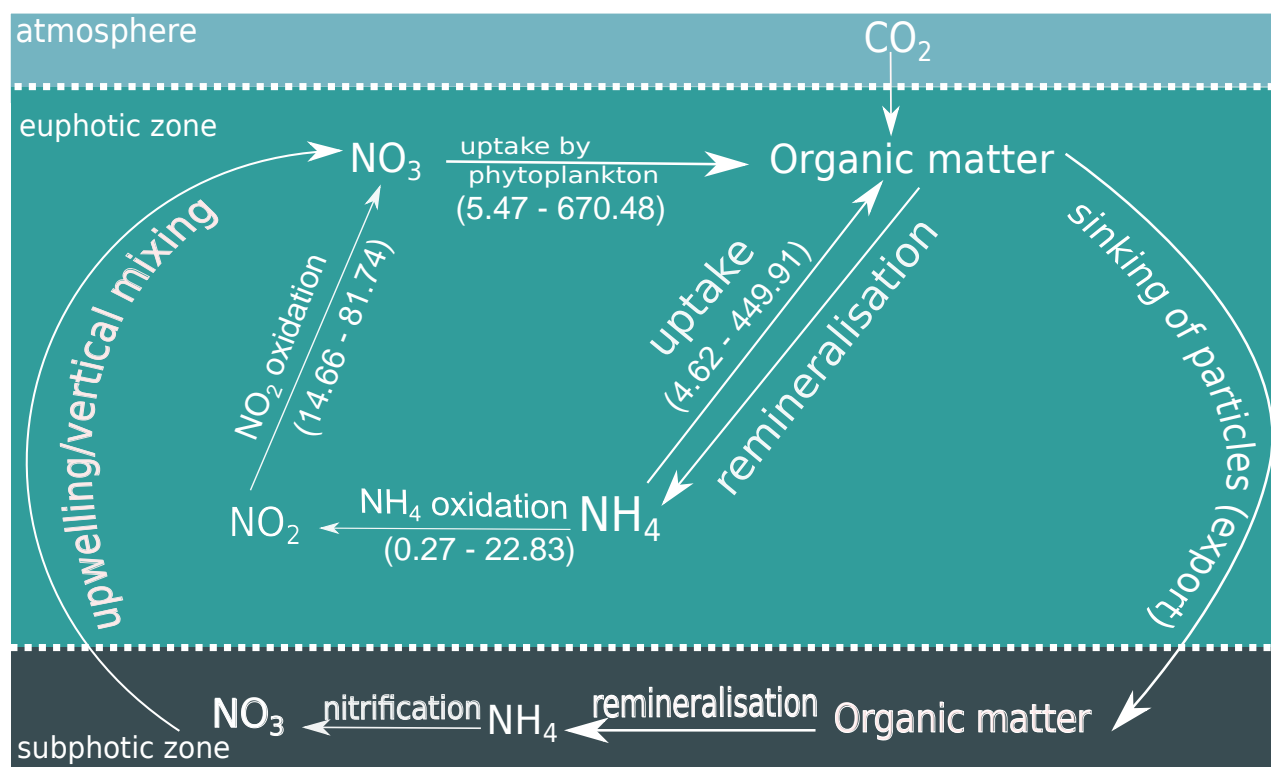
In St-Helena Bay, the rates of nitrate uptake, nitrite production and nitrite oxidation varied with the timing of sampling within a bloom cycle. Three field surveys were done in St-Helena Bay (November 2011, March 2012 and March 2013). The environmental conditions in November 2011 and March 2012 indicated active upwelling, which settled during the course of the survey. This predictably led to high nitrate concentrations and high nitrate uptake. On the other hand, in March 2013, the low nitrate, high oxygen and chlorophyll concentrations indicated post-bloom conditions. This was associated with low nitrate uptake. The changes in nitrogen uptake after an upwelling pulse have been well-studied in the past. However, the progression of nitrification throughout the bloom cycle is not as well understood (Benavides et al., 2014).

Nitrite production can be a result of ammonium oxidation as well as other processes such as the release of nitrite by phytoplankton. Nitrite production was much higher at the beginning of an upwelling cycle (November 2011 and March 2012) than at the end of the upwelling cycle (March 2013). Differences between day-time and night-time nitrite production rates in March 2012 were much larger than diel differences in March 2013. This indicates that in March 2012, a light-dependent process was enhancing the rates of nitrite production but that this was not the case in March 2013. One such process could be the release of nitrite by phytoplankton, which can be stimulated when nitrate concentrations are high. The importance of nitrification for the supply of nitrate also changed throughout the upwelling cycle. At the start of a bloom, when nitrate uptake was very high, the contribution of nitrification was low. The nitrification rates observed here were likely to have been underestimates, but even if they were up to ten times higher, they would not have exceeded the nitrate uptake rates. In contrast, at the end of a bloom cycle, nitrate uptake rates were low and were consistently exceeded by (reliable) nitrification rates.

In addition, the differences between the field campaigns in March 2012 and March 2013 highlight the fact that nitrogen cycling in the Benguela upwelling system are more strongly influenced by upwelling events and that these can cause high intra-seasonal variability. Seasonal variability in the Southern Ocean is expected to have a larger effect on the nitrogen cycle. In both seasons, ammonium uptake was higher than nitrate uptake. The differences between summer and winter nitrate uptake rates were greater than those between summer and winter ammonium uptake rates. In this study, the biogeochemical controls on the nitrogen uptake regime were investigated using multivariate statistical techniques. In winter, the fronts did not have a major influence on the nitrogen uptake regime. Stations having similar nitrogen uptake rates were sometimes located far away from each other rather than being in the same frontal zone. Nitrate uptake was strongly influenced by the southwards decrease in the number of day-light hours. The whole nitrogen uptake regime was influenced by the presence of ammonium, which both enhanced ammonium uptake and inhibited nitrate uptake. During the summer cruise, which focused on the sub-antarctic zone, increases in the mixed layer depth resulted in increases in the uptake rates. This suggested that low nutrient availability (e.g iron availability) was limiting primary productivity at this time of year. This is in agreement with the current understanding whereby the spring and summer bloom deplete nutrients in the surface layer.



(a) Southern Ocean



(b) St Helena Bay (Benguela upwelling)

Figure 6.1: Summary of nitrogen cycling rates in (a) the Southern Ocean and (b) St Helena Bay (Benguela upwelling system). Rates shown are in $\text{nmol} \cdot \text{L}^{-1} \cdot \text{h}^{-1}$. The range of nitrogen cycling rates is for the 55% light depth for both seasons in the Southern Ocean and from a depth of 3 m for the three field campaigns in the Benguela. The ammonium regeneration rates were calculated from the box model described in chapter 4. Nitrite production is shown here as ammonium oxidation. However, it is possible that part of the nitrite production could be due to release by phytoplankton.

6.5 Outlook

This study presents a rare dataset for surface nitrification (especially nitrite oxidation) and nitrate uptake rates for the Southern Ocean and the Southern Benguela upwelling system. However, the single field campaigns and cruises only provide snapshot views of the marine environment. In order to establish how high nitrification rates really are in the Southern Ocean, repeat experiments along regular transects are required. Similarly, for the Southern Benguela, time-series measurements as well as succession studies such as the ones done by Brown et al. (1991) for phytoplankton productivity and Benavides et al. (2014) would be extremely useful.

Moreover, the significance of nitrogen uptake and nitrification would be quantified more accurately if the rates of these processes had been measured throughout the water column and the mixed layer. Depth profiles of nitrification would contribute to a better understanding of this process with light and particulate matter. It would also help to resolve the vertical decoupling between nitrite production and nitrite oxidation. Furthermore, evaluating the source of nitrite using tracer experiments or natural abundance stable isotopes would be beneficial for a complete view of the nitrogen cycle. Finally, a characterisation of the bacterial and phytoplankton (including mixotrophs) communities would also contribute to understanding the drivers of the nitrogen cycle. Some mixotrophic phytoplankton are able to graze on bacteria resulting in a decrease in nitrification rates. The relationship between such organisms and nitrifying bacteria are poorly understood. In addition, different nitrifying organisms can occupy different niches and hence make varying contributions to nitrification. While the identification of these niches has been done in other regions (Fernández and Farías, 2012; Merbt et al., 2012), there are no such studies in the Southern Ocean and in the Benguela upwelling system. While this study has shown that nitrification rates in these two regions can be high and be major contributors to the nitrogen cycle, there are many open questions about the factors regulating the process.

Some of these questions can be addressed through new model studies incorporating both ammonium and nitrite oxidation would contribute to a better understanding of the nitrogen cycle. The results of this study can be used in such models as they provide nutrient concentrations with associated regeneration and uptake rates. A number of current models describe nitrification as a fixed rate. Based on the results in this study, this is clearly incorrect as both the nitrification rates have been found to be highly variable. Most models assume a coupling between ammonium and nitrite oxidation and a linear relationship between the concentration of ammonium and nitrate generation rates. This might need to be reconsidered in future models as this study suggests the decoupling between ammonium and nitrite oxidation is highly significant within the euphotic zone. Further studies investigating the extent and time-scales of this decoupling are required.

Bibliography

- Alonso-Sáez, L., Waller, A. S., Mende, D. R., Bakker, K., Farnelid, H., Yager, P. L., Lovejoy, C., Tremblay, J.-É., Potvin, M., Heinrich, F., Estrada, M., Riemann, L., Bork, P., Pedrós-Alíó, C., and Bertilsson, S.: Role for urea in nitrification by polar marine archaea, *Proceedings of the National Academy of Sciences*, 109, 17 989–17 994, URL <http://www.pnas.org/content/109/44/17989.abstract>, 2012.
- Ansorge, I., Speich, S., Lutjeharms, J., Goni, G., Rautenbach, C. d. W., Froneman, P., Rouault, M., and Garzoli, S.: Monitoring the oceanic flow between Africa and Antarctica : report of the first GoodHope cruise : research in action, *South African Journal of Science*, 101, p.29–35, 2005.
- Arrigo, K. R., Worthen, D., Schnell, A., and Lizotte, M. P.: Primary production in Southern Ocean waters, *Journal of Geophysical Research*, 103, 15 587–15,600, 1998.
- Aumont, O., Ethé, C., Tagliabue, A., Bopp, L., and Gehlen, M.: PISCES-v2: an ocean biogeochemical model for carbon and ecosystem studies, *Geoscientific Model Development Discussions*, 8, 1375–1509, doi: 10.5194/gmdd-8-1375-2015, URL <http://www.geosci-model-dev-discuss.net/8/1375/2015/>, 2015.
- Behrenfeld, M. J.: Abandoning Sverdrup’s Critical Depth Hypothesis on phytoplankton blooms, *Ecology*, 91, 977–989, doi:10.1890/09-1207.1, 2010.
- Beman, J., Sachdeva, R., and Fuhrman, J.: Population ecology of nitrifying archaea and bacteria in the Southern California Bight, *Environmental microbiology*, 12, 1282–1292, 2010.
- Beman, J. M., Popp, B. N., and Alford, S. E.: Quantification of ammonia oxidation rates and ammonia-oxidizing archaea and bacteria at high resolution in the Gulf of California and eastern tropical North Pacific Ocean, *Limnology and Oceanography*, 57, 711–726, doi:10.4319/lo.2012.57.3.0711, 2012.
- Beman, J. M., Leilei Shih, J., and Popp, B. N.: Nitrite oxidation in the upper water column and oxygen minimum zone of the eastern tropical North Pacific Ocean, *ISME Journal*, 7, 2192–2205, doi:10.1038/ismej.2013.96, 2013.
- Benavides, M., Santana-Falón, Y., Wasmund, N., and Arístegui, J.: Microbial uptake and regeneration of inorganic nitrogen off the coastal Namibian upwelling system, *Journal of Marine Systems*, in press, doi: 10.1016/j.jmarsys.2014.05.002, 2014.
- Berman-Frank, I., Cullen, J. T., Shaked, Y., Sherrell, R. M., and Falkowski, P. G.: Iron availability, cellular iron quotas, and nitrogen fixation in *Trichodesmium*, *Limnology and Oceanography*, 46, 1249–1260, doi: 10.4319/lo.2001.46.6.1249, 2001.
- Berounsky, V. M. and Nixon, S. W.: Temperature and the Annual Cycle of Nitrification in Waters of Narragansett Bay, *Limnology and Oceanography*, 35, 1610–1617, 1990.
- Bianchi, M. and Feliatra, D.: Regulation of nitrification in the land-ocean contact area of the Rhône River plume (NW Mediterranean), *Aquatic Microbial Ecology*, 18, 301–312, 1999.

- Bianchi, M., Feliatra, F., Tréguer, P., Vincendeau, M.-A., and Morvan, J.: Nitrification rates, ammonium and nitrate distribution in upper layers of the water column and in sediments of the Indian sector of the Southern Ocean, *Deep-Sea Research*, Part II, 44, 1017–1032, doi:10.1016/S0967-0645(96)00109-9, 1997.
- Bianchi, M., Fosset, C., and Conan, P.: Nitrification rates in the NW Mediterranean Sea, *Aquatic microbial ecology*, 17, 267–278, 1999.
- Bielicka-Daszekiewicz, K. and Voelkel, A.: Theoretical and experimental methods of determination of the breakthrough volume of SPE sorbents, *Talanta*, 80, 614–621, URL <http://www.sciencedirect.com/science/article/pii/S0039914009006122>, 2009.
- Bissett, W., Walsh, J., Dieterle, D., and Carder, K.: Carbon cycling in the upper waters of the Sargasso Sea: I. Numerical simulation of differential carbon and nitrogen fluxes, *Deep-Sea Research Part I: Oceanographic Research Papers*, 46, 205–269, doi:10.1016/S0967-0637(98)00062-4, 1999.
- Bopp, L., Monfray, P., Aumont, O., Dufresne, J.-L., Le Treut, H., Madec, G., Terray, L., and Orr, J. C.: Potential impact of climate change on marine export production, *Global Biogeochemical Cycles*, 15, 81–99, 2001.
- Borcard, D., Gillet, F., and Legendre, P.: *Numerical ecology with R*, Springer, 2011.
- Boyce, D. G., Lewis, M. R., and Worm, B.: Global phytoplankton decline over the past century, *Nature*, 466, 591–596, 2010.
- Boyd, P.: Environmental factors controlling phytoplankton processes in the Southern Ocean, *Journal of Phycology*, 38, 844–861, doi:10.1046/j.1529-8817.2002.t01-1-01203.x, 2002.
- Boyd, P. W., Strzepek, R., Fu, F., and Hutchins, D. A.: Environmental control of open-ocean phytoplankton groups: Now and in the future, *Limnology and Oceanography*, 55, 1353–1376, doi:10.4319/lo.2010.55.3.1353, 2010.
- Bronk, D., Killberg-Thoreson, L., Sipler, R., Mulholland, M., Roberts, Q., Bernhardt, P., Garrett, M., O’Neil, J., and Heil, C.: Nitrogen uptake and regeneration (ammonium regeneration, nitrification and photoproduction) in waters of the West Florida Shelf prone to blooms of *Karenia brevis*, *Harmful Algae*, doi:10.1016/j.hal.2014.04.007, 2014.
- Bronk, D. A., Gilbert, P. M., and Ward, B. B.: Nitrogen uptake, dissolved organic nitrogen release, and new production, *Science*, 265, 1843–1846, doi:10.1126/science.265.5180.1843, 1994.
- Brown, P. C. and Hutchings, L.: The development and decline of phytoplankton blooms in the southern Benguela upwelling system: 1. Drogue movements, hydrography and bloom development, *South African Journal of Marine Science*, 5, 357–391, doi:10.2989/025776187784522801, URL <http://dx.doi.org/10.2989/025776187784522801>, 1987.
- Brown, P. C., Painting, S. J., and Cochrane, K. L.: Estimates of phytoplankton and bacterial biomass and production in the northern and southern Benguela ecosystems, *South African Journal of Marine Science*, 11, 537–564, URL <http://www.tandfonline.com/doi/abs/10.2989/025776191784287673>, 1991.
- Buesseler, K. O.: The decoupling of production and particulate export in the surface ocean, *Global Biogeochemical Cycles*, 12, 297–310, 1998.
- Canfield, D. E., Glazer, A. N., and Falkowski, P. G.: The evolution and future of Earth’s nitrogen cycle, *Science*, 330, 192–196, 2010.

- Carini, S. A., McCarthy, M. J., and Gardner, W. S.: An isotope dilution method to measure nitrification rates in the northern Gulf of Mexico and other eutrophic waters, *Continental Shelf Research*, 30, 1795–1801, URL <http://www.sciencedirect.com/science/article/pii/S0278434310002463>, 2010.
- Cavagna, A.-J., Elskens, M., Griffiths, F. B., Fripiat, F., Jacquet, S. H., Westwood, K. J., and Dehairs, F.: Contrasting regimes of production and potential for carbon export in the Sub-Antarctic and Polar Frontal Zones south of Tasmania, *Deep-Sea Research, Part II*, 58, 2235–2247, doi:10.1016/j.dsr2.2011.05.026, 2011.
- Cavagna, A. J., Fripiat, F., Elskens, M., Dehairs, F., Mangion, P., Chirurgien, L., Closset, I., Lasbleiz, M., Flores?Leiva, L., Cardinal, D., Leblanc, K., Fernandez, C., Lefèvre, D., Oriol, L., Blain, S., and Quéguiner, B.: Biological productivity regime and associated N cycling in the vicinity of Kerguelen Island area, Southern Ocean, *Biogeosciences Discussions*, 11, 18 073?18 104, URL www.biogeosciences-discuss.net/11/18073/2014/, 2014.
- Chapman, P.: Nutrient cycling in marine ecosystems, *Journal of the Limnological Society of Southern Africa*, 12, 22–42, URL <http://dx.doi.org/10.1080/03779688.1986.9639397>, 1986.
- Chavez, F. P. and Messié, M.: A comparison of Eastern Boundary Upwelling Ecosystems, *Progress in Oceanography*, 83, 80–96, URL <http://www.sciencedirect.com/science/article/pii/S0079661109000998>, 2009.
- Chen, C.-T. A. and Borges, A. V.: Reconciling opposing views on carbon cycling in the coastal ocean: Continental shelves as sinks and near-shore ecosystems as sources of atmospheric CO₂, *Deep-Sea Research, Part II*, 56, 578–590, URL <http://www.sciencedirect.com/science/article/pii/S0967064509000162>, 2009.
- Clark, D. R., Fileman, T. W., and Joint, I.: Determination of ammonium regeneration rates in the oligotrophic ocean by gas chromatography/mass spectrometry, *Marine Chemistry*, 98, 121–130, URL <http://www.sciencedirect.com/science/article/B6VC2-4H9PN9W-3/2/cb71701624d42897e7f70fec715405c0>, 2006.
- Clark, D. R., Rees, A. P., and Joint, I.: A method for the determination of nitrification rates in oligotrophic marine seawater by gas chromatography/mass spectrometry, *Marine Chemistry*, 103, 84–96, doi:10.1016/j.dsr2.2011.05.026, 2007.
- Clark, D. R., Rees, A. P., and Joint, I.: Ammonium regeneration and nitrification rates in the oligotrophic Atlantic Ocean: implications for new production estimates, *Limnology and Oceanography*, 53, 52–62, 2008.
- Clark, D. R., Miller, P. I., Malcolm, E., Woodward, S., and Rees, A. P.: Inorganic nitrogen assimilation and regeneration in the coastal upwelling region of the Iberian Peninsula, *Limnology and Oceanography*, 56, 1689–1702, 2011.
- Clark, D. R., Brown, I. J., Rees, A. P., Somerfield, P. J., and Miller, P. I.: The influence of ocean acidification on nitrogen regeneration and nitrous oxide production in the North-West European shelf sea, *Biogeosciences Discuss.*, 11, 3113–3165, URL <http://www.biogeosciences-discuss.net/11/3113/2014/>, 2014.
- Cochlan, W. P.: Nitrogen uptake in the Southern Ocean, in: *Nitrogen in the marine environment*, edited by Capone, D. G., Bronk, D. A., Mulholland, M. R., and Carpenter, E. J., chap. 12, pp. 569–596, Academic Press, San Diego, doi:10.1016/B978-0-12-372522-6.00012-8, 2008.

- Codispoti, L., Brandes, J. A., Christensen, J., Devol, A., Naqvi, S., Paerl, H. W., and Yoshinari, T.: The oceanic fixed nitrogen and nitrous oxide budgets: Moving targets as we enter the anthropocene?, *Scientia Marina*, 65, 85–105, 2001.
- Colin F., P.: New trends in solid-phase extraction, *TrAC Trends in Analytical Chemistry*, 22, 362–373, URL <http://www.sciencedirect.com/science/article/pii/S0165993603006058>, 2003.
- Collos, Y.: Calculations of ^{15}N uptake rates by phytoplankton assimilating one or several nitrogen sources, *International Journal of Radiation Applications and Instrumentation. Part A. Applied Radiation and Isotopes*, 38, 275–282, doi:10.1016/0883-2889(87)90038-4, 1987.
- Cota, G., Smith, W., Nelson, D., Muench, R., and Gordon, L.: Nutrient and biogenic particulate distributions, primary productivity and nitrogen uptake in the Weddell-Scotia Sea marginal ice zone during winter, *Journal of Marine Research*, 50, 155–181, doi:10.1357/002224092784797764, 1992.
- Daims, H., Lückner, S., Le Paslier, D., and Wagner, M.: Diversity, environmental genomics, and ecophysiology of nitrite-oxidizing bacteria, in: *Nitrification*, edited by Ward, B. B., Arp, D. J., and Klotz, M. G., chap. 12, pp. 295–322, American Society of Microbiology, URL <http://www.asmscience.org/content/book/10.1128/9781555817145.ch12>, 2011.
- De Baar, H., Buma, A., Nolting, R., Cadée, G., Jacques, G., and Tréguer, P.: On iron limitation of the Southern Ocean: Experimental observations in the Weddell and Scotia Seas., *Marine Ecology Progress Series*, 65, 105–122, 1990.
- de Boyer Montégut, C., Madec, G., Fischer, A. S., Lazar, A., and Iudicone, D.: Mixed layer depth over the global ocean: An examination of profile data and a profile-based climatology, *Journal of Geophysical Research*, 109, C12 003–, URL <http://dx.doi.org/10.1029/2004JC002378>, 2004.
- Deal, C. J., Meibing, J., and Jia, W.: The significance of water column nitrification in the southeastern Bering Sea, *Chinese Journal of Polar Science*, 19, 185–192, 2008.
- Delille, D.: Abundance and function of bacteria in the Southern Ocean, *Cellular and Molecular Biology*, 50, 543–551, 2004.
- Deutsch, C. and Weber, T.: Nutrient ratios as a tracer and driver of ocean biogeochemistry, *Annual review of marine science*, 4, 113–141, 2012.
- Deutsch, Curtis, Sarmiento, Jorge L., Sigman, Daniel M., Gruber, Nicolas, and Dunne, John P.: Spatial coupling of nitrogen inputs and losses in the ocean, *Nature*, 445, 163–167, doi:10.1038/nature05392, 10.1038/nature05392, 2007.
- Devol, A. H.: Denitrification including Anammox, in: *Nitrogen in the marine environment*, edited by Capone, D. G., Bronk, D. A., Mulholland, M. R., and Carpenter, E. J., chap. 6, pp. 263–303, Academic Press, second edn., 2008.
- Diaz, F. and Raimbault, P.: Nitrogen regeneration and dissolved organic nitrogen release during spring in a NW Mediterranean coastal zone (Gulf of Lions): Implications for the estimation of new production, *Marine Ecology Progress Series*, 197, 51–65, doi:10.3354/meps197051, URL <http://www.int-res.com/abstracts/meps/v197/p51-65/>, 2000.
- Dickson, A. G., Sabine, C. L., and Christian, J. R.: Guide to best practices for ocean CO_2 measurements, 2007.

- DiFiore, P. J., Sigman, D. M., and Dunbar, R. B.: Upper ocean nitrogen fluxes in the Polar Antarctic Zone: Constraints from the nitrogen and oxygen isotopes of nitrate, *Geochemistry, Geophysics, Geosystems*, 10, Q11 016, doi:10.1029/2009GC002468, 2009.
- Doney, S. C.: The growing human footprint on coastal and open-ocean biogeochemistry, *Science*, 328, 1512–1516, URL <http://www.sciencemag.org/content/328/5985/1512>, 2010.
- Dore, J. E. and Karl, D. M.: Nitrification in the Euphotic Zone as a Source for Nitrite, Nitrate, and Nitrous Oxide at Station ALOHA, *Limnology and Oceanography*, 41, 1619–1628, URL <http://www.jstor.org/stable/2838650>, 1996.
- Dugdale, R. C. and Goering, J. J.: Uptake of new and regenerated forms of nitrogen in primary productivity, *Limnology and Oceanography*, 12, 196–206, doi:10.4319/lo.1967.12.2.0196, 1967.
- Dworkin, M.: Sergei Winogradsky: a founder of modern microbiology and the first microbial ecologist, *FEMS microbiology reviews*, 36, 364–379, 2012.
- Egan, L.: QuikChem® Method 31-107-04-1-C - Nitrate and/or Nitrite in brackish or seawater, Lachat instruments, 2008.
- Emerson, S. R. and Hedge, J. I.: *Chemical oceanography and the marine carbon cycle*, Cambridge University Press, New York, 1st edn., 2008.
- Eppley, R., Sharp, J., Renger, E., Perry, M., and Harrison, W.: Nitrogen assimilation by phytoplankton and other microorganisms in the surface waters of the central North Pacific Ocean, *Marine Biology*, 39, 111–120, doi:10.1007/BF00386996, 1977.
- Eppley, R. W. and Peterson, B. J.: Particulate organic matter flux and planktonic new production in the deep ocean, *Nature*, 282, 677–680, doi:10.1038/282677a0, 1979.
- Erguder, T. H., Boon, N., Wittebolle, L., Marzorati, M., and Verstraete, W.: Environmental factors shaping the ecological niches of ammonia- oxidizing archaea, *FEMS Microbiol Rev*, 33, 855 – 869, 2009.
- Falkowski, P.: Ocean Science: The power of plankton, *Nature*, 483, S17–S20, doi:10.1038/483S17a, 2012.
- Falkowski, P., Laws, E., Barber, R., and Murray, J.: Chapter 4 - Phytoplankton and their role in primary, new and export production., in: *Ocean biogeochemistry: The role of the ocean carbon cycle in global change*, edited by Fasham, M., Springer, 2003.
- Falkowski, P. G., Barber, R. T., and Smetacek, V.: Biogeochemical controls and feedbacks on ocean primary production, *Science*, 281, 200–206, doi:10.1126/science.281.5374.200, 1998.
- Farías, L., Fernández, C., Faúndez, J., Cornejo, M., and Alcaman, M.: Chemolithoautotrophic production mediating the cycling of the greenhouse gases N₂O and CH₄ in an upwelling ecosystem, *Biogeosciences*, 6, 3053–3069, 2009.
- Feliatra, F. and Bianchi, M.: Rates of nitrification and carbon uptake in the Rhône River plume (Northwestern Mediterranean Sea), *Microbial Ecology*, 26, 21–28, URL <http://dx.doi.org/10.1007/BF00166026>, 1993.
- Fernandes, S. O., Halarnekar, R., Malik, A., Vijayan, V., Varik, S., Kumari, R., V.K., J., Gauns, M. U., Nair, S., and LokaBharathi, P.: Nitrate reducing activity pervades surface waters during upwelling, *Journal of Marine Systems*, 137, 35–46, URL <http://www.sciencedirect.com/science/article/pii/S0924796314000979>, 2014.

- Fernández, C. and Farías, L.: Assimilation and regeneration of inorganic nitrogen in a coastal upwelling system: Ammonium and nitrate utilization, *Marine Ecology Progress Series*, 451, 1–14, URL <http://www.int-res.com/abstracts/meps/v451/p1-14/>, 2012.
- Fernández, C. and Raimbault, P.: Nitrogen regeneration in the NE Atlantic Ocean and its impact on seasonal new, regenerated and export production, *Marine Ecology Progress Series*, 337, 79–92, 2007.
- Fernández, C., Raimbault, P., Garcia, N., Rimmelin, P., and Caniaux, G.: An estimation of annual new production and carbon fluxes in the northeast Atlantic Ocean during 2001, *Journal of Geophysical Research: Oceans*, 110, 2005.
- Fernández, C., Farías, L., and Alcaman, M.: Primary production and nitrogen regeneration processes in surface waters of the Peruvian upwelling system, *Progress in Oceanography*, 83, 159–168, URL <http://www.sciencedirect.com/science/article/B6V7B-4WT3WG8-3/2/b842f66f1c3f431a84cd3fc1421147b1>, 2009.
- Fernández, C.: Cycle de l'azote et production primaire dans l'Atlantique Nord-Est: Suivi saisonnier et Influence de la meso échelle, Ph.D. thesis, Univ. de la Méditerranée, Marseille., 2003.
- Ferreira, V., Jarauta, I., Ortega, L., and Cacho, J.: Simple strategy for the optimization of solid-phase extraction procedures through the use of solid-liquid distribution coefficients: Application to the determination of aliphatic lactones in wine, *Journal of Chromatography A*, 1025, 147–156, URL <http://www.sciencedirect.com/science/article/pii/S0021967303019629>, 2004.
- Francis, C. A., Roberts, K. J., Beman, J. M., Santoro, A. E., and Oakley, B. B.: Ubiquity and diversity of ammonia-oxidizing archaea in water columns and sediments of the ocean, *Proceedings of the National Academy of Sciences of the United States of America*, 102, 14 683–14 688, URL <http://www.pnas.org/content/102/41/14683.abstract>, 2005.
- Francis, C. A., Beman, J. M., and Kuypers, M. M. M.: New processes and players in the nitrogen cycle: the microbial ecology of anaerobic and archaeal ammonia oxidation, *ISME Journal*, 1, 19–27, URL <http://dx.doi.org/10.1038/ismej.2007.8>, 2007.
- Fréon, P., Barange, M., and Aristegui, J.: Eastern Boundary Upwelling Ecosystems: Integrative and comparative approaches, *Progress in Oceanography*, 83, 1–14, URL <http://www.sciencedirect.com/science/article/pii/S0079661109001323>, 2009.
- Fulweiler, R., Emery, H., Heiss, E., and Berounsky, V.: Assessing the Role of pH in determining water column nitrification rates in a coastal system, *Estuaries and Coasts*, 34, 1095–1102, URL <http://dx.doi.org/10.1007/s12237-011-9432-4>, 2011.
- Füssel, J., Lam, P., Lavik, G., Jensen, M. M., Holtappels, M., Ganter, M., and Kuypers, M. M.: Nitrite oxidation in the Namibian oxygen minimum zone, *The ISME journal*, 6, 1200–1209, 2012.
- Gandhi, N., Ramesh, R., Laskar, A., Sheshshayee, M., Shetye, S., Anilkumar, N., Patil, S., and Mohan, R.: Zonal variability in primary production and nitrogen uptake rates in the southwestern Indian Ocean and the Southern Ocean, *Deep-Sea Research, Part I*, 67, 32–43, doi:10.1016/j.dsr.2012.05.003, 2012.
- Giddy, I., Swart, S., and Tagliabue, A.: Drivers of non-Redfield nutrient utilization in the Atlantic sector of the Southern Ocean, *Geophysical Research Letters*, 39, L17 604, 2012.
- Glibert, P. M., Lipschultz, F., McCarthy, J. J., and Altabet, M. A.: Isotope dilution models of uptake and remineralization of ammonium by marine plankton, *Limnology and Oceanography*, 27, 639–650, doi:10.4319/lo.1982.27.4.0639, 1982a.

- Glibert, P. M., Lipschultz, F., McCarthy, J. J., and Altabet, M. A.: Isotope dilution models of uptake and remineralization of ammonium by marine plankton, *Limnology and Oceanography*, 27, 639–650, doi:10.4319/lo.1982.27.4.0639, 1982b.
- Glibert, P. M., Lipschultz, F., McCarthy, J. J., and Altabet, M. A.: Has the mystery of the vanishing ^{15}N in isotope dilution experiments been resolved?, *Limnology and Oceanography*, 30, 444–447, doi:10.4319/lo.1985.30.2.0444, 1985.
- Goeyens, L., Tréguer, P., Baumann, M., Baeyens, W., and Dehairs, F.: The leading role of ammonium in the nitrogen uptake regime of Southern Ocean marginal ice zones, *Journal of Marine Systems*, 6, 345–361, doi:10.1016/0924-7963(94)00033-8, 1995.
- Gorham, E.: Biogeochemistry: its origins and development, *Biogeochemistry*, 13, 199–239, 1991.
- Grasshoff, K., Ehrhardt, M., and Kremling, K.: Methods of seawater analysis, Verlag Chemie, Weinheim, Germany, 1983.
- Grégoire, M. and Lacroix, G.: Study of the oxygen budget of the Black Sea waters using a 3D coupled hydrodynamical-biogeochemical model, *Journal of Marine Systems*, 31, 175 – 202, doi:http://dx.doi.org/10.1016/S0924-7963(01)00052-5, URL <http://www.sciencedirect.com/science/article/pii/S0924796301000525>, ventilation of Black Sea Anoxic Waters, 2001.
- Gregor, L. and Monteiro, P.: Is the southern Benguela a significant regional sink of CO_2 ?, *South African Journal of Science*, 109, 01–05, 2013.
- Großkopf, T., Mohr, W., Baustian, T., Schunck, H., Gill, D., Kuypers, M. M., Lavik, G., Schmitz, R. A., Wallace, D. W., and LaRoche, J.: Doubling of marine dinitrogen-fixation rates based on direct measurements, *Nature*, 488, 361–364, 2012.
- Gruber, N.: The marine nitrogen cycle: Overview and challenges, in: *Nitrogen in the Marine Environment*, edited by Capone, D. G., Bronk, D. A., Mulholland, M. R., and Carpenter, E. J., chap. 1, pp. 1–50, Academic Press, second edn., 2008.
- Gruber, N. and Sarmiento, J. L.: Global patterns of marine nitrogen fixation and denitrification, *Global Biogeochemical Cycles*, 11, 235–266, doi:10.1029/97GB00077, URL <http://dx.doi.org/10.1029/97GB00077>, 1997.
- Gruber, N., Gloor, M., Fletcher, S. E. M., Doney, S. C., Dutkiewicz, S., Follows, M. J., Gerber, M., Jacobson, A. R., Joos, F., Lindsay, K., Menemenlis, D., Mouchet, A., Müller, S. A., Sarmiento, J. L., , and Takahashi, T.: Oceanic sources, sinks, and transport of atmospheric CO_2 , *Global Biogeochemical Cycles*, 23, GB1005, doi:10.1029/2008GB003349, 2009.
- Grundle, D. S. and Juniper, S. K.: Nitrification from the lower euphotic zone to the sub-oxic waters of a highly productive British Columbia fjord, *Marine Chemistry*, 126, 173–181, URL <http://www.sciencedirect.com/science/article/pii/S0304420311000624>, 2011.
- Grundle, D. S., Juniper, S. K., and Giesbrecht, K. E.: Euphotic zone nitrification in the NE subarctic Pacific: Implications for measurements of new production, *Marine Chemistry*, 155, 113–123, URL <http://www.sciencedirect.com/science/article/pii/S0304420313001266>, 2013.
- Grzyski, J. J., Riesenfeld, C. S., Williams, T. J., Dussaq, A. M., Ducklow, H., Erickson, M., Cavicchioli, R., and Murray, A. E.: A metaproteomic assessment of winter and summer bacterioplankton from Antarctic Peninsula coastal surface waters, *ISME Journal*, 6, 1883–1900, URL <http://dx.doi.org/10.1038/ismej.2012.28>, 2012.

- Guerrero, M. and Jones, R.: Photoinhibition of marine nitrifying bacteria. I. Wavelength-dependent response, *Marine Ecology Progress Series*, 141, 183–192, URL <http://www.int-res.com/abstracts/meps/v141/p183-192/>, 1996a.
- Guerrero, M. and Jones, R.: Photoinhibition of marine nitrifying bacteria. II. Dark recovery after monochromatic or polychromatic irradiation, *Marine Ecology Progress Series*, 141, 193–198, URL <http://www.int-res.com/abstracts/meps/v141/p193-198/>, 1996b.
- Hansen, A., Ohde, T., and Wasmund, N.: Succession of micro- and nanoplankton groups in aging upwelled waters off Namibia, *Journal of Marine Systems*, in press, –, doi:10.1016/j.jmarsys.2014.05.003, 2014.
- Hatzenpichler, R.: Diversity, physiology, and niche differentiation of ammonia-oxidizing archaea, *Applied and Environmental Microbiology*, 78, 7501–7510, URL <http://aem.asm.org/content/78/21/7501.abstract>, 2012.
- Hedges, J., Baldock, J., G  linas, Y., Lee, C., Peterson, M., and Wakeham, S.: The biochemical and elemental compositions of marine plankton: A NMR perspective, *Marine Chemistry*, 78, 47–63, doi:10.1016/S0304-4203(02)00009-9, 2002.
- Hennion, M.-C.: Solid-phase extraction: method development, sorbents, and coupling with liquid chromatography, *Journal of Chromatography A*, 856, 3–54, URL <http://www.sciencedirect.com/science/article/pii/S0021967399008328>, 1999.
- Henson, S. A., Sanders, R., Madsen, E., Morris, P. J., Le Moigne, F., and Quartly, G. D.: A reduced estimate of the strength of the ocean’s biological carbon pump, *Geophysical Research Letters*, 38, L04 606–, doi:10.1029/2011GL046735, 2011.
- Herr, D.: The ocean and climate change: tools and guidelines for action, IUCN, 2009.
- Hoffmann, L., Peeken, I., and Lochte, K.: Iron, silicate, and light co-limitation of three Southern Ocean diatom species, *Polar Biology*, 31, 1067–1080–, doi:10.1007/s00300-008-0448-6, 2008.
- Holmes, R. M., Aminot, A., K  rouel, R., Hooker, B. A., and Peterson, B. J.: A simple and precise method for measuring ammonium in marine and freshwater ecosystems, *Canadian Journal of Fisheries and Aquatic Sciences*, 56, 1801–1808, doi:10.1139/f99-128, 1999.
- Horrigan, S., Carlucci, A., and Williams, P.: Light inhibition of nitrification in sea-surface films., *Journal of Marine Research*, 1981.
- Hutchins, D., Sedwick, P., DiTullio, G., Boyd, P., Queguiner, B., Griffiths, F., and Crossley, C.: Control of phytoplankton growth by iron and silicic acid availability in the subantarctic Southern Ocean: Experimental results from the SAZ Project, *Journal of Geophysical Research: Oceans*, 106, 31 559–31 572, doi:10.1029/2000JC000333, 2001.
- Ijichi, M. and Hamasaki, K.: Community structure of ammonia-oxidizing marine archaea differs by depth of collection and temperature of cultivation, *Journal of Oceanography*, 67, 739–745, URL <http://dx.doi.org/10.1007/s10872-011-0066-8>, 2011.
- Joubert, W. R., Thomalla, S. J., Waldron, H. N., Lucas, M. I., Boye, M., Le Moigne, F. A. C., Planchon, F., and Speich, S.: Nitrogen uptake by phytoplankton in the Atlantic sector of the Southern Ocean during late austral summer, *Biogeosciences*, 8, 2947–2959, doi:10.5194/bg-8-2947-2011, 2011.
- Kanda, J., Laws, E., Saino, T., and Hattori, A.: An evaluation of isotope dilution effect from conventional data sets of ¹⁵N uptake experiments, *Journal of Plankton Research*, 9, 79–90, doi:10.1093/plankt/9.1.79, 1987.

- Kuypers, M. M. M., Lavik, G., Woebken, D., Schmid, M., Fuchs, B. M., Amann, R., Jørgensen, B. B., and Jetten, M. S. M.: Massive nitrogen loss from the Benguela upwelling system through anaerobic ammonium oxidation, *Proceedings of the National Academy of Sciences of the United States of America*, 102, 6478–6483, URL <http://www.pnas.org/content/102/18/6478.abstract>, 2005.
- Lam, P., Lavik, G., Jensen, M. M., van de Vossenberg, J., Schmid, M., Woebken, D., Gutiérrez, D., Amann, R., Jetten, M. S. M., and Kuypers, M. M. M.: Revising the nitrogen cycle in the Peruvian oxygen minimum zone, *Proceedings of the National Academy of Sciences*, 106, 4752–4757, doi:10.1073/pnas.0812444106, URL <http://www.pnas.org/content/106/12/4752.abstract>, 2009.
- Lamont, T., Barlow, R., and Kyewalyanga, M.: Physical drivers of phytoplankton production in the southern Benguela upwelling system, *Deep-Sea Research Part I: Oceanographic Research Papers*, 90, 1–16, URL <http://www.sciencedirect.com/science/article/pii/S0967063714000399>, 2014.
- Lavrentyev, P., Gardner, W., and Johnson, J.: Cascading trophic effects on aquatic nitrification: experimental evidence and potential implications, *Aquatic microbial ecology*, 13, 161–175, 1997.
- Laws, E.: Isotope dilution models and the mystery of the vanishing ^{15}N , *Limnology and Oceanography*, 29, 379–386, doi:10.4319/lo.1984.29.2.0379, 1984.
- Laws, E. A., Falkowski, P. G., Smith, W. O., Ducklow, H., and McCarthy, J. J.: Temperature effects on export production in the open ocean, *Global Biogeochemical Cycles*, 14, 1231–1246, doi:10.1029/1999GB001229, 2000.
- Le Moigne, F., Boye, M., Masson, A., Corvaisier, R., Grosstefan, E., Gueneugues, A., and Pondaven, P.: Description of the biogeochemical features of the subtropical southeastern Atlantic and the Southern Ocean south of South Africa during the austral summer of the International Polar Year, *Biogeosciences*, 10, 281–295, doi:10.5194/bg-10-281-2013, 2013.
- Legendre, L. and Gosselin, M.: Estimation of N or C uptake rates by phytoplankton using ^{15}N or ^{13}C : revisiting the usual computation formulae, *Journal of Plankton Research*, 19, 263–271, URL <http://plankt.oxfordjournals.org/content/19/2/263.abstract>, 1997.
- Levipan, H. A., Molina, V., and Fernandez, C.: Nitrospina-like bacteria are the main drivers of nitrite oxidation in the seasonal upwelling area of the Eastern South Pacific (Central Chile (36°S)), *Environmental Microbiology Reports*, doi:10.1111/1758-2229.12158, 2014.
- Lima, I. D., Lam, P. J., and Doney, S. C.: Dynamics of particulate organic carbon flux in a global ocean model, *Biogeosciences*, 11, 1177–1198, URL <http://www.biogeosciences.net/11/1177/2014/>, 2014.
- Lipschultz, F.: Isotope tracer methods for studies of the marine nitrogen cycle, in: *Nitrogen in the Marine Environment*, edited by Capone, D. G., Bronk, D. A., Mulholland, M. R., and Carpenter, E. J., chap. 31, pp. 1345–1384, Academic Press, second edn., 2008.
- Lomas, M. W. and Glibert, P. M.: Temperature regulation of nitrate uptake: A novel hypothesis about nitrate uptake and reduction in cool-water diatoms, *Limnology and Oceanography*, 44, 556–572, doi:10.4319/lo.1999.44.3.0556, 1999a.
- Lomas, M. W. and Glibert, P. M.: Temperature regulation of nitrate uptake: A novel hypothesis about nitrate uptake and reduction in cool-water diatoms, *Limnology and Oceanography*, pp. 556–572, doi:10.4319/lo.1999.44.3.0556, 1999b.
- Lomas, M. W. and Glibert, P. M.: Comparisons of nitrate uptake, storage and reduction in marine diatoms and flagellates., *Journal of Phycology*, 36, 903–913, URL <http://dx.doi.org/10.1046/j.1529-8817.2000.99029.x>, 2000.

- Lomas, M. W. and Lipschultz, F.: Forming the primary nitrite maximum: Nitrifiers or phytoplankton?, *Limnology and Oceanography*, 51, 2453–2467, URL <http://www.jstor.org/stable/3841081>, 2006.
- Mackey, K. R., Bristow, L., Parks, D. R., Altabet, M. A., Post, A. F., and Paytan, A.: The influence of light on nitrogen cycling and the primary nitrite maximum in a seasonally stratified sea, *Progress in Oceanography*, 91, 545–560, 2011.
- Malerba, M. E., Connolly, S. R., and Heimann, K.: Nitrate-nitrite dynamics and phytoplankton growth: Formulation and experimental evaluation of a dynamic model, *Limnology and Oceanography*, 57, 1555, 2012.
- Martens-Habbena, W., Berube, P. M., Urakawa, H., de la Torre, J. R., and Stahl, D. A.: Ammonia oxidation kinetics determine niche separation of nitrifying archaea and bacteria, *Nature*, 461, 976–979, URL <http://dx.doi.org/10.1038/nature08465>, 2009.
- Martin, A. and Pondaven, P.: New primary production and nitrification in the western subtropical North Atlantic: a modeling study, *Global biogeochemical cycles*, 20, 2006.
- Martin, J. H., Gordon, R. M., and Fitzwater, S. E.: Iron in Antarctic waters, *Nature*, 345, 156–158, doi: 10.1038/345156a0, 1990.
- Mateus, M.: A process-oriented model of pelagic biogeochemistry for marine systems. Part I: Model description, *Journal of Marine Systems*, 94, URL <http://www.sciencedirect.com/science/article/pii/S0924796311002752>, 2012.
- Meeder, E., Mackey, K. R., Paytan, A., Shaked, Y., Iluz, D., Stambler, N., Rivlin, T., Post, A. F., and Lazar, B.: Nitrite dynamics in the open ocean-clues from seasonal and diurnal variations, *Marine Ecology Progress Series*, 453, 11–26, 2012.
- Menden-Deuer, S. and Lessard, E. J.: Carbon to volume relationships for dinoflagellates, diatoms, and other protist plankton, *Limnology and Oceanography*, 45, 569–579, 2000.
- Merbt, S. N., Stahl, D. A., Casamayor, E. O., Marti, E., Nicol, G. W., and Prosser, J. I.: Differential photoinhibition of bacterial and archaeal ammonia oxidation, *Fems Microbiology Letters*, 327, 41–46, doi: 10.1111/j.1574-6968.2011.02457.x, 2012.
- Messie, M., Ledesma, J., Kolber, D. D., Michisaki, R. P., Foley, D. G., and Chavez, F. P.: Potential new production estimates in four eastern boundary upwelling ecosystems, *Progress in Oceanography*, 83, 151–158, URL <http://www.sciencedirect.com/science/article/pii/S0079661109000731>, 2009.
- Mitchell, B. G., Brody, E. A., Holm-Hansen, O., McClain, C., and Bishop, J.: Light limitation of phytoplankton biomass and macronutrient utilization in the Southern Ocean, *Limnology and Oceanography*, 36, 1662–1677, doi:10.4319/lo.1991.36.8.1662, 1991.
- Miyazaki, T., Wada, E., and Hattori, A.: Capacities of shallow waters of Sagami Bay for oxidation and reduction of inorganic nitrogen, in: *Deep Sea Research and Oceanographic Abstracts*, vol. 20, pp. 571–577, Elsevier, 1973.
- Miyazaki, T., Wada, E., and Hattori, A.: Nitrite production from ammonia and nitrate in the euphotic layer of the western North Pacific Ocean, *Marine science communications*, 1975.
- Mohr, W., Großkopf, T., Wallace, D. W., and LaRoche, J.: Methodological underestimation of oceanic nitrogen fixation rates, *PLOS one*, 5, e12 583, 2010.

- Molina, V., Morales, C. E., Farfías, L., Cornejo, M., Graco, M., Eissler, Y., and Cuevas, L. A.: Potential contribution of planktonic components to ammonium cycling in the coastal area off central-southern Chile during non-upwelling conditions, *Progress in Oceanography*, 92, 43–49, 2012.
- Monteiro, P. M. and Roychoudhury, A. N.: Spatial characteristics of sediment trace metals in an eastern boundary upwelling retention area (St. Helena Bay, South Africa): A hydrodynamical-biological pump hypothesis, *Estuarine, Coastal and Shelf Science*, 65, 123–134, URL <http://www.sciencedirect.com/science/article/pii/S0272771405001654>, 2005.
- Moore, C. M., Hickman, A. E., Poulton, A. J., Seeyave, S., and Lucas, M. I.: Iron-light interactions during the CROZet natural iron bloom and EXport experiment (CROZEX): Taxonomic responses and elemental stoichiometry, *Deep-Sea Research, Part II*, 54, 2066–2084, doi:10.1016/j.dsr2.2007.06.015, 2007.
- Moore, C. M., Mills, M. M., Arrigo, K. R., Berman-Frank, I., Bopp, L., Boyd, P. W., Galbraith, E. D., Geider, R. J., Guieu, C., Jaccard, S. L., Jickells, T. D., La Roche, J., Lenton, T. M., Mahowald, N. M., Maranon, E., Marinov, I., Moore, J. K., Nakatsuka, T., Oschlies, A., Saito, M. A., Thingstad, T. F., Tsuda, A., and Ulloa, O.: Processes and patterns of oceanic nutrient limitation, *Nature Geoscience*, 6, 701–710, URL <http://dx.doi.org/10.1038/ngeo1765>, 2013.
- Moore, J. K. and Abbott, M. R.: Phytoplankton chlorophyll distributions and primary production in the Southern Ocean, *Journal of Geophysical Research*, 105, 28 709–28 722, URL <http://dx.doi.org/10.1029/1999JC000043>, 2000.
- Moore, J. K., Doney, S. C., Kleypas, J. A., Glover, D. M., and Fung, I. Y.: An intermediate complexity marine ecosystem model for the global domain, *Deep Sea Research Part II: Topical Studies in Oceanography*, 49, 403–462, 2001.
- Mulholland, M. R. and Lomas, M. W.: Nitrogen uptake and assimilation, in: *Nitrogen in the marine environment*, edited by Capone, D. G., Bronk, D. A., Mulholland, M. R., and Carpenter, E. J., chap. 7, pp. 303–385, Academic Press, second edn., 2008.
- Murawski, S. A., Steele, J. H., Taylor, P., Fogarty, M. J., Sissenwine, M. P., Ford, M., and Suchman, C.: Why compare marine ecosystems?, *ICES Journal of Marine Science: Journal du Conseil*, 67, 1–9, 2010.
- Nagel, B., Emeis, K.-C., Flohr, A., Rixen, T., Schlarbaum, T., Mohrholz, V., and Plas, A.: N-cycling and balancing of the N-deficit generated in the oxygen minimum zone over the Namibian shelf- An isotope-based approach, *Journal of Geophysical Research: Biogeosciences*, 118, 361–371, 2013.
- Newell, S. E., Babbitt, A. R., Jayakumar, A., , and Ward, B. B.: Ammonia oxidation rates and nitrification in the Arabian Sea, *GLOBAL BIOGEOCHEMICAL CYCLES*, 25, GB4016, doi:doi:10.1029/2010GB003940, 2011.
- Norton, J. M.: Diversity and environmental distribution of ammonia-oxidizing bacteria, in: *Nitrification*, edited by Ward, B. B., Arp, D. J., and Klotz, M. G., chap. 3, pp. 39–55, American Society of Microbiology, URL <http://www.asmscience.org/content/book/10.1128/9781555817145.ch03>, 2011.
- Olenina, I.: Biovolumes and size-classes of phytoplankton in the Baltic Sea, in: *HELCOM Balt. Sea Environ. Proc.*, vol. 106, 2006.
- Olson, R.: N-15 tracer studies of the primary nitrite maximum, *Journal of Marine Research*, 39, 203–226, 1981a.
- Olson, R.: Differential photoinhibition of marine nitrifying bacteria - a possible mechanism for the formation of the primary nitrite maximum, *Journal of Marine Research*, 39, 227–238, 1981b.

- Omand, M. M. and Mahadevan, A.: Large scale alignment of oceanic nitrate and density, *Journal of Geophysical Research: Oceans*, 118, 5322–5332, 2013.
- Orsi, A., Whitworth, T., and Nowlin, W.: On the meridional extent and fronts of the Antarctic Circumpolar Current, *Deep-Sea Research, Part I*, 42, 641–673, doi:10.1016/0967-0637(95)00021-W, 1995.
- Painter, S. C.: On the significance of nitrification within the euphotic zone of the subpolar North Atlantic (Iceland basin) during summer 2007, *Journal of Marine Systems*, 88, 332–335, URL <http://www.sciencedirect.com/science/article/pii/S0924796311001102>, 2011.
- Painting, S., Lucas, M., and Muir, D.: Fluctuations in heterotrophic bacterial community structure, activity and production in response to development and decay of phytoplankton in a microcosm., *Marine ecology progress series*. Oldendorf, 53, 129–141, 1989.
- Pitcher, G., Walker, D., Mitchell-Innes, B., and Moloney, C.: Short-term variability during an anchor station study in the southern Benguela upwelling system: Phytoplankton dynamics, *Progress in Oceanography*, 28, 39–64, URL <http://www.sciencedirect.com/science/article/pii/007966119190020M>, 1991.
- Pitcher, G. C., Brown, P. C., and Mitchell-Innes, B. A.: Spatio-temporal variability of phytoplankton in the southern Benguela upwelling system, *South African Journal of Marine Science*, 12, 439–456, URL <http://dx.doi.org/10.2989/02577619209504717>, 1992.
- Pollard, R., Lucas, M., and Read, J.: Physical controls on biogeochemical zonation in the Southern Ocean, *Deep-Sea Research Part II: Topical Studies in Oceanography*, 49, 3289–3305, doi:10.1016/S0967-0645(02)00084-X, 2002.
- Poole, C. F., Gunatilleka, A. D., and Sethuraman, R.: Contributions of theory to method development in solid-phase extraction, *Journal of Chromatography A*, 885, 17–39, URL <http://www.sciencedirect.com/science/article/pii/S0021967300002247>, 2000.
- Popova, E. E., Coward, A. C., Nurser, G. A., De Cuevas, B., Fasham, M. J. R., and Anderson, T. R.: Mechanisms controlling primary and new production in a global ecosystem model ? Part I: Validation of the biological simulation, *Ocean Science*, 2, 249–266, URL <http://hal.archives-ouvertes.fr/hal-00298300>, 2003.
- Preston, T., Zainal, K., Anderson, S., Bury, S. J., and Slater, C.: Isotope dilution analysis of combined nitrogen in natural waters. III. nitrate and nitrite, *Rapid Communications in Mass Spectrometry*, 12, 423–428, URL [http://dx.doi.org/10.1002/\(SICI\)1097-0231\(19980430\)12:8<423::AID-RCM178>3.0.CO;2-2](http://dx.doi.org/10.1002/(SICI)1097-0231(19980430)12:8<423::AID-RCM178>3.0.CO;2-2), 1998.
- Probyn, T.: The inorganic nitrogen nutrition of phytoplankton in the southern Benguela: new production, phytoplankton size and implications for pelagic foodwebs, *South African journal of Marine Science*, 12, 411–420, 1992.
- Probyn, T. A.: Nitrogen uptake by size-fractionated phytoplankton populations in the southern Benguela upwelling system., *Marine Ecology Progress Series*, 22, 249–, 1985.
- Probyn, T. A.: Nitrogen utilization by phytoplankton in the Namibian upwelling region during an austral spring, *Deep-Sea Research*, 35, 1387–1404, 1988.
- Probyn, T. A., Waldron, H. N., and James, A. G.: Size-Fractionated measurements of nitrogen uptake in aged upwelled waters: Implications for pelagic food webs, *Limnology and Oceanography*, 35, 202–210, URL <http://www.jstor.org/stable/2837356>, 1990.

- Probyn, T. A., Waldron, H. N., Searson, S., and Owens, N. J.: Diel variability in nitrogenous nutrient uptake at photic and subphotic depths, *Journal of Plankton Research*, 18, 2063–2079, URL <http://plankt.oxfordjournals.org/content/18/11/2063>, 1996.
- Quinones, R.: Eastern Boundary Current Systems, in: *Global Change - The IGBP Series*, edited by Liu, K.-K., Atkinson, L., Quinones, R., and Talaue-McManus, L., pp. 25–120, Springer Berlin Heidelberg, URL http://dx.doi.org/10.1007/978-3-540-92735-8_2, 2010.
- Raimbault, P., Slawyk, G., Boudjellal, B., Coatanoan, C., Conan, P., Coste, B., Garcia, N., Moutin, T., and Pujo-Pay, M.: Carbon and nitrogen uptake and export in the equatorial Pacific at 150°W: Evidence of an efficient regenerated production cycle, *Journal of Geophysical Research*, 104, 3341–3356, URL <http://dx.doi.org/10.1029/1998JC900004>, 1999.
- Raven, J. and Falkowski, P.: Oceanic sinks for atmospheric CO₂, *Plant, Cell & Environment*, 22, 741–755, 2002.
- Reay, D. S., Priddle, J., Nedwell, D. B., Whitehouse, M. J., Ellis-Evans, J. C., Deubert, C., and Connelly, D. P.: Regulation by low temperature of phytoplankton growth and nutrient uptake in the Southern Ocean, *Marine Ecology Progress Series*, 219, 51–64, doi:10.3354/meps219051, 2001.
- Redfield, A. C.: On the proportions of organic derivatives in sea water and their relation to the composition of plankton, University Press of Liverpool, 1934.
- Redfield, A. C.: The biological control of chemical factors in the environment, *American Scientist*, 46, 230A–221, 1958.
- Rees, A. P., Woodward, E. M. S., and Joint, I.: Concentrations and uptake of nitrate and ammonium in the Atlantic Ocean between 60°N and 50°S, *Deep-Sea Research, Part II*, 53, 1649–1665, URL <http://www.sciencedirect.com/science/article/B6VGC-4KJDWSR-3/2/06b04f4c9cd96cbd97346b1c3238f4bb>, 2006.
- Riebesell, U., Schulz, K. G., Bellerby, R. G. J., Botro, M., Fritsche, P., M. Meyerhöfer, C. N., Nondal, G., Oschlies, A., Wohlers, J., and Zöllner, E.: Enhanced biological carbon consumption in a high CO₂ ocean, *Nature*, 450, 545–549, doi:10.1038/nature06267, 2007.
- Robinson, D.: δ 15 N as an integrator of the nitrogen cycle, *Trends in Ecology & Evolution*, 16, 153–162, 2001.
- Salihoglu, B., Neuer, S., Painting, S., Murtugudde, R., Hofmann, E., Steele, J., Hood, R., Legendre, L., Lomas, M., Wiggert, J., Ito, S., Lachkar, Z., Hunt Jr., G., Drinkwater, K., and Sabine, C.: Bridging marine ecosystem and biogeochemistry research: Lessons and recommendations from comparative studies, *Journal of Marine Systems*, 109–110, 161–175, URL <http://www.sciencedirect.com/science/article/pii/S092479631200156X>, 2013.
- Sambrotto, R. N. and Mace, B. J.: Coupling of biological and physical regimes across the Antarctic Polar Front as reflected by nitrogen production and recycling, *Deep-Sea Research, Part II*, 47, 3339–3367, doi:10.1016/S0967-0645(00)00071-0, 2000.
- Sanders, R., Morris, P. J., Stinchcombe, M., Seeyave, S., Venables, H., and Lucas, M.: New production and the f ratio around the Crozet Plateau in austral summer 2004/2005 diagnosed from seasonal changes in inorganic nutrient levels, *Deep-Sea Research, Part II*, 54, 2191–2207, doi:10.1016/j.dsr2.2007.06.007, 2007.

- Santoro, A. E., Casciotti, K. L., and Francis, C. A.: Activity, abundance and diversity of nitrifying archaea and bacteria in the central California Current, *Environmental Microbiology*, 12, 1989–2006, URL <http://dx.doi.org/10.1111/j.1462-2920.2010.02205.x>, 2010.
- Santoro, A. E., Sakamoto, C. M., Smith, J. M., Plant, J. N., Gehman, A. L., Worden, A. Z., Johnson, K. S., Francis, C. A., and Casciotti, K. L.: Measurements of nitrite production in and around the primary nitrite maximum in the central California Current, *Biogeosciences*, 10, 7395–7410, URL <http://www.biogeosciences.net/10/7395/2013/>, 2013.
- Sarmiento, J. L., Gruber, N., Brzezinski, M. A., and Dunne, J. P.: High-latitude controls of thermocline nutrients and low latitude biological productivity, *Nature*, 427, 56–60, doi:10.1038/nature02127, 2004.
- Savoye, N., Dehairs, F., Elskens, M., Cardinal, D., Kopczyńska, E., Trull, T. W., Wright, S., Baeyens, W., and Griffiths, F. B.: Regional variation of spring N-uptake and new production in the Southern Ocean, *Geophysical Research Letters*, 31, L03 301, doi:10.1029/2003GL018946, 2004.
- Schlesinger, W. H. and Bernhardt, E. S.: *Biogeochemistry: an analysis of global change*, Academic press, 2013.
- Sedwick, P., Blain, S., Quéguiner, B., Griffiths, F., Fiala, M., Bucciarelli, E., and Denis, M.: Resource limitation of phytoplankton growth in the Crozet Basin, Subantarctic Southern Ocean, *Deep-Sea Research Part II: Topical Studies in Oceanography*, 49, 3327–3349, doi:10.1016/S0967-0645(02)00086-3, 2002.
- Semeneh, M., Dehairs, F., Elskens, M., Baumann, M., Kopczynska, E., Lancelot, C., and Goeyens, L.: Nitrogen uptake regime and phytoplankton community structure in the Atlantic and Indian sectors of the Southern Ocean, *Journal of Marine Systems*, 17, 159–177, doi:10.1016/S0924-7963(98)00036-0, 1998a.
- Semeneh, M., Dehairs, F., Fiala, M., Elskens, M., and Goeyens, L.: Seasonal variation of phytoplankton community structure and nitrogen uptake regime in the Indian Sector of the Southern Ocean, *Polar Biology*, 20, 259–272, doi:10.1007/s003000050302, 1998b.
- Serebrennikova, Y., Fanning, K. A., and Walsh, J. J.: Modeling the nitrogen and carbon cycling in Marguerite Bay, Antarctica: Annual variations in ammonium and net community production, *Deep-Sea Research Part II: Topical Studies in Oceanography*, 55, 393–411, URL <http://www.sciencedirect.com/science/article/pii/S0967064507003104>, 2008.
- Shillington, F., Reason, C., Duncombe Rae, C., Florenchie, P., and Penven, P.: 4 Large scale physical variability of the Benguela Current Large Marine Ecosystem (BCLME), in: *Benguela Predicting a Large Marine Ecosystem*, edited by Vere Shannon, Gotthilf Hempel, P. M.-R. C. M. and Woods, J., vol. Volume 14, pp. 49–70, Elsevier, URL <http://www.sciencedirect.com/science/article/pii/S1570046106800091>, 2006.
- Slawyk, G. and Raimbault, P.: Simple procedure for simultaneous recovery of dissolved inorganic and organic nitrogen in ^{15}N -tracer experiments and improving the isotopic mass balance, *Marine Ecology Progress Series*, 124, 289–299, doi:10.3354/meps124289, URL <http://www.int-res.com/abstracts/meps/v124/p289-299/>, 1995.
- Slawyk, G., Collos, Y., and Auclair, J.-C.: The use of the ^{13}C and ^{15}N isotopes for the simultaneous measurement of carbon and nitrogen turnover rates in marine phytoplankton, *Limnology and Oceanography*, 22, 925–932, URL <http://www.jstor.org/stable/2834930>, 1977.
- Smart, S.: Wintertime nitrate Isotope dynamics in the Atlantic sector of the Southern Ocean, Master's thesis, University of Cape Town, 2014.

- Smart, S. M., Fawcett, S. E., Thomalla, S. J., Weigand, M. A., Reason, C. J. C., and Sigman, D. M.: Isotopic evidence for nitrification in the Antarctic winter mixed layer, *Global Biogeochemical Cycles*, 2015.
- Smith, Jr, W. . and Nelson, D. M.: Phytoplankton growth and new production in the Weddell Sea marginal ice zone in the austral spring and autumn, *Limnology and Oceanography*, 35, 809–821, doi:10.4319/lo.1990.35.4.0809, 1990.
- Smith Jr., W. and Harrison, W.: New production in polar regions: The role of environmental controls, *Deep-Sea Research, Part I*, 38, 1463–1479, doi:10.1016/0198-0149(91)90085-T, 1991.
- Souza, A. C., Gardner, W. S., and Dunton, K. H.: Rates of nitrification and ammonium dynamics in northeastern Chukchi Sea shelf waters, *Deep-Sea Research Part II: Topical Studies in Oceanography*, 102, 68–76, URL <http://www.sciencedirect.com/science/article/pii/S0967064513004633>, 2014.
- Stigebrandt, A. and Wulff, F.: A model for the dynamics of nutrients and oxygen in the Baltic proper, *Journal of Marine Research*, 45, 729–759, doi:doi:10.1357/002224087788326812, URL <http://www.ingentaconnect.com/content/jmr/jmr/1987/00000045/00000003/art00009>, 1987.
- Strzepek, R. F., Hunter, K. A., Frew, R. D., Harrison, P. J., and Boyd, P. W.: Iron-light interactions differ in Southern Ocean phytoplankton, *Limnology and Oceanography*, 57, 1182–1200, doi:10.4319/lo.2012.57.4.1182, 2012.
- Sutka, R., Ostrom, N., Ostrom, P., and Phanikumar, M.: Stable nitrogen isotope dynamics of dissolved nitrate in a transect from the north Pacific subtropical gyre to the eastern tropical north Pacific, *Geochimica et Cosmochimica Acta*, 68, 517–527, URL <http://www.sciencedirect.com/science/article/pii/S0016703703004836>, 2004.
- Sverdrup, H.: On conditions for the vernal blooming of phytoplankton, *Journal du Conseil*, 18, 287–295, doi:10.1093/icesjms/18.3.287, 1953.
- Swart, S., Waldron, H., and Hutchings, L.: Evidence of carbon transport between shelf and slope waters in the Benguela upwelling system, *African Journal of Marine Science*, 29, 137–139, doi:10.2989/AJMS.2007.29.1.13.78, 2007.
- Sweeney, R., Liu, K., and Kaplan, I.: Oceanic nitrogen isotopes and their uses in determining the source of sedimentary nitrogen, *N. Z. Depart. Sci. Ind. Res. Bull.*, 9, 9–26, 1978.
- Takahashi, T., Sutherland, S. C., Wanninkhof, R., Sweeney, C., Feely, R. A., Chipman, D. W., Hales, B., Friederich, G., Chavez, F., Sabine, C., Watson, A., Bakker, D. C., Schuster, U., Metzl, N., Yoshikawa-Inoue, H., Ishii, M., Midorikawa, T., Nojiri, Y., Körtzinger, A., Steinhoff, T., Hoppema, M., Olafsson, J., Arnarson, T. S., Tilbrook, B., Johannessen, T., Olsen, A., Bellerby, R., Wong, C., Delille, B., Bates, N., and De Baar, H.: Climatological mean and decadal change in surface ocean pCO₂, and net sea-air CO₂ flux over the global oceans, *Deep-Sea Research, Part II*, 56, 554–577, doi:10.1016/j.dsr2.2008.12.009, 2009.
- Taylor, B. W., Keep, C. F., Hall, Robert O., J., Koch, B. J., Tronstad, L. M., Flecker, A. S., and Ulseth, A. J.: Improving the fluorometric ammonium method: Matrix Effects, background Fluorescence, and standard additions, *Journal of the North American Benthological Society*, 26, 167–177, doi:10.1899/0887-3593(2007)26%5B167:ITFAMM%5D2.0.CO;2, 2007.
- Thomalla, S., Fauchereau, N., Swart, S., and Monteiro, P.: Regional scale characteristics of the seasonal cycle of chlorophyll in the Southern Ocean, *Biogeosciences*, 8, 2849–2866, doi:doi:10.5194/bg-8-2849-2011, 2011a.

- Thomalla, S. J., Waldron, H. N., Lucas, M. I., Read, J. F., Ansorge, I. J., and Pakhomov, E.: Phytoplankton distribution and nitrogen dynamics in the southwest indian subtropical gyre and Southern Ocean waters, *Ocean Science*, 7, 113–127, doi:10.5194/os-7-113-2011, 2011b.
- Thompson, P. A., Levasseur, M. E., and Harrison, P. J.: Light-Limited Growth on ammonium vs. nitrate: What is the advantage for marine phytoplankton?, *Limnology and Oceanography*, 34, 1014–1024, URL <http://www.jstor.org/stable/2837191>, 1989.
- Tilzer, M. and Dubinsky, Z.: Effects of temperature and day length on the mass balance of Antarctic phytoplankton, *Polar Biology*, 7, 35–42, doi:10.1007/BF00286822, 1987.
- Touratier, F., Field, J. G., and Moloney, C. L.: Simulated carbon and nitrogen flows of the planktonic food web during an upwelling relaxation period in St Helena Bay (southern Benguela ecosystem), *Progress in Oceanography*, 58, 1–41, URL <http://www.sciencedirect.com/science/article/pii/S0079661103000879>, 2003.
- Tréguer, P. and Jacques, G.: Review dynamics of nutrients and phytoplankton, and fluxes of carbon, nitrogen and silicon in the Antarctic Ocean, in: *Weddell Sea Ecology*, pp. 149–162, Springer, 1993.
- Tyrrell, T.: The relative influences of nitrogen and phosphorus on oceanic primary production, *Nature*, 400, 525–531, 1999.
- Tyrrell, T. and Lucas, M. I.: Geochemical evidence of denitrification in the Benguela upwelling system, *Continental Shelf Research*, 22, 2497–2511, URL <http://www.sciencedirect.com/science/article/B6VBJ-475J3TH-5/2/a3c9207f2c46d7083397827836d207ab>, 2002.
- Van Oijen, T., Van Leeuwe, M., Granum, E., Weissing, F., Bellerby, R., Gieskes, W., and De Baar, H.: Light rather than iron controls photosynthate production and allocation in Southern Ocean phytoplankton populations during austral autumn, *Journal of Plankton Research*, 26, 885–900, doi:10.1093/plankt/fbh088, 2004.
- Vasechkina, E. and Yarin, V.: Object-based modeling of the coastal marine ecosystem, *Physical Oceanography*, 19, 315–338, URL <http://dx.doi.org/10.1007/s11110-010-9057-3>, 2009.
- Venables, H. and Moore, C. M.: Phytoplankton and light limitation in the Southern Ocean: Learning from high-nutrient, high-chlorophyll areas, *J. Geophys. Res.*, 115, C02015–, doi:10.1029/2009JC005361, 2010.
- Venables, H. J., Clarke, A., and Meredith, M. P.: Wintertime controls on summer stratification and productivity at the western Antarctic Peninsula, *Limnology and Oceanography*, 58, 1035–1047, doi:10.4319/lo.2013.58.3.1035, 2013.
- Venter, J. C., Remington, K., Heidelberg, J. F., Halpern, A. L., Rusch, D., Eisen, J. A., Wu, D., Paulsen, I., Nelson, K. E., and Nelson, W.: Environmental genome shotgun sequencing of the Sargasso Sea, *Science*, 304, 66–74, 2004.
- Vernet, M., Kozłowski, A., Yarmey, L., Lowe, A., Ross, R., Quetin, L., and Fritsen, C.: Primary production throughout austral fall, during a time of decreasing daylength in the western Antarctic Peninsula, *Marine Ecology Progress Series*, 452, 45–61, doi:10.3354/meps09704, 2012.
- Vichi, M., Masina, S., and Navarra, A.: A generalized model of pelagic biogeochemistry for the global ocean ecosystem. Part II: Numerical simulations, *Journal of Marine Systems*, 64, 110–134, doi:10.1016/j.jmarsys.2006.03.014, 2007.
- Volk, T. and Hoffert, M. I.: Ocean carbon pumps: Analysis of relative strengths and efficiencies in ocean-driven atmospheric CO₂ changes, *Geophysical Monograph Series*, 32, 99–110, 1985.

- Waldron, H.: Influences on the hydrology of the Cape Columbine/St Helena Bay region, Master's thesis, University of Cape Town, 1985.
- Waldron, H. and Probyn, T.: Short-term variability during an anchor station study in the southern Benguela upwelling system: Nitrogen supply to the euphotic zone during a quiescent phase in the upwelling cycle., *Progress in Oceanography*, 28, 153–166, 1991.
- Waldron, H., Monteiro, P., and Swart, N.: Carbon export and sequestration in the southern Benguela upwelling system: lower and upper estimates, *Ocean Science*, 5, 711–718, 2009.
- Waldron, H. N. and Probyn, T. A.: Nitrate supply and potential new production in the Benguela upwelling system, *South African Journal of Marine Science*, 12, 29–39, URL <http://dx.doi.org/10.2989/02577619209504688>, 1992.
- Waldron, H. N., Probyn, T. A., Lutjeharms, J. R. E., and Shillington, F. A.: Carbon export associated with the Benguela upwelling system, *South African Journal of Marine Science*, 12, 369–374, URL <http://dx.doi.org/10.2989/02577619209504712>, 1992.
- Waldron, H. N., Attwood, C. G., Probyn, T. A., and Lucas, M. I.: Nitrogen dynamics in the Bellingshausen Sea during the Austral spring of 1992, *Deep-Sea Research*, 42, 1253–1276, doi:10.1016/0967-0645(95)00063-V, 1995.
- Waldron, H. N., Probyn, T. A., and Brundri, G. B.: Carbon pathways and export associated with the southern Benguela upwelling system: a re-appraisal, *South African Journal of Marine Science*, 19, 113–118, URL <http://dx.doi.org/10.2989/025776198784126854>, 1998.
- Wankel, S. D., Kendall, C., Pennington, J. T., Chavez, F. P., and Paytan, A.: Nitrification in the euphotic zone as evidenced by nitrate dual isotopic composition: Observations from Monterey Bay, California, *Global Biogeochemical Cycles*, 21, GB2009–, URL <http://dx.doi.org/10.1029/2006GB002723>, 2007.
- Wanninkhof, R. e. a.: Global ocean carbon uptake: magnitude, variability and trends, *Biogeosciences*, 10, 1983–2000, doi:10.5194/bg-10-1983-2013, 2013.
- Ward, B.: Temporal variability in nitrification rates and related biogeochemical factors in Monterey Bay, California, USA, *Marine Ecology Progress Series*, 292, 97–109, 2005.
- Ward, B.: Nitrification in marine systems, in: *Nitrogen in the marine environment*, edited by Capone, D. G., Bronk, D. A., Mulholland, M. R., and Carpenter, E. J., chap. 5, pp. 199–261, Academic Press, second edn., 2008.
- Ward, B.: Measurement and distribution of nitrification rates in the oceans, in: *Research on Nitrification and Related Processes, Part A*, edited by Klotz, M. G., vol. Volume 486, chap. 13, pp. 307–323, Academic Press, URL <http://www.sciencedirect.com/science/article/pii/B9780123812940000134>, 2011a.
- Ward, B. and Zafiriou, O.: Nitrification and nitric oxide in the oxygen minimum of the eastern tropical North Pacific, *Deep-Sea Research Part A. Oceanographic Research Papers*, 35, 1127–1142, 1988.
- Ward, B. B.: Nitrification: an introduction and overview of the state of the field, in: *Nitrification*, edited by Ward, B. B., Arp, D. J., and Klotz, M. G., chap. Nitrification: an introduction and overview of the state of the field, pp. 3–8, American Society for Microbiology (ASM), 2011b.
- Ward, B. B. and O'Mullan, G. D.: Community level analysis: Genetic and biogeochemical approaches to investigate community composition and function in aerobic ammonia oxidation, in: *Environmental Microbiology*, edited by Leadbetter, J. R., vol. Volume 397, pp. 395–413, Academic Press, URL <http://www.sciencedirect.com/science/article/pii/S0076687905970249>, 2005.

- Ward, B. B., Kilpatrick, K. A., Renger, E. H., and Eppley, R. W.: Biological nitrogen cycling in the nitracline, *Limnology and Oceanography*, 34, 493–513, doi:10.4319/lo.1989.34.3.0493, 1989.
- Wasmund, N., Nausch, G., and Hansen, A.: Phytoplankton succession in an isolated upwelled Benguela water body in relation to different initial nutrient conditions, *Journal of Marine Systems*, in press, doi: 10.1016/j.jmarsys.2014.03.006, 2014.
- Westwood, K. J., Griffiths, F. B., Webb, J. P., and Wright, S. W.: Primary production in the Sub-Antarctic and Polar Frontal Zones south of Tasmania, Australia; SAZ-Sense survey, 2007, Deep-Sea Research, Part II, 58, 2162–2178, doi:doi:10.1016/j.dsr2.2011.05.017, 2011.
- Whitehouse, M. J., Atkinson, A., and Rees, A.: Close coupling between ammonium uptake by phytoplankton and excretion by Antarctic krill, *Euphausia superba*, Deep-Sea Research Part I: Oceanographic Research Papers, 58, 725–732, doi:10.1016/j.dsr.2011.03.006, 2011.
- Whitlock, D. R. and Feelisch, M.: Soil bacteria, nitrite and the skin, in: *The Hygiene Hypothesis and Darwinian Medicine*, pp. 103–115, Springer, 2009.
- Wuchter, C., Abbas, B., Coolen, M. J., Herfort, L., van Bleijswijk, J., Timmers, P., Strous, M., Teira, E., Herndl, G. J., and Middelburg, J. J.: Archaeal nitrification in the ocean, *Proceedings of the National Academy of Sciences*, 103, 12 317–12 322, 2006.
- Yool, A.: Modeling the role of nitrification in open ocean productivity and the nitrogen cycle, in: *Research on Nitrification and Related Processes, Part A*, edited by Klotz, M. G., vol. Volume 486, chap. 1, pp. 3–32, Academic Press, URL <http://www.sciencedirect.com/science/article/pii/B9780123812940000018>, 2011.
- Yool, A., Martin, A. P., Fernández, C., and Clark, D. R.: The significance of nitrification for oceanic new production, *Nature*, 447, 999–1002, doi:10.1038/nature05885, 2007.
- Zehr, J. and Ward, B.: Nitrogen cycling in the ocean: New perspectives on processes and paradigms, *Applied and environmental microbiology*, 68, 1015 – 1024, 2002.
- Zehr, J. P.: New twist on nitrogen cycling in oceanic oxygen minimum zones, *Proceedings of the National Academy of Sciences of the United States of America*, 106, 4575–4576, 2009.

Appendix A

CTD stations for the winter cruise

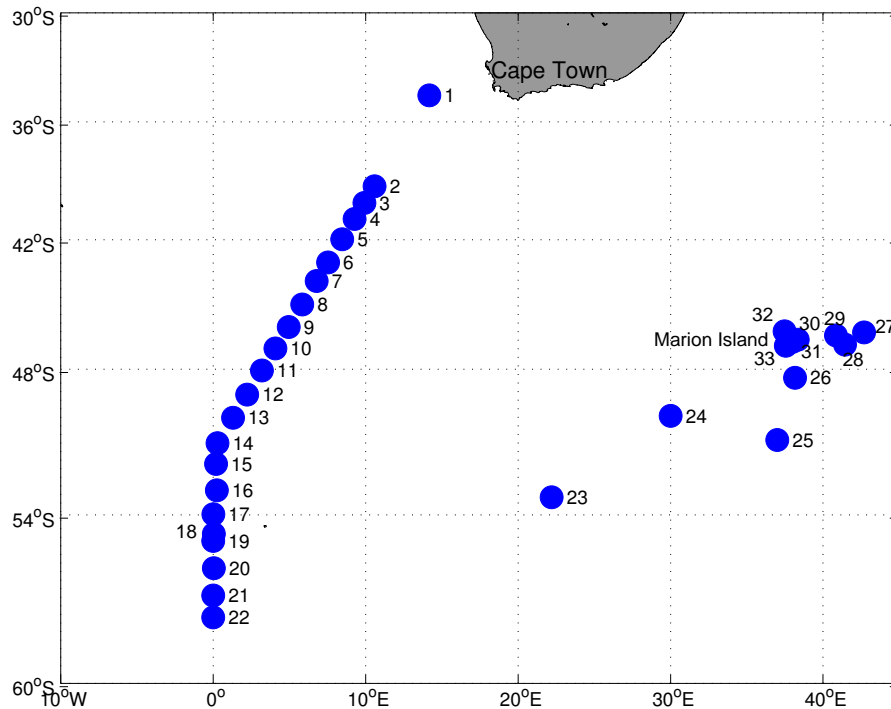


Figure A.1: CTD positions for the winter cruise. During leg 2, sampling was carried out from the ice edge to Marion Island in a straight line and then around the island in an anti-clockwise direction. For this reason, the profiles for leg 2 are shown by CTD number rather than by latitude as the circular nature of the transect gives rise to overlaps in the latitude. The positions of the ^{15}N stations where nitrogen uptake was measured are shown on figure 3.1 as well as on the CTD plots (figures 3.3 to 3.6)

Appendix B

Nitrate and nitrite profiles for the Southern Ocean stations

This appendix shows all the nitrate and nitrite profiles for the Southern Ocean stations where 15N experiments were conducted. Figures B.1 and B.2 show the summer profiles to maximum depth whereas figures B.3 and B.4 show the same profiles to a depth of 200 m. Figures B.5 to B.7 show the winter profiles to the maximum depth.

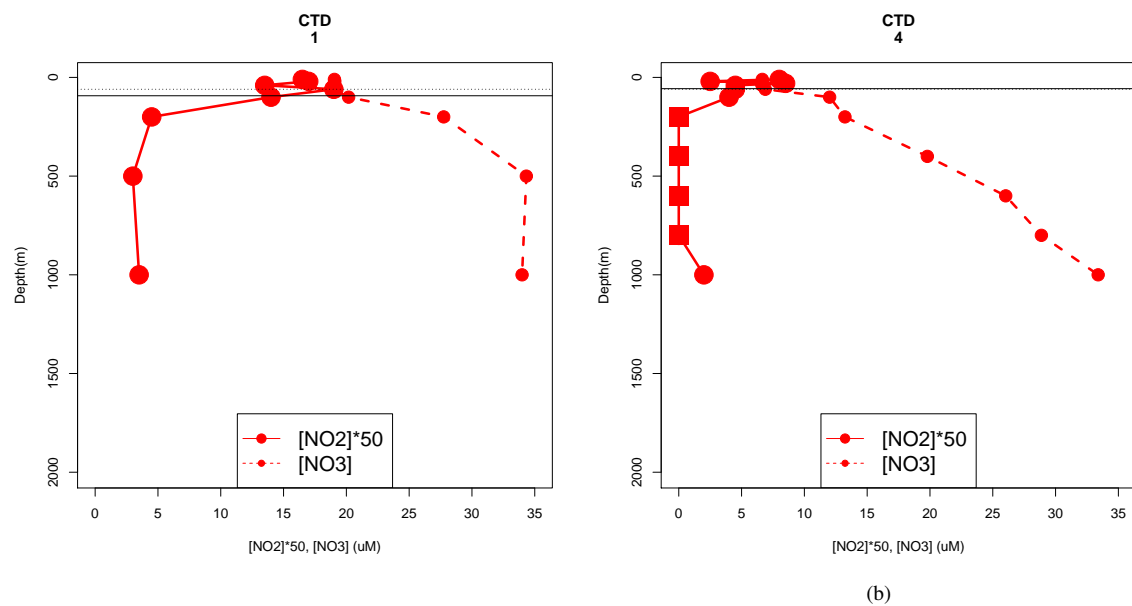


Figure B.1: Nitrate and nitrite profiles to maximum depth for the summer cruise . The black solid line shows the MLD and the black dotted line the 3% light depth. The red squares represent concentrations below the detection limit ($0.04 \mu\text{mol} \cdot \text{L}^{-1}$)

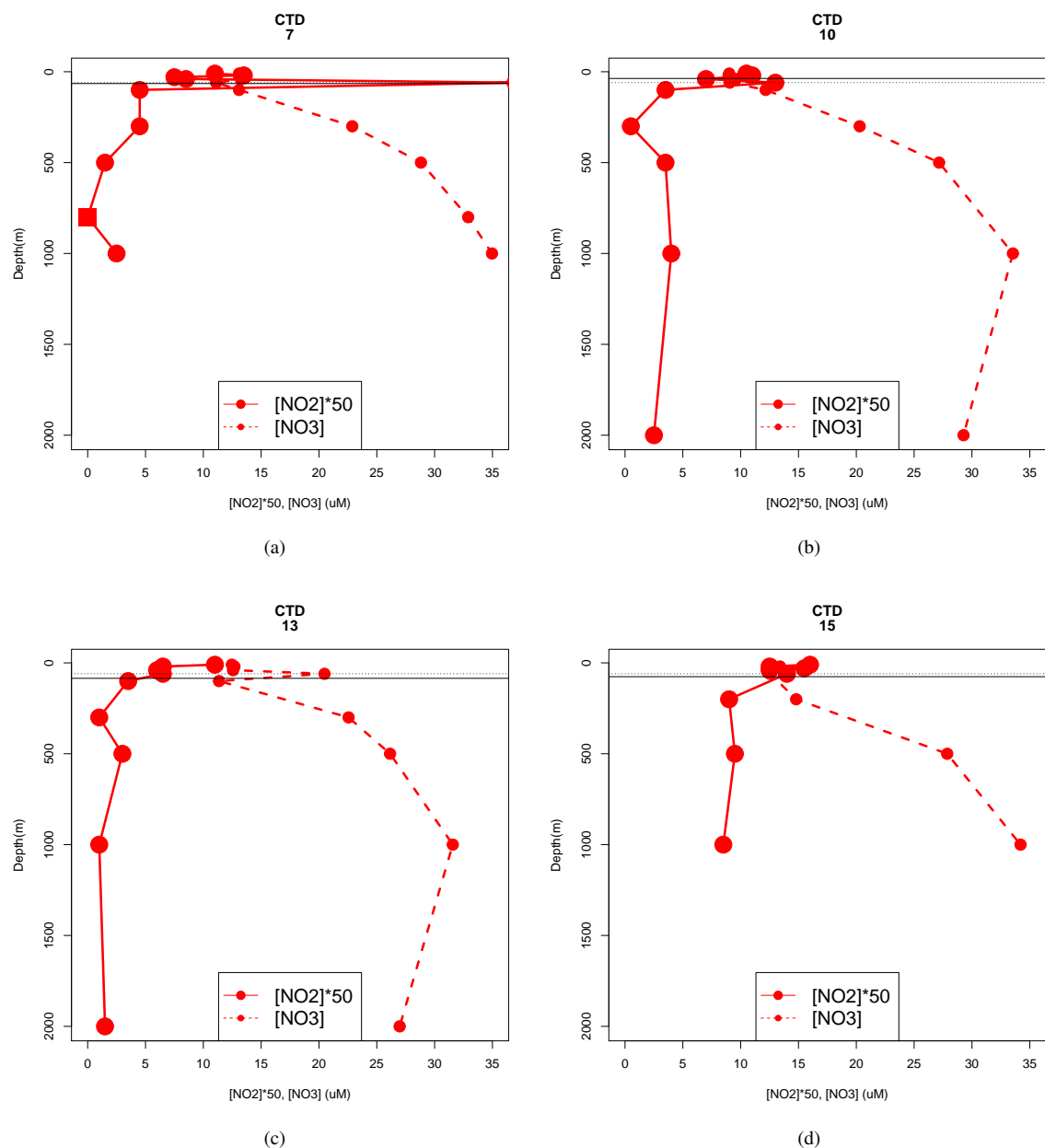


Figure B.2: Nitrate and nitrite profiles to maximum depth for the summer cruise (cont.). The black solid line shows the MLD and the black dotted line the 3% light depth. The red squares represent concentrations below the detection limit ($0.04 \mu\text{mol} \cdot \text{L}^{-1}$).

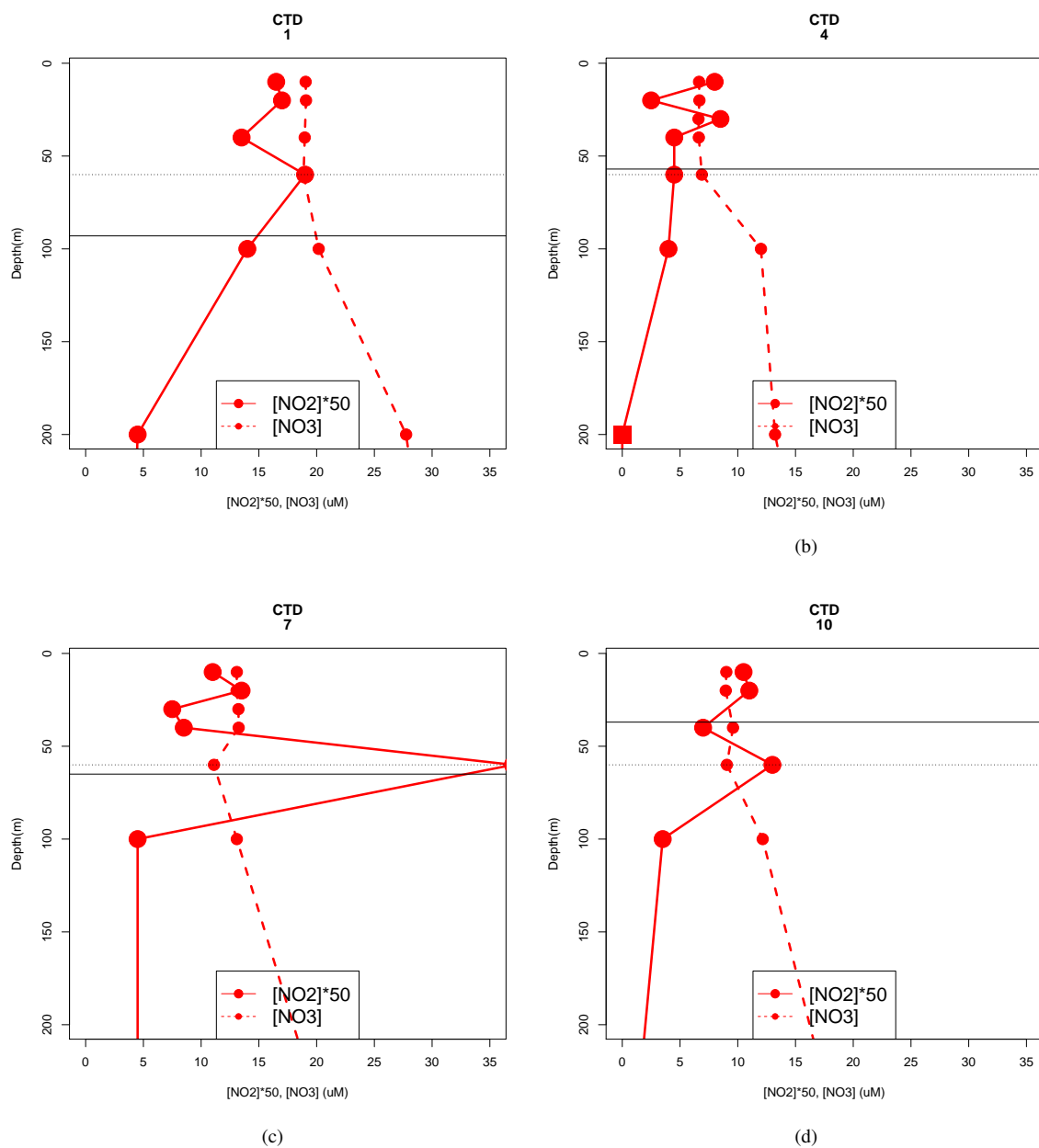


Figure B.3: Nitrate and nitrite profiles to 200 m for the summer cruise. The black solid line shows the MLD and the black dotted line the 3% light depth. The red squares represent concentrations below the detection limit ($0.04 \mu\text{mol} \cdot \text{L}^{-1}$)

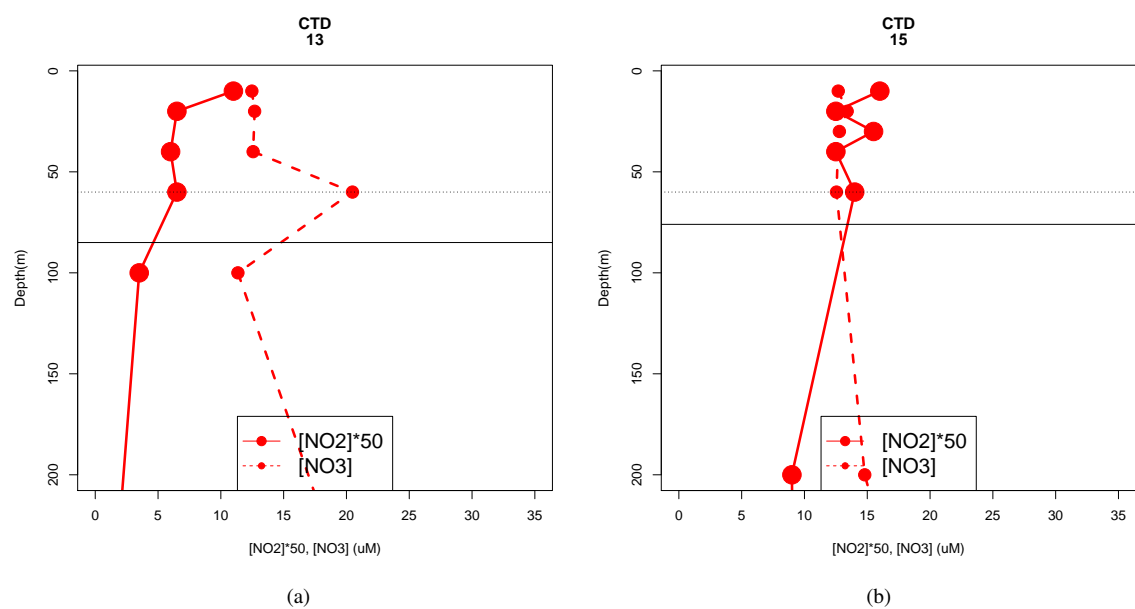


Figure B.4: Nitrate and nitrite profiles to 200 m for the summer cruise (cont.) The black solid line shows the MLD and the black dotted line the 3% light depth. . The red squares represent concentrations below the detection limit ($0.04 \mu\text{mol} \cdot \text{L}^{-1}$)

Figure B.5: Nitrate and nitrite profiles for the winter cruise. The y-axis is kept constant at 2000 m, the maximum depth available for the whole dataset. The 55% and 1% are shown as the black dashed and dotted line respectively while the mixed layer depth is shown as the solid black line. Nitrate profiles are represented by the red dashed line and nitrite profiles by the red solid line. The red squares represent concentrations below the detection limit ($0.04 \mu\text{mol} \cdot \text{L}^{-1}$).

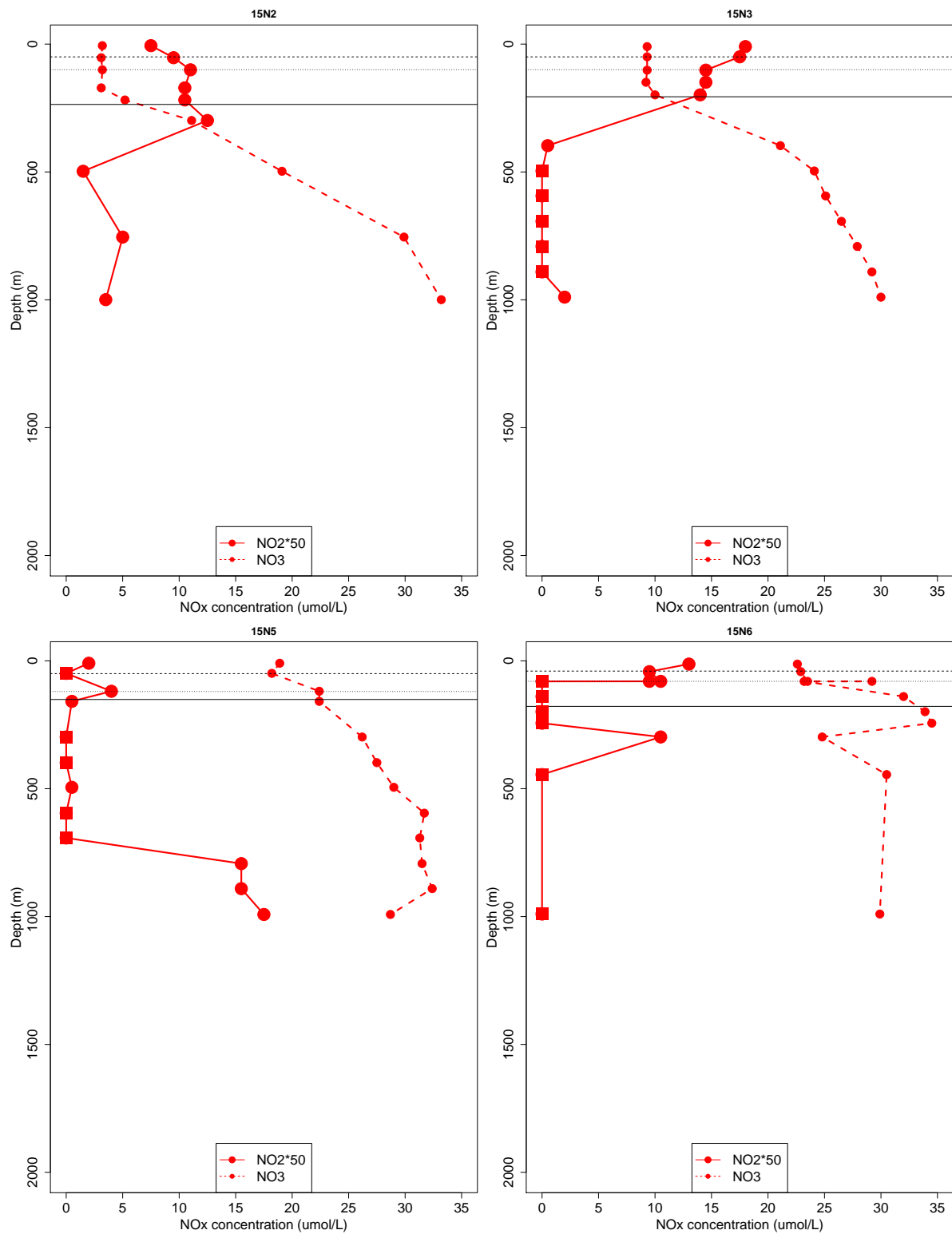


Figure B.6: Nitrate and nitrite profiles for the winter cruise (cont). The y-axis is kept constant at 2000 m, the maximum depth available for the whole dataset. The 55% and 1% are shown as the black dashed and dotted line respectively while the mixed layer depth is shown as the solid black line. Nitrate profiles are represented by the red dashed line and nitrite profiles by the red solid line. The red squares represent concentrations below the detection limit ($0.04 \mu\text{mol} \cdot \text{L}^{-1}$).

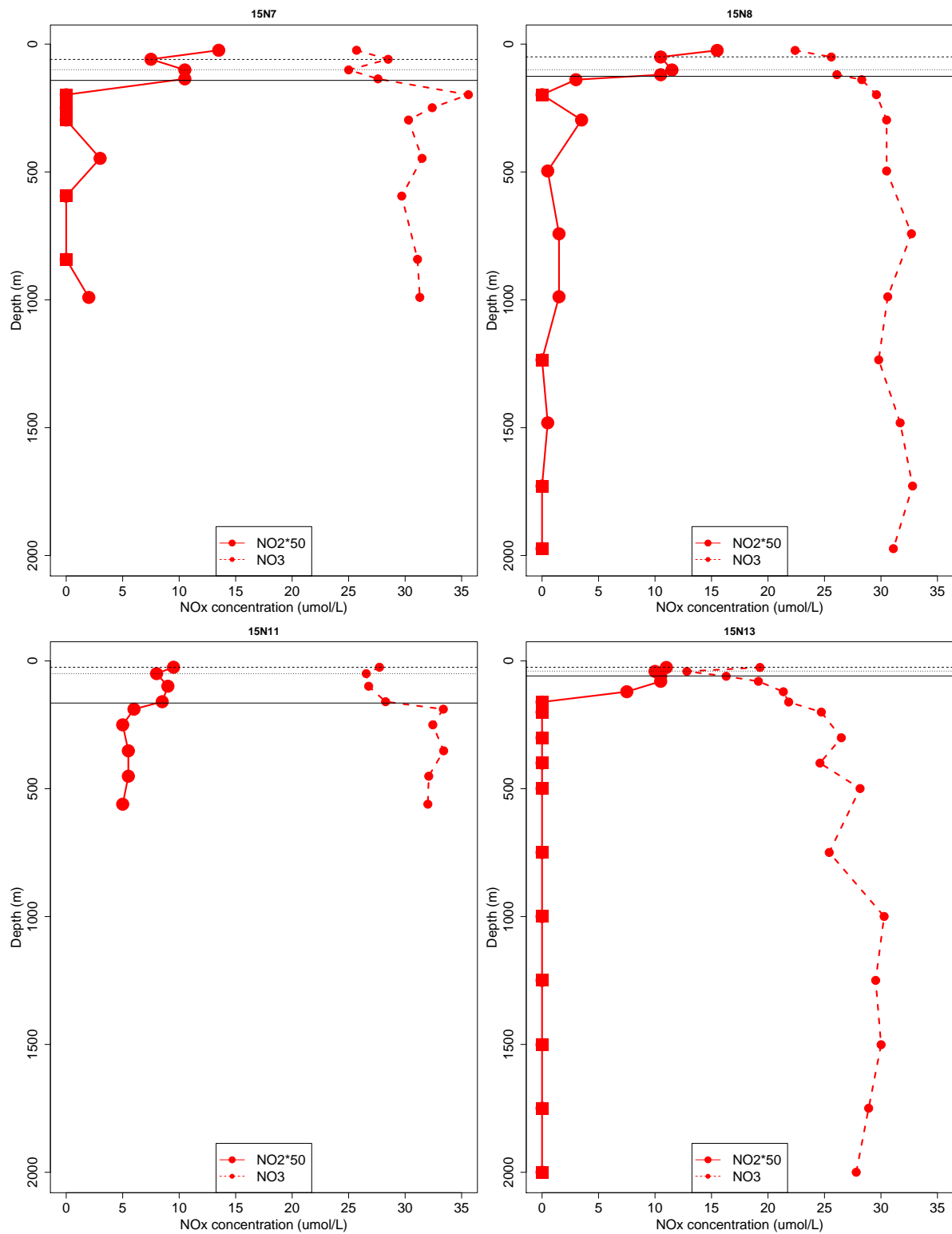


Figure B.7: Nitrate and nitrite profiles for the winter cruise (cont.). The y-axis is kept constant at 2000 m, the maximum depth available for the whole dataset. The 55% and 1% are shown as the black dashed and dotted line respectively while the mixed layer depth is shown as the solid black line. Nitrate profiles are represented by the red dashed line and nitrite profiles by the red solid line. . The red squares represent concentrations below the detection limit ($0.04 \mu\text{mol} \cdot \text{L}^{-1}$).

